Microbial Weathering of Volcanic Rocks

Thesis

Microbial Weathering of Volcanic Rocks

Annika Emilia Simpson

A thesis submitted for the degree of Doctor of Philosophy

Department of Physical Sciences

The Open University

August 2011

DATE OF SUBMISSION: 19 SEPTEMBER 2011

DATE OF AWARD: 20 SEPTEMBER 2013

Summary

The aim of this thesis was to further the knowledge on microbial weathering, by looking at the effect of model organisms (*Acidithiobacillus ferrooxidans* and *Geobacter metallireducens*) to natural microbial communities (from basaltic glass).

It was found that the medium water-rock ratio (50:1) provided the optimum conditions for *A. ferrooxidans* growth, whilst the low water-rock ratio (1:1) had a lower release of iron because of pH. The pH affected the release of iron and REEs, with less released the higher the pH. In addition, it was found that, though localised areas of hematite were found on the treated rocks, there were also oxidised layers that did not correspond to specific mineralogy. The lack of specific mineral signatures on the rock surface, but the apparent oxidation of the surface, suggested that the surface had been passivated with Fe^{3+} binding to the mineral surface. In contrast, *G. metallireducens* did not affect the production of Fe^{2+} from basalt glass when compared to controls. However, when low water-rock ratios and hematite were tested, a difference was observed between abiotic and biotic flasks. It was suggested the low water-rock ratio possibly allowed *G. metallireducens* to obtain the iron more easily by affecting the pH of the solution which in turn affected the stability of the bound iron.

In terms of studying microbial communities on rocks, it was found that community structure in Icelandic basaltic glass changed over time, becoming more diverse, with a switch from r- to K-selected microorganisms over the course of the year, similarly to results obtained in the field. DGGE results showed each flask had a distinctive population – with no correlation between ratios, and replicates different in composition to each other. It is suggested that, though community does change over time (as shown by the clone libraries), the ratios do not have an effect and each flask is developing with its own 'microbial island'. However, the results of the chemistry of the flask solutions

indicated that the biological experiments showed differences in pH and elemental release between ratios. Elemental release rates were faster in the biological experiments. The natural communities affected mineral dissolution, possibly through the release of organic acids, which would also account for the drop in pHs observed in the biological experiments.

It was noted that there were differences in dissolution rates between the results reported in this thesis and previous literature. It is suggested that these are caused by the rock surface area as in previous studies the rocks have typically been crushed into powder and fine particles. This crushed powder would have provided fresh rock surface for the microorganisms and also greater surface area for reactions to take place, accounting for generally higher weathering rates in previous literature per unit weight of material.

Acknowledgements

Dedicated to my parents, Richard and Pia Simpson, and my sister, Jennifer Simpson.

It has not been an easy road to get this PhD. However, I am glad I did it. Not only because of the character development the trials and tribulations gave me, but also for the people I would not have met had I not undertaken this journey. It is to those people that I owe my sanity and my forever thanks. Though not an exhaustive list, I would like to thank the following:

Thank you to two great supervisors: Dr Karen Olsson-Francus and Prof. Monica Grady. You went that extra mile for me and I cannot express how much it meant to me.

Thank you to Dr Tatjana Polacsek. Thank you for the curry and DVD nights as we both faced our PhDs. We made it!

Thank you to the EGL team: Graham, Emily, Ellie, Claire, Darren, Mike, Suzanne, Angus and Jason. You have given me a great time, both through my PhD and through my work.

I dedicated this thesis to my parents and my sister. I would also like to take the chance to thank them here as well. You made me who I am. I can never thank you enough. Even you, Jenska-poo!

Finally, I want to thank one special person: Dr Paul Wilkinson. We did this together. You listened to me when I needed to rant, you held me when it all got too much, and you were always there for me. I hope you know how much you mean to me. You, especially, made this worthwhile. Thank you.

Table of Contents

List of figures

List of tables

List of abbreviations

BLAST: Basic local alignment search tool

DGGE: Denaturing gradient gel electrophoresis

dH_2O: Distilled H_2O

DNA: Deoxyribonucleic acid

dNTP: Deoxyribonucleotide

DSMZ: Deutsche Sammlung von Mikroorganismen und Zellkulturen GmbH (German Collection of Microorganisms and Cell Cultures)

NCBI: National Center for Biotechnology Information

PCR: Polymerase chain reaction

rDNA: Ribosomal DNA

RDP: Ribosomal Database Project

rpm: Revolutions per minute

SEM: Scanning Electron Microscope

Chapter 1: Introduction

Weathering of rocks by microbes can occur in varying conditions. However, one rather significant variable has not been studied in relation to microorganisms and weathering: the ratio of liquid to rock. Yet, in natural environments, one can find differing ratios, from saturated water in rock vesicles to more dilute and varying environments such as rocks in a flowing river bed. When microbial weathering experiments are described in the literature, there is usually no evident explanation as to why a certain amount of rock is added to media. Why are 'A' grams of rock added to 'B' ml of media, rather than 'C' grams to 'D' ml?

1. The general aim of this thesis was to study microbial weathering of volcanic rocks, with an emphasis on water-rock ratios. The main objective was to gain a better understanding of the processes by which microbes contribute to weathering and if any knowledge learnt can be put to use in industrial applications (e.g. acid mine drainage) and in the field of astrobiology (e.g. life on Mars). The aim was to address the following broad questions: Do microbes contribute significantly to rock weathering?
2. How do microbial communtities develop under different water-rock ratios?
3. Can they acquire nutrients and energy supplies from volcanic environments?

To meet the aims described above, the objectives were as follows:

1.1. Chapter 4: Weathering with *Acidithiobacillus ferrooxidans*

The first year focused on an experiment to examine the effect of changing liquid to rock ratios on weathering of basalt by the bacterium *Acidithiobacillus ferrooxidans*, a well-known and characterised acidophilic iron oxidiser; the experiment is considered in Chapter 4. The hypothesis to be tested was that a high water-rock ratio would have an effect on release of iron, diluting it as soon as it was released, and thus limiting its supply. At the other extreme, a low water-rock ratio, the quenching effect of the rock would be increased, causing the pH of the medium to rise above optimum for bacterial growth. However, an intermediate water-rock ratio between the two would strike a balance between optimum iron concentration and pH. The key effect that changes in water-rock ratios might influence is the concentration of bioavailable iron, i.e. iron in solution. The ability of the rock to dissolve in the media, to form a solution depends on several parameters, including the physical and chemical properties of the rock and media, pressure, temperature and pH. The rock, media, temperature and pressure will be constant; however, the pH will not be controlled.

Though this study predominantly looked at the iron utilisation from the basalt by the bacteria since they require iron as a source of energy, the release and use of other elements was also investigated.

1.2. Chapters 7-8 Natural microbial communities and weathering

Following Chapter 4, the effect of changing the water to rock ratios on native microbial communities of basalt glass was studied, using a combination of culture and molecular techniques. It provided a year-long succession study on microbial communities in Iceland basalt glass and the experiment observed a community rather than a single organism. In addition, the microbial composition of the rock was known through

previous work, however, it was not known if all the phyla present were active in the rock, and if they contributed to the weathering process, which this thesis aimed to find out. It was hypothesised that the community would be dominated by microorganisms with a broad niche, whilst nutrients were low; however, this would change as time passed to microorganisms with more specific needs and narrower niches as they lived off other organisms and their by-products.

The work had implications for the rates of rock weathering in natural environments where water-rock ratios may affect the balance between optimum energy and nutrient supply. The use of ry crushed basalt glass rather than powdered also mimics a more natural environment and may be a possible explanation why weathering rates differ between the lab and field, as laboratory experiments have usually used crushed rocks.

1.3. Chapter 8: Weathering with *Geobacter metallireducens*

The final chapter focussed on investigating whether the iron reducer *Geobacter metallireducens* could weather basaltic glass. The thesis began with studying the effect of an iron oxidiser, *A. ferrooxidans*, and ends with the opposite - studying the effect of an iron reducer. It followed the astrobiology theme of Chapter 4, whereby if an anaerobic iron reducer such as *G. metallireducens* could weather basalt, it would open up possibilities of life having existed on Mars. The work also acted as preliminary work to further studies planned to investigate whether *G. metallireducens* would be able to obtain iron from a Martian meteorite, furthering the astrobiology aspect of the chapter.

Chapter 2: Background

2.1. Introduction to Weathering

Weathering is the breakdown of rocks, soils and minerals through contact with the Earth's atmosphere, biota and waters. It occurs *in situ* and is not to be confused with erosion, which involves the movement of rocks and minerals by water, ice and gravity.

Weathering affects the compositions of ground water, river and lake water, and ultimately of oceans (Banfield *et al.*, 1999). In addition, as a result of microbial attack and consequent mineral breakdown, ions are leached out into the surroundings and translocated (Lauwers and Heinen, 1974; Leyval and Berthelin, 1991; Brehm *et al.*, 2005). The ions are then used for growth and metabolism by primary producers such as plants and microorganisms (Lauwers and Heinen, 1974; Leyval and Berthelin, 1991; Brehm *et al.*, 2005). Mineral weathering impacts humans, which includes water quality, agriculture, architectural stability and landscape evolution (Banfield *et al.*, 1999). Weathering reactions have occurred throughout geological time and have shaped the compositions of the mantle, crust, hydrosphere, and atmosphere (Banfield *et al.*, 1999).

Rock weathering has a large effect on biogeochemical cycling. Weathering of volcanic minerals makes a significant contribution to the global silicate weathering budget (Dessert *et al.*, 2003), thus influencing carbon dioxide (CO_2) drawdown and climate control as CO_2 is consumed in mineral weathering reactions. The Deccan Traps in India, for example, have an estimated area of 10^6 km^2 and is thought to account for about 5 % of the global silicate weathering flux (Gaillardet *et al.*, 1999). In total, basalt rocks may account for over 30 % of the global CO_2 drawdown in silicate weathering (Dessert *et al.*, 2003). It is not the total weathering of continents that affect the carbon cycle, but the weathering of silicates in particular (Garrels and Mackenzie, 1971; Berner

et al., 1983). The process converts atmospheric CO_2 into bicarbonate in streams and, in the long term, leads to carbonate precipitation and sedimentation in the oceans (Dessert *et al.*, 2003).

2.1.1. The Carbon-Silicate Cycle

Since the work of Urey (1952), it had been postulated that, over geologic time scales, the level of atmospheric CO_2 was greatly affected, if not controlled by, the transformation of silicate rocks to carbonate rocks by weathering and sedimentation, and transformation back to silicate rocks by metamorphism and magmatism (Holland, 1978; Budyko and Ronov, 1979; Mackenzie and Pigott, 1981; Fisher, 1983). The carbon cycle is shown in Figure 2.1. Carbonic acid is produced from CO_2 combining with water (the CO_2 is taken up by plants and fixed in the soil), and it proceeds to weather carbonate and silicate rocks.

2.1.1.1. Carbonate weathering

For each molecule of CO_2 drawn down from the atmosphere, one molecule of carbonic acid is produced in the soil (Berner and Lasaga, 1989). The acid molecule produces two bicarbonate ions from dissolution of carbonate minerals (Berner and Lasaga, 1989). These are transported through groundwater to nearby streams, onto rivers and ultimately to the oceans. Here, one of these ions is transformed by marine organisms, such as plankton and corals, into carbonate to construct calcium carbonate skeletons and shells (Berner and Lasaga, 1989). When the organisms die, the calcium carbonate is deposited

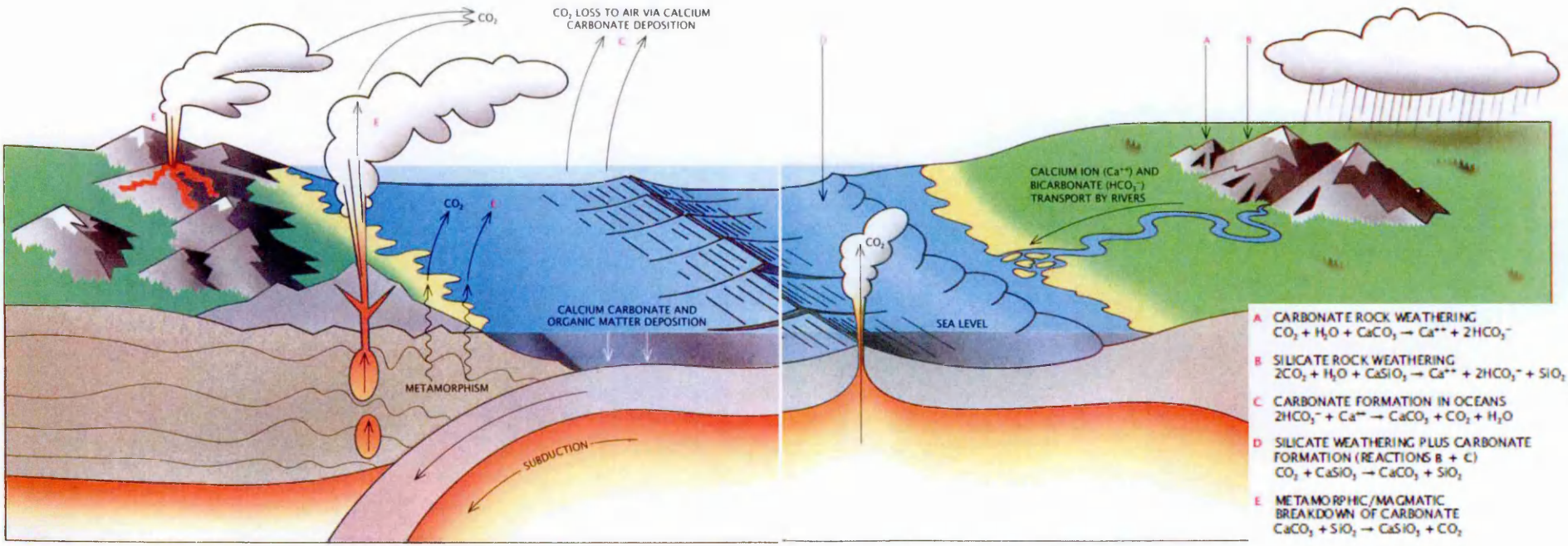

Figure 2.1. The carbon cycle as depicted by Berner and Lasaga (1989). CO_2 is taken up and fixed in the soil by plants. In the soil, the CO_2 combines with water to form carbonic acid (H_2CO_3), which weathers carbonate minerals (such as $CaCO_3$) and silicate minerals (such as $CaSiO_3$) to produce bicarbonate ions (HCO_3^-), calcium ions (Ca^{2+}) and dissolved silica (SiO_2). These are transported to the ocean, where they are incorporated into calcium carbonate by marine life, liberating CO_2, which re-enters the atmosphere. There is no net loss of atmospheric CO_2 (Berner and Lasaga, 1989). The bicarbonate and calcium ions produced during silicate weathering also combine to form calcium carbonate. However, in these reactions only half of the CO_2 is returned to the atmosphere, resulting in a net loss of atmospheric CO_2.

onto the ocean floor and buried, eventually to become sedimentary rock. The other ion is transformed into CO_2. Ultimately, however, all the CO_2 drawn down for carbonate weathering is returned to the atmosphere. However, this is not the case for silicate weathering.

2.1.1.2. Silicate weathering

Carbonic acid weathers silicates to produce two bicarbonate ions in addition to calcium ions (Berner and Lasaga, 1989). As with carbonate weathering, these products are washed into oceans and used by marine organisms. However, unlike carbonate weathering, only half of the CO_2 from the atmosphere is returned to the atmosphere (Berner and Lasaga, 1989). Therefore, silicate weathering is extremely important as it results in a net loss of atmospheric CO_2 (Berner and Lasaga, 1989; Dessert *et al.*, 2003). The balance is eventually made up during volcanic eruptions – calcium carbonate and silicon dioxide are heated deep in the Earth until combined, producing calcium silicate and CO_2, the latter which is released by the eruptions and returned to the atmosphere (Berner and Lasaga, 1989). This is the completing stage in the cycle.

As mentioned previously, the weathering of silicates is a significant CO_2 sink (Dessert *et al.*, 2003). As a result of the high prevalence of volcanic silicates, Iceland is particularly relevant to climate change (Stefansson and Gislason, 2001; Dessert *et al.*, 2003; Sigmarsson and Steinthórsson, 2007).

2.2. Iceland

Iceland was formed approximately 60 million years ago, during a massive volcanic eruption from the underlying mantle plume of the mid-Atlantic Ridge (Lauwer and Muller, 1994; Korenaga, 2004). The island itself is still volcanically active (Lauwer and Muller, 1994), with recent volcanic eruptions including Eyjafjallajökull (in southern Iceland, north ofSkógar and to the west of Mýrdalsjökull) in 2010 and Grimsvotn (under the Vatnajokull glacier in south-east Iceland) in 2011. Iceland's major volcanoes are shown in Figure 2.2.

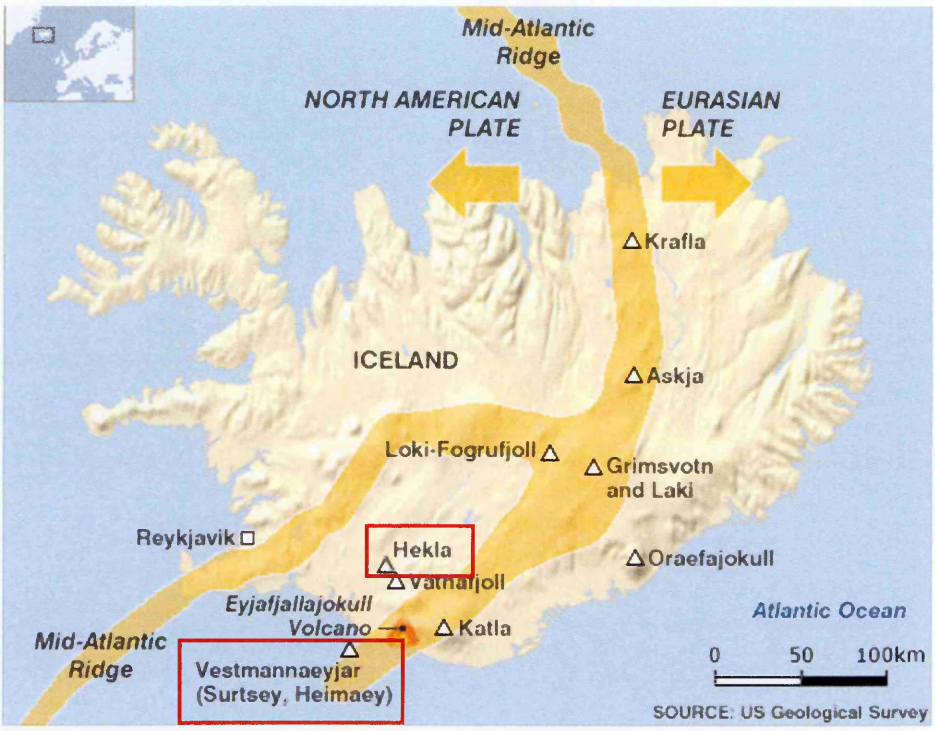

Figure 2.2. Iceland's major volcanoes (denoted by triangles) and tectonic boundaries (shaded orange) (BBC). Iceland lies on a mantle plume of the mid-Atlantic, which is caused by the diverging Eurasia and North American tectonic plates (Korenaga, 2004). The volcanoes highlighted in a red box denote the sampling areas in this thesis.

Iceland primarily consists of basaltic lava and tephra from Pleistocene subglacial eruptions and Holocene lava flows (Sigmarsson and Steinthórsson, 2007). This thesis focussed on crystalline basalt from Eldfell, Heimaey, and basaltic glass from Valafell, north East of Hekla. The basalt was fresh basalt formed from the volcano's eruption in 1973 and a mixture of olivine, FeTi oxides and plagioclase. The glass was produced in a subglacial volcanic eruption during the upper Pleistocene less than 0.8 Myr (Crovisier *et al.*, 2003) and was a mixture of basaltic glass weathered to palagonite which incorporates clasts of crystalline basalt (Furnes, 1978). The crystalline basalt was used as an iron source for *Acidithiobacillus ferrooxidans* (Chapter 4), whilst the succession of microbial community in volcanic glass was studied (Chapters 5-7). The glass was also used as an iron source for *Geobacter metallireducens* in Chapter 8.

2.2.1. Iceland and Astrobiology

In addition to being of particular relevance to climate change, Iceland and its volcanic silicates also offer significance to the field of astrobiology. Iceland's unique geological setting (on a high-point of the mid-Atlantic Ridge) leads to on-going and often intense volcanic activity, much of which is highly analogous to Mars surface processes (Cousins, 2011). The current geological features found on Mars are similar to ones observed in Iceland (Cavicchioli, 2002; Smellie, 2009; Warner and Farmer, 2010).

As Iceland lies on a near-Arctic latitude, much of the volcanism is in direct interaction with glacial activity. For example, Vatnajökull (Europe's largest glacier) lies over seven volcanic centres (Cousins, 2011). This leads to increased glaciation of volcanic centres, despite their relatively high heat flow (Cousins, 2011). The large sudden floods of glacial melt water produced by subglacial volcanic eruptions can cause catastrophic floods (Baker, 2002). These flow waters cut through the landscape, changing it. It is the

topography of these channels that is very similar to that observed in Cerberus Fossea by the High-resolution Mars Orbiter Camera (Baker, 2001), as shown in Figure 2.3. In addition, on both Mars and in Iceland, volcanic units are interfingered with fluvial units (McEwen *et al.*, 2001). Well-preserved flood lavas in SE Elysium Planitia, Amazonis Planitia, and portions of the Tharsis rise are dominated by a distinctive morphology of plates and ridges, very similar to the 'apalhraun' or 'rubbly pahoehoe' of Iceland (Keszthelyi *et al.*, 2000; McEwen *et al.*, 2001). Iceland and Mars also share geochemical similarities, with both environments being predominately theolitic basalt (McSween *et al.*, 2009).

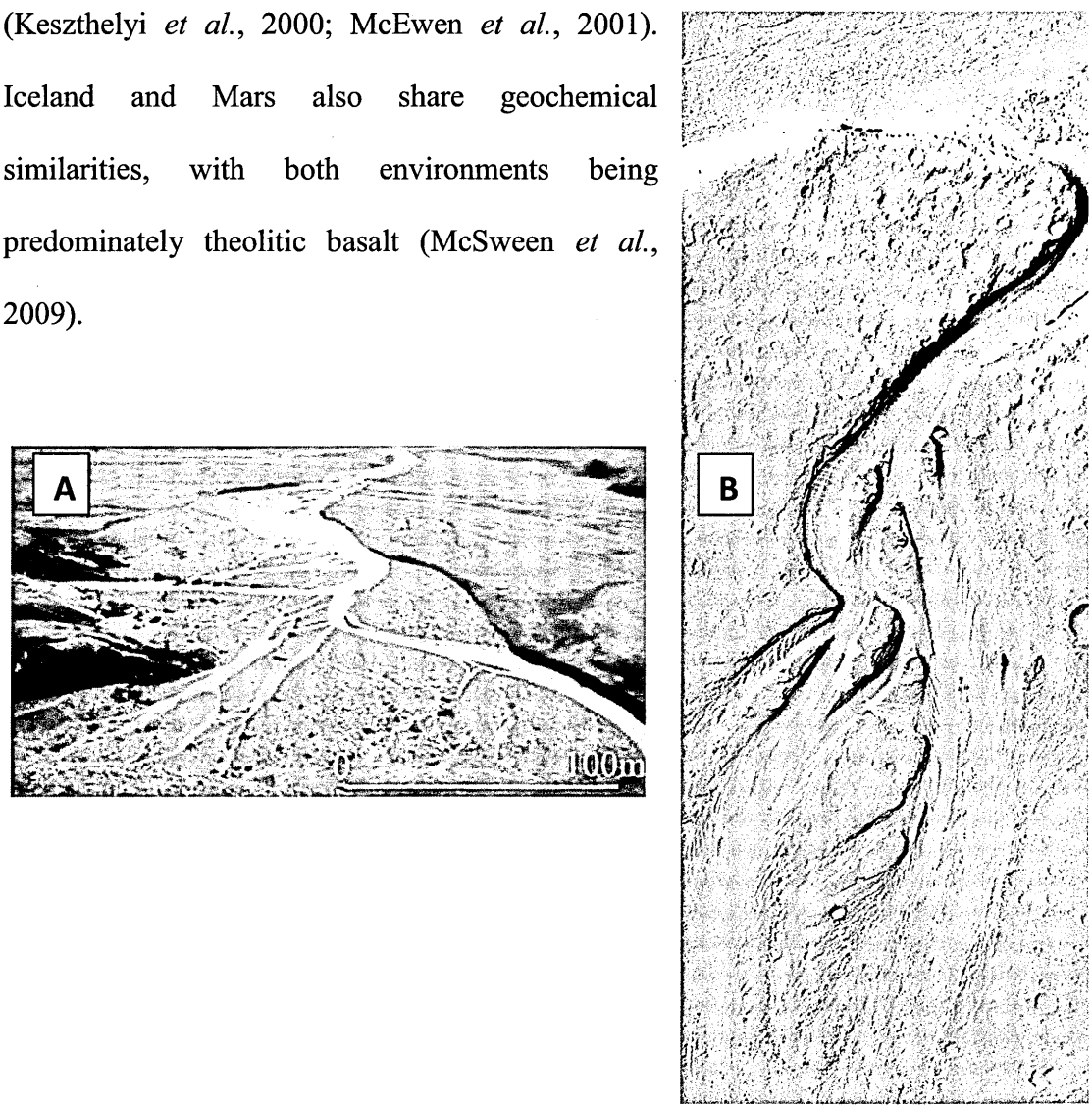

Figure 2.3. An example of flood channels found in Iceland (A) (Russell *et al.*, 2010) and similar fluvial channel systems observed in Cerberus Fossea (B) by the High-resolution Mars Orbiter Camera (Baker, 2001).

2.3. Microbes and Weathering

2.3.1. Introduction

The weathering of rocks is a complex interaction of physical weathering (temperature, wedging, crystallisation), chemical reactions (air pollutants, soil moisture, acid rain), and biological processes (Hirsch *et al.*, 1995a,b; Goudie and Parker, 1999). However, the majority of geochemical research on mineral weathering has focused on inorganic aspects (White and Brantley, 1995; Banfield *et al.*, 1999). However, understanding the weathering process requires an integrated approach of abiotic and biotic analysis (Banfield *et al.*, 1999). Although there are experimental variations, the importance of biological effects has been shown by the bacterial oxidation of ferrous iron released from pyrite (FeS_2) surfaces; the rate is up to one million times faster than the inorganic oxidation rate at low pH (Singer and Stumm, 1970; Banfield *et al.*, 1999). In addition, Wu *et al.* (2007a), in their characterisation of elemental release during microbe-basalt interactions at 28 °C, observed faster rates of release of elements (including Mg and Si) when bacteria were present. The authors reported linear release rates for Mg and Si as 0.54×10^{-12} and 1.11×10^{-12} mol/m^2/s, respectively when bacteria were present, compared to 0.09×10^{-12} and 0.57×10^{-12} mol/m^2/s in the abiotic controls.

The microorganisms involved in rock weathering are lichens (Barker and Banfield, 1998), fungi (Hirsch *et al.*, 1995b), cyanobacteria (Ferris and Lowson, 1997), many species of bacteria (Adams *et al.*, 1992), and microalgae (Hirsch *et al.*, 1995b). Microorganisms covering surfaces, fissures, and pore spaces of rocks sometimes form biofilms (De la Torre *et al.*, 1993; Gorbushina *et al.*, 2002; Puente *et al.*, 2009), contributing to the breakdown of rocks. Microbial weathering has been observed in both hot (Adams *et al.*, 1992) and cold deserts (Friedmann and Kibler, 1980). However,

little is known about weathering mechanisms (current knowledge is summarised in Section 2.3.2). It has been reported that iron and sulphides in rocks can be oxidised by bacteria at great sea depths and in deserts (Bach and Edwards, 2003; Bawden *et al.*, 2003; Edwards *et al.*, 2003; Hossner and Doolittle, 2003; Puente *et al.*, 2009). In addition, acids (Section 2.3.2.2.1.) produced by microorganisms, as by-products of their metabolism, can dissolve rocks and the resulting minerals can be utilised by microorganisms and plants (Hinsinger and Gilkes, 1993, 1995; Illmer and Schinner, 1995; Illmer et al., 1995; Chang and Li, 1998; Vazquez et al., 2000; Yamanaka et al., 2003; Puente, 2009). However, though studies have been carried out on microbial weathering, precise data on weathering rates in most environments are not abundant (Danin and Caneva, 1990; Danin, 1993; Puente et al., 2006).

Early studies on the biological weathering of volcanic rocks focused on the role of lichens (Fry, 1927; Jackson and Keller, 1970; Adamo and Violante, 1991, 2000; Banfield *et al.*, 1999). Fry (1927) conducted the earliest study of biological weathering and showed that lichens could cause etching, fragmentation and weakening of the silica-rich volcanic glass, obsidian.

It is these early studies that revealed two important factors in microbial weathering. Firstly, changes in the microenvironment induced by microorganisms at the rock surface play a role in weathering, with changes including pH, redox state and water retention (Blum and Lasaga, 1988; Parasuraman, 1995; Barker *et al.*, 1998). Indeed, chemo-organotrophic microbial communities may lower the pH to 2-4, while phototrophic communities may increase pH to above 10 due to CO_2 utilisation (Golubic, 1973; Krumbein *et al.*, 1991). The equilibrium of the rock chemistry is affected, affecting dissolution and secondary mineral formation, which accelerates weathering.

Secondly, minerals have different susceptibilities to weathering by bacteria. For example, calcium-containing plagioclase tends to weather faster than minerals such as K-feldspars (Burger, 1968). These differences are determined by the susceptibility of minerals to weathering agents produced by microorganisms or changes in chemical equilibrium.

The effect of microbial weathering is to accelerate both the physical breakdown of rock and the chemical breakdown. In addition to accelerating the weathering of all elements from volcanic rocks, microbial weathering can cause preferential leaching or enrichment of elements. Prokaryotic involvement in volcanic rock weathering has been inferred in deep ocean basalt glass in which a diversity of microbial alteration textures has been reported (e.g. Thorseth *et al.*, 1992; Fisk *et al.*, 1998; Torsvik *et al.*, 1998; Furnes and Staudigel, 1999; Thorseth *et al.*, 2001; Etienne and Dupont, 2002; Thorseth *et al.*, 2003). In addition, the idea that microbes can influence basalt weathering is not new (Staudigel *et al.*, 1995, 1998; Daughney *et al.*, 2004).

There have been several studies related to the weathering of minerals and rocks that have indicated a complex interaction of not only physical and chemical factors, but also of the activity of microorganisms (Thorseth *et al.*, 1995). In nature, the diversity of microorganisms offers a variety of direct and indirect mechanisms that may be responsible for basalt weathering (Karl, 1995; Daughney *et al.*, 2004). Microorganisms selectively oxidise, reduce and chelate a large number of elements.

In a study of basaltic glass weathering using a microbial enrichment culture from Loihi seamount, Hawaii, Staudigel *et al.* (1998) showed that the population of microorganisms, which included heterotrophic bacteria, cyanobacteria and diatoms, induced an enrichment of calcium in the sediments produced by weathering, but a loss of magnesium. In contrast, the controls showed the opposite trend. Herrera *et al.*

(2008) examined bacterial communities within obsidian in Iceland. They showed a diverse population of bacteria, which were shown to be associated with weathering alteration fronts in the rocks. However, Einen *et al.* (2006) observed that the bioalteration of glass with a community of microorganisms present was not different from abiotic controls. This difference may be explained by the timescale that the two studies looked at. The obsidian studied by Herrera *et al.* (2008) was approximately 2000 years old and from the field, whilst Einen *et al.* (2006) studied weathering of glass for one year in the laboratory. It may take centuries for visible alterations to occur which may explain why bioalteration in the lab does not always occur. The one drawback of Einen *et al.*'s (2006) work, however, is that they did not study the weathering rates of the glass or monitor the pH of the flasks, relying on visual observations of alterations instead which would have provided a more comprehensive study of weathering. This thesis aims to rectify this by providing further information on weathering rates in basalt and basalt glass.

2.3.2. Physical and chemical weathering by microbes

Upon exposure of a rock at the Earth's surface, communities of bacteria, algae, fungi, and/or lichens attach to the newly available solid surfaces (Konhauser, 2007). The fresh surfaces offer a rich source of bioessential elements. However, the microorganisms must be able to extract them. Certainly, in nutrient-poor terrestrial environments, mineral solubilisation and elemental cycling can be a requisite for the survival of the communities (Konhauser *et al.*, 1994). The effect of microbial weathering is to accelerate both the physical and chemical breakdown of rocks. Colonising microorganisms can physically penetrate into the rock, causing disaggregation of the minerals they are obtaining, or they can use chemical mechanisms. These latter

mechanisms include the production of organic acids that act as dissolving agents, changing the local pH at the rock surface through the secretion of protons (Blum and Lasaga, 1988; Parasuraman, 1995; Barker *et al.*, 1998), and the production of complexing ligands such as siderophores, which chelate oxidised iron.

Figure 2.4 shows a zone model developed by Barker and Banfield (1998) for microbially mediated mineral weathering. It is based on a correlation of different styles of silicate mineral weathering with pore size-controlled microbial distributions (Barker and Banfield, 1998; Banfield *et al.*, 1999). Zone 1 consists of the upper lichen thallus and is devoid of weathering of substratum-derived mineral particles (Barker and Banfield, 1998; Banfield *et al.*, 1999). Zone 2 is a region of extreme mineral weathering, characterised by direct contact between cells (in addition to extracellular polymers and associated compounds) and the mineral surfaces (Barker and Banfield, 1998; Banfield *et al.*, 1999). In Zone 3, although accelerated by microbial products, the weathering reactions are not mediated by direct microbial contact (Barker and Banfield, 1998; Banfield *et al.*, 1999). Unweathered minerals and minerals undergoing early, predominantly inorganic reactions comprise Zone 4 (Barker and Banfield, 1998; Banfield *et al.*, 1999).

2.3.2.1. Physical weathering by microbes

In the case of fungi, the penetration of the rock by hyphae is one primary means by which they can invade the interior of a rock and accelerate weathering. The microorganisms exploit cracks, cleavages and grain boundaries, causing alteration features such as simple surface roughing of etching and pitting, to extreme physical disintegration of the minerals (Barker *et al.*, 1997; Konhauser, 2007).

The biological processes work alongside abiotic physical weathering processes such as frost wedging, alternate wetting-drying and thermal expansion. These processes all break down the rock into smaller lithic fragments that are more susceptible to dissolution by rain and organic acids. As the minerals become loosened, macrofauna such as nematodes accentuate the erosional process through mechanical abrasion as they graze (Schneider and Le Campion-Alsumard, 1999). Eventually, the original rock has been transformed into finer-grained mineral components comprising primitive soils.

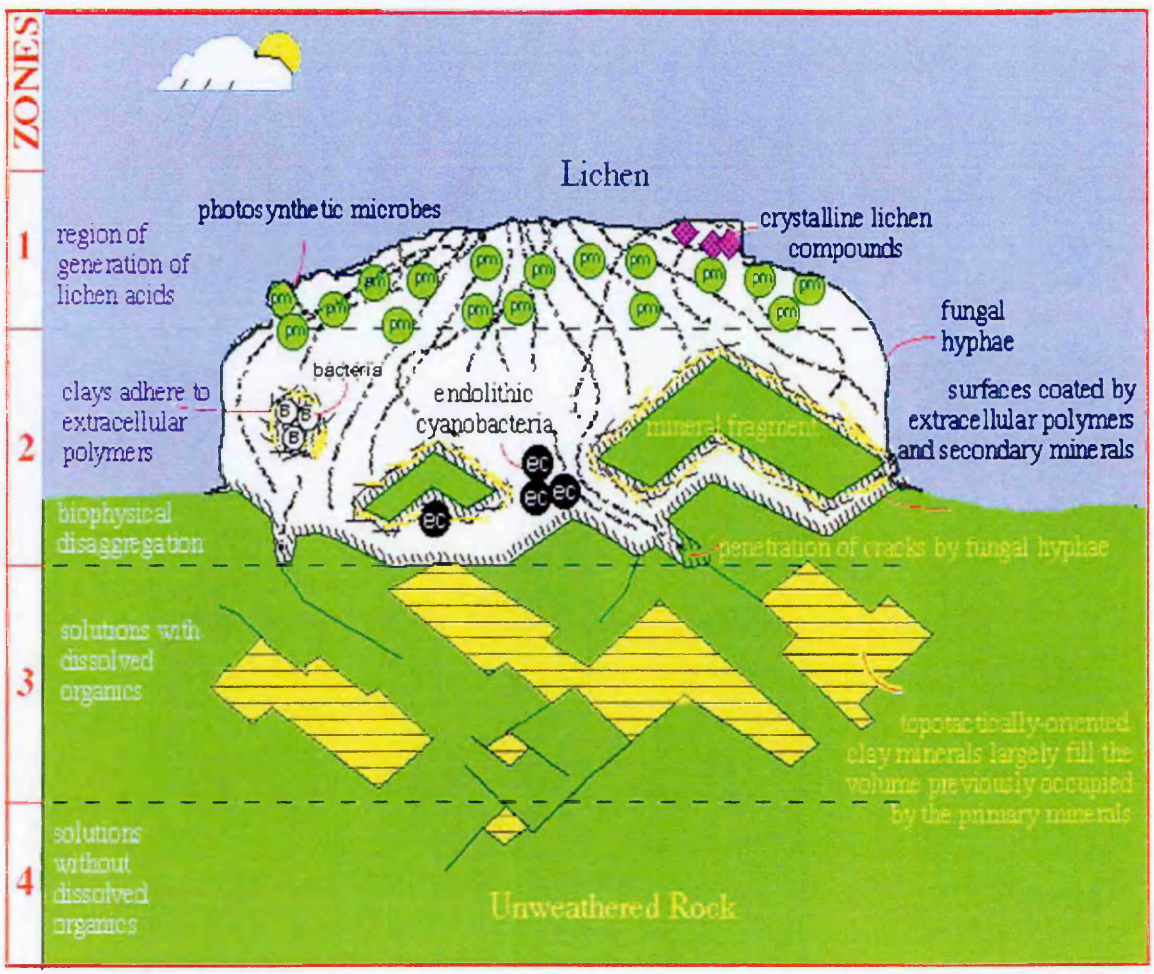

Figure 2.4. A diagram of four zones proposed for biogeochemical weathering by Barker and Banfield (1998), illustrating mineral weathering occurring in zones that are impacted by microbes to different degrees and ways. Zone 1 is where photosynthetic members of the lichen symbiosis generate fixed carbon and where crystalline lichen acids precipitate. Zone 2 is the area of direct contact between microbes, organic

products, including polymers, and mineral surfaces. Zone 3 is where reactions are accelerated by dissolved organic molecules (predominantly acids) but cells are in direct contact with reacting mineral surfaces. Zone 4 includes un-weathered rock and rock beginning to be weathered by inorganic reactions (Barker and Banfield, 1998; Banfield *et al.*, 1999).

2.3.2.2. Chemical weathering by microbes

Bacteria produce extracellular polysaccharides (EPS) which cover exposed mineral surfaces. The EPS retains water which helps to promote mineral fracturing and increases the residence time for water to fuel hydrolysis and other chemical reactions (Welch *et al.*, 1999; Konhauser, 2007). The EPS also serves as a substrate for heterotrophic bacteria, some of which generate acids that chemically attack the underlying minerals (e.g. Ferris and Lowson, 1997).

2.3.2.2.1. Organic acids

Once microorganisms become established on the mineral surface, they accelerate dissolution through the production of organic acids (organic compounds with acidic properties). The majority of these acids are by-products of fermentation and/or various intermediate steps of the aerobic respiration of glucose (Jones, 1998). However, when growth is limited by the absence of an essential nutrient, some microorganisms excrete organic acids (Jones, 1998).

Acid production is the most basic mechanism by which microorganisms can affect weathering reactions (Banfield *et al.*, 1999). Drever (1994) and Drever and Vance (1994) reported that solutions of organic acids in concentrations that were the same or slightly higher than ground water showed increases in dissolution rates of less than one order in magnitude. Though these are relatively small effects, there may be much larger

responses in natural systems where local microenvironments may be characterised by very high acid concentrations because of cell proximity (Banfield *et al.*, 1999). As previously mentioned earlier in this introduction, microorganisms have been shown to cause low pH microenvironments at mineral surfaces (Blum and Lasaga, 1988; Parasuraman, 1995; Barker *et al.*, 1998; Banfield *et al.*, 1999). Lowering the pH to 3 or 4 can correspond to a 10- to 1000-fold increase in dissolution rate (Blum and Lasaga, 1988; Parasuraman, 1995; Barker *et al.*, 1998; Banfield *et al.*, 1999). In addition elements such as Fe and Al are relatively insoluble at neutral pH (Banfield *et al.*, 1999), but their solubility increases as acidity increases (Banfield *et al.*, 1999). Elemental release rates determined under different pHs have been reported in the literature. For example, Gislason and Eugster (1987b) determined their rates under pH 9 conditions. Here dissolution proceeds more rapidly relative to the pH 4.5-6 Wu et al. (2007a) determined their rates at (Oelkers and Gislason, 2001; Brantley, 2003; Gislason and Oelkers, 2003).

Figure 2.5 shows the Eh–pH diagram for iron (a plot of oxidation potential for iron against pH). Eh-pH diagrams are useful tools for visualising the stability areas of metal species in a solution depending on the solution's redox potential (Eh) and pH. This diagram illustrates the general rules for the aqueous geochemistry of iron, where the solubility of iron is favoured under acidic, reducing conditions and disfavoured under basic, oxidising conditions. In the diagram, it can be seen that the only soluble iron species are ferrous iron (Fe^{2+}) and ferric iron (Fe^{3+}). Ferric iron is only stable at a limited area at low pH-values and high redox potential while ferrous iron is stable over a wider region at lower redox potential and extending to higher pH-values.

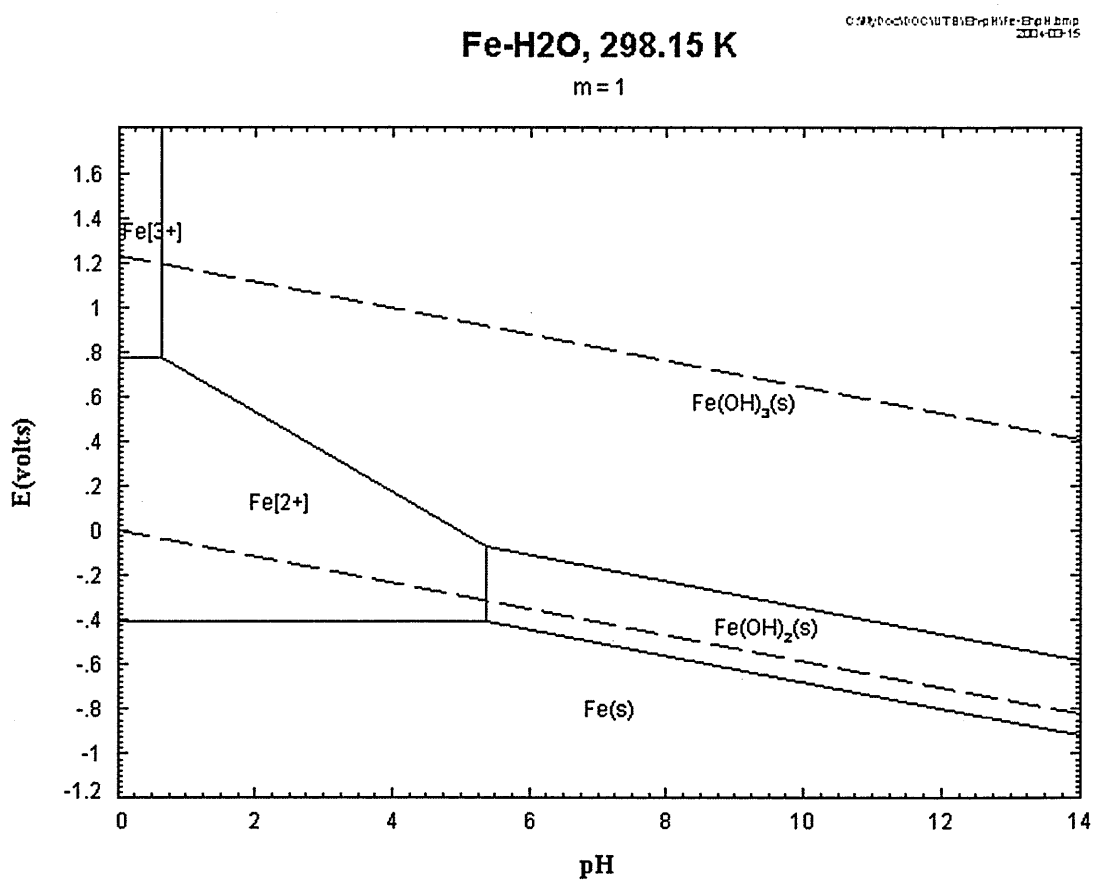

Figure 2.5. This figure shows the Eh–pH diagram for iron (Williamson, 1998). It illustrates the general rules for the aqueous geochemistry of iron advanced by Goldschmidt (1958), where the solubility of iron is favoured under acidic, reducing conditions and more limited under basic, oxidising conditions. The dashed lines represent the stability area of water, i.e. the area of relevance for hydrometallurgy. The upper dashed line is the equilibrium between water and oxygen gas. If the solution potential is increased above this line, water is oxidised forming oxygen and hydrogen ions. The lower dashed line shows where hydrogen ions in a solution are reduced to hydrogen gas. Metallic iron (Fe(s)) is not stable in water since iron is located below the stability region of water. This is why iron corrodes in aqueous solutions. If iron metal is placed in water it is oxidised to Fe^{2+} and if pH is higher than 5-6 the ferrous iron is precipitated as $Fe(OH)_2(s)$ (Williamson, 1998).

This pH dependant solubility is seen in particular in industrial applications where alkaline precipitation is a commonly used technology for removing of heavy metals from water (National Metal Finishing Resource Center, 2009). It is based on the occurrence of the following reaction:

$$M^{++}_{(aq)} + 2(OH^-) \longleftrightarrow M(OH)_{2(s)} \qquad \textit{Equation 1}$$

The M^{++} represents any divalent heavy metal. The metal ion combines with a hydroxide ion to form the insoluble metal hydroxide solid. This reaction is pH dependent; as pH is increased, the reaction is driven further to the right to precipitate more of the metals (as shown for Fe in Figure 2.5). Conversely, as the pH is decreased, the thermodynamic equilibrium moves to the left, causing more of the metals to resolubilise. This reaction is fully reversible and results in a solubility curve similar to that shown in Figure 2.6.

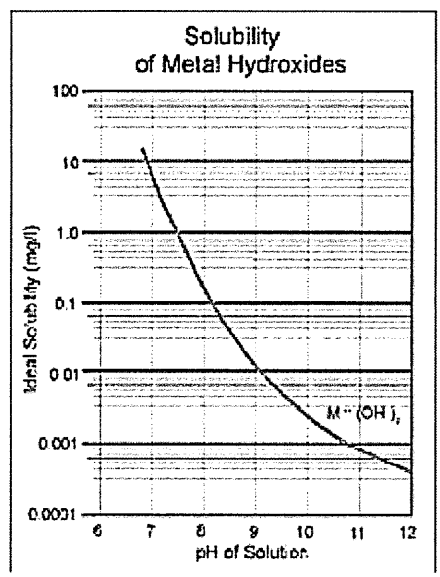

Figure 2.6. A solubility curve for metal hydroxides. As pH increases, the less soluble the metals (UniPure Technology, 2012).

In the case of fungal acids, the acids contain multiple carboxyl groups that dissociate at circumneutral pH (Berthelin, 1983). For example, citric acid is a tricarboxylic acid with

three pKa values (tridentate) at pH 3.1, 4.7, and 6.4, and oxalic acid has two (bidentate) at pH 1.3 and 4.2 (Drever and Stillings, 1997; Konnhauser, 2007). Lichens also produce 'lichen acids' which are a suite of compounds synthesised by the fungi from carbohydrates supplied by the phycobiont (Easton, 1997); 300 compounds unique to lichens have been identified (Konnhauser, 2007).

The majority of organic acids dissociate into organic anions and protons (Drever and Stillings, 1997; Konnhauser, 2007). The protons react with the ligands of the mineral surface (i.e. protonation reactions), causing a weakening of the metal-oxygen bonds and the release of a metal cation from the surface (Drever and Stillings, 1997; Konnhauser, 2007). The organic anions, on the other hand, react with metal cations on the mineral surface, destabilising the metal-oxygen bonds, and promoting dissolution through the formation of a metal-chelate complex (Drever and Stillings, 1997; Konnhauser, 2007). The eventual detachment of the chelate exposes underlying oxygen atoms to further protonation reactions (Drever and Stillings, 1997; Konnhauser, 2007). Systems with high concentrations of tridentate or bidentate organic acids tend to contribute to high levels of ion release compared to monofunctional groups (e.g. acetic acid) which have a lesser effect (Welch and Ullman, 1993; Konnhauser, 2007). Deprotonated organic anions, such as oxalate and citrate, indirectly affect dissolution rates by complexing with metals in solution (rather than the mineral's surface), lowering the solution's saturation state (Bennet *et al.*, 1988; Konnhauser, 2007).

2.3.2.2.2. Organic ligands and siderophores

As well as organic acid production, microorganisms can also produce organic ligands to catalyse mineral weathering rates (Banfield *et al.*, 1999). Ligands are ions or molecules

that bind to a central metal atom to form a coordination complex. The ligands complex with ions on the mineral surface and can weaken metal-oxygen bonds (Banfield *et al.*, 1999). In addition, they can form complexes with ions in solution, decreasing the solution saturation state and thus indirectly affecting reactions (Banfield *et al.*, 1999). The effect of ligands is somewhat similar to organic acids as the ligands affect silicate mineral dissolution stoichiometry by complexing with, and increasing the solubility of, less soluble major ions such as Fe and Al (Antweiler and Drever, 1983; Wogelius and Walther, 1991; Welch and Ullman, 1993; Banfield *et al.*, 1999).

Siderophores are one example of organic ligands and are important in iron transport to cell surfaces (Neilands, 1981, 1982; Banfield *et al.*, 1999; Konhauser, 2007). They are by definition Fe(III) specific and, under iron limitation, microorganisms that possess the capability produce siderophores that chelate oxidised iron (Banfield *et al.*, 1999; Konhauser, 2007). Mineral weathering experiments with naturally occurring siderophores have shown that these compounds can accelerate the rate of iron oxide and silicate mineral dissolution by about one order of magnitude and thus impacting iron cycling in soils (Watteau and Berthelin, 1994; Hersman *et al.*, 1995, 1996; Stone, 1997).

Siderophores average around 10^{-6} mol L^{-1} in soil pore water (Hersman, 2000). With a 1:1 binding of a siderophore to Fe (and assuming that each siderophore is used only once), these ligands could remove up to 10^{-6} mol L^{-1} of Fe from solution. This chelating ability will affect the dissolution of Fe(III)-bearing oxyhydroxide and silicate minerals (Kraemer, 2004; Konnhauser, 2007). For example, the coordination of the Fe(III) in the crystal lattice is altered during the dissolution of ferric oxyhydroxides (Kraemer, 2004; Konnhauser, 2007). The O^{2-} or OH^- ligands are exchanged for water or an organic ligand (Stumm and Sulzberger, 1992; Kraemer, 2004; Konnhauser, 2007). This leads to

a weakening of the Fe(III)-anion bond and the subsequent detachment of Fe^{3+} into solution (Stumm and Sulzberger, 1992).

Although siderophores are generally better able to chelate dissolved Fe(III) species because they can form a complete five-member ring, the hydroxamate groups of a siderophore can also bind to Fe atoms on mineral surfaces (Kraemer, 2004; Konnhauser, 2007). For example, in the case of goethite, a single hydroxamate group is adsorped to the mineral's surface, followed by structural rearrangement, dewatering and detachment of a molecule of Fe(III)-hydroxamate (Holmén and Casey, 1996; Konnhauser, 2007). Siderophores can also dissolve hematite at rates comparable to oxalic and ascorbic acids or dissolution induced by proton adsorption (Hersman *et al.*, 1995; Konnhauser, 2007). It is likely that siderophores work in tandem with protons and other organic ligands to promote ferrix oxyhydroxide mineral dissolution (Konnhauser, 2007).

2.3.3. Weathering of minerals

The weathering of volcanic minerals is recognised to make a significant contribution to the global silicate weathering budget (Louvat and Allégre, 1998; Dessert *et al.*, 2001; Kisakurek *et al.*, 2004). As previously described, this influences CO_2 drawdown and climate control, since the CO_2 is consumed in mineral weathering reactions. Approximately 30 % of all minerals are silicates and it is estimated that 90 % of the Earth's crust is made up of silicate-based material (Konnhauser, 2007).

Due to the variation in mineral constituents, texture, and porosity, different types of rocks are affected in different ways during the weathering process (Chen *et al.*, 2000). For instance, in the case of sandstone, Friedmann (1982) and Friedmann and Weed

(1987) demonstrated a characteristic weathering pattern in which the surfaces of Beacon sandstone were exfoliated in the Antarctic cold desert (Chen *et al.*, 2000). Fluid from cryptoendolithic lichens had been shown to dissolve the cementing substance between sandstone grains, reducing the cohesion of sandstone grains in the upper level of the lichen colonised zone, which resulted in surface exfoliation (Chen *et al.*, 2000). In addition, iron compounds within the sandstone were mobilised and moved to the surface where they were precipitated (Chen *et al.*, 2000).

In terms of granitic rocks weathered by lichens, aluminum silicate minerals appear to be the most significantly affected (Chen *et al.*, 2000). Biotite has been shown to be most subject to attack by organic acids under laboratory conditions (Song and Huang, 1988; Chen *et al.*, 2000), and as a result, flakes of biotite suffer much more extensive morphological and chemical alteration (Chen *et al.*, 2000). Varadachari *et al.* (1994) examined weathered biotite residues and revealed that major changes in crystal morphology occur during weathering. For example, flakes that show perfect layering in the original mineral become smaller in size, the edges etched, the thickness of the layers reduced and numerous fragmented particles are present (Varadachari *et al.*, 1994; Chen *et al.*, 2000). These morphological features of altered biotite have also been observed in granitic rocks naturally colonised by various lichens (Prieto *et al.*, 1994; Wierzchos and Ascaso, 1994, 1996; Ascaso *et al.*, 1995; Silva *et al.*, 1997).

The release of structural cations from biotite is also noticeable in weathering of granitic rocks, as demonstrated by Purvis (1984) who found that disintegration and surface dissolution of feldspar grains was apparent where there was direct contact with lichens. Wierzchos and Ascaso (1996) also reported that where the lichen thallus came into contact with granitic biotite, a considerable depletion of potassium from the interlayer

positions occurred, together with removal of other elements, corresponding to a 9.7% loss in matter (Chen *et al.*, 2000).

In basaltic rocks (the focus of this thesis), the main rock-forming minerals (pyroxene, olivine and feldspar) have been shown to be subject to attack by organic acids (Chen *et al.*, 2000). For example, Eick *et al.*, (1996) reported that pyroxene surfaces exposed to oxalic acid treatment showed side-by-side etching along the boundaries of basal lamellae whilst olivine grains exhibited a pitted or wavy surface. Varadachari *et al.* (1994) also observed that after treatment with oxalic acid of higher concentrations, a very large number of small crystals appeared and parts of the original grains became amorphous (Chen *et al.*, 2000). With this in mind, it would be expected that the dissolution of these minerals would mean that Fe and Mg (major constituents of pyroxene and olivine) could be released in the greatest amounts, followed by Ca and Al (Iskandar and Syers, 1972; Eick *et al.*, 1996). Indeed, when lichens colonise basalt, the weathering process is characterised by mobilisation of Fe and Mg and release of Ca and Al from the primary minerals, and by coating of hydrous ferric oxide on mineral surfaces and formation of amorphous materials (Chen *et al.*, 2000).

The composition and texture of volcanic rocks has been reported to have an influence on weathering rates (Cockell *et al.*, 2009a). Chemical weathering has been shown to be faster in natural silicate glasses than their crystalline counterparts in crystalline basalt, when the glasses are silica rich (Wolff-Boenisch *et al.*, 2006). This might be due to the high silica concentrations impeding rock weathering as the breakdown of SiO bonds limits weathering rates (Cockell *et al.*, 2009a). Silica-rich rocks such as rhyolite weather more slowly than less Si-rich materials such as andesitic glasses (Furnes, 1975;

Cockell *et al.*, 2009a). Figure 2.7 shows a Total Alkali Silica (TAS) diagram, demonstrating the relationships between combined alkali content and the silica content.

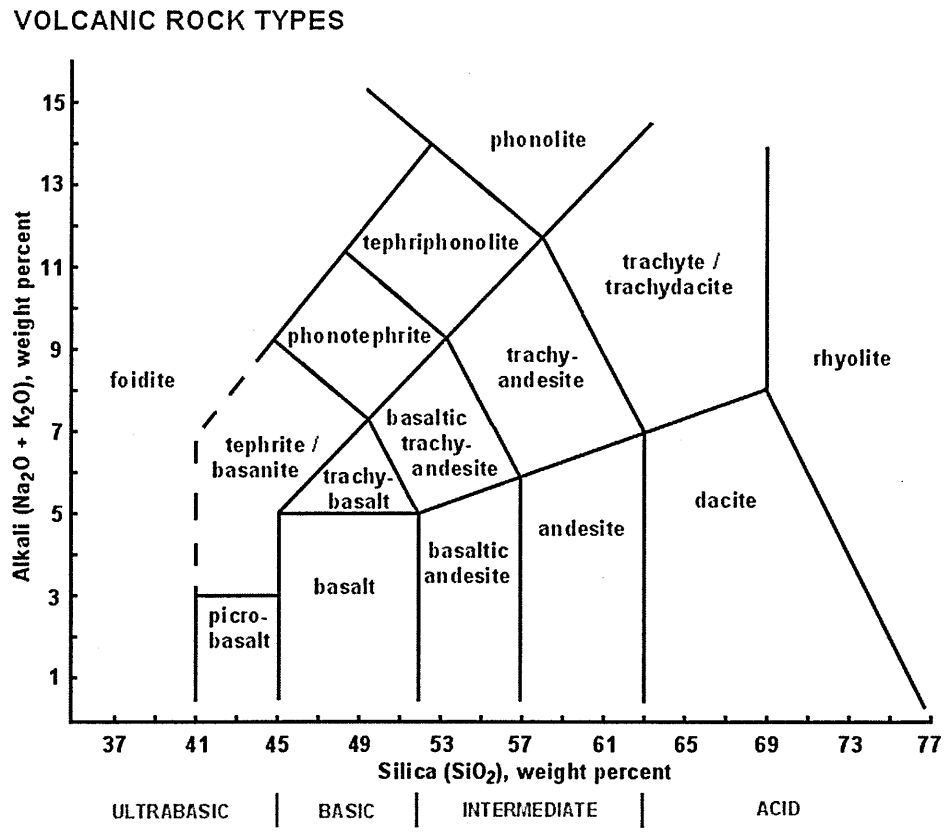

Figure 2.7. Total Alkali Silica (TAS) diagram, demonstrating the relationships between combined alkali content and the silica content (adapted from Le Bas *et al.*, 1986). Rhyolite is more silica rich than basaltic andesite, which in turn has higher silica content than basalt.

As previously mentioned, prokaryotic involvement in volcanic rock weathering has been inferred in deep ocean basalt glass in which a diversity of microbial alteration textures has been reported (e.g. Thorseth *et al.*, 1992; Fisk *et al.*, 1998; Torsvik *et al.*, 1998; Furnes and Staudigel, 1999; Thorseth *et al.*, 2001; Etienne and Dupont, 2002; Thorseth *et al.*, 2003). Cockell *et al.*, (2009a) reported that the abundance of alteration

textures in volcanic minerals is related to the original rock texture, where silica-rich rocks were found to lack alteration textures, such as elongate features and had lower abundances of pitting textures, compared to basaltic glass. It is not clear, however, whether the differences arise because of differences in texture (porosity) or composition (silica content).

In the case of the microenvironment, the surface of silica-rich rocks is different to basaltic glass. Silica-rich rocks do not have the well-developed palagonitic rinds found in weathered basaltic glass (Cockell *et al.*, 2009a). However, organisms have been shown by fluorescent *in situ* hybridization (FISH) to be exclusively associated with the rock surface in these materials (Herrera *et al.*, 2008). Due to the water-rich clay-like material of palagonite, microorganisms are likely to be able to extract nutrients more easily than a solid rock matrix. The rind might also provide a relatively protected microenvironment for organisms compared to the relatively exposed surfaces of silica-rich rocks (Cockell *et al.*, 2009a). Cockell *et al.* (2009a) supported this assumption by the high numbers of cells they observed in the basaltic glass.

2.4. Summary

To summarise, the weathering of volcanic minerals is recognised to make a significant contribution to the global weathering budget (Louvat and Allègre, 1998; Dessert *et al.*, 2001, 2003; Kisakurek *et al.*, 2004), influencing CO_2 drawdown and climate control. Microorganisms are thought to play an important part in rock weathering, and the role of lichens in volcanic weathering has received a large amount of attention (Jackson and Keller, 1970; Adamo *et al.*, 1993). However, it is only recently that work has begun in the laboratory to understand the role of bacteria (e.g. Puente *et al.*, 2004, 2009; Wu *et*

al., 2007a, 2007b; Lopez *et al.*, 2011). The involvement of bacteria has been inferred in deep-ocean basaltic glass in which a diversity of microbial alteration textures has been reported (e.g. Thorseth *et al.*, 1992; Fisk *et al.*, 1998; Torsvik *et al.*, 1998; Furnes and Staudigel, 1999; Thorseth *et al.*, 2001; Etienne and Dupont, 2002; Thorseth *et al.*, 2003). As described in Chapter 1, this thesis aims to further the knowledge into microbial weathering, by looking at the effect of model organisms (*Acidithiobacillus ferrooxidans* and *Geobacter metallireducens*) to natural microbial communities (from basaltic glass).

Chapter 3: Materials and Methods

3.1. Introduction

This chapter describes the material and the methods employed in this thesis. The decision to put materials and methods in one chapter rather than in each data chapter allows for each subsequent chapter to focus on the data collected and its interpretation.

3.2. Basalt and basaltic glass substrates

This thesis set out to test the effect that bacteria have on basalt and basaltic glass through measuring pH and elemental release. The rocks selected were:

Basalt from Eldfell, a volcano on the island of Heimaey in Iceland. It was fresh basalt, formed from the volcano's eruption in 1973. Microprobe (Cameca SX100, Kent, UK) data have shown it to be a mixture of olivine, FeTi oxides and plagioclase. The data provided the mineralogy of the basalt, allowing one to know what nutrients were available for the bacteria to utilise. To determine the surface area of the basalt the multi-point BET (Brunauer, Emmett and Teller)-N_2 (5-point) specific surface area was sent off for analysis (Meritics Ltd., Dunstable, UK) and determined as 0.56 $m^2\ g^{-1}$ ±0.01 $m^2\ g^{-1}$ (Brunauer *et al.*, 1938).

Basaltic glass collected from near Valafell, north East of Hekla volcano at 64°4.83'N, 19°32.53'W, Iceland (Cockell *et al.*, 2009a). The material was produced in a subglacial volcanic eruption during the upper Pleistocene less than 0.8 Myr (Crovisier *et al.*, 2003) and is a mixture of basaltic glass weathered to palagonite which incorporates clasts of crystalline basalt (Furnes, 1978). The samples came from blocks that lay on the ground and were 3-10 cm in diameter (Cockell *et al.*, 2009a). The multi-point BET (Brunauer,

Emmett and Teller)-N_2 (5-point) specific surface area of the glass (109.46 m^2 g^{-1} ±0.01 m^2 g^{-1}) was determined (Meritics Ltd., Dunstable, UK) (Brunauer *et al.*, 1938).

The locations of the volcanos are shown in Figure 2.2 in Chapter 2.

For both substrates, the material was collected into aseptic bags (Whirlpak, Fisher Scientific, Loughborough, UK) and initially maintained at ambient outside temperatures (Cockell *et al.*, 2009a). The samples were frozen at -20°C upon return from the field (Cockell *et al.*, 2009a).

3.2.1. Preparation of the substrates

Preparation of the basalt was as follows:

1. The rock was broken into approximately 1 cm by 1 by 0.5 cm pieces.
2. Fine particles resulting from the crushing process were removed by ultrasonication in MilliQ water and dried at 60°C (Wu *et al.*, 2007).
3. The dried basalt pieces were sterilised with an autoclave (120 °C for 20 minutes) before use.

Autoclaving the rock samples should have no effect at 121 °C as the duration is short (15 min). Furthermore, the rocks were dry and sealed in dry bottles (so they did not come into contact with the steam).

In the case of the basalt, some of the basalt was set aside for analysis by ICP-MS and XANES (as described in section 3.2.2.).

In the case of the glass, it was processed in two ways. Firstly, one batch of rock was processed in the same way as the basalt, crushed into approximately 1 × 1 × 0.5 cm pieces and sterilised by autoclaving (120 °C for 20 minutes). Another batch was kept in

a -20 °C freezer until the start of the experiment, when it was thawed in a sterile environment before being aseptically broken up into approximately 1 × 1 × 0.5 cm diameter pieces. The latter was used as the inoculating material for the experiment.

3.2.2. Analysis of the rock and solutions

3.2.2.1. Scanning electron microscopy (SEM)

Technique adopted in: Chapter 4 and 6.

Surface morphology of the rocks in Chapter 4 was examined under a Zeiss Supra 55V field emission gun scanning electron microscope (FEG-SEM), which provided high spatial resolutions. Samples were imaged with a beam size of 15 keV, at a working distance of 4-6 mm. This allowed the rock samples, and the microorganisms, to be seen on the micron scale. One of the pieces of rock (a polished piece of rock for the experiments describe in Chapter 4) placed in each flask was carbon-coated and examined under the SEM to see whether the different conditions had an effect on surface morphology, details of which cannot be seen accurately with a light microscope. In addition, in Chapter 4, the number of *Acidithiobacillus ferrooxidans* cells per 100 fields of view were counted for each water-rock ratio to ascertain whether any differences in cell numbers between ratios was replicated in solution and on the rock.

In the experiments described in Chapter 6, SEM was used at the end of the experiment to observe whether biofilms had grown on the surface of the rocks.

3.2.2.2. Elemental analysis

Technique adopted in: Chapter 4 and 6.

Inductively coupled plasma mass spectrometry (ICP-MS) and atomic emission spectroscopy (ICP-AES) were employed on the samples, using the Agilent 7500s ICP-MS with New Wave 213 laser system (Agilent, Berkshire, UK) and the Teledyne Leeman Prodigy (Quantitech, Milton Keynes, UK), respectively. These were used to measure the concentration of elements leaching out from the basalt into solution. ICP-MS was also carried out on the rock.

The kinetics of elemental release was calculated using the linear (R_i^l) release rate, as given by the equation:

$$R_i^l = \frac{dC_i^*}{dt}\frac{V_0}{Am} \qquad \textbf{\textit{Equation 3.1}}$$

R_i^l is the linear release rate of element i (mol/m^2/d), $\frac{dC_i^*}{dt}$ is the slope of the line describing C_i^*, the corrected elemental concentration, which corresponds to a change in $C_{j,i}^*$ values versus time. V_0 is the initial fluid volume, A is the BET-N_2 specific surface area and m is the mass of the rock particles (Wu *et al.*, 2007a).

3.2.2.2.1. Analysis of rock

ICP-MS was used to measure the concentration of rare earth and heavy metal elements in the basalt. The basalt was crushed into a fine powder with a mortar and pestle before being digested using HF/HNO_3 as described by Bailey *et al.* (2003). After digestion, the samples were run on the ICP-MS in a continuous run.

3.2.2.2.2. Analysis of solution

ICP-MS was employed to measure the concentration of rare earth and heavy metals in solution over the duration of the experiment. One ml was removed from each flask on each sampling day and placed into a sterile 4 ml sample tube. To each tube, 1 ml of 2 % HNO_3 was added and mixed by inverting the tube by hand. The nitric acid prevented the elements from adhering to the sides of the tubes, and thus preventing loss of elements whilst in storage at 4 °C. The samples for Chapter 4 and 6 were run at the end of their respective experiments (after 43 and 213 days). There have been no reports on the effects of long term storage on the quality of data acquired from a sample. This observation was supported by technical staff in the laboratory that had never had problems with degradation of samples during long term storage (i.e. for storage much greater than the 213 days of the experiment in Chapter 5). No literature has addressed long term storage. If there were some loss, e.g. through binding with sample vessels, proportionally it should be the same in all samples, so that whilst there would be an overall underestimation of release rates, the relative trends would be the same.

All samples were analysed in one continuous run, and sampled three times by the machine, with a mean and standard deviation calculated for each time point and flask (accuracy was to ±5 % RSD). In addition, blanks were also run (which consisted of one tube containing distilled water, and another containing 2% HNO_3). This was to check that elemental concentrations detected would not be due to the solutions used to dilute the samples. A set of calibration standards was run through the machine at the beginning of the run, and a standard was also run after every ten samples to monitor any instrumental drift that would affect the results. It is assumed that the drift affecting the chosen standard would also affect the samples. Therefore, data can be corrected for drift during the data analysis stage. Once the samples were run through and data

acquired, the data were converted from parts per billion to moles per litre (M) and corrected for drift if needed.

ICP-AES was employed to measure Al, Ca, Cr, Cu, Fe, K, Mg, Na, Ni, Si and Zn in solution. Preliminary analysis of solutions using ICP-AES showed that 1:5 dilution of the samples was needed to fit in the range of the calibration chosen (0 to 7.5 ppm) and also to accommodate the limited amount of liquid that could be removed from the flasks. One ml was removed from each flask, on each sampling day and placed into sterile 15 ml polycarbonate centrifuge tubes (Fisher Scientific, Loughborough, UK). To each tube, 4 ml 2% HNO_3 was added and mixed by inverting the tube by hand.

As with the ICP-MS, all samples were analysed in one continuous run. They were sampled three times by the machine, with a mean and relative standard deviation (RSD) calculated for each time point and flask, accuracy was to 5% RSD. The data were corrected for drift if needed and converted from parts per billion to M using the following method:

Concentration in ppb ÷ 1 000 000 = Concentration in g l^{-1}

Concentration in g l^{-1} ÷ molar mass of element = M

3.2.2.3. XANES Analysis

Technique adopted in: Chapter 4.

X-ray near-edge spectroscopy (XANES) was used to study the oxidation state of iron present in minerals on the surface of the polished basalts placed in the flasks in Chapter 4, as described by Cockell *et al.* (2011). It was hoped that the investigation would show

effects from the weathering of basalt at the surface. As in the case of the SEM, a piece of basalt (previously polished) was removed from the flasks at the end of the experiment for analysis. Original basalt (not placed in the flasks) was also analysed.

The work was conducted at the microfocus spectroscopy beamline (I18) at the Diamond Light Source (Mosselmans *et al.*, 2008; Cockell *et al.*, 2011). The beamline produces a focused X-ray beam, typically 3 μm in size, and operates over a 2–20 keV energy range. The spectra were collected using a 9-element Ortec Gemonolithic solid state detector with XSPRESS2 processing electronics (STFC, UK). The beamline has a cryogenically cooled Si(111) monochromator. Data were gathered at the Fe-K edge region, with randomly selected areas on the surface analysed to get an overview. The energy range for analysis was from 7,000 to 7,200 eV. Data were gathered at 0.3 eV increments until 7,170 eV and at 3 eV increments thereafter. All spectra were calibrated against the spectrum obtained from metallic Fe foil with the first inflection point of the Fe-K edge set at 7,111.08 eV.

The polished basalts were attached to aluminium sample holders. Samples of control iron oxide minerals and siderite were examined (Richard Tayler Minerals, Cobham, UK). $FeSO_4$ was obtained from Sigma-Aldrich (Dorset, UK). Ferrihydrite (2-line) was prepared in the laboratory by the method of Schwertmann and Cornell (2008). Some of the control minerals and oxyhydroxides (hematite, magnetite, ferrihydrite) were examined in transmission mode. To prepare samples for transmission mode analysis, approximately 20 mg of sample was added to 100 mg of boron nitride and pressed into a ~1 mm-thick disc. Two spectra were collected at each point to improve data quality and to rule out beam damage to the sample by comparison of the first and second spectra.

Data reduction and XANES analysis was carried out using the program Athena (Ravel and Newville, 2005). To determine the closest match of the standards to the surface iron oxyhydroxides, Linear Combination fitting was used in the analysis suite of Athena using ferrihydrite, goethite, hematite and magnetite as standards.

3.3. Bacteria

The experiments in Chapter 4 were conducted using *Acidithiobacillus ferrooxidans*, obtained from the German Collection of Microorganisms and Cell Cultures (DSMZ). The strain used was DSMZ 584, as this is a well characterised iron oxidiser with well defined growth requirements.

The experiments in Chapters 5-7 were conducted using a community of microorganisms from the volcanic glass used in the experiment. They would later be identified using molecular techniques (Chapter 5, Section 5.2).

The experiments in Chapter 8 used a stock culture of *Geobacter metallireducens*, obtained from the German Collection of Microorganisms and Cell cultures (DSMZ). The strain used was DSMZ 7210, as, again, this is well characterised with well defined growth requirements.

3.3.1. Cell counts

Technique adopted in: Chapter 4.

Cell counts of cells were carried out using fluorescence microscopy. One ml of the culture was filtered onto 0.2 μm black polycarbonate film (Whatman, Fisher Scientific, Leicestershire, UK) using vacuum filtering equipment to collect any cells present. Using the same filtering equipment, the cells were then washed twice, each time with 1

ml of sterile water to remove any acid present. One ml of a 1000x diluted DNA-binding dye SYBR Green (2 µl SYBR Green stock in 10 ml of distilled water) was added to stain the cells. The dye was left on the filter paper for one minute, before being drawn through using the vacuum. The filter, with the now dyed cells, was removed from the apparatus and placed on a slide, and left in a dark box for 10 minutes.

The cells were viewed under a fluorescence microscope (Leica DMRP, Wetzlar, Germany), using a blue filter, and magnification of x100. Any bacteria that were present fluoresce green. For each sample slide, 50 fields of view were counted, and the average number of cells was calculated using the following equation:

(Cells/fields counted) × (filter area/field area) × (1/ml filtered) = Cells per ml

Where, filter area is 201.06 mm^2 and field area is 0.0314 mm^2.

3.4. Media

The media used in the different experiments are described below, in the order that they appear in the thesis.

3.4.1. Chapter 4 – *Acidithiobacillus ferrooxidans*

For *A. ferrooxidans* we used Silverman and Lundgren (modified K9) medium, a well-characterised medium for this organism (Silverman and Lundgren, 1951). The components of the medium are listed in Appendix A.

Through previous experience in the laboratory group, it was noted that adding basalt to the media produced a precipitate, thought to be a sulphide produced by reactions between the iron in the rock and sulphate in the medium, which clouded the media (this was also true when $FeSO_4$ was added). This occurred despite the addition of bacteria.

At the time this was not investigated but future work should analyse this precipitation. As the precipitation and clouding might affect the results of mineral leaching by increasing the amount of elements present during analysis, steps were taken to prevent this. Preliminary experiments were carried out, that aimed to investigate how varying the concentration of Solution A of the modified K9 medium affected both precipitation and *A. ferrooxidans*. The concentration of $FeSO_4$ (Solution B) remained the same. The concentrations can be found in Appendix A. In short, a $1/10^{th}$ and $1/100^{th}$ strength solutions were all tested alongside the normal strength (flasks were duplicated). Table 3.1 summarises the conditions investigated.

Table 3.1. Summary of conditions investigated with regards to finding optimum Sol A concentration that prevented precipitation with minimal impact to the bacteria. 'B' denotes biological flasks (with bacteria added) and 'C' denotes controls (no bacteria added). Each condition was carried out in duplicate.

Flask label	Solution A strength	Addition of *A. ferrooxidans*
B1	Normal	+
B2	$1/10^{th}$	+
B3	$1/100^{th}$	+
C1	Normal	-
C2	$1/10^{th}$	-
C3	$1/100^{th}$	-

The flasks were sampled over 14 days and iron concentrations measured, in duplicate, using the ferrozine assay and the averages were calculated (Section 3.5.2). The media that showed the least amount or no precipitation, whilst not affecting *A. ferrooxidans*,

would be used for the basalt experiments. Cultures were incubated static at 29°C. After the preliminary experiments, a $1/100^{th}$ (Solution A_{low}) strength solution was selected (data described in Chapter 4).

3.4.2. Chapter 5-7 – Natural communities and volcanic glass

A low yeast extract (LP0021 Oxoid, Cambridge, UK) medium (0.2 g per litre of distilled water) was added to each experimental flask before the addition of the inoculating rock that contained the native microbial community.

3.4.3. Chapter 8 – *Geobacter metallireducens*

The culture media used was DSMZ 579 *Geobacter* medium, recommended by the culture company for this strain, and is described in Appendix A. The media was prepared anaerobically and 5 ml was added to Hungate tubes (SciQuip Ltd., Shropshire, UK). A 100 µl inoculum of *G. metallireducens* was added to each Hungate and incubated stationary at 29 °C.

3.5. Specific techniques

3.5.1. Measuring pH

Technique adopted in: Chapter 4 and 6.

To monitor how biotic and abiotic weathering affects the pH of a solution in experiments, pH measurements were carried out using a Fisherbrand Hydrus 300 benchtop pH meter (Fisher Scientific, Leicestershire, UK). One millilitre of sample was

taken from the solution being measured and was placed in an eppendorf tube. Using a thin pH probe, the pH was read.

3.5.2. Ferrozine assay

Technique adopted in: Chapter 4 and 8.

The iron oxidation by microorganisms was monitored using a Fe^{2+} specific assay using ferrozine (3-(2-pyridyl)-5,6-diphenyl-1,2,4 triazine-4', 4''-disulfonic acid sodium salt) (Stookey, 1970). Ferrozine is an iron-chelating agent that forms a complex with ferrous iron, producing a purple colour and has an absorption peak at 564 nm. The ferrozine assay is a standard method used to measure changing iron concentrations in solution. The oxidation of iron can be used as a proxy for growth of microorganisms in cultures. Abiotic oxidation of Fe^{2+} can also be monitored using this assay, thus allowing one to compare biotic and abiotic oxidation together.

The assay also includes a reduction step which allows one to measure the total iron concentration in the sample, that is, the step allowed one to determine how much oxidised iron had been removed from solution as precipitates or had yet to be oxidised.

A modified version of the ferrozine assay was used to measure Fe^{2+} concentrations over time, as described by Viollier *et al.* (2000). Three reagents were prepared to perform the assay:

1. **Ferrozine** was prepared to a concentration of 0.01 M by adding 24.6 mg Ferrozine to 5 ml of 10^{-1} mol/l ammonium acetate (0.38 g ammonium acetate in 50 ml of distilled water, adjusted to pH 9.9)
2. **Reducing agent**, 1.4 M hydroxylamine hydrochloride ($H_2NOH.HCl$), was prepared by adding 0.97 g of hydroxylamine hydrochloride to 10ml of 2M HCl.

3. **Buffer solution** (10 M ammonium acetate) was prepared by adding 7.7 g ammonium acetate to 10 ml distilled water and adjusted to pH 9.9 using 30% ammonium hydroxide.

The initial concentration of reduced iron (A_1) in solution was determined by adding 100 µl of ferrozine solution to 900 µl of sample in a cuvette. The absorbance was measured at 564 nm using a spectrophotometer (Helios Spectrophotometer, Thermo Scientific, UK). After taking the reading, 800 µl of the solution was transferred to a new cuvette and 150 µl of reducing agent was added. The solution was left for 10 minutes to allow reduction of Fe^{3+} to Fe^{2+}. After 10 minutes, 50 µl of buffer solution was added and the absorbance (A_2) corresponding to the total iron (Fe^{2+} from soluble Fe^{2+} and reducible Fe^{3+}) was then recorded at 564 nm. The quantity of iron in µM was determined using calibration curves obtained with standards using $FeSO_4$.

3.6. Statistical and data analysis

There are two different types of data in my thesis, each of which requires a different type of statistical treatment to gain an idea of the validity of my data. The statistics implemented are described below.

The first type of data could loosely be called 'inorganic', and includes elemental analysis, pH determination etc. The T-test was used for this type of data to compare differences in pH and elemental release between different treatments, where a *P* value of less than 0.05 was considered significant. The T-test is a method that is used to determine if two sets of data are significantly different from each other. It is the only appropriate statistical method that can be applied when there are only a limited number of replicate analyses, as here, where the number of replicates, n, is two.

The second type of data is that coming from analysis of my microbial community, which requires a completely different evaluation technique, such as the system known as MOTHUR, version 1.18.0 (Schloss *et al.*, 2009). This is a code-based software with built-in algorithms specifically designed to calculate such things as richness, diversity, and rarefaction curves from a molecular data set. Cluster analysis on the DGGE is qualitative. These analytical packages are used commonly by molecular biologists (Bonetta *et al.*, 2008; Oros-Sichler *et al.*, 2006; Manzano *et al.*, 2013; Schloss *et al.*, 2009; Walker *et al.*, 2011; Bik *et al.*, 2010)

Through analysis of papers and from discussion with staff in the laboratory expert in the techniques, MOTHUR and Gelcompar analysis were evaluated as the best tools for the data set.

In Chapter 5, diversity and richness estimators (Shannon diversity index, Simpson's reciprocal index and Chao1 (Chao 1984) on clone libraries were computed. In addition, MOTHUR was also used to:

- Assign sequences to OTUs – this identifies a representative sequence from each OTU, allowing for a tree to be constructed with representative OTUs.
- Calculate rarefaction curves – the curves provide a way of comparing the richness observed in different samples.
- Calculate rank abundance curves – a means for visually representing species richness and species evenness.

Clone libraries were compared at species (97 %) sequence similarity levels using the Libshuff (Singleton *et al.*, 2001) function available in MOTHUR. The DNADIST program of PHYLIP (Felsenstein, 1989), using the Jukes-Cantor (Jukes *et al.,* 1969) for nucleotide substitution, was employed to generate the distance matrix analysed by Libshuff. Neighbor-Joining phylogenetic trees were constructed in MEGA4 (Tamura *et*

al., 2007) using the Jukes-Cantor nucleotide substitution model and 1000 bootstrap replicates.

In the case of DGGE, the DGGE patterns were normalised using the software GelCompar II v.6.0 (Applied Maths, Belgium). During this processing, the different lanes and bands were defined and background was subtracted. A cluster analysis was created based on the presence and absence of bands in the community profile, creating a dendogram diagram. Distance was calculated using the Jaccard algorithm (Jaccard, 1908).

Chapter 4: Effect of Water-Rock Ratios on Basalt Weathering by *Acidithiobacillus ferrooxidans*

4.1. Introduction

4.1.1. Aim of Chapter

The aim of this chapter is to focus on the effect of changing water-rock ratios on weathering of basalt by the bacterium *Acidithiobacillus ferrooxidans*. *A. ferrooxidans* is a well characterised acidophilic iron-oxidiser. This work has implications for the rates of rock weathering in natural environments where water-rock ratios may affect the balance between optimum energy and nutrient supply, as for example in the case of microorganisms in vesiculated basalt (low water-rock ratio) and acid mine drainage sites (high water-rock ratio). Water-rock ratio effects may contribute to differences in laboratory and field measured weathering rates. From an astrobiological perspective, this work has implications for micro-scale conditions for habitability in basaltic environments on Mars, where low water-rock ratios have been postulated to be present in combination with acidic conditions. Such conditions may also have existed in geothermal regions on the Archaean Earth.

The hypothesis to be tested was that a high ratio of water to rock would have a diluting effect, diluting the iron as soon as it is released and thus limiting its supply. At the other extreme, a low water-rock ratio would cause the acid in the media to be quickly quenched by protons being used up in reactions with the rock, raising pH above optimum for bacterial growth. However, a ratio between the two would strike a balance between optimum iron concentration and pH. Though this study predominantly looked

at the iron utilisation from the basalt by the bacteria, since they require iron as a source of energy, the release and use of other elements was also investigated.

4.1.2. Iron-oxidising bacteria and weathering

Iron is the fourth most abundant element in the Earth's crust (5.63 %) (Taylor, 1964). On Earth's surface, it exists naturally as metal and in two oxidation states: ferrous (Fe^{2+}) and ferric (Fe^{3+}) (Madigan and Martinko, 2005). In nature, the oxidation of Fe^{2+} occurs both chemically and as a form of chemolithotrophic metabolism (Madigan and Martinko, 2005). Under oxidising conditions, Fe-oxidising bacteria and archaea can utilise reduced iron as an electron donor in energy generation (Santelli *et al.*, 2001) according to the reaction:

$$Fe^{2+} + ¼\ O_2 + H^+ \rightarrow Fe^{3+} + ½\ H_2O \qquad \textit{Equation 4.1}$$

It is known that ferrous oxidation by *A. ferrooxidans* rapidly decreases at pH greater than 2.5 (Nakamura *et al.*, 1986; Pesic *et al.*, 1989; Kupka and Kupsáková, 1999). In most reports of ferrous oxidation by acidophiles, bacterial catalysis is significant only up to pH ~3.5 (MacDonald and Clark, 1970; Pesic *et al.*, 1989; Kupka and Kupsáková, 1999). At neutral pH and under fully aerated conditions, Fe^{2+} rapidly oxidises to Fe^{3+}, which then hydrolyses to form ferric hydroxide (Konhauser, 2007). The kinetic relationship that describes chemical Fe^{2+} oxidation at circumneutral pH values is:

$$-d[Fe(II)] / dt = k[Fe(II)][OH^-]^2[O_2] \qquad \textit{Equation 4.2}$$

Where $k = 8\ (\pm\ 2.5) \times 10^{13}\ min^{-1}\ atm^{-1}\ mol^{-2}\ l^{-2}$ at 25°C (Singer and Stumm, 1970). As pH and oxygen availability have strong influences on the reaction rate, this explains why at low pH or low oxygen concentrations Fe^{2+} is quite stable (e.g., Liang *et al.*, 1993). Thus, not surprisingly, the most efficient way for a microbe to overcome the

stability limitations is to either grow under acidic conditions (as an acidophile) or under low oxygen concentrations at circumneutral pH (as a microaerophile) (Konhauser, 2007).

4.1.3. *A. ferrooxidans*

The bacterium *A. ferrooxidans*, reclassified in 2000 from *Thiobacillus ferrooxidans* (Kelly and Wood, 2000), is an acidophilic iron- and sulphur-oxidiser that converts Fe^{2+} to Fe^{3+}. When iron oxidising bacteria such as *A. ferrooxidans* are present under acidic conditions, the oxidation of a wide range of sulphide minerals (Lawrence *et al.*, 1997) can be 10^6 times faster than the abiotic rate (Singer and Stumm, 1970).

A. ferrooxidans is not 100 % efficient in its use of energy from iron oxidation. Baas *et al.* (1927) calculated the ΔG (change in free energy) for iron oxidation to be around 10 kCal mol^{-1}. Lees *et al.* (1969) determined the free energy yield from this oxidation to be closer to 6.4 kCal mol^{-1}, a value which is barely enough to synthesise 1 mol of ATP (Leduc and Ferroni, 1994). Approximately 18.5 mol of Fe^{2+} would have to be oxidised to assimilate 1 mol of carbon, the assumption being that it requires 120 kCal of energy to fix this much carbon at 100 % efficiency (Silverman and Lundgren, 1959; Leduc and Ferroni, 1994). Efficiency values as low as 3.2 % (Temple and Colmer, 1951) to as high as 30 % (Lyalikova, 1958) have been reported. Thus, the bacteria must oxidise a large amount of Fe^{2+} in order to grow, and even a small number of bacteria can be responsible for generating significant concentrations of dissolved Fe^{3+}.

A. ferrooxidans is traditionally regarded as a mesophilic microorganism, with a minimum temperature growth near 15°C, an optimum around 30°C, and a maximum of approximately 37°C (Leduc and Ferroni, 1994). However, psychrotrophic strains of this bacterium have been isolated with a growth range on iron of 2-37°C (Leduc *et al.*,

1993; Leduc and Ferroni, 1994). They are also able to grow anaerobically, with ferric ions as electron acceptors for the oxidation of reduced sulphur compounds (Pronk *et al.*, 1992; Singleton and Sainsbury, 2006).

The bacterium has been generally regarded as a strict acidophile (Madigan and Martinko, 2005), its optimum pH range generally given between 1.5 and 2. However, there are varying reports on its pH range. Temple and Colmer (1951) described their isolate as growing well in the pH range of 2.0-2.5 (Leduc and Ferroni, 1994; Temple and Colmer, 1951). However, in 1959, the bacterium was shown to oxidise iron optimally in the pH range 3.0-3.6 (Leduc and Ferroni, 1994; Silverman and Lundgren, 1959). Another strain of the bacterium was shown to oxidise iron optimally at pH 1.6 (Landesman *et al.*, 1966; Leduc and Ferroni, 1994). It is now generally agreed that the optimal growth and iron oxidation for *A. ferrooxidans* occurs at approximately pH 2 (Leduc and Ferroni, 1994), and the bacterium has a range of 1.5 to 6, with variations in the literature resulting from the differences in strain composition and experimental conditions (Leduc and Ferroni, 1994). However, a recent study by Mielke *et al.* (2003) reported survival of *A. ferrooxidans* at pH 7, and an ability to initiate pyrite oxidation and localised acidification within two weeks of colonisation. Essentially an acidic nanoenvironment is developed between the bacteria and the pyrite mineral surface (Mielke *et al.*, 2003). Meruane and Vargas (2003) also reported ferrous oxidation at pH 7 for *A. ferrooxidans*.

4.1.4. The Wider Picture: Implications and Use

Gaining a better understanding on microbial weathering, specifically on how water-rock ratios affect it, has implications in two main areas: environmentally and astrobiology

4.1.4.1. Environment: Acid Mine Drainage

Environmentally, the work on microbial weathering can help one understand the rates of weathering in natural environments, for example in acid mine drainage sites. In these environments, a balance between optimum energy, nutrient supply and pH occurs. Although such sites are not generated through weathering of basalts, they are environments with a low water-rock ratio, hence understanding the influence of water-rock ratios on weathering by *A. ferrooxidans* may be important in understanding the fundamental mechanisms of acid mine drainage.

Acid mine drainage (AMD) refers to the outflow of acidic water from usually abandoned metal or coal mines, producing scenes such as the Rio Tinto River in Spain (Figure 4.1). AMD is produced when pyrite is oxidised on exposure to oxygen and water to form ferric hydroxides and sulphuric acid (Soucek *et al.*, 2000). The acid runs off into clean rivers, which dissolves heavy metals, contaminating surface and ground water and damaging the surrounding ecosystems, (Roback and Richardson, 1969; Soucek *et al.*, 2000; Madigan and Martinko, 2005). It has been suggested that microbial activity accounts for about 75% of the AMD produced (Edwards *et al.*, 2000; Baker and Banfield, 2003).

Figure 4.1. An example of acid mine drainage in the Rio Tinto River in Spain (Stoker, 2003).

4.1.4.2. Astrobiology: Life on Mars?

Through several paleoclimate models, it is known that early Mars was a wet and warm planet, similar to early Earth, before losing its atmosphere and becoming a cold, dry planet (Hurowitz and McLennon, 2007; Hurowitz, 2008; Quinn *et al.*, 2005). From an astrobiology perspective, this work has implications for microbial habitability in basalt environments on Mars, where low water-rock ratios have been postulated to be present with acidic conditions (Hurowitz, 2008). From chemical and mineralogical composition of rocks and soils from the sites where landed missions (Viking, Pathfinder, MER) have operated on Mars and modelling and experimental studies, it has been suggested that water-limited, acidic weathering conditions have more than likely been the defining characteristic of the Martian aqueous environment for billions of years (Hurowitz, 2008). If bacteria were to survive in acidic, low water-rock ratio experiments, this could prove promising in terms of life having been or currently residing on Mars. Through understanding the influence of water-rock ratios on microbial weathering it may be possible to postulate suitable sites that would or could

have sustained life. Would rock vesicles be the place to look? River beds? Or impact craters?

4.2. Experimental design

4.2.1. Chapter 4: *Acidithiobacillus ferrooxidans*

4.2.1.1. Overview

The objective of this chapter was to gain a better understanding of the processes by which *A. ferrooxidans* weathers basalt, and how this may (or may not) be affected by water-rock ratios. What follows is a detailed description of how the experiments were set up, from the preparation of the basalt to setting up the flasks. Table 4.1 summarises the experiments carried out in this chapter and their measurements and sampling frequencies.

Table 4.1. An overview of the experiments carried out in Chapter 4, including the measurements and sampling frequencies.

Experiment	Measurements	Sampling frequency
Preliminary: Choosing culture media strength	Ferrozine assay and cell counts	Four points over 14 days
Preliminary: Effect of three water-rock ratios on pH	pH	Seven points over 120 hrs
Experiment 1: Effect of water-rock ratios on *A. ferrooxidans*	Cell counts, Ferrozine assay, pH, elemental analysis, SEM, XANES analysis	Eight points over 37 days
Experiment 2: Effect of water-rock ratios on *A. ferrooxidans*	Cell counts, Ferrozine assay, pH, elemental analysis, SEM	Five points over 43 days

Side experiment: pH tolerance	Ferrozine assay	Per day over eight days
Side experiment: heavy metal tolerance	Ferrozine assay	Five points over eight days

4.2.1.2. Experimental set up

The aim of this chapter was to look at the effect of changing water-rock ratios on weathering by *A. ferrooxidans*. The setup of the experiment was as follows:

1. Preparation of the rock.
2. A stock *A. ferrooxidans* culture started to inoculate the experimental flasks.
3. After one week of growth, the cell count was determined in the stock.
4. The stock was prepared for addition to experimental flasks.
5. Experimental flasks were set up with differing ratios of media to basalt, and biological flasks were incubated with *A. ferrooxidans*.

The flasks were incubated stationary, at 29 °C, for 37 days.

4.2.1.2.1. A. ferrooxidans *preparation*

A stock culture of *A. ferrooxidans* was grown up in 1/100th strength modified K9 media. A sterile 250 ml conical flask was used, with a 1:1 ratio of Solution A_{low} and B (75 ml each). The stock was inoculated with 2 ml of a previous *A. ferrooxidans* culture and incubated stationary at 29 °C for one week.

4.2.1.2.2. Flask preparation (water-rock ratio batch cultures)

Three water-rock ratios were chosen for the experiment, as described in Table 4.2. Solution A_{low} was made up and sterilised by autoclaving, whilst the basalt was prepared as described in Chapter 3.

Table 4.2. The water-rock ratios used in the experiments.

Ratio	Basalt (g)	Solution A_{low} (ml)
High (400:1)	2.001	800
Medium (50:1)	2.004	100
Low (1:1)	50.010	50

Polycarbonate conical flasks were used instead of glass to prevent any possible leaching of elements from the flasks because of the acidic pH of the media, and thus affecting results. Each condition was carried out in duplicate, and controls were also run alongside (no bacteria added). Figure 4.2 summarises the experimental set up of the flasks. Figure 4.3 shows photographs taken of the medium water-rock and low water-rock flasks when both rock and media were added. With regards to the low water-rock ratio, the liquid completely covered the rocks. In addition to the chips of basalt, two polished thin pieces (approx. 0.5 by 0.5 by 0.1 cm) of basalt were added to each flask. These would be removed at the end of the experiment and used for SEM observation (to observe any changes in surface morphology of the basalt) and XANES analysis. The addition of the polished rocks may bring up the question of whether this would affect the water-rock ratios. As the polished pieces were added to all flasks, including the controls, no flask would have had its conditions changed more than any other flask. The polished pieces were relatively small, but we can calculate their contribution to the

overall active surface area available for reaction, assuming they have the same surface area characteristics (as measured by BET) as the rock chips:

Assuming the active area = 0.56 $m^2 g^{-1}$ (BET results)

For the polished section:

Volume = 0.5 × 0.5 × 0.1 cm^3

Volume = 0.025 cm^3 and Density = 3 g cm^{-3}

Mass = 0.075 g

Surface area = 0.56 $m^2 g^{-1}$ × 0.075 g = <u>0.042 m^2</u>

For the rock chips:

Mass = 50 g

Surface area = 0.56 $m^2 g^{-1}$ × 50 g = <u>28 m^2</u>

Polished section accounts for:

(0.042 m^2 / 28 m^2) × 100 % = <u>0.15 % of the total active surface area.</u>

However, if these experiments were to be repeated, one should run parallel flasks with no polished pieces (but have the identical weight to volume ratio) to ascertain whether the addition of the polished pieces would have made a difference.

4.2.1.2.3. Adding A. ferrooxidans

In tandem with preparing the flasks, the stock culture of *A. ferrooxidans* was being prepared for addition to the biological flasks. First, the cell count in the flasks was determined using fluorescence microscopy (Chapter 3, Section 3.3.1). From the cell counts, it was determined that the number of cells in each flask would be 3.07 × 10^4

cells per ml. This ensured that each flask would have the same number of cells per ml regardless of media volume.

The stock culture was filtered onto a polycarbonate membrane filter 25 mm in diameter and with a pore size of 0.2 μm (Whatman, Fisher Scientific) and washed with Solution A_{low} twice. This was to remove any iron sulphate from the bacteria and the solution so as not to introduce iron into the experimental flasks; the only iron available should be from the basalt. The filter with the cells was then resuspended in fresh Solution A_{low} and mixed thoroughly. The resuspended bacteria were then added to each flask in the required volume. The flasks were incubated stationary at 29 °C.

4.2.1.2.4. Sampling and data analysis

The flasks were sampled over 37 days. Aliquots of 4 ml were collected with sterile pipettes. One ml of the sample was used to measure concentrations of Fe^{2+} and total Fe^{3+} using the ferrozine assay; 1 ml for pH measurements; and 2% nitric acid was added to the final two ml for ICP-MS (and ICP-AES for the second experiment) analysis and stored at 4°C until use at a later date. Cell counts were performed at the start and end of the experiment, when one ml was removed for fluorescence microscopy. In addition, at the end of the experiment the polished pieces of basalt were removed and viewed under FEG-SEM and for XANES analysis.

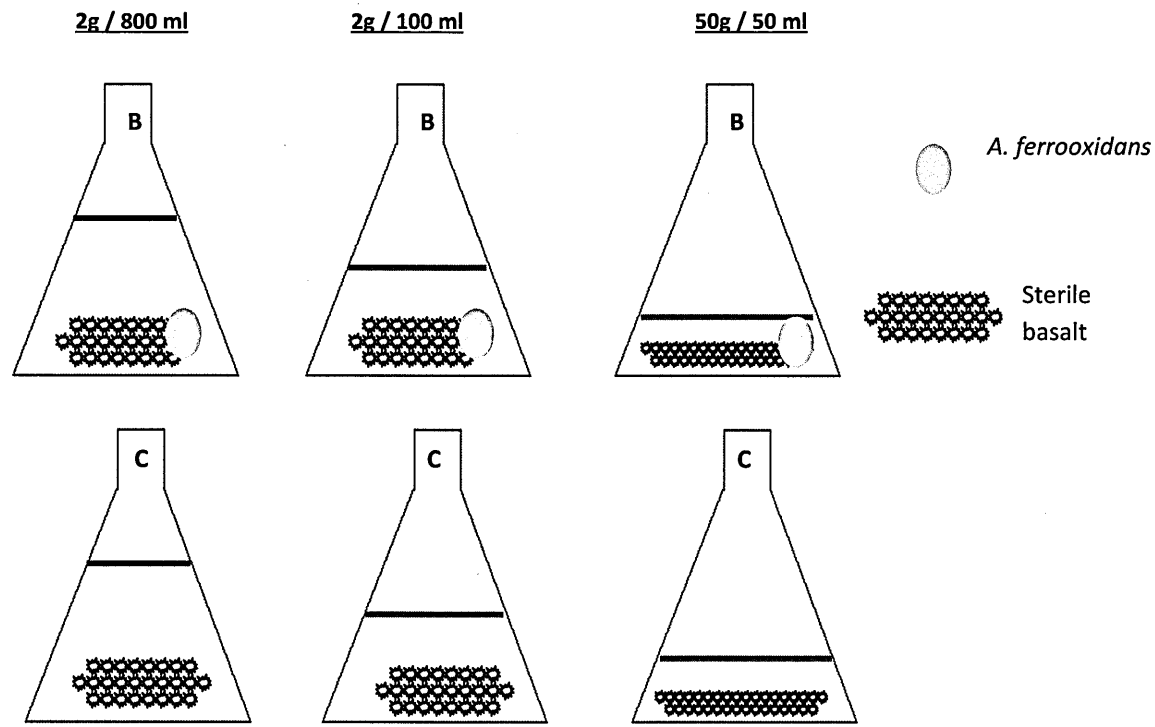

Figure 4.2. An overview of the experimental set up of the flasks for Experiment 1 and 2. The diagram shows the three different ratios used (high: 2 g in 800 ml; medium: 2 g in 100 ml; low: 50 g in 50 ml). The letter 'B' denotes the biological flasks (inoculated with *A. ferrooxidans*), and 'C' the controls (only sterile rock added).

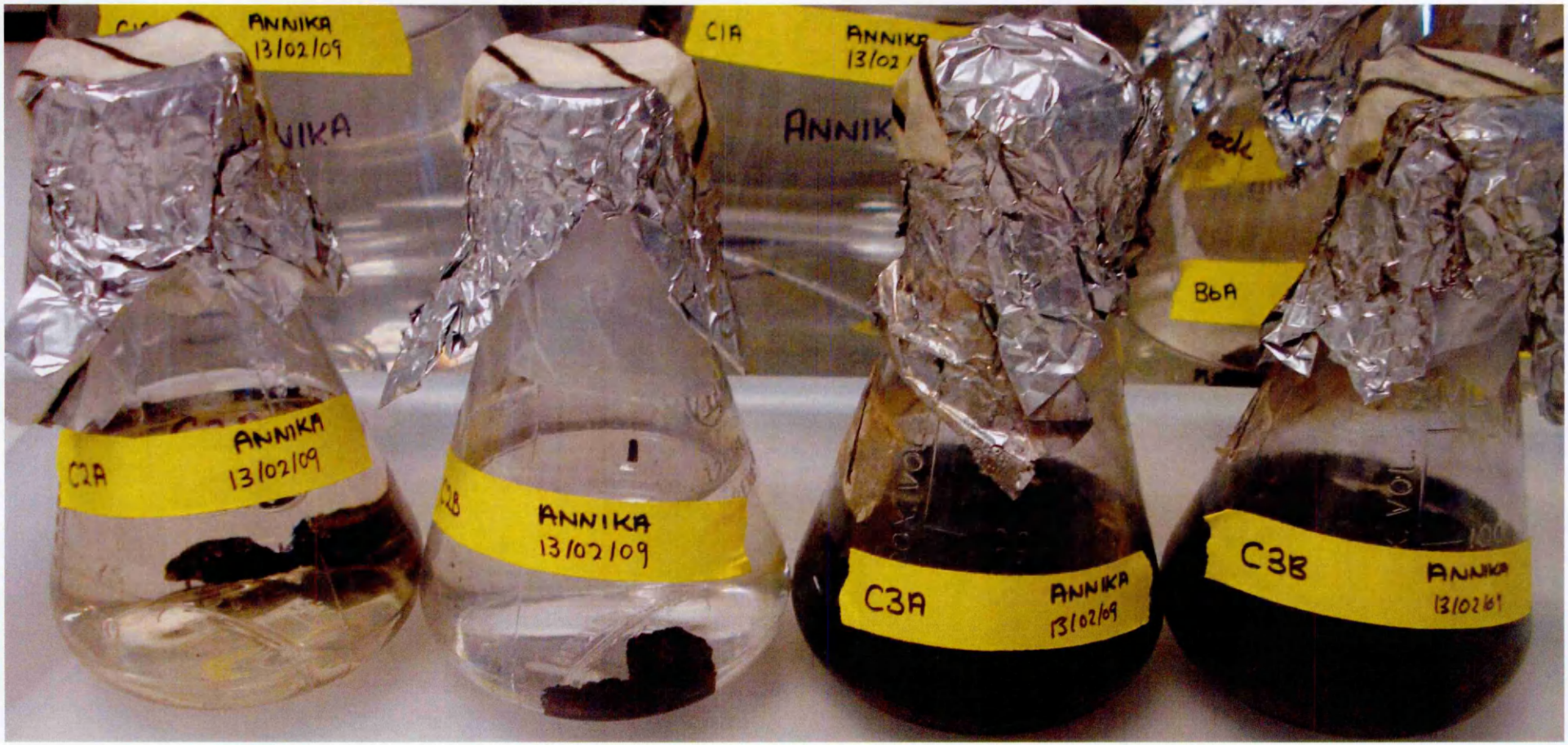

Figure 4.3. Photographs of medium (left) and low (right) water-rock ratio flasks, with basalt and media added.

4.2.1.3. Second experiment

After the experiment was completed and data collected and analysed, the experiment was repeated to determine if the results could be reproduced. The experiment set up was as before, with one exception. The low ratio this time round had its starting pH raised from 1.5 to 3.5 using NaOH. The reason for this was to ascertain whether a higher starting pH in the low ratio affected the rate of iron oxidation at the beginning of the experiment.

XANES analysis was not carried out on the second experiment; however, ICP-AES analysis was, in conjunction with ICP-MS.

4.2.1.4. Tolerance experiments

The pH and heavy metal tolerance of *A. ferrooxidans* was tested. Table 4.3 outlines the different conditions set up.

For the heavy metal tolerance tests, concentrations were based on ICP-MS data obtained on the basalt. Table 4.4 lists the heavy metals added to Sol A_{low} and the concentrations tested. The concentrations were as found in the rock. Untreated flasks were also set up. Fifty ml of media and heavy metals were added to 100 ml flasks and 1 ml of *A. ferrooxidans* inoculum was also added. The Ferrozine assay was used to measure iron concentrations, which would give an indication if heavy metals would affect iron oxidation (which would indicate whether the bacteria were affected).

The pH tolerance of the bacteria was determined by growing them on Sol A_{low} media that had been adjusted to the required pH with HCl or NaOH. As with the heavy metal tests, 1 ml of inoculum was added to 50 ml of media, and the iron concentrations were monitored using the Ferrozine assay.

Table 4.3. Set up of pH and heavy metal tolerance experiments. Flasks were in duplicate, set up with 50 ml Sol A_{low} media and 1 ml *A. ferrooxidans* inoculum. Controls were also set up (no bacteria added). The composition of the heavy metal mixtures are shown in Table 4.4.

Flask	Tolerance	Concentration
Condition 1	Heavy metals	Basalt
Condition 2	Untreated	-
Condition 3	pH 1	-
Condition 4	pH 2.5	-
Condition 5	pH 3	-
Condition 6	pH 3.5	-
Condition 7	pH 4	-
Condition 8	Normal pH (pH 2)	-

Table 4.4. Heavy metal composition in heavy metal tolerance flasks. They are the concentrations as found in the basalt (from ICP-MS data).

Metal	Chemical form	Basalt concentration (mM)
Copper	$CuSO_4.5H_2O$	0.71
Cobalt	$CoSO_4.7H_2O$	0.62
Zinc	$ZnSO_4.7H_2O$	1.89
Chromium	K_2CrO_4	0.18
Nickel	$NiSO_4.6\ H_2O$	0.25
Lead	$Pb(NO_3)_2$	0.01
Vanadium	$VOSO_4$	4.98
Tin	$SnCl_2$	9.69×10^{-3}
Molybdenum	Na_2MoO_4	0.02
Manganese	$MnSO_4.H_2O$	35.00

4.3. Results

4.3.1. Preliminary experiments

Preliminary experiments were carried out to ascertain the best media concentration to use (with minimal or no precipitation without affecting the bacteria), and what ratios would give a range of pH changes. To determine the media strength, Fe^{2+} concentrations and cell counts were analysed. Figure 4.4 shows Fe^{2+} at three different Sol A strengths (normal, $1/10^{th}$, and $1/100^{th}$). Fe^{2+} concentrations were different between the biological experiments and controls (abiotic oxidation of $FeSO_4$). However, in terms of media strength, iron oxidation by *A. ferrooxidans* did not appear to be affected by the concentration of Sol A. Precipitation was noted in both the normal strength and $1/10^{th}$ concentration, when basalt was added to the media, however, none was observed in the $1/100^{th}$ media (Sol A_{low}).

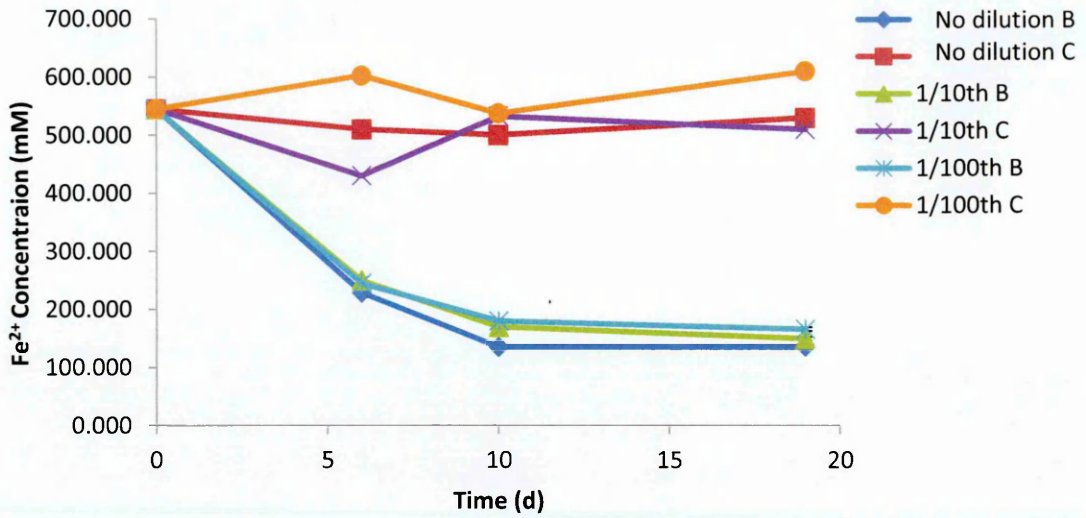

Figure 4.4. Effect of Sol A concentration on oxidation of $FeSO_4$ by *A. ferrooxidans,* over time. 'B' denotes biological flasks (bacteria added) and 'C' denotes controls. The volume of liquid available limited the amount of sampling, thus only four sampling points on the graph.

Cell counts (Figure 4.5) also show that decreasing the concentration of Sol A was not detrimental to cell numbers. From these results, a Sol A_{low} was decided upon for the main experiment – the concentration did not produce precipitation and it did not adversely affect the bacteria.

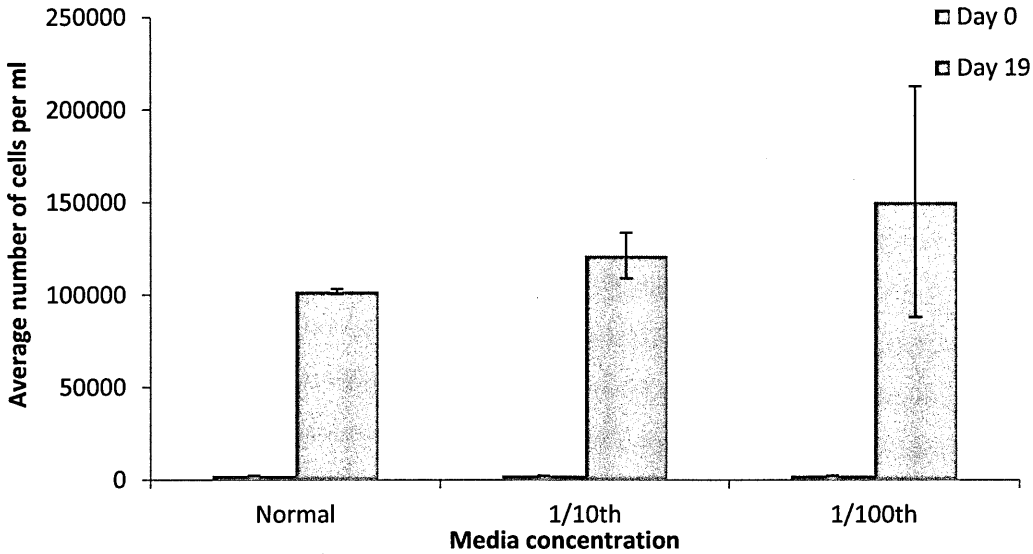

Figure 4.5. Average number of cells per ml at day 0 and day 19 with different Sol A concentrations.

Figure 4.6 shows how pH changed over time with the three different ratios. The aim of this preliminary experiment was to determine suitable ratios for the main experiment, specifically for the low ratio. A ratio was wanted that would raise the pH by two or more orders of magnitude to provide an environment where quenching of protons would occur. From adding basalt to varying volumes of Sol A_{low}, a 2 g in 2 ml set up raised the pH from 1.75 to nearly pH 4 in ten hours. A 2 g in 100 ml raised pH from pH 1.75 to pH1.84 after 120 hours. A 1:1 ratio was decided for the low ratio (50 g in 50 ml), whilst the medium ratio had 2 g in 100 ml (1:50), and the high ratio had 2 g in 800 ml (1:400). The large volume of media for the high ratio was also chosen to mimic the more dilute environment of a river bed, and thus possibly limiting iron to the bacteria through its diluting effect.

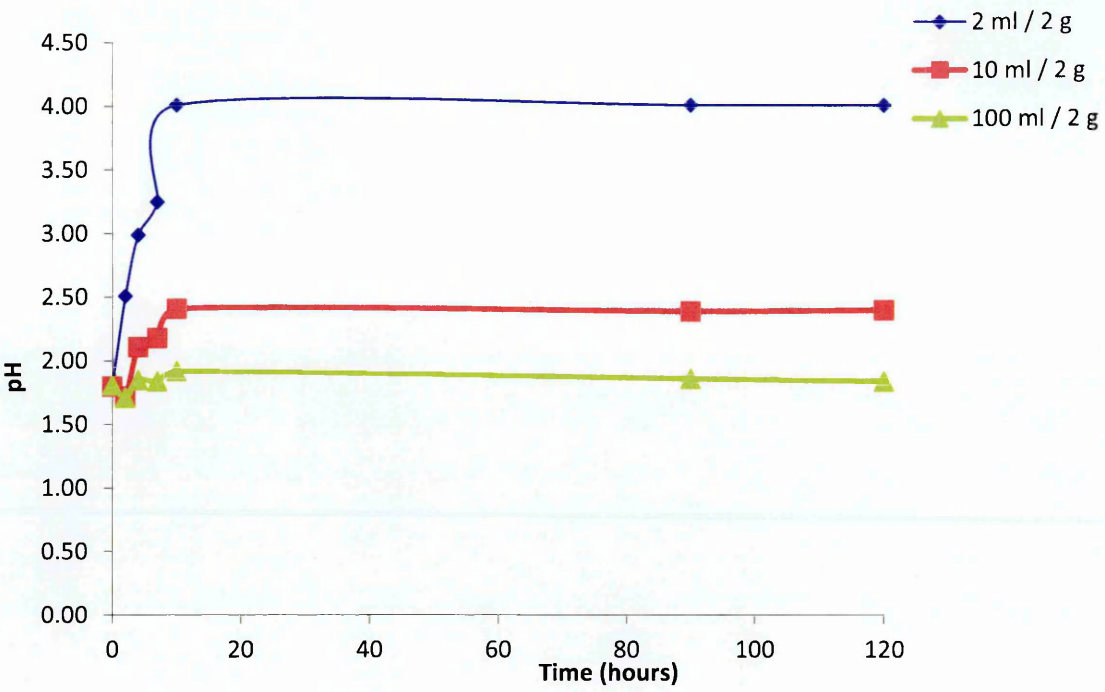

Figure 4.6. Effect of three different ratios on the pH of Sol A_{low}.

4.3.2. Experiment 1

Experiment 1 was the first experiment looking at how *A. ferrooxidans* was affected by varying water-rock ratios and how this would affect weathering. Experiment 2 repeated Experiment 1 for the most part to ascertain whether the main results could be replicated. This section describes the results from Experiment 1.

4.3.2.1. pH and cell counts

The change in pH over time with the different water-rock ratios is shown in Figure 4.7. The starting pH of the media is around pH 1.5. In all three water-rock ratios the pH rose, however, to different degrees depending on the ratio. The high ratio only rose slightly in pH over the course of the experiment, from pH 1.5 to 1.77. The medium ratio rose to 2.86 and 2.39 in the control and biological experiment, respectively.

However, the low ratio showed the largest increase in pH, from 1.5 to 3.88, over three times as much. The pH in the low ratio tripled in the first 24 hours before stabilising. A similar trend was seen in the high and medium ratios; however, they continued increasing over 24 days. Between 0 and 7 days there was a degree of oscillation in pH for the medium and high ratios. The pH rose over the first day before dropping by the third day, and then rising again by the seventh day. This is addressed in the discussion (Section 4.4.1).

The biological experiment and abiotic controls were very similar in the high and low ratios, with error bars taken into account ($P > 0.05$). However, the medium control had a higher pH than its counterpart biological experiment ($P < 0.05$).

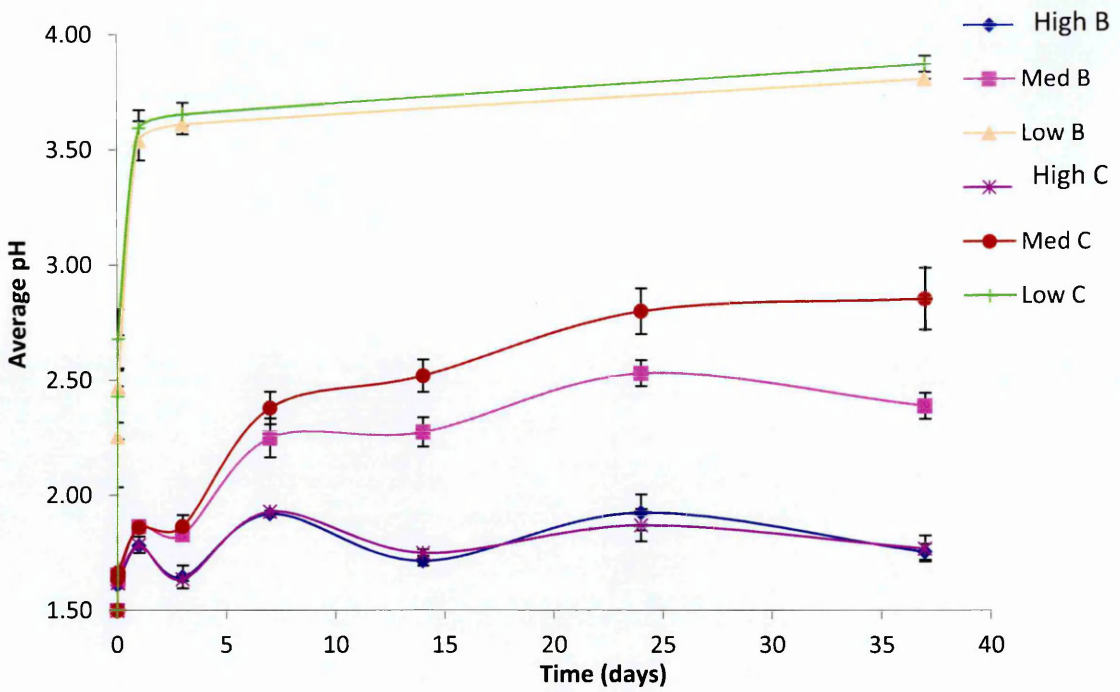

Figure 4.7. Experiment 1. The average pH over time for the three ratios, with *A. ferrooxidans* added and sterile conditions. In the legend, 'B' denotes biological flasks and 'C' control.

Cell counts (Table 4.5) showed that cell numbers were highest in the medium ratio on day 37 at 14,018 cells per ml, and lowest in the low ratio (635.5 cells per ml). Cell numbers decreased between day 0 and day 37 for all three ratios. SEM cell counts of cells on the rock surface are also shown in Table 3.5. As with the solution cell counts, the medium ratio had the highest number of cell counts, whilst no cells were observed on the surface of the low ratio rocks.

Table 4.5. Cell counts of cells in solution at day 0 and day 37 for the three water-rcok ratios (standard error 5%), alongside rock surface cell counts using SEM at day 37.

	Day 0	Day 37	SEM Day 37 (per 100 fields of view)
High	30700	1278	19
Medium	30700	14018	206
Low	30700	636	No cells

4.3.2.2. Elemental analysis

Elemental analysis in the form of Ferrozine assays and ICP-MS were performed on samples from Experiment 1. The average Fe^{2+} and Fe^{3+} released per gram of rock over time is shown in Figure 4.8. The high control had the largest amount of Fe^{2+} released per gram of rock, whilst the low ratio had the lowest release amount (Figure 4.8C). The biological experiment ratios did not show any Fe^{2+} being released. Fe^{3+} release showed a similar pattern, with the high control having the highest release, whilst the low ratio had the lowest.

Both high and medium controls had a similar pattern: Fe^{2+} concentration did not rise until day 4, after which it continued to increase to day 24 before plateauing. The low control did not rise until day 14, and by day 37 rate increase had reduced. In the case of Fe^{3+}, it began to rise by day 4 for Med B and Med C but then reached a plateau. No significant difference was observed between the medium biology and the control (*P*-value >0.05). In the case of the high biological flasks, Fe^{3+} concentration rose rapidly from 0 to just above 0.015 M between 25 and 37 days. For the low ratios, there was a

sharp rise in Fe^{3+} between 0 and 7 days before concentrations dropped to 0 for the rest of experiment. More Fe^{3+} was released in the biology than the control (approx. 5×10^{-5} compared to approx. 3.2×10^{-5}). This was a significant difference (P-value <0.05).

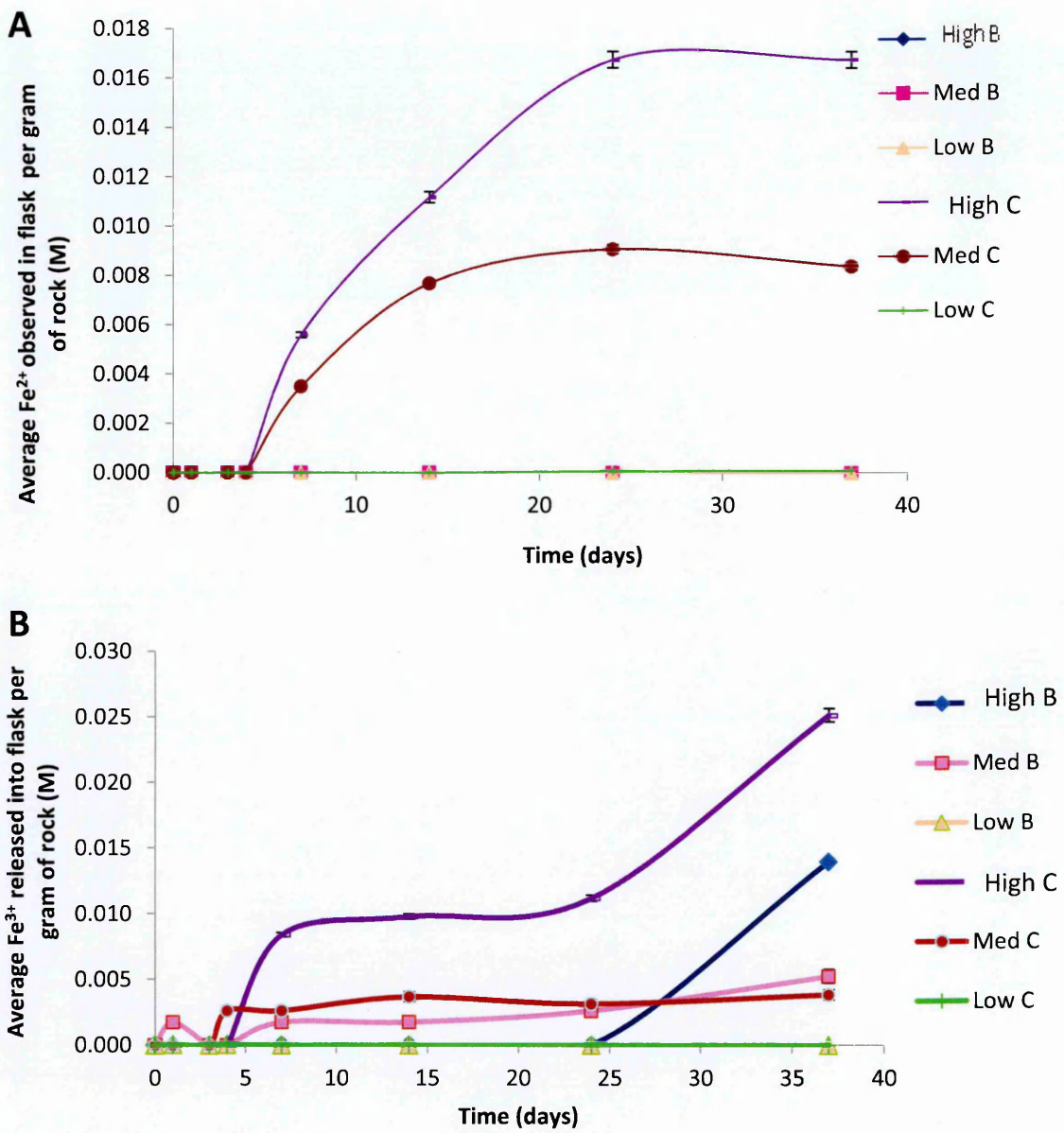

Figure 4.8 continued overleaf.

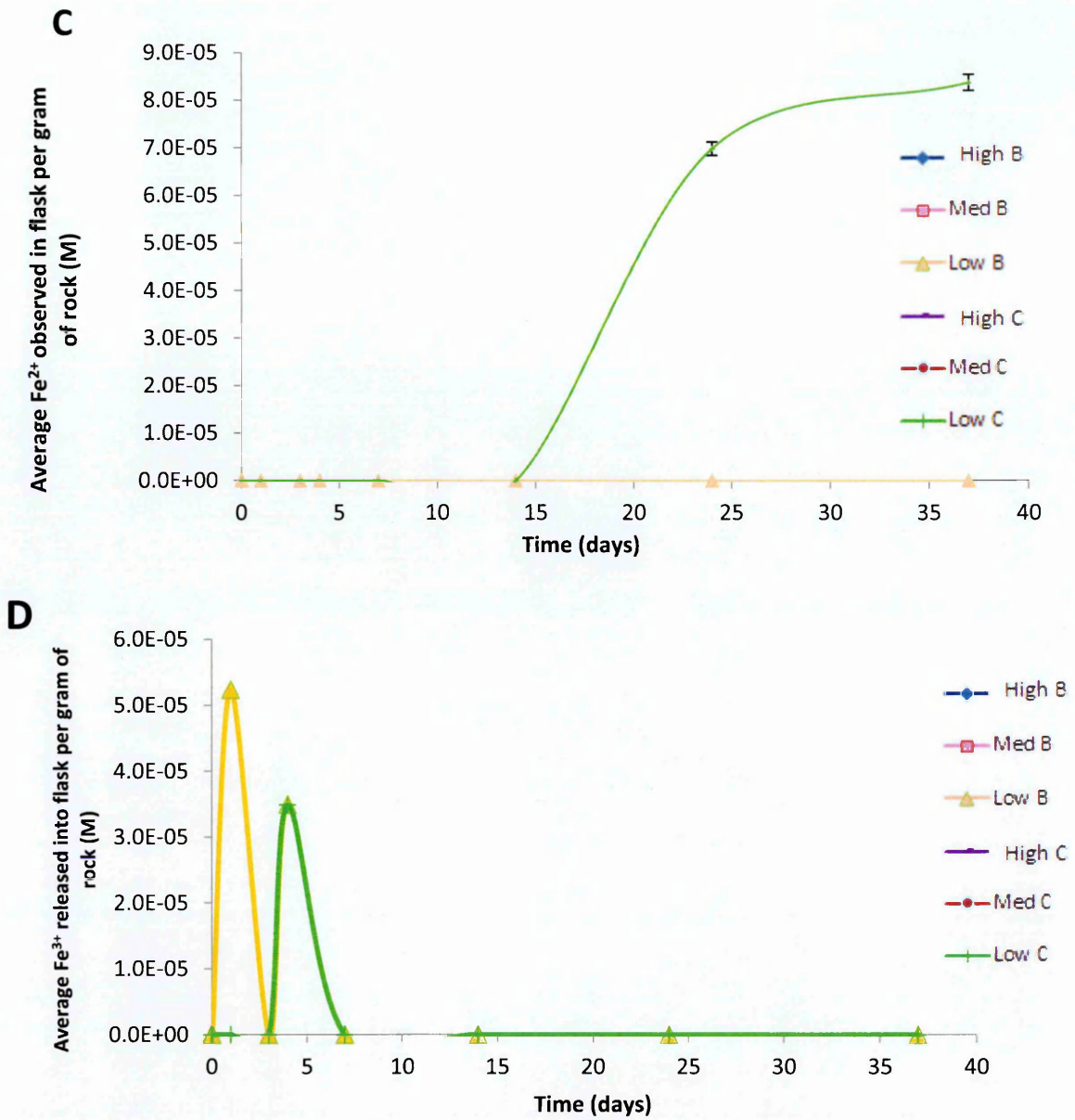

Figure 4.8. Experiment 1. Average Fe^{2+} and Fe^{3+} concentrations observed in flask per gram of rock in the three ratios. (A) Fe^{2+} for all ratios, (B) Fe^{3+} for all ratios, (C) Fe^{2+} for low biology and control, and (D) Fe^{3+} for low biology and control. In the legend, 'B' denotes biological flasks and 'C' control.

Figure 4.9 shows the concentration of the rare earth element (REE) Lutetium released per gram of rock. The pattern shown for this element is replicated by all REEs (data in Appendix). As in the case of Fe^{2+}, the high ratio had the highest amount released whilst

the low ratio had the lowest. The biological experiment showed an increased release over the control in the high ratio. However, T-test statistics show no significant difference between the biological experiment and control for both the medium and low ratios (P-value >0.05).

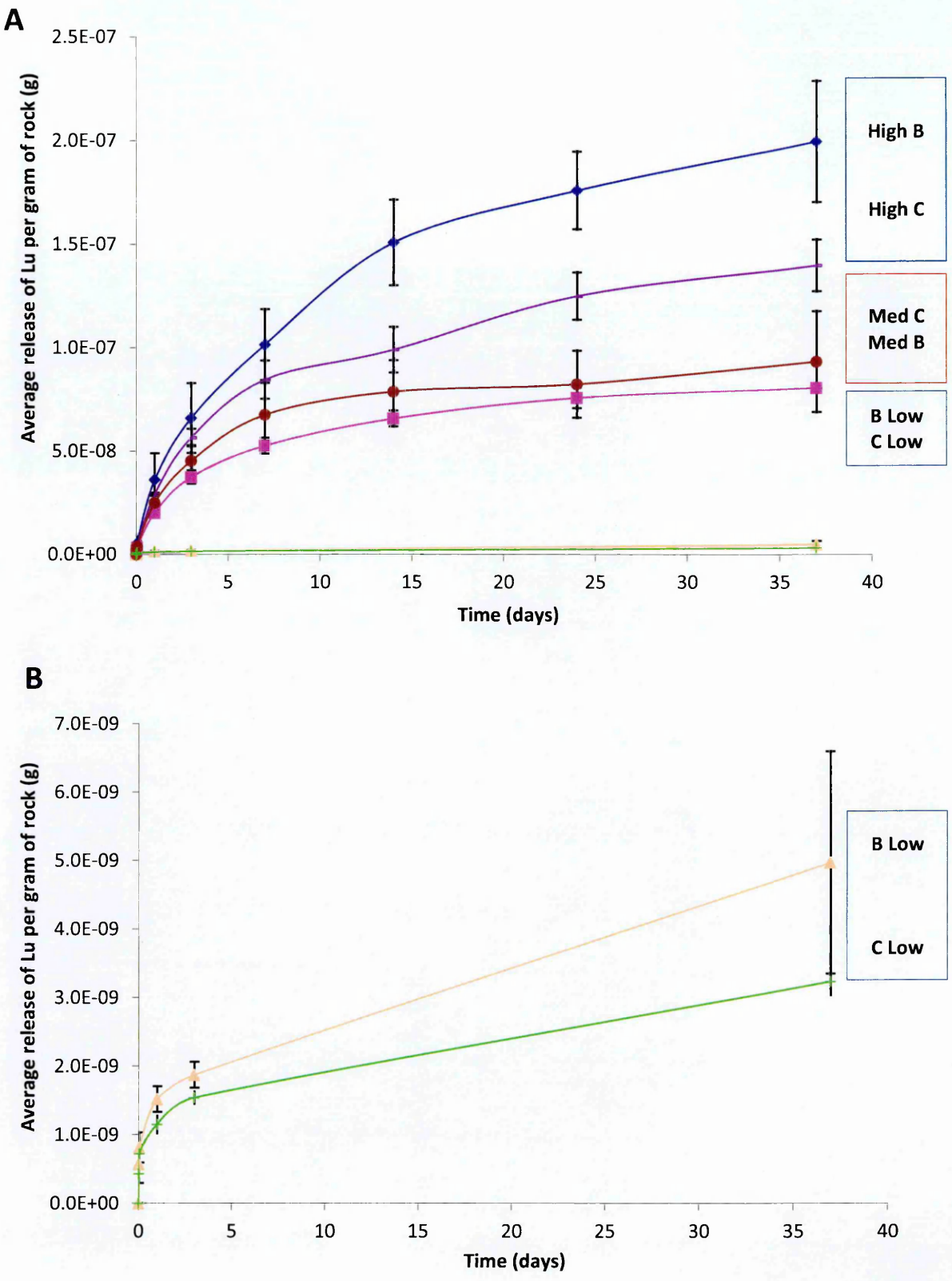

Figure 4.9. Experiment 1. The average release of REE Lu per gram of rock over time for (A) all ratios and for (B) the low ratio only. The trend for Lu is representative of all REEs. In the legend, 'B' denotes biological flasks and 'C' control.

4.3.2.3. XANES Analysis

Figure 4.10 shows X-ray absorption spectra (XAS) of the biological experiment and untreated basalt with control compounds. XAS showed localised areas of hematite, but the surface of the rock also showed iron oxidation without a change in gross mineralogy. An important observation is that the control rocks (in solution without organisms) also showed partial oxidation of the surface.

Figure 4.10 (overleaf). X-ray absorption spectra of the basalt from the three ratios with bacteria added and from untreated basalt (which had not been placed in media). Control compounds are also shown, and expected location of peaks corresponding to Fe^{2+} and Fe^{3+} are shown with dotted lines. In addition, example spectra are shown, including signatures for hematite, basalt glass and palagonite.

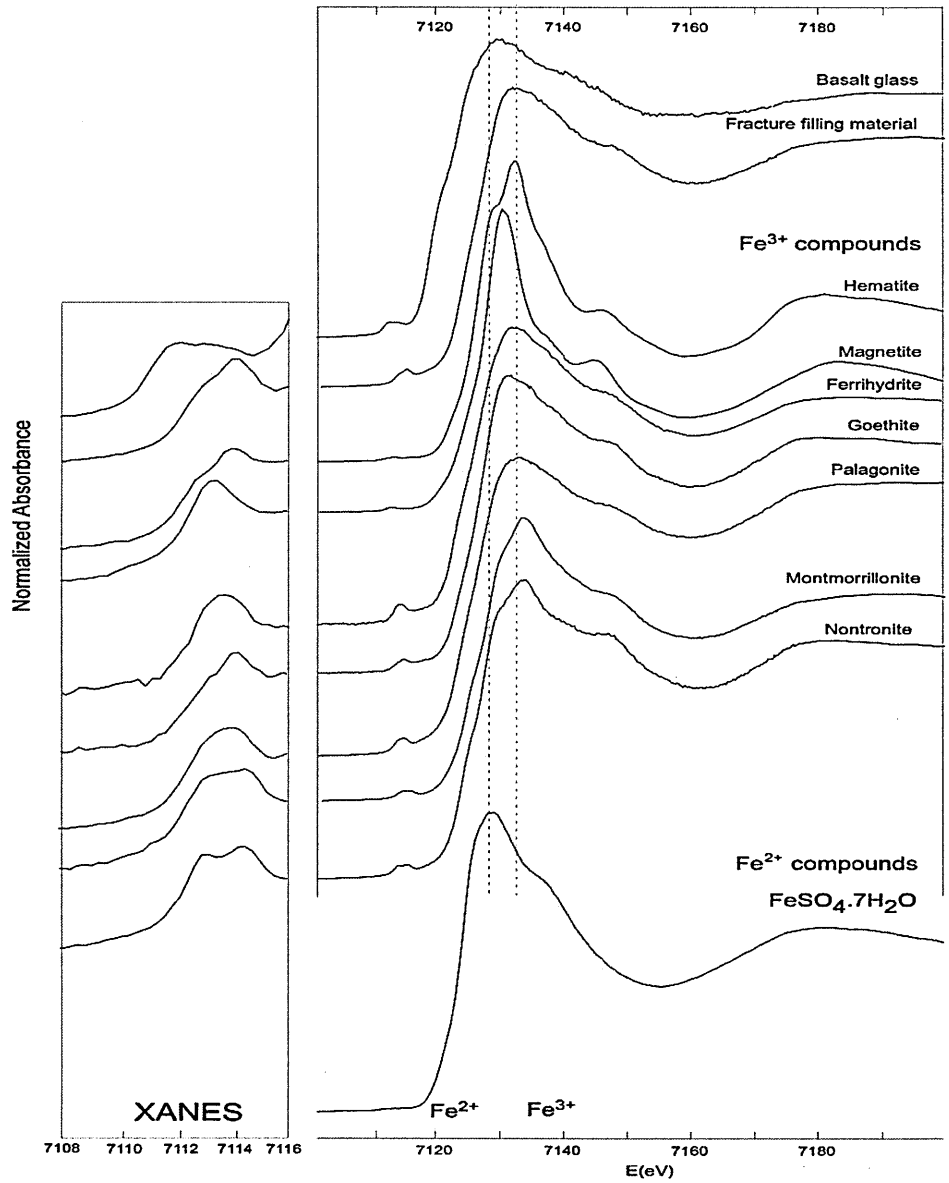
Normalized Absorbance
XANES
7108 7110 7112 7114 7116
7120 7140 7160 7180
Basalt glass
Fracture filling material
Fe3+ compounds
Hematite
Magnetite
Ferrihydrite
Goethite
Palagonite
Montmorrillonite
Nontronite
Fe2+ compounds
FeSO4.7H2O
Fe2+ Fe3+
7120 7140 7160 7180
E(eV)

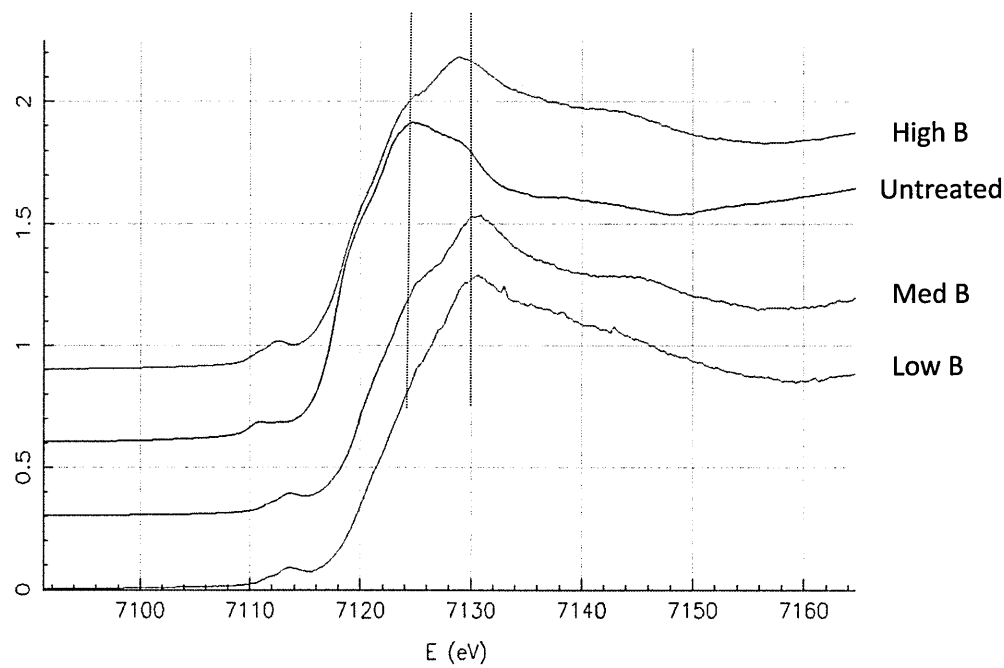
0 0.5 1 1.5 2
7100 7110 7120 7130 7140 7150 7160
E (eV)
High B
Untreated
Med B
Low B

4.3.2.4. SEM

Figure 4.11 shows a comparison of the rock surfaces of the three biological flasks and the high ratio control (representative of all controls). With regards to cell density in the biological experiment, numbers were sparse in the high ratio, whilst no cells were visible on the low ratio rock surface. Clumps of bacteria, however, were found in the medium ratio (Figure 4.11B). This trend corresponded with liquid cell numbers previously reported. As for surface morphology, it was relatively smooth for all except in the case of the medium biological experiment (Figure 4.12), where pitting on the surface was observed.

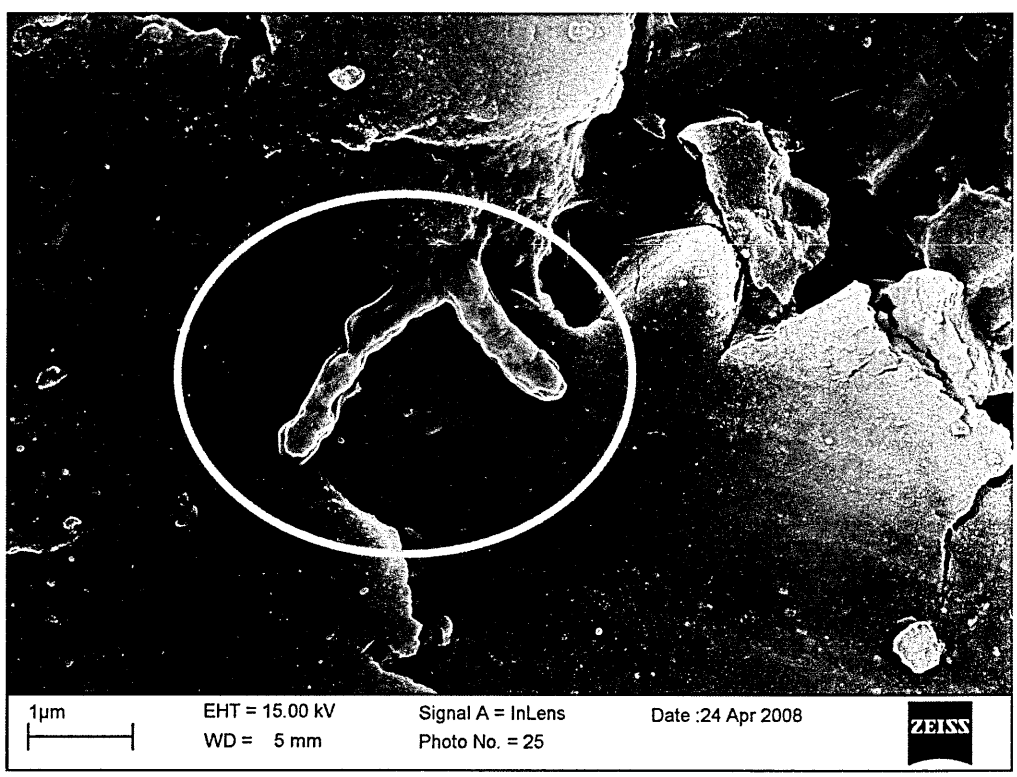

A

Figure 4.11 continued overleaf.

B

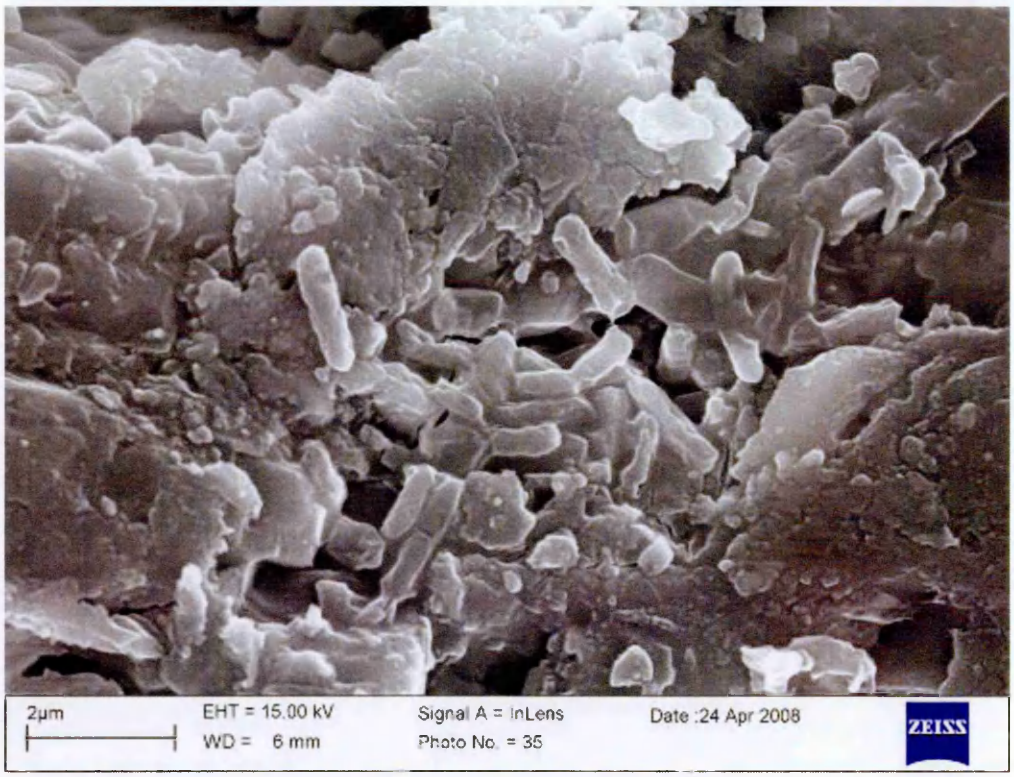

C

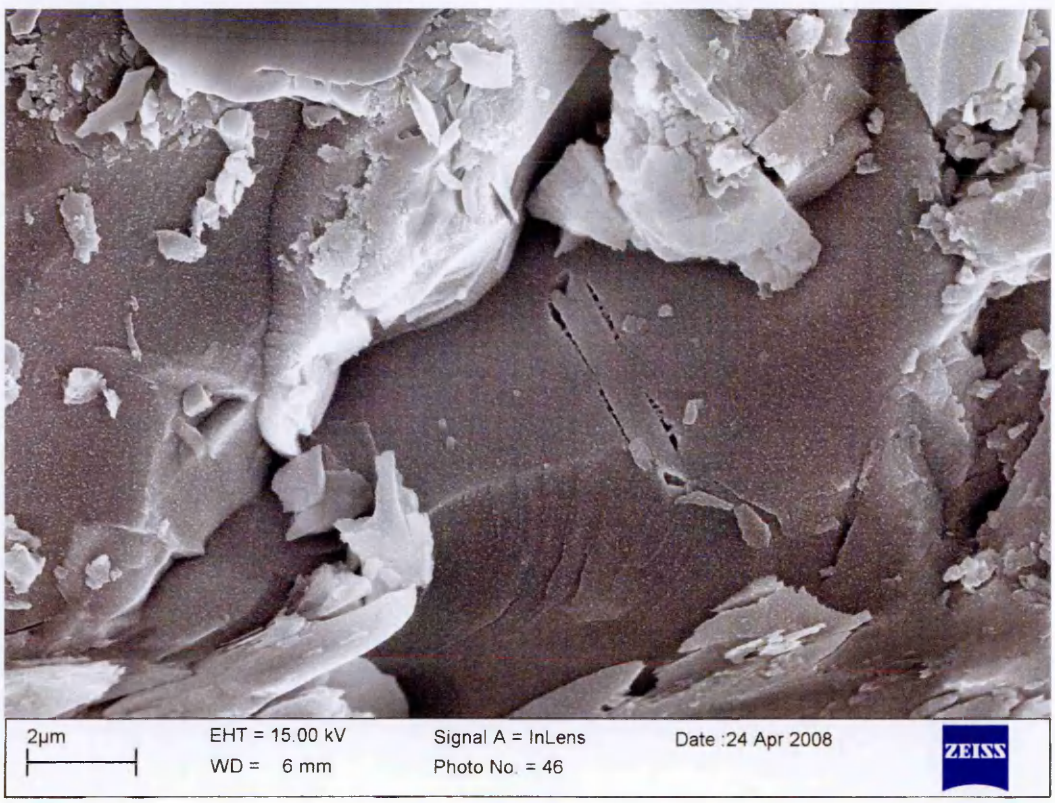

Figure 4.11 continued overleaf.

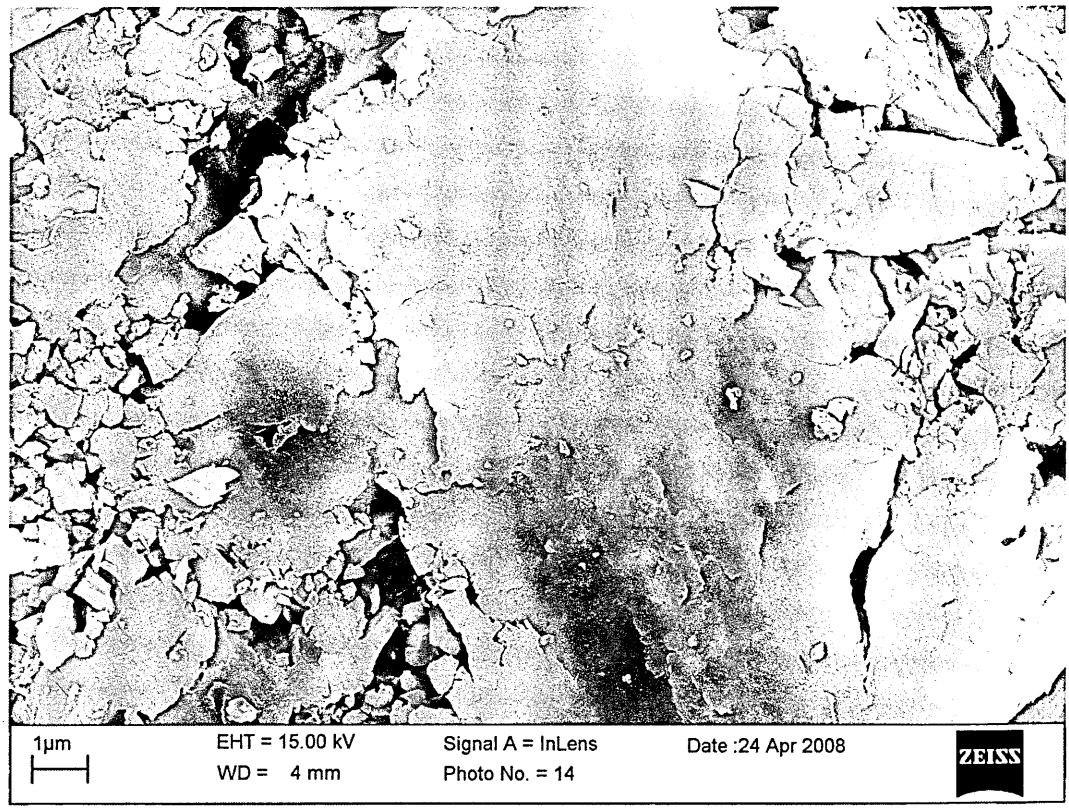

D

Figure 4.11. SEM comparison of the rock surfaces in the (A) High B water-rock ratio condition (three cells circled), (B) Med B, (C) Low B, and (D) High C, representative of all controls. Surface morphology was relatively smooth except for the biological medium water-rock ratio which had pitting.

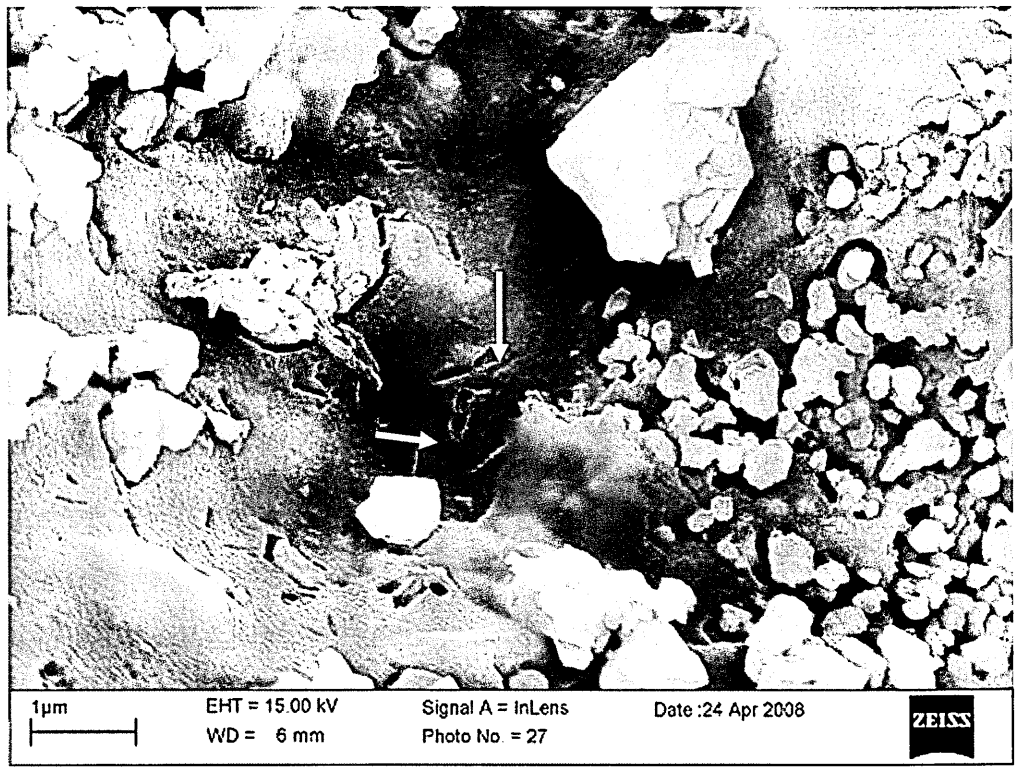

Figure 4.12. A SEM picture of the Med B rock surface with evident pitting (examples shown by arrows).

4.3.3. Experiment 2

Experiment 2 was a repeat of Experiment 1 for the most part in terms of conditions, except for the low ratio which had its starting pH increased to pH 3.50. The analysis involved pH and elemental analysis which are detailed in this section.

4.3.3.1. pH

As with Experiment 1, pH had the highest increase in the low ratio and the lowest in the high ratio (Figure 4.13). In the low ratio, the pH rose from 3.50 to 5.63 in the control and 5.04 in the biological experiment before plateauing for both. The pH was higher in the controls in the case of the medium and low ratios; however, the pH in the high ratio was similar between the biological experiment and control (the high ratio saw a rise

from pH 1.5 to approximately pH 1.75). This was seen in Experiment 1 as well. In all three ratios, pH increased over 6 days before stabilising.

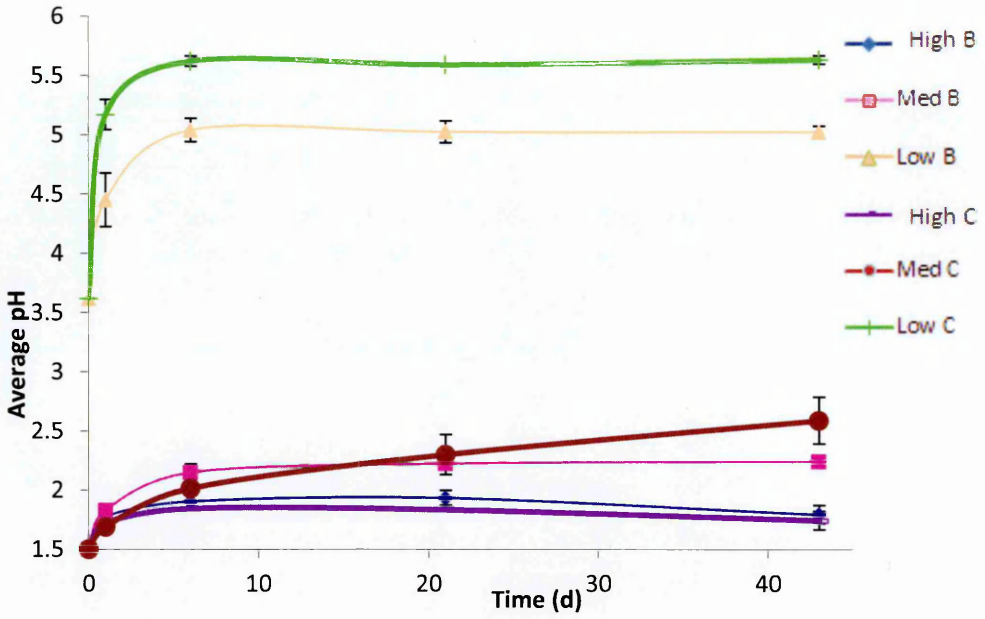

Figure 4.13. Experiment 2. The average pH over time in the three ratios, with *A. ferrooxidans* added and sterile conditions. In the legend, 'B' denotes biological flasks and 'C' control.

4.3.3.2. Elemental analysis

In a replication of Experiment 1 results, the high control had the largest amount of Fe^{2+} released per gram of rock (2.4 mM at 43 days) (Figure 4.14A). The low ratio (control and biological experiment) exhibited no release of Fe^{2+} when sampled. However, in contrast to Experiment 1, the high and medium biological experiment conditions had an increase in Fe^{2+} over 1 and 6 days, respectively (Figure 4.14B). In the case of Experiment 1, no Fe^{2+} was released. Both decreased after the increase, with the

medium biological experiments having the greatest decrease, from 0.31 mM to 0.01 mM, compared to 0.17 to 0.06 mM in the high biological experiment.

The concentration of the REE Samarium (Sm) released per gram of rock is shown Figure 4.15. As with Experiment 1, the pattern of release over time is similar in all REEs. Samarium was chosen as an example and the data for all other REEs are included in the appendix. In addition, as with Experiment 1, the difference between biological experiments and controls is replicated. A greater increase in concentrations was observed in the controls compared to the biology-containing flasks in the medium ratio experiment, whilst biology-containing flasks were higher in the high and low ratios. Again the high ratio exhibited the greatest REE concentrations whilst the low ratio had the lowest.

ICP-AES analysis was carried out on samples from Experiment 2 and the linear elemental release rates are shown in Table 4.6 (calculated from the slopes of the plotted results – data in Appendix D). The rates show that the high ratios had the greatest release of elements for all, except in the case of Na, where the low ratio biological experiment had the greatest (0.64 $\mu mol\ m^{-2}\ d^{-1}$ compared to 0.19 $\mu mol\ m^{-2}\ d^{-1}$). The low ratios had the slowest rate for all elements (except for Na, as already described). In terms of controls versus biological experiments, faster rates are shared almost equally between controls and biological experiments. K, Mg and Na have a faster rate in the high and medium biological experiments, whilst the low control has a faster rate compared its biological experiments counterpart. Ca and Fe have faster rates in the high and medium controls in comparison to the biological experiments.

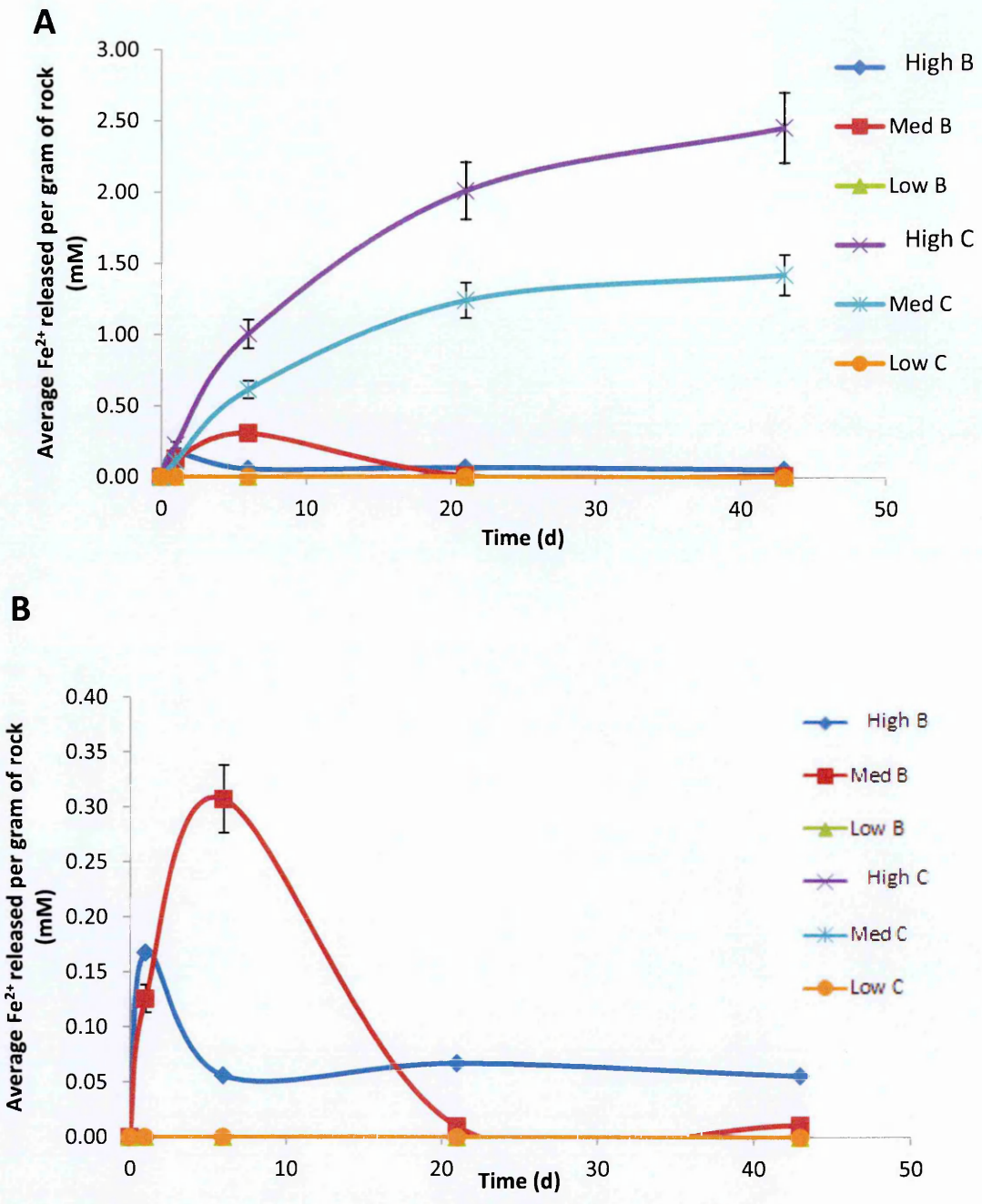

Figure 4.14. Experiment 2. Average Fe^{2+} concentration released per gram of rock in the three ratios. (A) All ratios shown, with biological experiments and controls, and (B) low control only along with biological experiments of all three ratios. In the legend, 'B' denotes biological flasks and 'C' control.

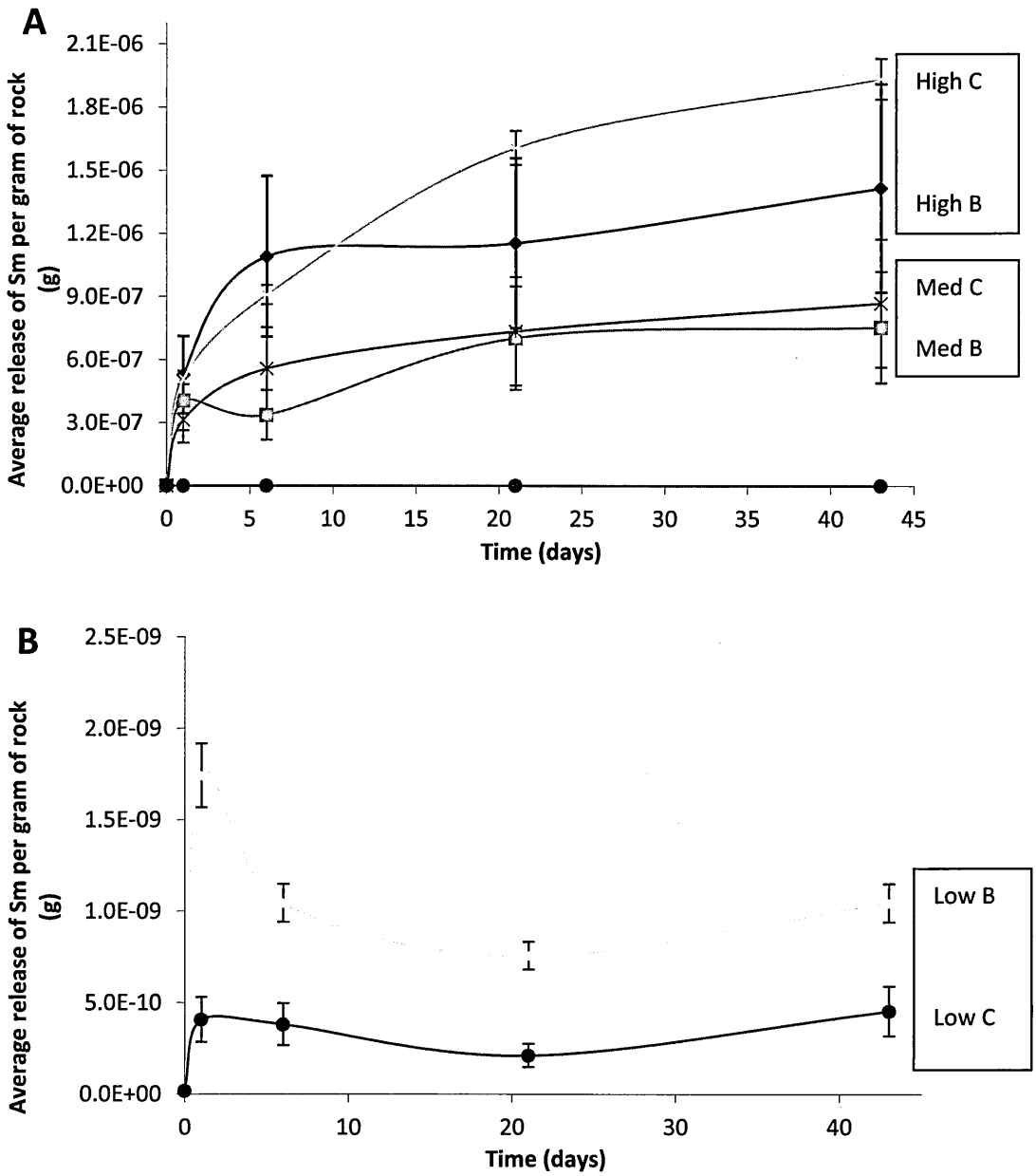

Figure 4.15. Experiment 2. The average release of REE Sm per gram of rock over time for (A) all ratios and for (B) the low ratio only. As with Experiment 1, all REEs share the same trend. In the legend, 'B' denotes biological flasks and 'C' control.

Table 4.6. Linear elemental release rates (μmol per m^2 per day) from ICP-AES analysis of Experiment 2. The fastest release rates, when comparing biological experiments and controls, are underlined. 'B' denotes biological flasks and 'C' control.

μmol/m^2/d	Ca	Fe	K	Mg	Na	Si
High B	175.56	304.16	287.53	183.77	0.19	38.51
High C	221.23	372.19	45.21	151.75	-	63.18
Med B	42.76	197.56	35.54	113.86	0.07	9.59
Med C	48.24	199.43	2.19	99.44	0.05	8.62
Low B	0.36	0.16	0.06	-	0.64	-
Low C	0.72	0.06	0.33	0.06	0.09	0.00

The linear elemental release rates of the REEs shown in Figures 4.9 and 4.15 are shown in Table 4.7. In terms of Experiment 1 the rates followed a similar trend as seen with Figure 4.9. The high ratio biological experiment and low ratio biological experimental conditions had faster rates compared to their controls whilst the medium ratio had a greater rate in the control compared to the biological experiment. In addition, the high ratio had the fastest rate, whilst the low ratio had the slowest. In controls versus biology-containing flasks for Experiment 2, however, biological experiments had the faster rates over controls for all three ratios. As with Experiment 1, the high ratio had the overall fastest rate whilst low ratio had the slowest.

Table 4.7. Linear elemental release rates (μmol per m^2 per day) of representative REEs (Lu and Sm) for both experiments. The fastest release rates, when comparing biological experiments and controls, are underlined. 'B' denotes biological flasks and 'C' control.

μmol/m^2/d	Experiment 1 (Lu)	Experiment 2 (Sm)
High B	$\underline{1.48 \times 10^{-4}}$	$\underline{6.18 \times 10^{-3}}$
Med B	7.67×10^{-5}	$\underline{4.80 \times 10^{-3}}$
Low B	$\underline{7.25 \times 10^{-6}}$	$\underline{2.05 \times 10^{-5}}$
High C	1.23×10^{-4}	5.95×10^{-3}
Med C	$\underline{9.85 \times 10^{-5}}$	3.71×10^{-3}
Low C	4.71×10^{-6}	4.62×10^{-6}

When analysing the rates of Fe^{2+} by Ferrozine assays, the fastest rates are found in the controls (for both Experiment 1 and 2) (Table 4.8). The fastest rate was observed in the high ratio, whilst the slowest rate was found in the low ratio. On the whole, this matched with the ICP-AES results for Fe. The one exception was the low control had a slower rate than the biological experiment in the ICP-AES analysis, whilst the Ferrozine assays showed a faster rate in the control (Experiment 1) or no difference (Experiment 2).

Table 4.8. Linear elemental release rates (μmol per m^2 per day) of Fe^{2+} as obtained through Ferrozine assays for both experiments. 'B' denotes biological flasks and 'C' control.

μmol/m^2/d	Experiment 1	Experiment 2
High B	0.00	0.30
Med B	0.00	1.64
Low B	0.00	0.00
High C	22.32	5.36
Med C	12.09	3.27
Low C	0.11	0.00

4.3.4. Tolerance experiments

4.3.4.1. pH

The effect of pH on *A. ferrooxidans* is detailed in Table 4.9, which shows the rate of Fe^{2+} removal from solution in biological experiments and controls, over a pH range of 1.0 to 5.0. pH did not appear to affect iron oxidation by the bacteria, with the rate of Fe^{2+} removal from solution ranging from 4.58 to 4.67 mM per day in the biological flasks. The controls showed an increase of Fe^{2+} in solution at pH 1 to 3 (denoted by the plus sign in Table 4.9), and no change at 3.5. The less acidic the solution, the more Fe^{2+} is removed from solution in the controls.

Table 4.9. Rate of Fe^{2+} oxidation between the start and end of the experiment at different pHs, with *A. ferrooxidans* added (biological experiments) and sterile flasks (controls). The plus signs denote a rate of increase of Fe^{2+} in solution rather than a rate of removal of Fe^{2+}. 'B' denotes biological flasks and 'C' control. Standard error 10%.

	Rate of Fe^{2+} oxidation (mM per day)	
pH	Biological	Control
1	4.67	+1.50
1.5	4.65	+0.33
2	4.67	+0.50
2.5	4.58	+1.00
3	4.67	+1.42
3.5	4.62	0.00
4	4.60	0.83
4.5	4.60	1.67
5	4.63	1.83

4.3.4.2. Heavy metals

The effect of heavy metals (at a concentration as found in the basalt) on *A. ferrooxidans* is shown in Figure 4.16, alongside untreated solutions. Both untreated and heavy metal controls have a higher Fe^{2+} concentration than in biological experiments. However, there is no significant difference between the untreated and heavy metal conditions in either the biological experiment or control (*P*-value >0.05). Thus, *A. ferrooxidans* is not affected by the addition of heavy metals.

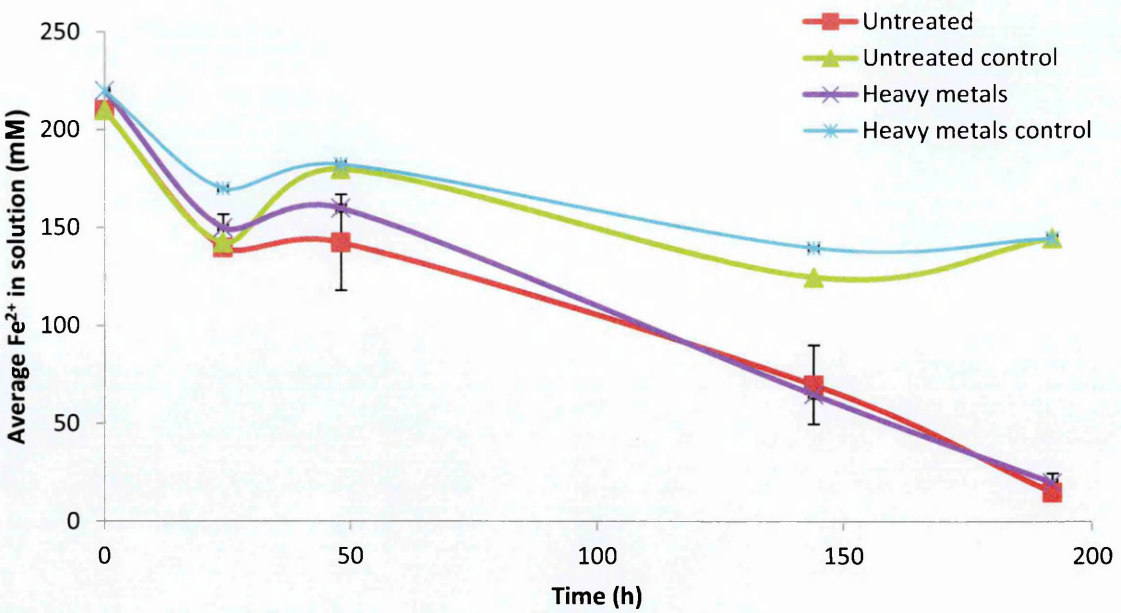

Figure 4.16. The effect of heavy metals on Fe^{2+} release by *A. ferrooxidans* over time.

4.3.5. Summary of results

In summary for the two experiments, pH increased in all three water-rock ratios, with the greatest increase seen in the low ratio and the lowest in the high ratio (figures 4.7 and 4.13). The medium control had a higher pH than the equivalent biological experiment, whilst in the high and low ratios the biological experiments and controls were very similar to each other. Cell counts (Table 4.5) showed that that the medium ratio had the largest number of cells per ml; the low ratio had the lowest. Release of Fe^{2+} was greatest in the high control, however, very little to no Fe^{2+} was released in the biological experiments for all three ratios (Figures 4.8 and 4.14). Fe^{3+} release showed a similar pattern, with the high control having the highest release and the low ratio had the lowest. In the case of the medium ratio, Fe^{3+} began to rise by day 4 for Med B and Med C but then plateaud. For the low ratios, there was a sharp rise in Fe^{3+} between 0 and 7 days before concentrations dropped to 0 for the rest of experiment, with more Fe^{3+} released in the biology (Figure 4.8).

In terms of REEs, the average release of REEs was greatest in the high ratios and lowest in the low ratios (Figure 4.9 and 4.15). Biological experiments showed a greater release than their counterpart controls in the case of the high and low ratios. The medium ratio, on the other hand, exhibited a greater release in the control.

Linear elemental release rates showed trends when looking at REEs and Fe^{2+} (Table 4.7). Rates for Fe^{2+} were fastest in the controls, with the high ratio being fastest overall and the low ratio the slowest. On the whole, REEs showed a faster rate in the biological experiments. The rates for trace element releases for Experiment 2 exhibited the fastest rates in the high ratios and the lowest in the low ratios. However, compared to biology-containing flasks, neither had the majority of faster rates.

XANES analysis showed localised areas of hematite but also iron oxidation without a change in gross mineralogy (Figure 4.10). However, the controls also showed oxidation of the surface. SEM pictures of the rock surfaces showed pitting in the Med B as well as biofilms of *A. ferrooxidans* (Figure 4.11). No pitting was observed in the controls.

4.4 Discussion

The objective of this chapter was to gain a better understanding of the processes by which *A. ferrooxidans* weathers basalt, and how this may (or may not) be affected by water-rock ratios. As previously mentioned in the introduction to this chapter, this work has implications from an astrobiological perspective in terms of microbial habitability in basalt environments on Mars. Low water-rock ratios have been postulated to have been present with acidic conditions (Hurowitz and McLennon, 2007; Hurowitz, 2008; Quinn

et al., 2005). In terms of the environment, the work could also help to understand the rates of weathering in natural environments, such as acid mine drainage sites.

A variety of analytical techniques were used to determine whether *A. ferrooxidans* was affected by water-rock ratios. Ferrozine assays and ICP-MS/AES were used to measure the release of elements, whilst the pHs of the solutions were monitored throughout the experiment. Cell counts were carried out at the end of the experiment and SEM images were taken of the rock surfaces. In addition, XANES analysis was used on the rocks to analyse any mineral signatures present.

The hypothesis was that a high water-rock ratio would have a diluting effect, diluting the iron as soon as it was released and thus limiting its supply. At the other extreme, a low ratio would cause the acid in the media to be quickly quenched by protons being used up in reactions with the rocks, raising pH above optimum for bacterial growth. However, a ratio between the two would strike a balance between optimum iron concentration and pH.

4.4.1. Iron oxidation

A trend seen in both Experiments 1 and 2 was that low to no Fe^{2+} being released into solution in the biological flasks (with bacteria), regardless of water-rock ratio. This was most likely because the iron was being used by the bacteria as soon as it was released. For experiment 1, release of Fe^{3+} was shown in Figure 4.8. This showed that oxidation of iron was occurring to some degree in all the ratios. In the case of Experiment 1, and for the most part in Experiment 2, the highest release of Fe^{2+} was observed in the controls. However, with respect to the controls, differences between the high, medium

and low water-rock ratios in terms of Fe^{2+} release can be explained by the pH. Greater release of Fe^{2+} coincided with a lower pH (i.e. more acidic). The higher the pH, the slower the release rate and the less iron was released, as demonstrated by the low water-rock ratio control which had the highest pH out of the three. This is supported by Santelli *et al.* (2001) who studied the effect of iron-oxidising bacteria on iron-silicate mineral dissolution. They found that, as pH increased, the iron released into solution was several orders of magnitude lower than for experiments run at a lower pH.

This is typical of Fe solubility, as it is governed by pH. If pH is defined as the concentration of hydrogen ions, this concentration is calculated by the negative logarithm of the hydrogen ion (H+) concentration, which means the higher the pH level, the less free hydrogen ions. Additionally, this means a change in one pH value represents a ten-fold change in the concentration of hydrogen ions. Therefore, there are 10 times as many hydrogen ions available at a pH of 7 than at a pH of 8, and 100 times as any at a pH of 6. Solubility refers to the amount of a substance that can be dissolved in water and the lower pH level, the more soluble the iron will be.

Santelli *et al.* (2001) suggest that initial dissolution rates are due primarily to proton consumption and preferential dissolution of more reactive material (Santelli *et al.*, 2001). Slower release rates reflect conditions where solution pH is higher, and solutions are supersaturated with respect to several possible secondary phases (Santelli *et al.*, 2001). A decrease in rates also occurs over time because 30-50 % of the available material reacts within the first few days of experiments (Santelli *et al.*, 2001), which would explain the plateauing of elemental release seen with regards to Fe^{2+}, and later with the REEs.

As mentioned in the results, there was a small degree of of oscillation in pH for Experiment 1 for the medium and high ratios between 0 and 7 days. Here the pH rose

over the first day before dropping by the third day, and then rising again by the seventh day. There is no apparent explanation for this and it is not repeated in Experiment 2. The explanation could be equipment drift. The pH probe was changed after pH began to oscillate. Because no drift was observed following replacement of the pH probe, it was concluded that the oscillations resulted from faulty equipment. Fortunately, the oscillations did not affect the overall large-scale trend in the data, so results for experiment 1 could still be used.

The effect of the three ratios on *A. ferrooxidans* cell numbers is not as straightforward to explain. It is possible that the numbers in the high ratio (lower than the medium but higher than the low water-rock ratio) could be due to the iron being diluted as soon as it was released. However, further studies need to be carried out to ascertain the minimum levels of iron *A. ferrooxidans* can survive on. In addition, cell counts at regular intervals rather than at the start and end of the experiment should be carried out to ascertain whether the medium water-rock ratio always had the highest number of cells compared to the other two water-rock ratios.

Cell numbers were lowest in the low ratio which also had the highest pH. One could postulate that the increased pH affected the cell numbers directly. However, results from pH tolerance tests and previous literature suggest that the pH should not have affected the bacteria. The tolerance studies have shown no difference in iron oxidation at pH 1.5 or pH 5.0. *A. ferrooxidans* has been shown to oxidise iron at pH 7 (Meruane and Vargas, 2003; Mielke *et al.*, 2003). Mielke *et al.* (2003) found that *A. ferrooxidans* develops an acidic nano-environment between the cells and the pyrite mineral surface they were studying. Figure 4.17 is a schematic representation of this process, as drawn out by Mielke *et al.* (2003).

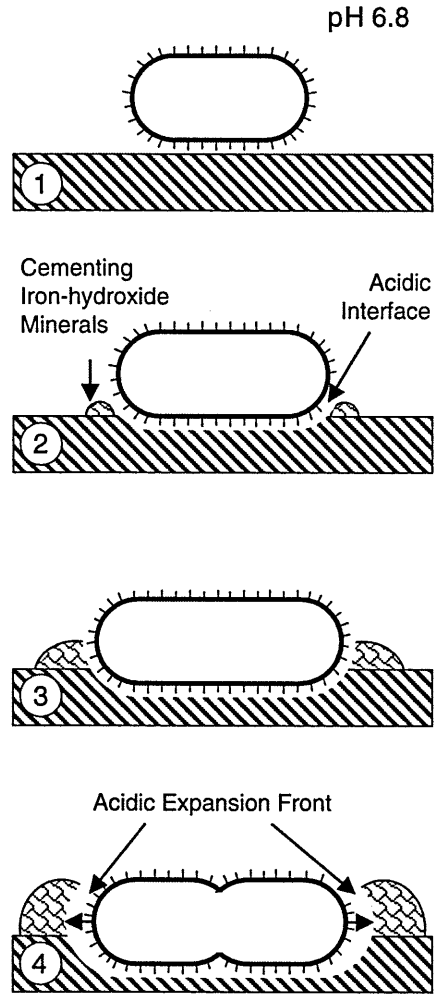

Figure 4.17. A schematic representation by Mielke *et al.* (2003) of the colonisation of pyrite under circumneutral pH conditions. *A. ferrooxidans* create an acidic nano-environment under these conditions as follows: in Phase 1 salt bridging occurs between the bacterium and the phosphate-enriched mineral surface. In Phase 2 an iron oxy-hydroxide matrix around the bacterium is formed as corrosion is initiated. This helps maintain the acidic nano-environment at the bacteria–mineral interface by limiting the diffusion of acid or iron away from the cell. The continued growth of the bacterium outward across the mineral surface and inward as the pyrite is consumed as its source of energy, eventually resulting in cell division is demonstrated in Phases 3 and 4 (Mielke *et al.*, 2003).

One theory as to why the cell numbers were so low is that iron oxides may have formed in the flasks, which coated the rock surfaces. As the acid was quickly quenched under the low ratio, the formation of iron oxides would have occurred faster than in the high and medium ratios. In addition, as the low ratio had a relatively small area of the flask covered in media, the only place for the iron oxides to form was the rock surface. The iron precipitation could have prevented further release of Fe^{2+}, starving the bacteria. This theory is further supported when looking at Fe^{3+} concentrations in Experiment 1 for the low ratios. Fe^{3+} concentrations peaked between 0 and 7 days before dropping to 0. The higher concentration was found in the biology which may be explained by the addition of *A. ferrooxidans* increasing the rate. However, as the pH rose rapidly, iron oxides could have formed on the rock surface, preventing further oxidation and thus explain the drop in Fe^{3+} concentrations.

This theory may explain why no cells were observed on the rocks during SEM cells counts – a coating of iron precipitation may have prevented access of iron from the rock and the bacteria were forced to acquire any iron in solution instead. The iron precipitation theory is backed by findings by Meruane and Vargas (2003) when they studied the iron oxidation by *A. ferrooxidans* in the pH range 2.5-7.0. Their results showed that the inhibition of iron oxidation activity by *A. ferrooxidans* observed at pH values above 3.0 was partially linked to the formation of ferric iron precipitates, which apparently hindered transport processes on the cell surface (Meruane and Vargas, 2003).

Another theory was that the leaching of heavy metals into solution affected the bacteria in the low water-rock ratio. However, this theory was tested in tolerance tests whereby iron oxidation by *A. ferrooxidans* was monitored when heavy metals were added in the concentration as found in the basalt, and compared to untreated conditions. The iron oxidation when heavy metals were added was not different from the untreated. This

would suggest that, even at the maximum of concentrations possible under these conditions, *A. ferrooxidans* was not affected. In addition, according to the literature, *A. ferrooxidans* is capable of resisting high concentrations of heavy metals such as copper, zinc, arsenic and uranium (Tuovinen *et al.*, 1971; Leduc *et al.*, 1997; Dopson, 2003; Cabrera *et al.*, 2005). Table 4.10 shows the maximum tolerated concentrations (MTC) of a selection of heavy metals as found in literature (Cabrera *et al.*, 2005). The concentrations cited in literature are above the concentrations found in the basalt used in this experiment (Table 4.10).

Table 4.10. Maximum tolerated concentrations of a selection of heavy metals as found in literature (Cabrera *et al.*, 2005).

Heavy metal	MTC (g/l)	Reference
Cr(III)	0.52	Sisti *et al.* (1998)
	0.78	Wong *et al.* (1982)
	3.9	Baillet *et al.* (1998)
Cu(II)	0.6–10	Leduc *et al.* (1997)
	19	Boyer *et al.* (1998)
	16	García Jr. and Silva (1991)
	10	Das *et al.* (1997)
	5	Brahmaprakash *et al.* (1988)
Cd(II)	5.6	Baillet *et al.* (1997)
	1.12	Imai *et al.* (1975)
Zn(II)	40	Kondratyeva *et al.* (1995)
	40	Das *et al.* (1997)
Ni(II)	0.6–9.4	Leduc *et al.* (1997)
	6.3	Dopson *et al.* (2003)
	10	Huber and Stetter (1990)

As heavy metals do not appear to be affecting cell numbers, it is proposed that though pH was not affecting cell numbers directly, it was indirectly affecting numbers by limiting iron release.

XANES analysis shows some signs in favour of the theory that iron oxides are coating the rocks (Cockell 2009). The analysis showed that following weathering of the rocks, the basalt surface showed areas of an oxidised layer (Fe^{3+}) that did not correspond to any specific mineralogy. Patches of hematite were observed on the surface which suggests that some of the rock material is released into solution and oxidised to iron-bearing oxides. The lack of specific mineral signatures on the rock surface, but the apparent oxidation of the surface could suggest that the surface has been passivated with Fe^{3+} binding to the mineral surface. This is consistent with speculations advanced by Santelli *et al.* (2001) who observed the passivation of olivines during microbial dissolution. This chapter has provided some XANES support for this supposition but the analysis was preliminary and more work would need to be carried out to be more conclusive.

The work is important because not only has it provided empirical evidence for a mechanism by which organisms might weather and oxidise volcanic rocks, but it may also explain how microorganisms can reduce weathering rates in some environments. Certainly, in addition to studies showing an increase in weathering with microorganisms present (e.g. Staudigel *et al.*, 1998; Brehm *et al.*, 2005; Wu *et al.*, 2007a), there have also been studies where microorganisms have retarded weathering (e.g. Benedict, 1993; Arinõ *et al.*, 1995; Santelli *et al.*, 2001; Lüttge and Conrad, 2004). Arinõ *et al.* (1995), who investigated lichen colonisation on the flagstones and sandstones used in some historical buildings, revealed that stones without lichen cover showed greater

deterioration than those colonised by lichens. Lüttge and Conrad (2004) found that the addition of *Shewanella oneidensis* MR-1 significantly inhibited the dissolution rate of calcite.

An important observation made during the analysis is that the control rocks (in solution without *A. ferrooxidans*) also showed partial oxidation of the surface. Thus, this would suggest that the process is not exclusive to microbial activity and occurs naturally when fresh basalt surfaces come into contact with water.

It would appear that the medium water-rock ratio was the optimum ratio, providing enough iron for the bacteria to reach the highest numbers of the three as neither pH (as in the case of the low ratio) nor dilution (as in the case of the high ratio) are adversely affecting the release of iron.

4.4.2. Rare earth and trace elements

The analysis of REEs was carried out to ascertain how they were affected with different conditions. REEs were chosen as they are used in geochemical analysis of weathering rates; investigations have shown that REEs provide useful information concerning the origin and genesis of various kinds of geological materials because of their unique chemical characteristics (e.g., Henderson, 1984; Bünzli and Choppin, 1989, Sholkovitz, 1995). As a result of their similar geochemical behaviour, REEs have been used as environmental tracers for soil earth, sedimentary and aqueous systems (Nance and Taylor, 1976; Taylor and McLennan, 1985; McLennan, 1989; Johannesson *et al.*, 2006; Welch *et al.*, 2009). In systems with low water-rock ratios, such as soils and groundwater, the extent of water-rock ratio interactions has a profound impact on the geochemistry of the REE in both solution and the solid phase (Johannesson *et al.*, 1996; Åström, 2001; Hannigan and Sholkovitz, 2001; Åström and Corin, 2003; Haley *et al.*,

2004; Verplanck *et al.*, 2004; Welch *et al.*, 2009). In most other natural waters such as rivers and lakes, where there is a high water-rock ratio, the major controls on REE composition and concentration are solution variables, predominantly acidity (Elderfield *et al.*, 1990; Wood, 1990; Johannesson *et al.*, 1996; Johannesson *et al.*, 2006; Welch *et al.*, 2009).

It was predicted that a similar pattern, as seen with Fe^{2+}, would be seen with the REEs. This proved correct. As with Fe^{2+}, a higher pH in the media coincided with less leaching of elements from the rock. As with the iron the difference in rates with pH may be a case of solubility, with REEs becoming more soluble the lower the pH.

The biological experiments showed a higher release than the corresponding control for all ratios except the medium, where the control was higher. An explanation for this may lie in the number of cells.

The medium biological experiment had the highest number of cells at the end of Experiment 1. Clumps of bacteria could be seen on the rock surface using SEM. Biofilms of *A. ferrooxidans* covered the medium ratio rocks, something not seen in the high and low ratios. It is conceivable that the bacteria were retarding the release of REEs by covering the surface of the rocks. This would have prevented the release of REEs into solution in the same concentration as the control. The inhibition of elemental release has already been touched upon in terms of iron release, and literature has examples of inhibition and retardation (e.g. Benedict, 1993; Arinõ *et al.*, 1995; Santelli *et al.*, 2001; Lüttge and Conrad, 2004). Benedict (1993) suggested that granodiorite weathering in Colorado Front range, USA was retarded in the presence of crustose lichens which discouraged granular disintegration by binding the rock surface together. In addition, on sites where lichens are removed by snowkill, weathering proceeds rapidly (Viles, 1995). Biofilms of bacteria have also been shown to inhibit weathering

of sandstone by restricting penetration of salt water (Mustoe, 2010). In addition, Wu *et al.* (2007a) suggested that it is possible that discrepancies between abiotic and biotic release rates may in part result from the presence of organic molecules (such as extracellular polysaccharides) in biotic experiments that bind to mineral surfaces and effectively shield reactive surface sites from dissolution reactions (Sverdrup, 1990; White, 1995; Ullman *et al.*, 1996; Welch *et al.*, 1999; Benzerara *et al.*, 2004; Benzerara *et al.*, 2005).

In the case of the high and low ratios, where the biological experiments produced higher concentrations of REEs, it is more difficult to explain. Two theories are proposed. Firstly, the attachment of the bacteria to the basalt may have increased weathering with the bacteria destroying the rock as they oxidise iron. The problem with this theory, however, is that neither of the ratios had a large enough biomass for this to be plausible; SEM cell counts of the rock surface showed no bacteria in the low ratio and a low number in the high ratio compared to the medium ratio. The second, and more likely, explanation is that as the bacteria oxidised the iron, the saturation state of the solution may have been reduced, allowing a greater release of REEs.

As described previously, whilst having faster rates in the high ratios and slowest rates in the low ratios, linear elemental release rates for the trace elements showed no overall preference towards either the controls or biological experiments. Trace elements were analysed only for Experiment 2, thus one cannot say whether the results are true representatives. In terms of Fe^{2+} and REEs there is a difference between controls and biological experiments. The exception of the trace elements may be due to preferential uptake of some of the elements by the cells.

A number of studies have shown that biotic weathering can cause preferential leaching or enrichment of elements at the weathering front or within the sediments produced by

volcanic rock weathering. Staudigel *et al.* (1998), in a study of basaltic glass weathering using a microbial enrichment culture from Loihi seamount, Hawaii, showed that the population of microorganisms induced an enrichment of calcium in the sediments produced by weathering, but a loss of magnesium, in contrast to the controls which showed the opposite trend. These results show that microorganisms can cause a differential rate of leaching of different elements from rocks. It could be conceivable that the lack of preference for either controls or biology-containing flasks could be due to uptake of some of the elements by the cells as soon as the elements were released. For future work, elemental uptake by cells could be measured by analysing intracellular elemental concentrations of the cells as described by Wu *et al.* (2007a). If elements that had faster rates of release in the controls, but found in large concentrations inside the cells in the biological experiments, it could be argued that the elements were being taken up by the cells as soon as they were released from the rock. This work was not carried out for this thesis due to time constraints and availability of the equipment.

4.4.3. Implications

What does this mean in terms of Mars? At the beginning of this chapter, different water-rock ratios were mentioned; the low ratio of water in rock vesicles, to the more dilute water of a river bed (high ratio). In terms of Mars, would rock vesicles or river beds have harboured life? On the basis of the results in this chapter, neither the low nor high ratio would be ideal places to look. However, a medium water-rock ratio would, at least in terms of the results, provide the optimum conditions for *A. ferrooxidans*-like organisms. Thus, impact craters rather than rock vesicles (low ratios) or river channels (high ratio) may be more appropriate sites to search for life that may have been on Mars.

The results from this experiment may also be relevant to a variety of natural processes, as well as to reactions that occur in sites impacted by acid rain or acid drainage. Though bulk solution pH for most natural environments is typically 'near neutral', it is not unreasonable that in microbial microenvironments, conditions could be significantly more acidic (Barker *et al.*, 1998; Santelli *et al.,* 2001). Indeed, Mielke *et al.* (2003) observed that *A. ferrooxidans* formed microcolonies which produced acidic nano-environments despite circumneutral conditions. In terms of acid mine drainage, the results suggest that the bacteria may need an optimum water-rock ratio (medium) to cause serious pollution. Diluting or creating a low water-rock ratio may help to reduce the amount of sulphuric acid produced by *A. ferrooxidans* as these conditions reduce the number of *A. ferrooxidans* present considerably.

4.5. Conclusions

In conclusion, it has been found that water-rock ratios affect *A. ferrooxidans*, with the medium water-rock ratio (50:1) providing the optimum conditions of those tested for growth whilst the low water-rock ratio (1:1) had a lower release of iron due to pH. pH affected the release of iron and REEs, with less released the higher the pH.

In the medium biological experiment, it is postulated that bacteria retarded the release of REEs through formation of biofilms on the surface of the basalt. In the high and low ratios, biology-containing flasks increased the release of REEs, most likely due to the bacteria decreasing the saturation state of the solution through iron oxidation.

Linear elemental release rates for the trace elements showed no overall preference for controls or biology-containing flasks. It is possible that a lack of preference for either controls or biology-containing flasks could be due to uptake of some of the elements by

the cells as soon as the elements were released. If elements that had faster rates of release in the controls, but found in large concentrations inside the cells in the biological experiments, it could be argued that the elements were being taken up by the cells as soon as they were released from the rock.

Preliminary XANES analysis suggested localised areas of hematite were found on the treated rocks in addition to also oxidised layers that did not correspond to specific minerals. The lack of specific mineral signatures on the rock surface, but the apparent oxidation of the surface, could provide evidence that the surface has been passivated with Fe^{3+} binding to the mineral surface. This is consistent with speculations advanced by Santelli *et al.* (2001) who observed the passivation of olivines during microbial dissolution.

Chapter 5: Molecular Analysis Related to the Microbial Successional Changes in a One Year Laboratory Experiment on the Weathering of Basalt Glass with Different Water-Rock Ratios

5.1. Introduction

5.1.1. Aim of Chapter

Following the water-rock ratio experiments with *A. ferrooxidans* in Chapter 4, it was decided to look at how a natural microbial community, native to Icelandic basalt glass, would be affected by water-rock ratios. The reason for this was two-fold. Firstly, one would be looking at a more natural set up – communities rather than a single organism. Weathering studies have typically tended to focus on single microorganisms rather than communities (e.g. Santelli *et al.*, 2001; Lüttge and Conrad, 2004; Song *et al.*, 2007; Wu *et al.*, 2007a; Wu *et al.*, 2008). Secondly, the microbial community was a diverse community (Cockell *et al.*, 2009a), the composition of which is depicted in Figure 5.1. However, we did not know if all these phyla were active in the rock, and if they contributed to the weathering, and if they were affected by water-rock ratios.

This work has implications for the rates of rock weathering in natural environments where water-rock ratios may affect the balance between optimum energy and nutrient supply. The chemistry of the flasks might vary depending on the ratio, which could then in turn affect the communities. As with Chapter 4, this study also mimics a more natural environment as the basalt glass used is crushed rather than powdered; a more accurate portrayal of the environment.

This chapter will focus on the molecular analysis related to this experiment (what microorganisms are emerging over the year and how this may or may not vary between ratios). It will also allow the observation of succession over a year-long period. Chapter 5 will focus on the chemical analyses and weathering rates related to the experiment.

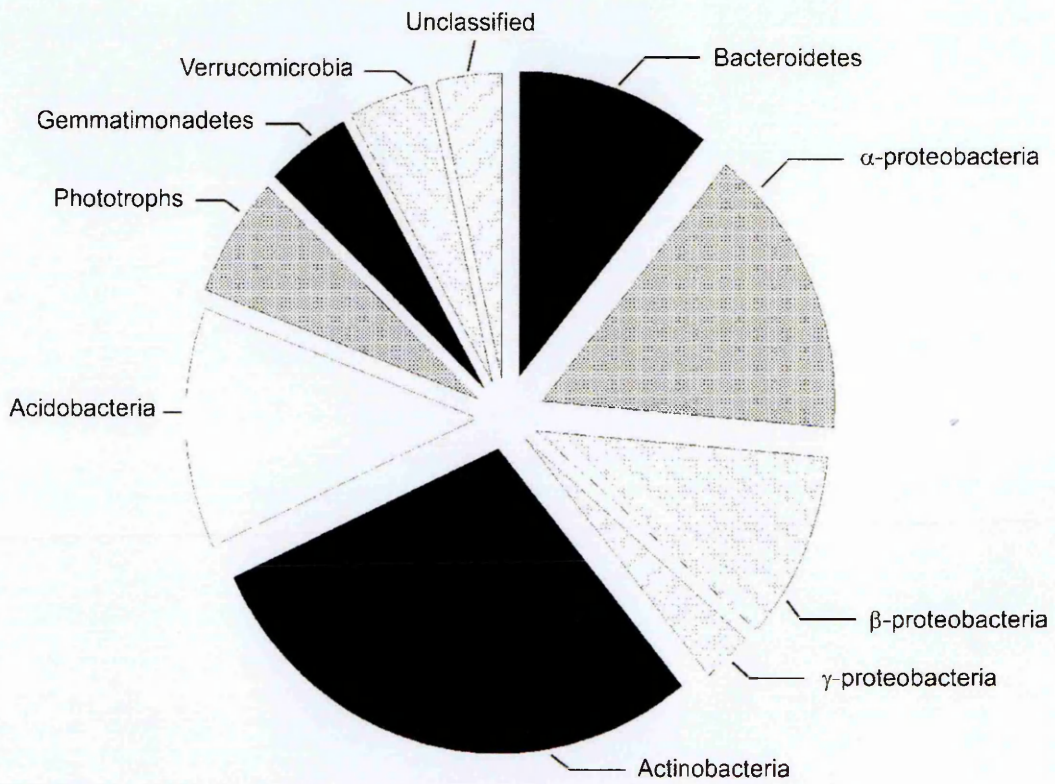

Figure 5.1. Pie chart showing the 16S rDNA phylum composition of a subglacial basalt sample (Cockell *et al.*, 2009a).

5.1.2. Weathering of volcanic glass

Volcanic glass is an amorphous product from rapidly cooling magma; it is the speed at which it cools that prohibits crystallisation. The glass is abundant in the Earth's crust (Staudigel and Hart, 1983). Due to the concentration of biologically important elements

present (including iron), alteration of glass makes it an important process in global biogeochemical cycling.

Microbes have been associated with alteration of basalt glass, with microbially-mediated alteration textures described in both terrestrial and deep-ocean settings (e.g. Thorseth *et al.*, 1992, 1995, 2003; Fisk *et al.*, 1998; Staudigel *et al.*, 1998; Torsvik *et al.*, 1998; Furnes & Staudigel, 1999; Etienne & Dupont, 2002; Banerjee & Muehlenbachs, 2003; Storrie-Lombardi & Fisk, 2004; Furnes *et al.*, 2005, 2007; Staudigel *et al.*, 2006, 2008; Walton, 2008).

5.1.3. The rock and its community

To provide the phylogenetic context for the microbial community in the rock, the phylum composition is briefly described below, along with broad characteristics of each respective phylum.

Acidobacteria: This is a relatively new phylum. They contain few cultured representatives but are believed to be ubiquitous in a number of soil environments (Quaiser *et al.*, 2003). The ecological characteristics are poorly understood as its members have been difficult to culture and few molecular investigations have focused exclusively on this group (Jones *et al.*, 2009). Due to this, we would predict that these do not appear in the flasks. However, the phylogenetic diversity, ubiquity and abundance of this group, particularly in soil habitats, suggest an important ecological role and extensive metabolic versatility (Quaiser *et al.*, 2003). A clear relationship has been identified between pH and abundance of acidobacteria (Jones *et al.*, 2009).

Actinobacteria: In terms of number and variety of identified species, this phylum represents one of the largest taxonomic units of the bacteria (Stackebrandt *et al.*, 1997) and thus we could expect find them in the cultures. They are the most morphologically diverse prokaryotes and are widely distributed in both terrestrial and aquatic environments (Embley & Stackebrandt, 1994; Servin *et al.*, 2007). The phylum comprises Gram-positive bacteria with a high G+C content in their DNA (Ventura *et al.*, 2007).

It has been suggested that the filamentous growth habit of some Actinobacteria make them particularly suitable for colonising rock substrates (Cockell *et al.*, 2009b). The filaments are capable of directionally growing across the rock surface and branching into the vesicular pore spaces (Cockell *et al.*, 2009b).

Bacteroidetes: Formerly known as Cytophaga-Flexibacter-Bacteroidetes, bacteria of this phylum are believed to be prevalent in the natural environment. They have previously been associated with soil crusts and soils (Shivaji *et al.*, 2004; Nagy *et al.*, 2005; Gundlapally *et al.*, 2006), but are also prevalent in aquatic environments (O'Sullivan *et al.*, 2006; Stevens *et al.*, 2005) having been found in freshwater (McCammon *et al.*, 1998; Wu *et al.*, 2007b), temperate rivers (Böckelmann *et al.*, 2000), marine sediments (Humphry *et al.*, 2001) and sea ice (Brown & Bowman, 2001). However, they have also been identified in microbial mats (Abed *et al.*, 2007), and in Arctic environments, such as tundra soil (Nemergut *et al.*, 2005), where they can dominate the population (Männistö *et al.*, 2009).

Bacteroidetes have been implicated as major utilisers of high-molecular-mass dissolved organic matter in marine ecosystems (Cottrell & Kirchman, 2000) and are often

abundant in nutrient-rich waters where biomacromolecules accumulate (Reichenbach, 1989).

Gemmatimonadetes: This is a recently described phylum (Zhang *et al.*, 2003). The phylum is present in diverse environments, including arctic permafrost (Steven *et al.*, 2007), cave soils (Zhou *et al.*, 2007), water treatment plants (Zhang *et al.*, 2003, Qin *et al.*, 2007), and the hyper-arid core of the Atacama desert (Drees *et al.*, 2006).

Phototrophs: Phototrophs comprise any organism that uses light as primary source of energy for metabolism and growth (Singleton and Sainsbury, 2002), including cyanobacteria and algae. The emergence of phototrophs in an environment provides additional nutrients, which benefit other microorganisms. We would expect these to appear near the beginning of the experiment as in the absence of a large pool of organic carbon, carbon-fixing organisms would have a greater advantage.

Proteobacteria: This phylum presently comprises the largest and most diverse group of Bacteria and account for the vast majority of the known Gram-negative bacteria (Stackebrandt *et al.*, 1988; Gupta, 2000). We would expect the presence of members of this phylum due to their diversity and abundance in the environment.

Verrucomicrobia: 16S rDNA sequences from this phylum have been retrieved from various soils (Hackl *et al.*, 2004; He *et* al., 2006), lake mesocosms (Haukka *et al.*, 2005; Haukka *et al.*, 2006), lakes (Eiler and Bertilsson, 2004; Lindstrom *et* al., 2005), marine sediments (Polymenakou *et al.,* 2005), and even from hot springs (Kanokratana *et al.*,

2004). They have also been detected in a mesocosm simulating the flooding of an unplanted paddy soil (Noll *et al.*, 2005). Their late appearance after flooding suggested that they were adapted to low substrate concentrations (Noll *et al.*, 2005). Therefore, if this phylum does appear in the flasks, we would expect it to be near the end of the year-long sampling period, when phototrophs in the flasks would have increase carbon availability.

5.1.4. Succession

In addition to studying the effect of water-rock ratios on microbial communities, the succession of the communities over time was also investigated. Succession is defined as the orderly and predictable manner by which communities change over time following the colonisation of a new environment (Fierer *et al.*, 2010). However, despite most of the phylogenetic diversity on Earth being microbial (Pace, 1997), the majority of succession research has focussed on plants.

Fierer *et al.* (2010) put forward three categories of microbial succession (Table 5.1). The categorisation was based on the fact that microbes can be divided into autotrophs and heterotrophs. Autotrophs use CO_2 as their carbon source, whilst heterotrophs require organic carbon compounds as their carbon source. Fierer *et al.* (2010)'s rationale was that as these physiologies are fundamentally dissimilar, and since the two categories may co-occur but are likely to dominate in very distinct type of environments, initial stages of succession could be divided into categories determined by the source of carbon biosynthesis. The heterotrophic succession is further divided into exogenous and endogenous categories. Exogenous succession is fuelled by continuous external inputs of organic carbon, whilst the majority of organic carbon

supplies in endogenous succession are derived from a single initial input contained within the substrate itself (Fierer *et al.*, 2010).

The study of microbial succession may provide insight into applied areas such as plaque formation on teeth, microbial colonisation and corrosion of pipes, and composting, which could all be considered examples of microbial succession (Fierer *et al.*, 2010). With the developments in molecular phylogenetic methods, comprehensive surveys of microbial diversity and succession patterns can be thoroughly documented. This was not possible previously as the majority of microbial taxa cannot be identified using standard culture based methods (Fierer *et al.*, 2010). This study aims to use molecular techniques to further understand succession in basaltic glass, as well as the effect of water-rock ratios.

Table 5.1. As given by Fierer *et al.* (2010), the three general categories of microbial succession, their distinguishing features, and some specific examples.

General succession categories	Distinguishing features	Where this type of microbial succession is likely to be found
Autotrophic	Initial colonizers are predominately autotrophs using light or the oxidation of inorganic compounds to generate energy	Metal and concrete pipes (Okabe *et al.*, 2007).
	Little to no organic C initially available	Glacial till, volcanic deposits, and other newly-exposed mineral surfaces (Hoppert *et al.*, 2004; Gomez-Alvarez *et al.*, 2007; Nemergut *et al.*, 2007; Schutte *et al.*, 2009).
	Organic C supply changes relatively slowly over time	Aquatic biofilms receiving light (Johnson *et al.*, 1997; Besemer *et al.*, 2007).
Endogenous Heterotrophic	Initial colonizers are predominately heterotrophs, respiring or fermenting organic compounds to generate energy	Decomposing wood and litter, compost (Nakasaki *et al.*, 2005; Danon *et al.*, 2008; Novinscak *et al.*, 2009; Rui *et al.*, 2009).
	Succession primarily fueled by organic carbon derived from the substrate itself	Food products including cheese, alcoholic beverages, cured meats, vinegar, cacao fermentation, etc. (Ercolini *et al.*, 2004; Haruta *et al.*, 2006).
	Initial community development can be fast	Leaf surface (Osono, 2005; Redford and Fierer, 2009).
	Substrate quality changes over time as succession progresses and substrate is directly modified by microbes	Skin surface (Fierer *et al.*, 2008; Costello *et al.*, 2009).
Exogenous Heterotrophic	Initial colonizers are predominately heterotrophic respirers or fermenters	Sewage and wastewater bioreactors (Santegoeds *et al.*, 1998; van der Gast *et al.*, 2008).
	Organic carbon supplied by external inputs	Teeth (Kolenbrander *et al.*, 2006).
	Initial community development can be fast	Aquatic biofilms forming under reduced light conditions (Martiny *et al.*, 2003).
	Organic C quality and quantity not directly controlled by the microbes and can be highly variable over time	Human gut (Palmer *et al.*, 2007; Balamurugan *et al.*, 2008).

5.2. Experimental design for Chapters 5-7: Natural communities

5.2.1. Overview

The effect of changing the water to rock ratios on native microbial communities of basalt glass was studied in Chapters 5 to 7, using a combination of culture and molecular techniques. It provided a year-long succession study on microbial communities in Iceland basalt glass and the experiment would observe a community rather than a single organism. An overview of the methods used in the three chapters is shown in Table 5.2.

Table 5.2. An overview of the experiments carried out in Chapters 5-7, including the measurements and sampling frequencies. Elemental analysis was only monitored over 213 days, rather than 12 months because of equipment availability.

Experiment	Measurements	Sampling frequency
Chapter 4: Molecular biology	Clone libraries, DGGE, isolation and sequencing	Five points over 12 months (days 5, 76, 160, 213, 371)
Chapter 5: Chemistry	pH, elemental analysis, SEM	Eight points over 12 months (pH) (days 0, 5, 39, 76, 119, 160, 188, 213) Eight points over 213 days (Elemental analysis) (days 0, 5, 39, 76, 119, 160, 188, 213)
Chapter 7: Isolates	Biolog plates, show of growth	N/A

5.2.1.1. Experimental design

Three ratios were set up in duplicate in polycarbonate flasks (Table 5.3).

Table 5.3. The water-rock ratios used in the experiments in Chapters 5-6.

Ratio	Basalt (g)	Media (ml)
High (400:1)	2	800
Medium (50:1)	2	100
Low (1:1)	100	100

Sterile volcanic glass was weighed and placed in the appropriate flask. As with Chapter 4, the medium covered the rocks completely. A small amount of carbon was added to increase the rate of succession as the time of the experiment was limited to a year. The flasks were incubated stationary at 21 °C in Milton Keynes, UK, in natural sunlight with a natural diurnal cycle for one year from February 2009 to February 2010. The incubation temperature was chosen as during summer in Iceland, the rock temperature is usually around this, and can even go higher (Herrera *et al.*, 2009). Summer would also have more water and thus higher water-rock ratios. Higher temperatures might have artificially enhanced weathering rates, although they would be applicable to summer. However, slower weathering rates might cause a decrease in rates as solubility is affected by temperature and so it would be interesting in future to examine this.

It is important to note, as well, that different minerals have different activation energies which would be affected by temperature changes. For example, activation energies, based on laboratory measurements, for many silicate minerals are on the order of 60 kJ mol^{-1} (e.g. albite (Lasaga, 1995, Chen and Brantley, 1997)), which would yield a sixfold increase in rate after raising temperature from 5 to 25 °C (Turner *et al.* 2010).

Biological activity is also dependent on temperature. Examples are the production of acids needed for weathering reactions, including organic acids (e.g. van Wesemael and Verstraten, 1993), and CO_2 respired from roots and decaying organic matter (e.g. Davidson and Trumbore, 1995) (Turner *et al.* 2010). Ugolini *et al.* (1977) has documented that, in general, upper soil pore waters, where the temperature is higher, have higher concentrations of organic acids compared to lower samples which tend to be dominated by carbonic acid. Increased biological productivity at higher temperatures may result in greater production of these acids (Turner *et al.* 2010).

Over this period, the flasks were sampled for pH, redox potential and elemental release. SEM was carried out on the rocks at the end of the 12 months. DNA was extracted to build a community profile over time using denaturing gradient gel electrophoresis (DGGE) in combination with 16S rDNA clone libraries and sequencing of isolates.

5.2.1.2. Cultivation and identification of microorganisms

The cultivation and isolation of microorganisms from the flasks was undertaken to provide the physiological and metabolic information required to place the microorganisms identified through molecular techniques into context. Isolates obtained from culturing allowed further investigations to be carried out (to understand adaptations to rock environments). This included the effect of heavy metals and pH (to ascertain whether changes in pH and heavy metals could affect communities), and the use of Biolog plates to obtain carbon utilisation profiles of the isolates (to increase understanding of the nutritional requirements of the isolates).

5.2.1.2.1. Isolation of microorganisms from flasks

For the purpose of isolating microorganisms from the flasks, each month 100 µl was removed from each flask and spread plated on to 0.2 g l^{-1} yeast extract agar plates and incubated at 21°C, under same conditions as the flasks. Once growth had occurred, individual colonies were selected and streaked out onto new yeast extract plates and grown up again. The cycle was repeated until pure colonies were obtained. A single colony was then picked and resuspended in 20 µl of sterile distilled water and stored at -20°C until further use.

5.2.1.2.2. Extraction of DNA from cultured isolates

Two extraction protocols were employed for the isolates. For the majority, a freeze-thaw cycle was used. The resuspended colony was left at -80°C overnight after which it was heated to 100°C for 15 minutes using a heat block. The sample was then used for downstream applications.

In the case of some isolates, a freeze-thaw cycle did not work. In these instances a DNA extraction kit was used – FastDNA SPIN Kit for Soil (Qbiogene, California, USA) according to manufacturer's instructions.

5.2.1.2.3. Polymerase chain reaction (PCR) amplification

The isolates were amplified using polymerase chain reaction (PCR) using primers that were appropriate (Table 5.4). PCR master mixes were prepared in sterile MilliQ water (18.2 Ω.cm; Millipore, MA, USA), and composed of 5 µl of template DNA; 1 µM primers each (Biomers.net); 1x buffer without Mg (Invitrogen, Paisley, UK); 1.5 mM $MgCl_2$ (Invitrogen, Paisley, UK); 200 µM dNTP (New England BioLabs, MA, USA)

and 2.5 units of *Taq* DNA polymerase (Invitrogen, Paisley, UK). The PCR machine used was a G-Storm GS1 Thermocycler (GeneTechnologies Ltd, Essex, UK). The amplification program for each primer pair used is summarised in Table 5.5.

The PCR products (total 5 µl) were loaded onto a 0.8% w/v agarose gel (prepared in 1x TAE buffer) to check if the PCRs had been successful. Electrophoresis was carried out at 120 V for 20-40 min (depending on the size of the gel used). The gels were then stained with ethidium bromide (0.2% v/v) for 20 minutes, after which they were observed under UV (GeneFlash, Syngene, Cambridge, UK).

Table 5.4. Details of the primers used for microorganisms isolated from flasks using plates and their purpose.

Purpose	Primer Name	Sequence (5' – 3')	Target region	Reference
Bacterial isolates	pAF	AGAGTTTGATCCTGGCTCAG	V1-V9	Bruce *et al.* (1992)
	Com2R	CCGTCAATTCCTTTGAGTTT		Schwieger and Tebbe (1998)
DGGE	338F-GC	CGCCCGCCGCGCGCGGCGGG CGGGGCGGGGGCACGGGGGG ACTCCTACGGGAGGCAGCAG	V3-V9	Muyzer *et al.* (1993)
	Com2R	CCGTCAATTCCTTTGAGTTT		Schwieger and Tebbe (1998)

F: forward primer; R: reverse primer.

Table 5.5. Summary of PCR programs for each set of primers used on isolates.

Steps	Temperature (°C)	pA-Com2	338F-GC-Com2
Initial denaturation	94	10 min	5 min
Cycles	-	30	35
Denaturation	94	1 min	30 s
Annealing	55	40 s	30 s
Elongation	72	40 s	30 s
Final elongation	72	10 min	10 min

5.2.1.2.4. Purification of PCR products

The PCR products were purified to remove any unbound nucleotides and primer dimers from the target product. The purification was carried out using the illustra GFX PCR DNA and Gel Band Purification Kit (GE Healthcare, Buckinghamshire, UK) according to manufacturer's instructions. If no multiple bands were present on the gel, the PCR product was purified directly using the protocol for purification of DNA from solution or an enzymatic reaction. If multiple bands were found, the total volume of PCR product was loaded and run on an electrophoresis gel and the target band extracted using a sterile scalpel blade. This was then purified using the protocol for purification of DNA from TAE and TBE agarose gels. In both methods, the cleaned products were eluted into 50 µl of elution buffer type 4. The purified DNA was stored at -20°C until further use.

5.2.1.2.5. Sequencing of isolates

Isolates were sequenced at Molecular Cloning Laboratories (MCLAB) in San Francisco, USA for sequencing. The sequences were classified using the GenBank database and the tool Classifier in the Ribosomal Database Project II (RDP II,

http://rdp.cme.msu.edu/html/) (Cole *et al.,* 2003) and the BLASTN program (Altschul *et al.* 1997).

5.2.1.3. Microbial Community Analysis

5.2.1.3.1. Sampling from flasks and processing

For microbial community analysis, 1 ml was aseptically removed from the biological flasks over 12 months (five points) and placed in 1.5 ml eppendorfs. These were spun down at 14,000 RPM for 10 min to obtain a pellet. The supernatant was carefully removed so as not to disturb the pellet and discarded. The pellet was then resuspended in 100 µl of sterile ddH_2O. The resuspended samples were subjected to a freeze thaw cycle, as described in 4.2.3.3. The samples were stored at -20°C until further use.

At the end of the 12 months, one rock piece was removed from flasks B1A (high ratio, replicate A) and B3A (low ratio, replicate A). A clone library was performed on both of these to analyse the microbial community composition in the rock. The outside of the rocks were blowtorched for 30 seconds to remove any microorganisms on the outside of the rock. The rocks were then aseptically crushed into a powder and 500 mg was processed with a DNA extraction kit. The extracted DNA was stored at -20 °C until used.

5.2.1.3.2. Community analysis by DGGE

The liquid samples collected from the flasks and the isolates cultured were amplified using 338F-GC-Com2 primers. After confirming that amplification had worked through electrophoresis, the PCR products were separated by DGGE (Muyzer *et al.*, 1993). DGGE was performed on 6 % w/v acrylamide gel with a gradient of 30 to 65 %

denaturant (7 M urea and 0.5 M formamide is referred to as 100 % denaturant). To establish the gradient, a gradient maker was used and each gel was produced between 20 cm sandwich plates (BioRad, Hertfordshire, UK). Once the gel had set, it was clamped onto the cassette of the DGGE system (DCodeSystem, Biorad, Hertfordshire, UK) and immersed into the DGGE tank, which contained 1x TAE that had been warmed to 60°C. PCR products (0.5 μg – measured using a NanoDrop 1000 from ThermoScientific, Wilmington, USA) were mixed with a loading dye (ratio 1:1) and loaded onto the gel. One of the samples (B1A at 5 days) was used as a marker on all gels run (loaded at the beginning, middle and end of the gel) to allow for the gels to be compared with each other during the analysis stage. Once all samples had been loaded, the buffer was again heated until it reached 60°C and the voltage was switched on. Electrophoresis was carried out at 75 V for 17.75 hours.

After electrophoresis, the gel was removed from the system and stained in SYBRGreen (Invitrogen, Paisley, UK) for 40 min before being photographed on the UV transilluminator. Any bands of interest were stabbed with a sterile pipette, which was then dipped into 20 μl of sterile ddH_2O and swirled around. This solution was reamplified with 338F-GC-Com2 primers as before. The products were run on a DGGE gel to ensure only the band picked had been amplified. The products were sent to MCLAB for sequencing.

5.2.1.3.3. 16S clone library construction and analysis

Clone libraries were carried out on flasks B1A (high ratio, replicate 1) and B3A (low ratio, replicate 1) every other month, and on the rocks from these flasks at the end of the experiment. The libraries were performed using the TOPO TA Cloning Kit for Sequencing (Invitrogen, Paisley, UK) according to the manufacturer's instructions. In

brief, samples were amplified with pA-Com2 primers. The products were purified. A TOPO cloning reaction was set up that consisted of fresh PCR product (4 µl), 1 µl salt solution and 1 µl TOPO vector. The reaction was mixed gently and incubated at room temperature for 30 min. Five µl of the reaction was then added to 25 µl of OneShot Chemically Competent *E. coli* and incubated for 30 min on ice. Cells were heat-shocked for 30 s at 42°C and immediately placed on ice. S.O.C. medium (250 µl; Invitrogen, Paisley, UK) was added to the transformed cells and incubated horizontally at 37 °C for one hour at 200 rpm. Aliquots of the suspension (50 µl) were spread plated onto pre-warmed (37°C) Luria Broth (LB) agar plates (Appendix A) containing ampicillin (50 mg ml^{-1}; Sigma-Aldrich, Poole, UK). The plates were incubated overnight at 37°C and stored at 4°C until further use.

For each clone library, 96 clones were picked with sterile pipette tips and transferred to 140 µl LB-Amp in 96-well plates (Fisher Scientific, Loughborough, UK). The suspensions were incubated overnight at 37°C, after which the cultures were sent to MCLAB for sequencing with T3 primers (forward).

The sequences were edited and aligned using BioEdit (www.mbio.ncsu.edu/BioEdit/bioedit.html) and ClustalX, respectively. Chimeras were identified in the clone libraries by submitting sequences to the chimera check application on the Bellerophon server (Huber et al., 2004). As with the isolates, the sequences were classified using RDP and BLASTN (Altschul *et al.* 1997).

5.3. Results

Over the span of the year-long experiment, microorganisms from the flasks were isolated and sequenced, and communities were analysed using DGGE and 16S rDNA clone libraries. The following sections will detail the results from these analyses.

5.3.1. Culturing and identifying organisms

Through plating on yeast extract and BG11 agar plates, it was observed that both non-phototrophic and phototrophic organisms (from 76 days onwards) grew. Microscopy of the phototrophs showed a highly diverse community of both filamentous and coccoid morphology (Figure 5.2).

The flasks were sampled every month and an aliquot was spread onto yeast extract agar plates. Microorganisms that grew up were subsequently isolated and sequenced. Bacterial isolation proved non-problematic in terms of PCR and sequencing and freeze-thaw cycling was sufficient for DNA extraction for amplification. Table 4.5 lists the isolates obtained from successful sequencing and their closest matches. All isolates were amplified using the pA-com2 primer set.

What is apparent is that a majority of the isolates affiliate closely to bacteria isolated from soil. There are also a few that are from cold habitats, such as *Microbacterium* sp. DVS4a2 (Medium-7-213d, 99%) from the Dry Valley, Antarctica, and *Streptomyces* sp. ZS1-2 (Medium-7-213d, 100%) which was also isolated from Antarctica. In addition, two isolates affiliate to bacteria that have been reported to associate with phototrophs: *Arthrobacter* sp. DC2a-1 (High-11-371d, 99%) isolated from an algal-bacterial consortia, and *Sphingomonas* sp. AKB-2008-VA4 (Low-16-371d, 99%) which associated with cyanobacterial water blooms (Berg *et al.* 2009).

The isolates grouped into three different phyla: Firmicutes, Proteobacteria, and Actinobacteria (Figure 5.3, Table 5.6). In the case of the Actinobacteria, isolates were affiliated to *Streptomyces* sp., *Arthrobacter* sp., *Microbacterium* sp. and *Rhodococcus erythropolis* (Table 5.6). As the clone libraries demonstrate, the diversity shown in the plates is less than that seen in the libraries.

Phototrophs also grew on plates and were subsequently isolated. Table 5.7 shows the isolates obtained and their closest matches, whilst Figure 5.4 shows them in a phylogenetic tree. All except one (Medium-P1-76d) matched to the same isolate, uncultured bacterium clone QB78 isolated from high-altitude tundra in Central Tibet, despite having different colony morphologies. RDP analysis, however, showed that all the phototrophs isolated were from the genus *Chlorophyta* (the green algae).

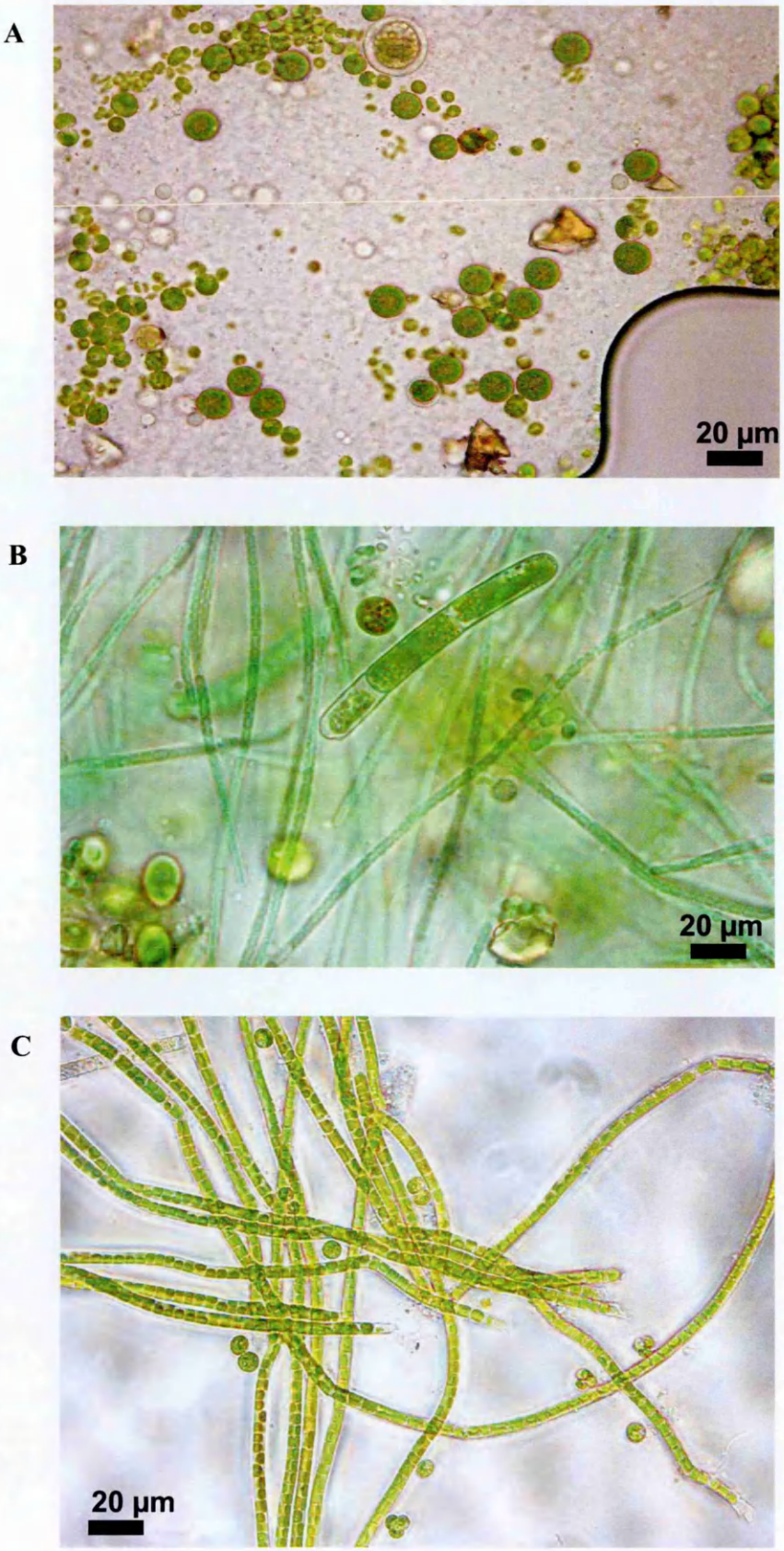

Figure 5.2. Representative light microscope images of phototrophs from the medium ratio at 213 days (A), low ratio at 213 days (B), and high ratio at 296 days (C).

Table 5.6. Closest matching sequences for sequences obtained from bacterial isolates from the flasks over one year. Primer set used was pA-com2 and isolates were cultured on 0.2 g^{-1} yeast agar plates. Accession numbers are listed alongside the closest matches.

Isolate (Accession #)	Closest relative (BLASTn)		
	ID (Accession #)	Max. ident. (%)	Sampling environment
HIGH RATIO			
High-1-5d (JN627967)	Arthrobacter sp. tz21 (HM151732.1)	98%	Air
High-2-39d (JN627968)	Bacillus sp. DB88(2010) (HM566968.1)	99%	Dung beetle
High-3-213d (JN627969)	Uncultured soil bacterium (DQ129209.1)	99%	Agricultural and forest soils
High-4-213d (JN627970)	Uncultured soil bacterium (DQ129209.1)	99%	Agricultural and forest soils
High-5-213d (JN627971)	Humicoccus sp. A24MTO (FN293194.1)	99%	Alpine tundra
High-6-296d (JN627972)	Uncultured bacterium (GQ396990.1)	97%	Unvegetated, perhumid, recently-deglaciated soils
High-7-296d (JN627973)	Cohnella sp. GT-L22 (GQ355279.1)	96%	Tidal flat sediment
High-8-296d (JN627974)	Uncultured bacterium (DQ510035.1)	96%	Arctic tundra tussock and shrub soils
High-9-371d (Not accepted)	Rhizobium sp. 01xTSA12A_B10 (HM113645.1)	71%	Cold Alaskan soil
High-10-371d (JN627961)	Rhizobium sp. 01xTSA12A_B10 (HM113645.1)	98%	Cold Alaskan soil
High-11-371d (JN627962)	Arthrobacter sp. DC2a-1 (AB552850.1)	99%	Algal-bacterial consortia

High-12-371d (JN627963)	Uncultured Paenibacillaceae bacterium (FJ608208.1)	99%	Larvae and adult midgut of *Anopheles stephensi*
High-13-371d (JN627964)	Paenibacillus alginolyticus strain ST7 (FJ982934.1)	80%	Granular sludge
High-14-371d (JN627965)	Rhodococcus sp. Y1E (EU293153.1)	92%	Petroleum-oil contaminated soil
High-15-371d (JN627966)	Rhizobium sp. 3-4 (FJ598330.1)	98%	Soil
MEDIUM RATIO			
Medium-1-5d (JN627998)	Bacterium B5B (GU458352.1)	99%	Gut of *Microcerotermes diversus* (termite)
Medium-2-160d (JN628000)	Uncultured bacterium (FJ595591.1)	98%	Rock varnish (Black Canyon, New Mexico)
Medium-3-188d (JN628001)	Bradyrhizobium sp. CCBAU 85080 (EU256466.1)	99%	Rhizobial resource in Tibet
Medium-4-188d (JN628002)	Rhodococcus erythropolis strain cmmb1 (GU120079.1)	100%	Marine water from the Gulf of Mannar
Medium-5-188d (JN628003)	Rhodococcus erythropolis strain cmmb1 (GU120079.1)	100%	Marine water from the Gulf of Mannar
Medium-6-188d (JN628004)	Arthrobacter sp. MNPB6 (FM213396.2)	100%	Glacier and cold environments of Lahaul and Spiti, India
Medium-7-213d (JN628005)	Streptomyces sp. ZS1-2 (DQ408296.1)	100%	Antarctica
Medium-8-213d (JN628006)	Uncultured firmicute (DQ829413.1)	99%	Agricultural soil
Medium-9-296d (JN628007)	Uncultured alpha proteobacterium (DQ463724.2)	98%	Lake Tanganyika anoxic hypolimnion

Medium-10-296d (JN627992)	Uncultured bacterium (EF693509.1)	99%	Well FW104 sediment sample from the Field Research Center at Oak Ridge National Laboratory (system for biostimulating the microbial remediation of uranium (VI) in groundwater)
Medium-11-371d (JN627993)	Paenibacillus alginolyticus (FJ982934.1)	78%	Anaerobic granular sludge
Medium-12-371d (JN627994)	Microbacterium sp. DVS4a2 (AY864634.1)	99%	Dry Valley in Antarctica
Medium-13-371d (JN627995)	Bosea thiooxidans strain MGV6-VS (AJ250799.1)	99%	Rhizoplane of *Medicago sativa* (alfalfa)
Medium-14-371d (JN627996)	Paenibacillus sp. Eur1 9.35 (DQ444989.1)	89%	Permafrost sample from the Canadian high Arctic
Medium-15-371d (JN627997)	Arthrobacter sp. RS-33 (FN377737.1)	99%	Kongsfjorden and Ny-Alesund, Svalbard, Arctic
Medium-16-371d (JN627999)	Bacillus sp. DS3sK3a (HM216203.1)	100%	Coal Mine Drainage
LOW RATIO			
Low-1-5d (JN627981)	Bacillus sp. BAM271 (GU003855.1)	100%	Wastewater influent, activated sludge, and a sequencing batch reactor
Low-2-5d (JN627984)	Pseudomonas sp. Air152 (GQ484873.1)	100%	Air sample collected 25 meters above sea level
Low-3-5d (JN627985)	Rhodococcus erythropolis (FN796872.1)	100%	Host stem endophyte (*Cytisus striatus* - Portuguese broom)
Low-4-39d (JN627986)	Variovorax paradoxus strain B55 (EU169153.1)	100%	Rhizosphere soil of *Bashania fangiana* (bamboo)
Low-5-76d (JN627987)	Pseudomonas sp. Air152 (GQ484873.1)	100%	Air sample collected 25 meters above sea level

Low-6-160d (JN627988)	Uncultured Rhodomicrobium sp. (FM175375.1)	100%	Recent tufa core sample formation
Low-7-160d (JN627989)	Brevundimonas sp. pfB9 (AY336538.1)	100%	Field-grown potato plant
Low-8-188d (JN627990)	Bacillus cereus strain ZY-02 (GU181319.1)	100%	Wastewater of Sibao (China) sewage treatment plant
Low-9-188d (JN627991)	Bacillus sp. PC IW 15 (FJ765236.1)	100%	Warm spring water from Western Ghats, India
Low-10-188d (JN627975)	Uncultured bacterium (AB487229.1)	99%	Rice Paddy Soil
Low-11-213d (JN627976)	Paenibacillus alginolyticus strain ST7 (FJ982934.1)	99%	Anaerobic granular sludge
Low-12-213d (JN627977)	Bacillus sp. KSA18 (GU048935.1)	100%	Water polluted with petroleum hydrocarbons and allied wastes
Low-13-296d (JN627978)	Uncultured bacterium clone BACu-B5C7 (GQ128078.1)	99%	Kobresia Meadow Soil from Mount Mila in Tibetan Plateau
Low-14-371d (JN627979)	Bacillus sp. ISP5-41-3 (HM044352.1)	99%	Root area soil of carnation in green-house
Low-15-371d (JN627980)	Skermanella sp. VTT E-073090 (EU438962.1)	98%	Paper mill pulps containing recycled fibres
Low-16-371d (JN627982)	Sphingomonas sp. AKB-2008-VA4 (AM989065.1)	99%	Treated drinking water
Low-17-371d (JN627983)	Uncultured Paenibacillaceae bacterium MFC85 (FJ608208.1)	99%	Larvae and adult midgut microflora of *Anopheles stephensi* (an Asian malarial vector)

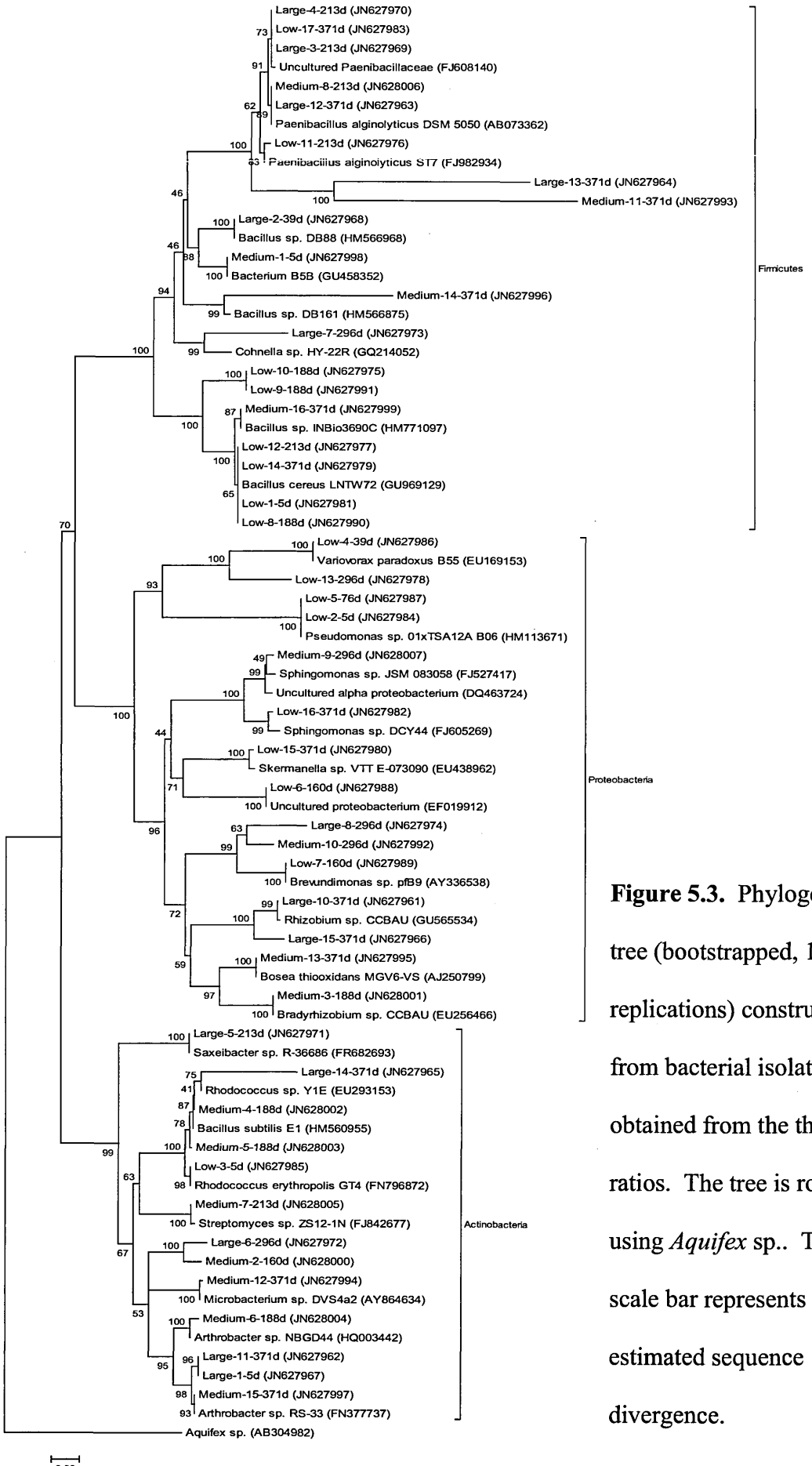

Figure 5.3. Phylogenetic tree (bootstrapped, 1000 replications) constructed from bacterial isolates obtained from the three ratios. The tree is rooted using *Aquifex* sp.. The scale bar represents 2% estimated sequence divergence.

Table 5.7. Closest matching sequences for sequences obtained from phototroph isolates from the flasks over one year. Primer set used was pA-com2 and isolates were cultured on 0.2 g $^{-1}$ yeast agar plates. Accession numbers are listed alongside the closest matches. Matches to the phylum level from RDP are also listed.

Isolate (Accession #)	Closest relative (BLASTn)			
	ID (Accession #)	Max. ident. (%)	Sampling environment	RDP Phylum
HIGH RATIO				
High-P1-188d (JN628009)	Uncultured bacterium clone QB78 (FJ790633.1)	99	Quartz Pavement in the High-Altitude Tundra of Central Tibet	Chlorophyta
High-P2-188d (JN628010)	Uncultured bacterium clone QB78 (FJ790633.1)	97	Quartz Pavement in the High-Altitude Tundra of Central Tibet	Chlorophyta
MEDIUM RATIO				
Medium-P1-76d (JN628012)	Uncultured bacterium clone C_13 (FJ490250.1)	98	Antarctica: Dry Valleys	Chlorophyta
Medium-P2-160d (JN628013)	Uncultured bacterium clone QB78 (FJ790633.1)	98	Quartz Pavement in the High-Altitude Tundra of Central Tibet	Chlorophyta
LOW RATIO				
Low-P1-188d (JN628011)	Uncultured bacterium clone QB78 (FJ790633.1)	99	Quartz Pavement in the High-Altitude Tundra of Central Tibet	Chlorophyta
SEEN IN ALL				
Algal-1-160d (JN628008)	Uncultured bacterium clone QB78 (FJ790633.1)	99	Quartz Pavement in the High-Altitude Tundra of Central Tibet	Chlorophyta

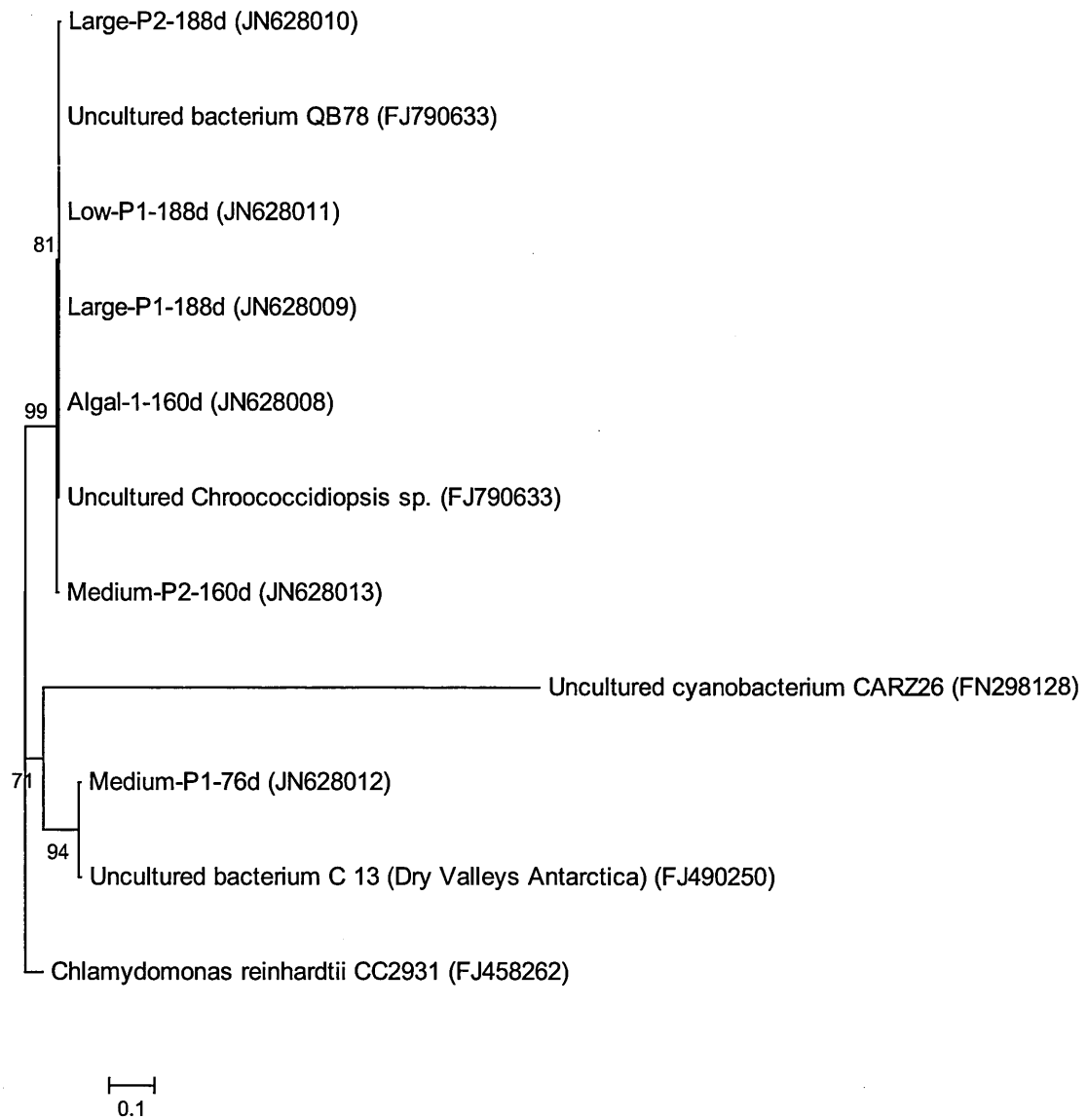

Figure 5.4. 16S rDNA phylogenetic tree constructed from phototroph isolates obtained from the three ratios. The tree is bootstrapped (1000 replicates) and the scale bar represents 10% estimated sequence divergence. The tree is rooted using *Chlamydomonas reinhardtii.*

5.3.2. Community analysis by DGGE

Amplification of 16S rDNA, using primers 338F-GC and com2, was carried out on all the samples collected over the year from the different ratios. The obtained products were then electrophoresised on DGGE gels. The results are shown in Figure 5.5. A cluster analysis based on the presence or absence of bands in the gel is shown alongside. It, however, shows no discernable clustering pattern between ratios, or between time points.

In an attempt to identify bands, two approaches were taken: approach one observed bands picked, amplified and then sequenced; approach two had isolates run on DGGE gels to match them with bands; however, both approaches did not prove successful. Sequences bands picked showed contamination, with no sequence able to provide a clear reading. Running isolates on gels had a low success rate as well, with multiple bands appearing in the lanes, despite the isolate being pure (Figure 5.6).

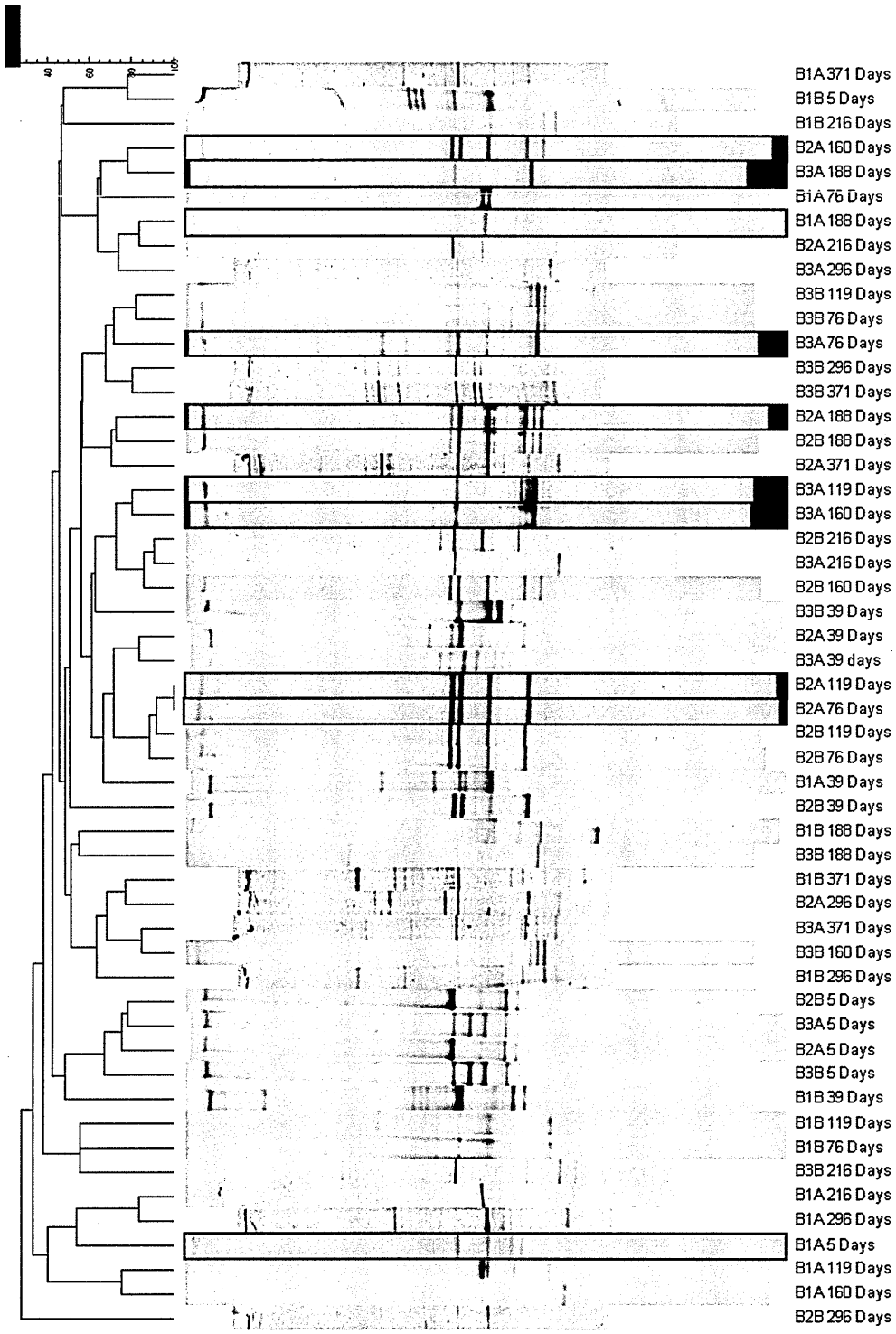

Figure 5.5. DGGE cluster analysis based on the presence and absence of bands. Labelling is as follows: B1 = high ratio, B2 = medium ratio and B3 = low ratio.

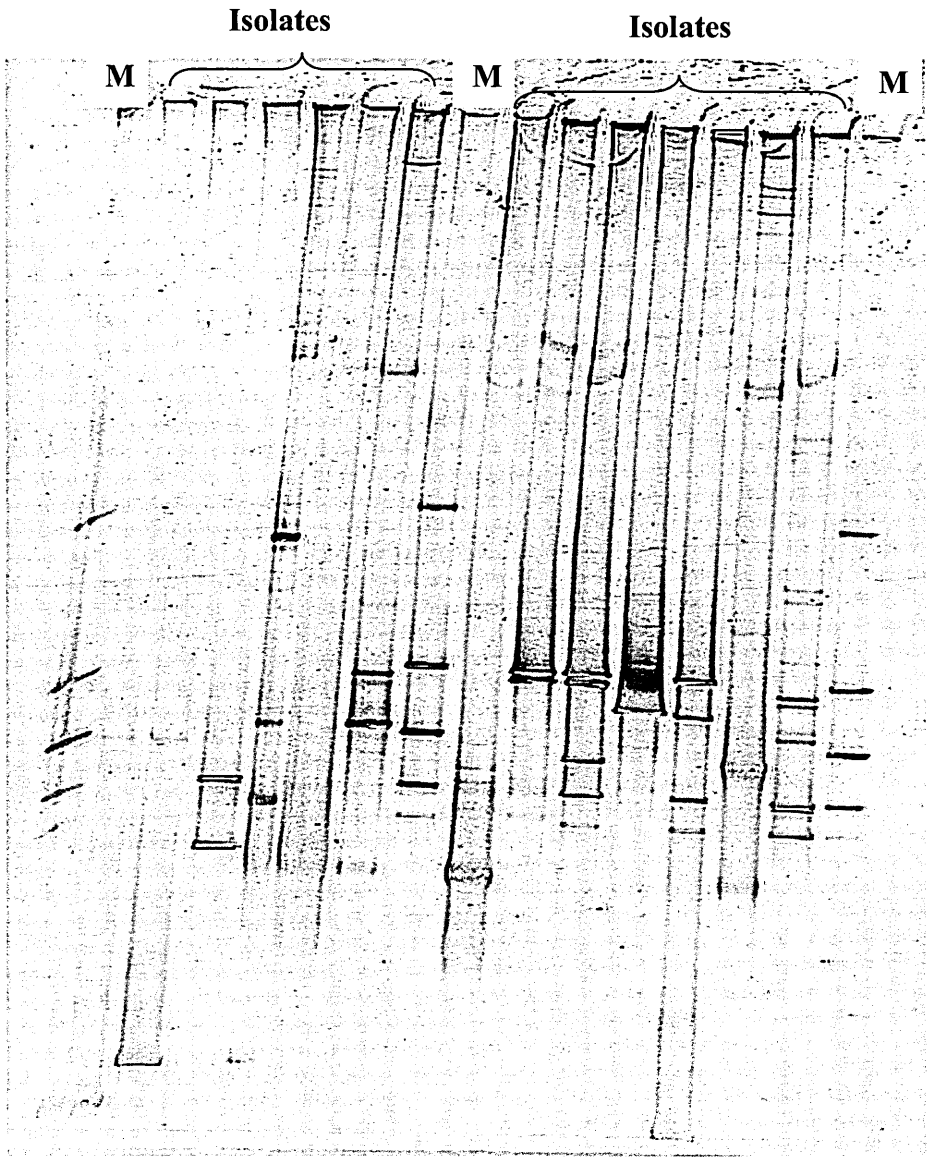

Figure 5.6. An example of isolates amplified and run on a DGGE gel. Markers are marked with an M.

5.3.3 Community analysis by 16S rDNA clone libraries

16S rDNA clone libraries were also carried out on the high and low ratios every other month (except at 160 days for the high ratio where the clone library was not successful). The distribution of clones within their respective phyla is represented in Figure 5.7. The sequence analysis of clone libraries at 5 days showed that both high and low ratios were made up of Firmicutes (such as *Paenibacillus* sp.) and Betaproteobacteria (such as members of the Oxalobacteria family), with Betaproteobacteria making up the majority.

However, the composition changes and diversifies with time. For example, by 213 days, Betaproteobacteria still made up a large part of the high ratio but no Firmicutes were found. Furthermore, phyla such as Verrucomicrobia, Bacteroidetes and Gammaproteobacteria were identified.

In terms of the low ratio at 213 days, Betaproteobacteria and Firmicutes were still present. However, there were a large number of unclassified bacteria, as well as Acidobacteria, Planctomycetes, Gemmatimonadetes and Deltaproteobacteria. The unclassified bacteria make up a large portion of the low ratio at 76, 160 and 213 days. However, at 371 days none were present.

A small number of cyanobacteria were sequenced for the high (371 days, and the rock) and low ratio (rock) but none were detected in the earlier time points despite the presence of phototrophs from 76 days onwards. Another phylum absent in the earlier time points was Actinobacteria. Though isolated on plates from as early as 5 days, they did not appear in the clone libraries until 371 days and they were also found in the rock.

The most diverse composition was found in the clone libraries from the rocks at the end of the experiment (371 days). The high ratio had 12 different phyla, and the low ratio had nine.

Libshuff revealed a combined 129 OTUs at 97% sequence identities among the libraries. The phylogenetic relationships of these OTUs are demonstrated in Figure 5.8, where each OTU is represented by one clone. The sampling time and ratios of the clones associated with each of the OTUs are listed in Appendix C.

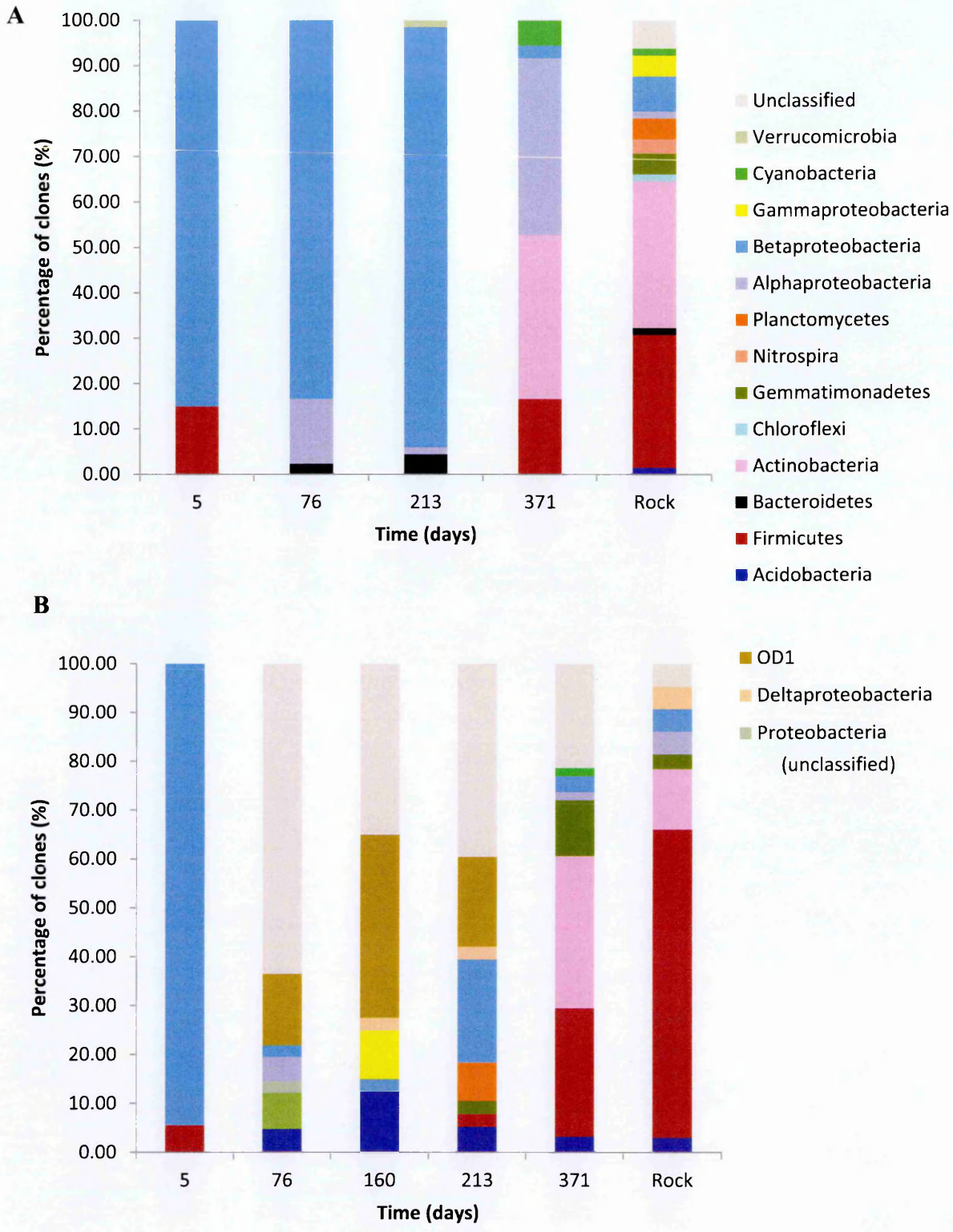

Figure 5.7. Stacked bar charts showing the percentage of community composition of the high ratio (A) and low ratio (B) over time, as found through 16S rDNA clone libraries.

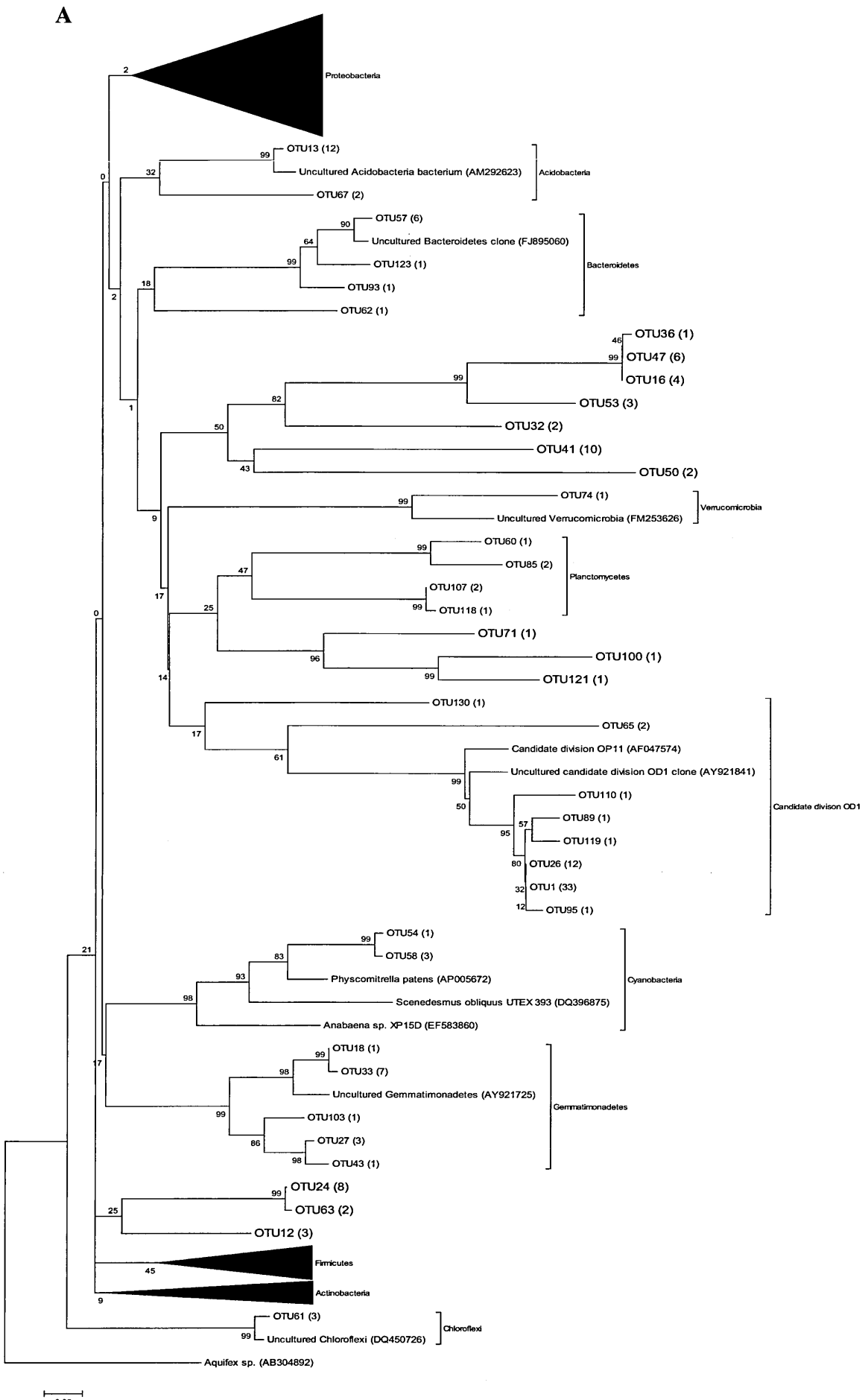
A
Proteobacteria
OTU13 (12)
Uncultured Acidobacteria bacterium (AM292623)
OTU67 (2)
Acidobacteria
OTU57 (6)
Uncultured Bacteroidetes clone (FJ895060)
OTU123 (1)
OTU93 (1)
OTU62 (1)
Bacteroidetes
OTU36 (1)
OTU47 (6)
OTU16 (4)
OTU53 (3)
OTU32 (2)
OTU41 (10)
OTU50 (2)
OTU74 (1)
Uncultured Verrucomicrobia (FM253626)
Verrucomicrobia
OTU60 (1)
OTU85 (2)
OTU107 (2)
OTU118 (1)
Planctomycetes
OTU71 (1)
OTU100 (1)
OTU121 (1)
OTU130 (1)
OTU65 (2)
Candidate division OP11 (AF047574)
Uncultured candidate division OD1 clone (AY921841)
OTU110 (1)
OTU89 (1)
OTU119 (1)
OTU26 (12)
OTU1 (33)
OTU95 (1)
Candidate divison OD1
OTU54 (1)
OTU58 (3)
Physcomitrella patens (AP005672)
Scenedesmus obliquus UTEX 393 (DQ396875)
Anabaena sp. XP15D (EF583860)
Cyanobacteria
OTU18 (1)
OTU33 (7)
Uncultured Gemmatimonadetes (AY921725)
OTU103 (1)
OTU27 (3)
OTU43 (1)
Gemmatimonadetes
OTU24 (8)
OTU63 (2)
OTU12 (3)
Firmicutes
Actinobacteria
OTU61 (3)
Uncultured Chloroflexi (DQ450726)
Chloroflexi
Aquifex sp. (AB304892)
0.02

Figure 5.8. Neighbour-joining phylogenetic tree of 16S rDNA clone sequences from high and low ratios libraries over one year. **(A)** full phylogenetic tree, **(B)** *Actinobacteria* phylum as represented by a wedge in (A), **(C)** Firmicutes phylum, **(D)** Proteobacteria phylum. Clones are represented at the OTU-level (defined at 97% sequence similarities) by one sequence from each Libshuff-indentified OTU. OTU designations are followed in parenthesis by the number of clones represented by that OUT and its accession number. The tree is bootstrapped (1000 replicates) and the scale bar represents 2% estimated sequence divergence. *Aquifex* sp. was used as an outgroup. Accession numbers for clones are JN222427-JN222544, and are listed in Appendix C.

B

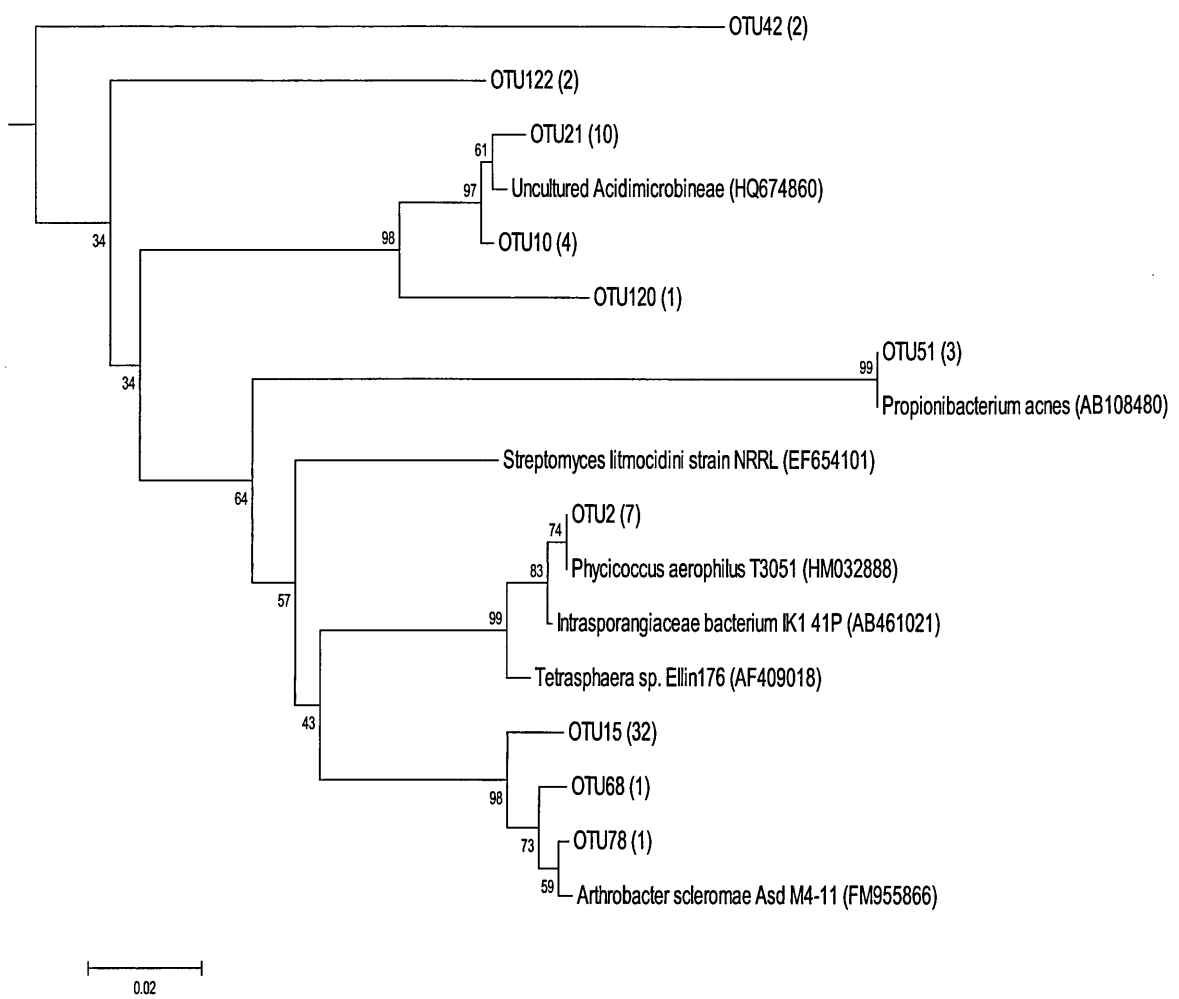

Figure 5.8. (continued)

C.

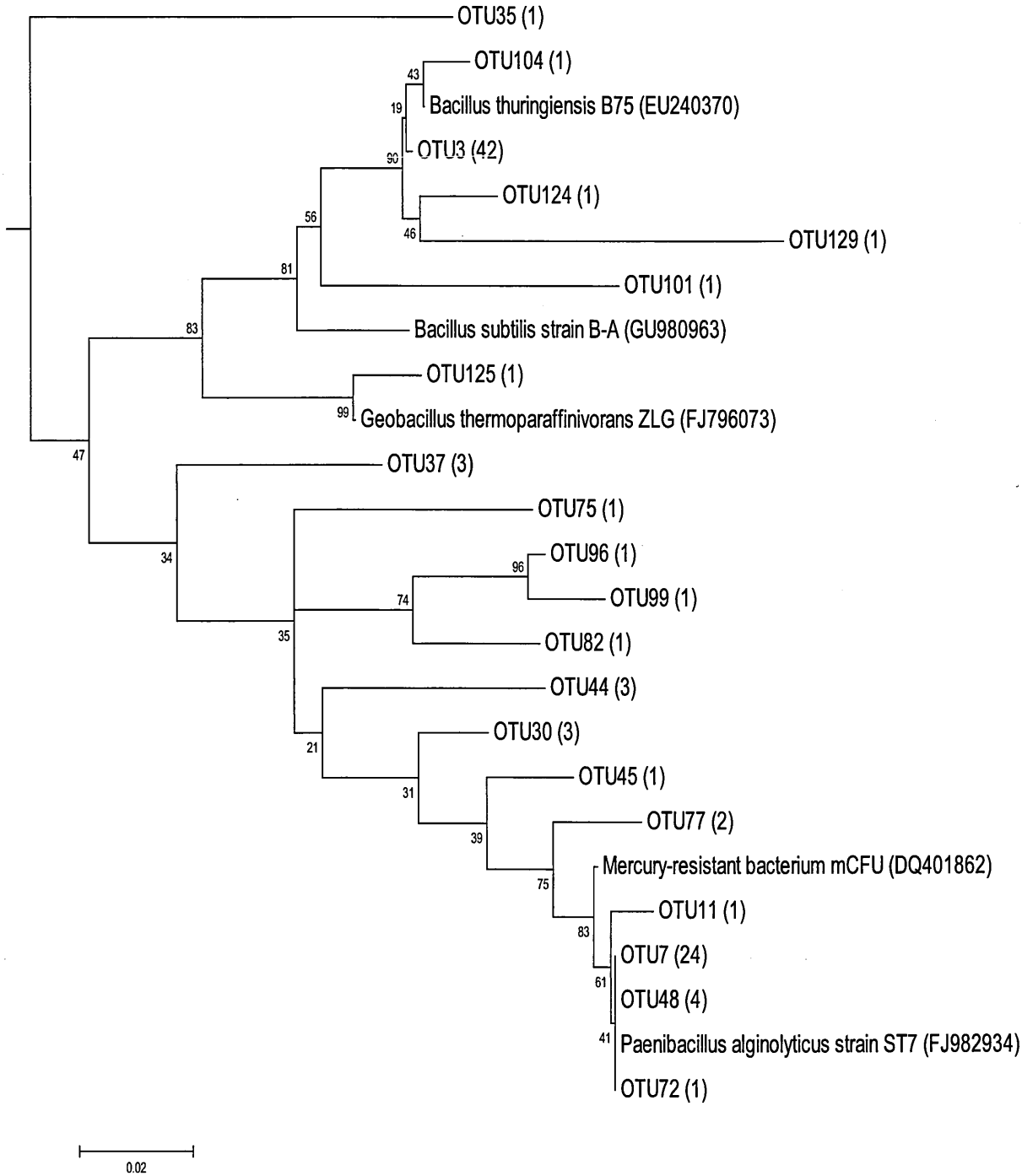

Figure 5.8. (continued)

D.

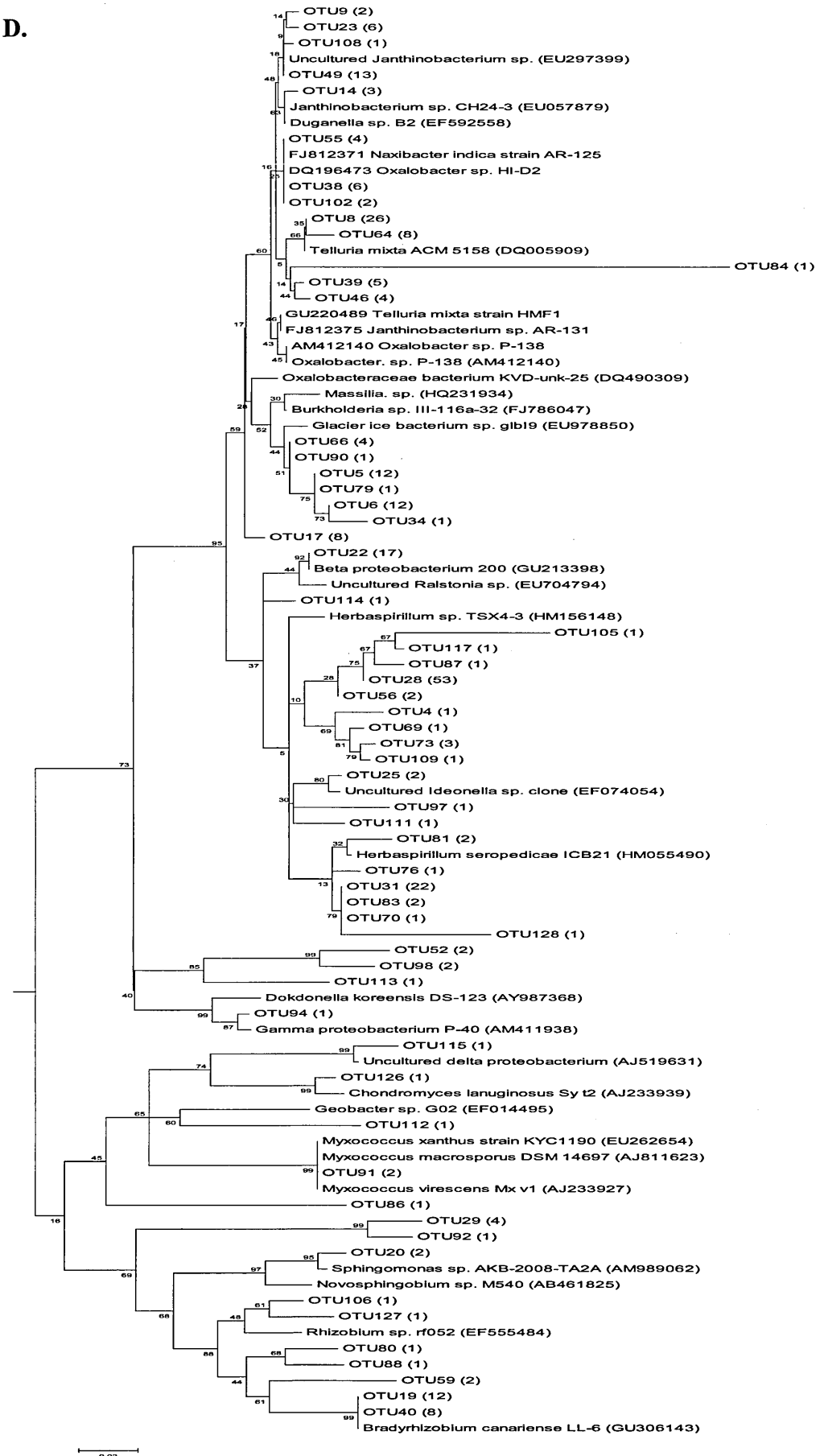

Figure 5.8. (continued)

5.3.4 Statistical Analyses on the 16S rDNA clone libraries

5.3.4.1. Clone library comparisons

Results from Libshuff (Singleton *et al.*, 2001) analysis on significant differences between the clone libraries is shown in Appendix B. For comparison of multiple libraries, the Bonferri correction (Bonferroni, 1935) was used to determine the critical p-value at or below which the libraries can be considered statistically different with 95% confidence (Singleton *et al.*, 2001; Henriksen, 2004). This critical value is calculated from the relationship: $p = 1-(1-a)^{k(k-1)}$, where 'p' is the experiment-wise p-value of 0.05, 'a' is the critical p-value, and 'k' is the number of libraries. The critical p-value in this case (with 11 libraries) was 0.00046. For each pairwise comparison, if the lower of the two p-values calculated by Libshuff was less than or equal to 0.00046, the result indicated a significant difference in the composition of the communities sampled by each library (Singleton *et al.*, 2001; Henriksen, 2004).

All libraries showed significant differences except those shown in Table 5.8. The complete Libshuff results are shown in Appendix B.

Table 5.8. Libshuff results for pairwise library comparisons that were not classed as statistically different (where the lower of the two p-values calculated by Libshuff was >0.00046).

Pairwise Comparison	Critical p-value
High 76 d – High 213 d	0.2376
High 213 d – High 76 d	0.2803
High rock – Low rock	0.0038
Low rock – High rock	0.0367
Low 76 d – Low 160 d	0.0693
Low 160 d – Low 76 d	0.0456
Low 160 d – Low 213 d	0.3915
Low 213 d – Low 160 d	0.0008

A phylogenetic tree created by MOTHUR to demonstrate clustering patterns between libraries is shown in Figure 5.9. The tree separates into two main clusters: low ratios and high ratios. The exceptions are with the rocks (High Rock library clusters with the Low Rock in the low ratio branch) and at five days where Low 5 d library clusters with High 5 d in the high ratio branch.

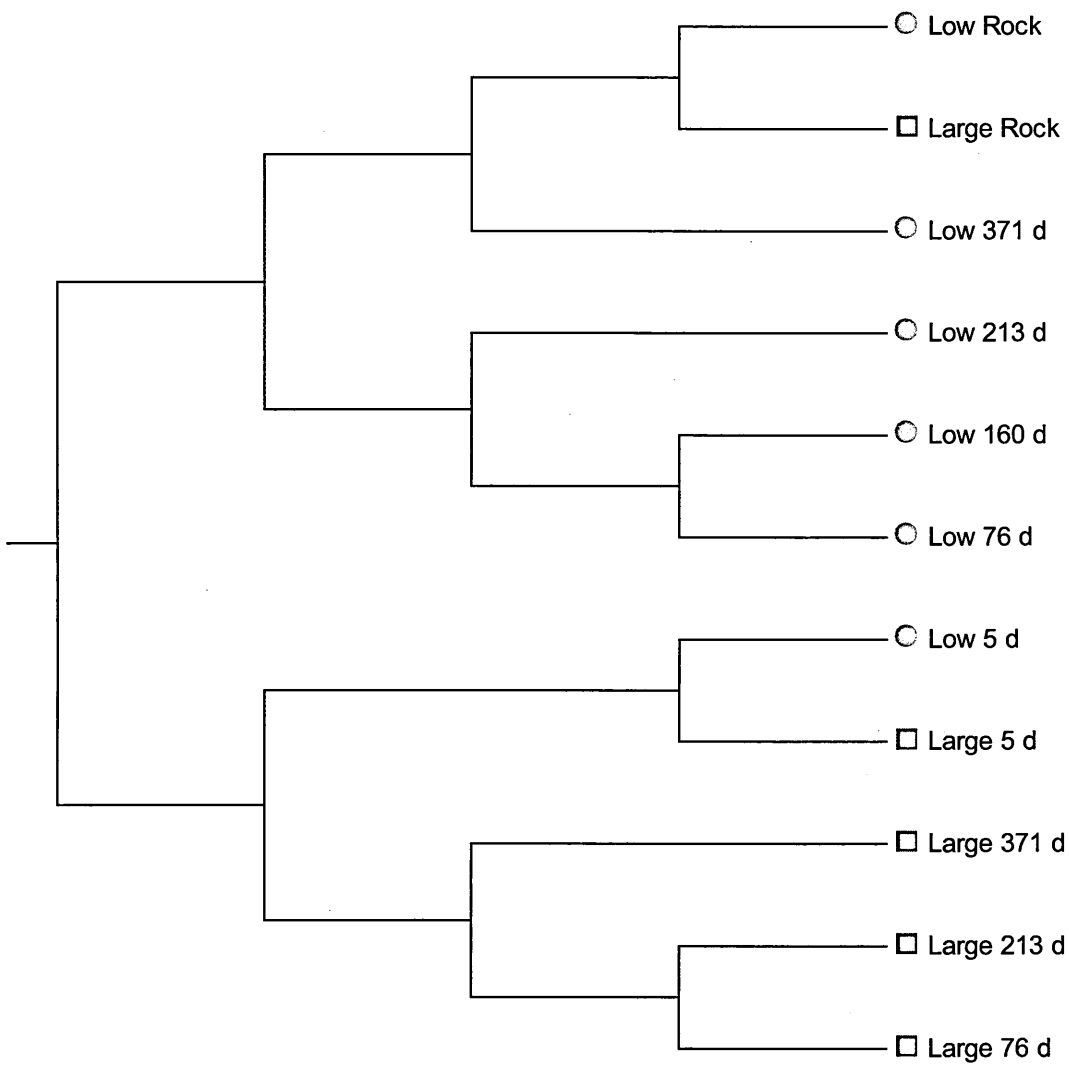

Figure 5.9. MOTHUR-created phylogenetic tree using the Jaccard index, showing high and low clone libraries at different time points (cut-off at 97%). Green circles denote the low ratios and the red squares the high ratios.

5.3.4.2. Richness, Evenness and Diversity

Using MOTHUR, species richness, evenness and diversity were calculated for the clone libraries (after sequences were chimera checked). Species richness is the number of different species in a given area, whilst species evenness is a measure of the relative abundance of the different species making up the richness of an area. As richness and evenness increase, so does diversity. The richness is represented here with rarefaction curves (Figure 5.10) and Chao1 richness estimates in Table 5.6, the evenness with rank abundance plots (Figure 5.11) and Simpson's Evenness Index (Table 5.7), and diversity using the Shannon diversity and Simpson's Reciprocal Indices (Table 5.6).

Rarefaction curves (Figure 5.10) were plotted as the number of OTUs as a function of the number of 16S rDNA sequences analysed for all the libraries (at species level). The analysis showed a high diversity of microbial phylotypes associated with both rock libraries in comparison to the solution libraries. However, analysis at species level indicated that libraries were not sampled to saturation, as some of the time points only had approximately 40 sequences analysed due to problems with sequencing, though Low 5 d and Low 371 d libraries were nearing saturation. Though a general trend can be elucidated from the rarefaction analysis, the non-saturation of the curves means that a complete picture cannot be put forth. The lower number of sequences will have an effect on statistics, such as richness, diversity, and evenness analyses.

Though a general trend can be elucidated from the rarefaction analysis, the non-saturation of the curves means that a complete picture cannot be put forth. We do not need to have saturation to do statistics; however, we are limited in understanding the complete phylogenetic diversity as we do not have full species numbers. The numbers of species quoted are not absolute as more clones would need to be sequenced to reach saturation to do this. Diversity indices will always be better with more clones as we will

have sampled the common (larger number) species found as well as the rarer (fewer number) species in the community, but one can still extract meaningful results at below saturation as it can provide an overview of the differences in species numbers.

Chao1 richness estimates (Table 5.9) indicate similar results to the rarefaction curves, with the High Rock and Low Rock libraries having higher richness values than the solution libraries at 46.43 and 48.00, respectively.

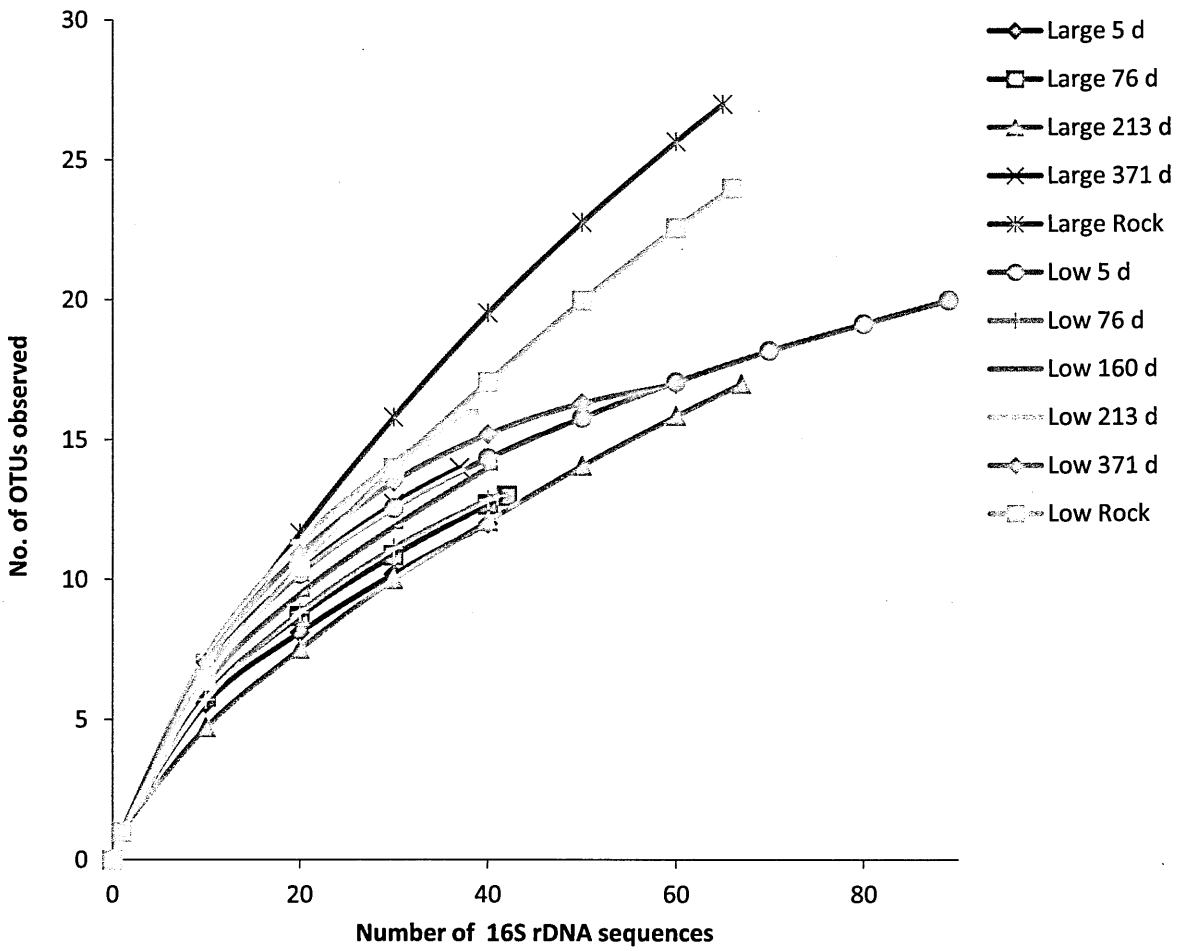

Figure 5.10. Rarefaction analysis of the diversity of bacterial clones from the high and low ratio clone libraries at different time points. The number of OTUs was plotted as a function of the number of 16S rDNA sequences analysed. Curves were calculated with sequence similarity values of 97% (species level).

Table 5.9. Richness (Chao1) and diversity estimates for bacterial 16S rDNA clone libraries from high and low ratios over time (species level) as calculated by MOTHUR.

Condition	Index		
	Chao1 (LCI, HCI)	Shannon (LCI, HCI)	Inv Simpson (LCI, HCI)
High 5 d	22.50 (14.03, 66.19)	1.98 (1.67, 2.29)	5.95 (4.21, 10.16)
High 76 d	20.00 (14.34, 49.54)	2.07 (1.76, 2.38)	6.28 (4.31, 11.61)
High 213 d	35.33 (21.48, 92.08)	1.75 (1.39, 2.11)	2.99 (2.19, 4.72)
High 371 d	17.00 (14.50, 31.95)	2.34 (2.06, 2.62)	10.09 (6.84, 19.22)
High Rock	46.43 (33.06, 89.32)	2.67 (2.35, 2.99)	8.42 (5.58, 17.20)
Low 5 d	27.00 (21.45, 53.75)	2.50 (2.29, 2.70)	9.48 (7.23, 13.78)
Low 76 d	16.00 (13.50, 30.95)	2.04 (1.70, 2.37)	5.73 (3.92, 10.64)
Low 160 d	28.00 (16.92, 81.11)	2.20 (1.89, 2.51)	7.50 (5.02, 14.80)
Low 213 d	23.00 (17.45, 49.75)	2.50 (2.23, 2.77)	12.78 (8.63, 24.59)
Low 371 d	17.43 (17.03, 22.57)	2.51 (2.29, 2.74)	10.47 (7.33, 18.33)
Low Rock	48.00 (31.12, 104.89)	2.44 (2.12, 2.77)	6.46 (4.39, 12.25)

Evenness for the libraries is shown in Table 5.10 (Simpson's Evenness Index) and in Figure 5.11 (rank abundance curves). Simpson's Evenness Index ranges between 0 (low) and 1 (high evenness); high evenness equates to the abundances of different species being similar. High 213 d had the lowest evenness at 0.18, whilst Low 213 d had the highest evenness at 0.80. The two rock libraries were second and third lowest (Low Rock second with 0.27, and High Rock third with 0.31).

Table 5.10. Simpson's Evenness Index for bacterial 16S rDNA clone libraries from high and low ratios over time (species level) as calculated by MOTHUR. The conditions are ranked based on their evenness score; the higher the rank, the higher the evenness.

Condition	SimpsonEven	Rank
High 213 d	0.18	1
Low Rock	0.27	2
High Rock	0.31	3
Low 76 d	0.44	4
Low 5 d	0.47	5
High 76 d	0.48	6
High 5 d	0.5	7
Low 160 d	0.54	8
Low 371 d	0.62	9
High 371 d	0.72	10
Low 213 d	0.80	11

The rank abundance curves offered similar results. High 213 d had the steepest gradient, whilst Low 213 d had the shallowest gradient. Both rocks also had steeper gradients compared to the rest of the curves, suggesting a larger number of rarer phylotypes.

Evenness did not appear to follow a pattern whereby evenness increased or decreased over time, nor did either ratio have more libraries with high or low evenness (both were equally distributed).

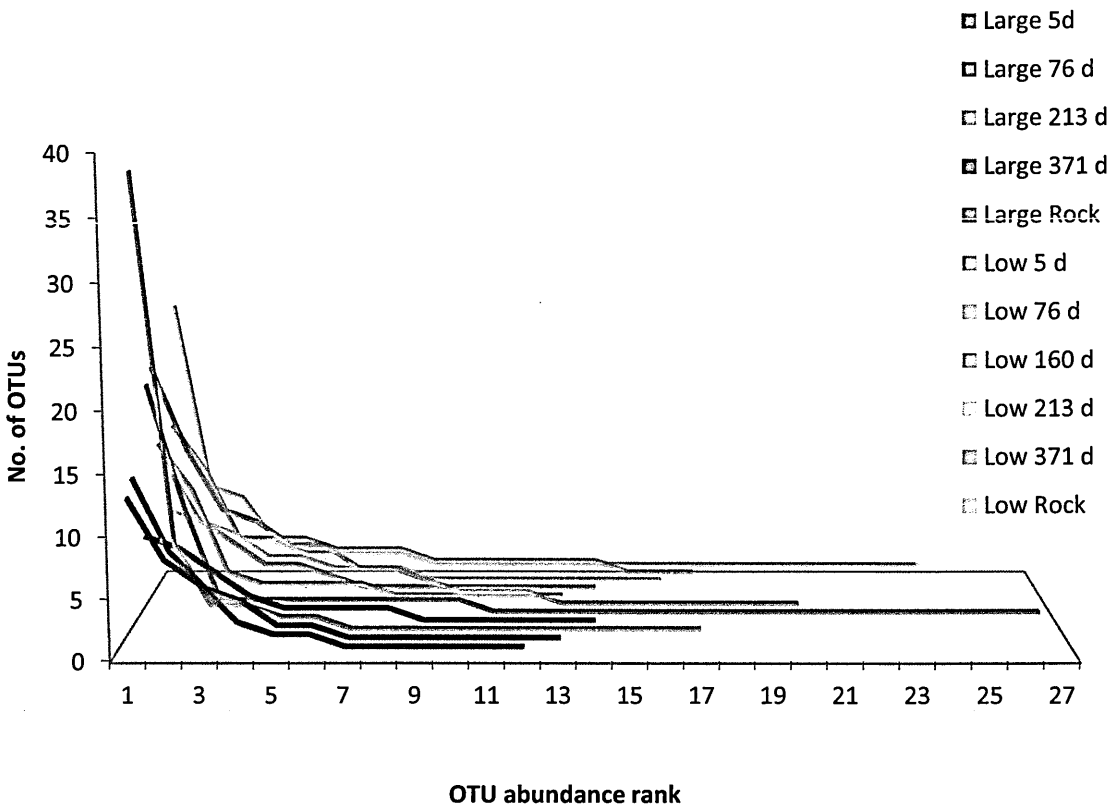

Figure 5.11. Rank abundance plots for high and low clone libraries over time (species level) as calculated by MOTHUR. Rank abundance provides a mean for visually representing species evenness. Species evenness is derived from the slope of the line that fits the graph. A steep gradient indicates low evenness as the high ranking species have much higher abundances than the low ranking species. A shallow gradient indicates high evenness as the abundances of different species are similar.

Shannon's diversity and Simpson's Reciprocal indices were calculated for the libraries using MOTHUR. From Figure 5.7, phyla were becoming more diverse over time for both ratios. This is somewhat replicated by the diversity indices in Table 5.8, which shows the diversity is lowest at 5 d (Shannon: 1.98; InvSimpson: 5.95) and highest at 371 d (Shannon: 2.34; InvSimpson: 10.09) in the high ratio. In the low ratio libraries, Low 5 d (Shannon: 2.50; InvSimpson: 9.48) is less diverse than 371 d (Shannon: 2.51;

InvSimpson: 10.47. In terms of diversity in the rocks, the high ratio (Shannon: 2.67; InvSimpson: 8.42) had a higher diversity than the low (Shannon: 2.44; InvSimpson: 6.46).

Table 5.11 summarises the richness, diversity and evenness results for the libraries, with the highest and lowest libraries for each category. High 213 d had the lowest diversity and the least abundance. The high water-rcok ratio rock had the highest richness and diversity, according to Shannon. However, InvSimpson showed low water-rock ratio 213 d to have the highest diversity. This condition also had the lowest evenness. The difference between Shannon and InvSimpson in terms of the lowest diversity may be explained by the error bands previously shown in Table 5.9, which are fairly large. The error bands for 'High Rock' and 'Low 213 d' overlapped, in the case of both diversity indeces, thus either could be classed with lowest diversity. The large error bands may have been due to the low number of clones sequenced (average of 40 sequences). Had more clones been successfully sequenced, the margin for error would most likely have been reduced.

Table 5.11. Summary of richness, diversity and evenness, showing the highest and lowest libraries for each category.

Rank	Chao1	Shannon	Inv Simpson	SimpsonEven
Highest	High Rock	High Rock	Low 213 d	Low 213 d
Lowest	Low 76 d	High 213 d	High 213 d	High 213 d

5.4 Discussion

As described in Chapter 2, rock weathering contributes to the carbonate-silicate cycle and long-term climate by consuming CO_2 in rock weathering reactions (Caldeira, 1995; Dessert *et al.*, 2001, 2003). Due to its importance, studying volcanic glass alteration in terms of microbial weathering, a less known contribution, is vital. The addition of water-rock ratios provides a broader understanding due to the varying ratios out in the field, where water-rock contact can be found with water in rock vesicles (low ratios), to rocks in a river bed (high ratios). To the best understanding, no study has been reported yet that has addressed water-rock ratios in relation to microbial weathering.

As mentioned in the introduction to this chapter, the bacterial community of the rock was known, and proved to be diverse. However, this chapter has demonstrated change in community structure over the course of a year and whether ratios would have an effect. This study has provided a snapshot of succession in subglacial basalt.

5.4.1. Change in community over time

The microbial activity in the rock is important to ascertain in order to understand weathering of rocks in more detail. From previous studies, the microbial content was known but not its activity (Cockell *et al.*, 2009a). A year-long experiment was decided upon to give an adequate time period to study changes in community, if any. Einen *et al.* (2006) carried out a year-long study on microbial colonisation and alteration of basalt glass under seafloor conditions. The study used DGGE in combination with sequencing to provide a fingerprint of bacterial community composition over time. This chapter has used a similar approach but using terrestrial volcanic glass rather than seafloor basalt, as though the potential geochemical nutrient and energy availability from terrestrial and deep-ocean basaltic glass is similar due to similar mineralogy, the

terrestrial environment is very different from the deep-ocean. Terrestrial basalt is exposed to freshwater (snowmelt), acidic rainwater, large temperature fluctuations and exposure to light, which probably account for different phylotypes (Cockell *et al.*, 2009b). This experiment also employed 16S rDNA clone libraries to increase the understanding of succession.

Einen *et al.* (2006) found Firmicutes and Proteobacteria dominating their microcosms. This was a similar case in this chapter, at least in the beginning.

The bacteria isolated from yeast extract plates fell into three phyla: Firmicutes, Proteobacteria and Actinobacteria. DNA was also extracted from bands on the DGGE where samples were run. However, attempts at sequencing failed as extraction appeared to pick up more than one sequence, either from contamination on the gel (which is not cast and kept in a sterile environment) or from more than one band being picked and sequenced. Sequencing was therefore limited to isolates and clone libraries.

A large number of isolates matched to soil bacteria, an observation also made by Kelly *et al.* (2010). They found that all the phyla identified in their clone libraries on terrestrial Icelandic volcanic glass contained clones most similar to sequences from soil environments. Actinobacteria and Proteobacteria are important groups in soils and have previously been shown to be abundant in endolithic habitats (Cockell *et al.*, 2009b; de la Torre *et al.*, 2003; Walker and Pace, 2007).

The affiliation to soil bacteria may not be so surprising considering the composition of the rock at the microscopic level is very much like soil, as basaltic glass weathers to palagonite, which is a soft secondary weathering material whose cations may be more amenable to microbial access compared to the solid rock (Kelly *et al.*, 2010). The isolates affiliating to bacteria from cold habitats are also not a surprise considering the location of the rock; Iceland's average temperature between December and February

is -2°C. Caution, however, must be attached to this statement as there is a small percentage difference between the isolates' sequences and that of the matched sequences. Though three phyla emerged through the isolates, the clone libraries showed that diversity was much higher than the isolates purported.

By the end of the year, clone libraries showed that phyla numbers totalled five and eight in the high and low ratios, respectively. Firmicutes and Betaproteobacteria dominated early on. Nemergut *et al.* (2007) studied microbial community succession in an unvegetated, recently deglaciated soil in south eastern Peru, along a chronosequence of three early successional soils. They showed that Betaproteobacteria were most dominant in the youngest soils, with abundance decreasing markedly with soil age. In this chapter's experiment, Betaproteobacteria made up 94.38% of clones at 5 d in the low ratio. However, from 76 days onwards they only accounted for a small percentage of the total (the maximum being 21.05% at 213 d). In the case of the high ratio, Betaproteobacteria were the dominant phylum (ranging from 83 to 92.54%) up until 371 d where they made up 2.78% of the total number of clones. Work done by Lysnes *et al.* (2004) on microbial community diversity in seafloor basalts from the Arctic spreading ridges found that the diversity of sequences retrieved from the basalts was dominated by Proteobacteria.

Fierer *et al.* (2010) described three general categories of microbial succession: autotrophic, endogenous heterotrophic and exogenous heterotrophic. Autotrophic succession is most likely seen in glacial till, volcanic deposits, and other newly exposed mineral surfaces (Fierer *et al.*, 2010; Hoppert *et al.*, 2004; Gomez-Alvarez *et al.*, 2007; Nemergut *et al.*, 2007; Schutte *et al.*, 2009). Its initial colonisers are predominantly autotrophs using light or the oxidation of inorganic compounds to

generate energy (Fierer *et al.*, 2010). Little or no organic carbon is initially available and the organic carbon supply changes relatively slowly over time (Fierer *et al.*, 2010). Both ratios at 5 d were dominated by *Betaproteobacteria*, specifically from the family *Oxalobacteraceae* and were heterotrophic, not autotrophs. However, Fierer *et al.* (2010) restrict their classification to primary succession dynamics, the community changes that occur following the colonisation of sterile or nearly sterile environments by microorganisms. The basalt glass in this chapter was already colonised with microbes and a carbon source was added in the form of the yeast in the media. Therefore we are beginning the succession stages with an established community and viewing the succession from that point onwards. In addition, as carbon was being added with the addition of the yeast and from the existing microorganisms in the rocks, the succession stage could be classified as both endogenously and exogenously heterotrophic, i.e. a mixture of both.

As time progressed the communities became more diverse; statistics have shown 5 d being less diverse than 371 d in both ratios. The increase in phyla diversity has been previously reported by Nemergut *et al.* (2007). They found that diversity was lowest in the youngest soils, and increased in the intermediate aged soils, before plateauing in the oldest soils. Perhaps if the experiment in this chapter had been run for longer, a plateau would have also been seen.

The diversity increase has also been reported in other studies. For example, Nicol *et al.* (2005) demonstrated an increase in archaeal diversity along a succession gradient. However, a ribosomal fingerprinting study carried out by Sigler and Zeyer (2002b) suggested a decrease in microbial diversity with soil age in early successional soils. Nemergut *et al.* (2007), however, puts forward the point that clone library techniques

are more sensitive to sequence variation in the 16S rDNA molecule, and thus may be a more accurate reflection of community dynamics.

The increase in microbial community diversity may be due to an increase in the diversity and the amount of energy and carbon inputs into the system (in forms of available light and organic material deposition) (Nemergut *et al.*, 2007). This would permit the growth of a more diverse set of microorganisms. The diversity could also be affected by changes in microecological interactions, such as competition (Nemergut *et al.*, 2007).

5.4.1.1 Nutrients and Selection

The chemistry of the flasks will be addressed in Chapter 6, where elemental concentrations and pH are discussed. However, inferences may be made already on nutrient availability from the microorganisms appearing and current literature.

At 76 days, phototrophs began to appear in all biological flasks, as witnessed by the solution turning green, microscopy and isolation on plates. For Nemergut *et al.* (2007), phototrophs appeared to be common in all soil ages. The importance of phototrophs in early successional environments is clear; in the absence of a large pool of organic carbon, carbon-fixing organisms would have a greater advantage. The emergence of phototrophs could mean additional nutrients in the flasks, which would in turn lead to the emergence of more microorganisms which would benefit from the extra nutrients. One cannot unequivocally say whether phototrophs affected the community. A repeat of the experiment should be carried out with flasks in the dark, preventing the growth of

phototrophs. If phototrophs did have an effect on the community, differences should be seen between the bacterial communities grown in the light and in the dark.

The dependence of microbes on others is illustrated in the case of *Nitrospirae* (found in the High Rock at the end of the experiment). They are nitrite oxidisers and are slow-growing specialists dependent on the supply of nitrite from ammonia oxidisers (Ehrich *et al.*, 1995), such as the Betaproteobacteria *Nitrosomonas* (Head *et al.*, 1993; Teske *et al.*, 1994). *Nitrosomonas* were found at 213 d in the high ratio. One could postulate that the appearance of these nitrite oxidisers was only possible due to the appearance of ammonia oxidisers such as *Nitrosomonas*.

Succession studies have predominantly focussed on plants. Though some studies of forefield bacterial population diversity and evenness have revealed trends different from those of plants (Sigler *et al.*, 2002a; Sigler and Zeyer, 2002b), categorisation of two sets of populations in succession can be extended to microorganisms. The characterisation is known as the r- to K-selection.

The r- and K-selection theory was developed by MacArthur and Wilson (1967), whilst Andrews and Harris (1986) provided a framework to apply the terms of r- and K-selection to microbial community succession. The theory proposes that, as communities develop, r-selected species with investment of energy mainly in reproduction will be replaced by K-selected species with relatively higher energy in maintenance and lower energy demands. Sigler and Zeyer (2002b) have shown that late succession bacterial population were less opportunistic than early succession bacteria, and Sigler and Zeyer (2004) found that there was an apparent shift from r- to K- strategists with successional age.

Ecologists have labelled organisms that are able to rapidly respond and dominate following a disturbance event as 'opportunists' (Odum, 1985) whereas 'maintenance'-type organisms are characterised by a slower response. If applied in the case of microbes, opportunistic microbes (r-strategists) would be able to rapidly take advantage of transient alterations in their environment, while less opportunistic types (K-strategists) tend to respond relatively slowly.

Early successional communities will be dominated by species with broad niche width, rapid growth, and high investment in reproduction (i.e. opportunistic organisms), whereas later successional communities will be dominated by species with narrow niche width, slower growth, and lower investment in reproduction (i.e. equilibrium organisms). These later successional communities may also account for the long tails observed in the rank abundance plot (Figure 5.11), seen predominantly in the later months of the experiments. The long tails in rank abundance plots account for less than 0.1% of the abundant species in a particular ecosystem (Sogin *et al.*, 2006). However, at the same time it represents thousands of populations, accounting for most of the phylogenetic diversity in an ecosystem. These are known as the 'rare biosphere' (Sogin *et al.*, 2006) – low abundance, high diversity groups.

Based on the descriptions of the two successional groups, predictions could also be made with regards to culturability of microorganisms in these groups.

5.4.1.2 The unculturables and succession

The diversity between isolates and clone libraries was different; isolates were not as diverse. The difference between the phyla emerging between the two may be explained by culturability. In addition phyla present in later stages of the experiment, such as *Acidobacteria*, *Verrucomicrobia* and *Gemmatimonadetes*, are known to be difficult to

culture and molecular techniques are relied upon to identify them in samples (Nemergut *et al.*, 2007). The issue of culturability is something that could be related to succession. Through the r- and K-selection theory, it could be predicted that early successional microbial communities would contain a higher proportion of culturable types; the ability to grow on non-selective medium requires that an organism directs energy into growth and not be overly specialised in its growth environments (i.e. have a broad niche width). Conversely, an increasing proportion of non-culturable types may be associated with later succession states since these types direct less energy into growth and/or have very specific growth requirements that may not be readily provided in artificial media.

The fastidious nature of the non-culturable microorganisms may be a result of the specific growth factor requirements, specialised use of a narrow range of carbon sources, or susceptibility to high nutrient concentration known to inhibit the ability to culture oligotrophic bacteria (Button *et al.*, 1993). Common to all of these mechanisms, from the perspective of successional theory, is that these organisms have become adapted to narrower, specialised niches. Garland *et al.* (2000) tested the potential of culturability as an indicator of community successional state and found that culturability decreased over time. Nemergut *et al.* (2007) also found that later successional soils showed an increase in difficult-to-culture groups including *Acidobacteria*, candidate division WYO, *Gemmatimonadetes*, and *Verrucomicrobia*. Similar findings were found in this chapter and it may also go some way in explaining why only *Actinobacteria*, *Firmicutes* and *Betaproteobacteria* were isolated on plates.

Previous studies have reported a decrease in culturability along the successional gradient (Sigler *et al.*, 2002a; Nemergut *et al.*, 2007). Nemergut *et al.* (2007) showed an increase in difficult-to-culture groups such as *Acidobacteria*, *Gemmatimonadetes*,

and *Verrucomicrobia* in later successional soils. These three phyla were also found in this study, and only in later stages for the majority, but only through clone libraries and not isolation. It is possible that these organisms utilise complex carbon substrates that would be more common in older and more developed soils, as suggested by Nemergut *et al.* (2007), and would not be replicated on plates. Another possibility is that the bacteria from these phyla require interactions with other bacteria which would also make it difficult to obtain pure cultures.

The question of culturability can also be extended to the phototrophs. Several were isolated on plates and matched to the phylum *Chlorophyta*. Five isolates matched to the same uncultured bacterium clone, despite colony morphologies being dissimilar enough to warrant sequencing. However, microscopy on the samples has shown both filamentous and coccoid phototrophs, but attempts to isolate filamentous organisms have proven unsuccessful. Perhaps, as described previously, they require nutrients that are not available in a defined medium or need the interaction with other microorganisms.

5.4.2. Rock vs. Liquid

There were several differences in community composition between rock and liquid. *Chloroflexi* and *Nitrospirae* were only detected in the rocks, whilst *Bacteroidetes*, Candidate division OD1, *Chlorophyta* and *Verrucomicrobia* were only found in the liquid. The distinction between rock and liquid has been previously noted by Lysnes *et al.* (2004). They demonstrated that seafloor basalt harboured a distinctive microbial community, as the majority of the sequences differed from those retrieved from surrounding seawater (Lysnes *et al.*, 2004). It was found that seawater was dominated by *Proteobacteria*, in contrast to the basalt samples which had several main

phylogenetic groups (*Firmicutes, Chloroflexi, Actinobacteria, Bacteroidetes, Proteobacteria* and *Crenarchaeota*) (Lysnes *et al.*, 2004). The seawater also contained *Verrucomicrobia* which, as in this experiment, was not detected in the basalts (Lysnes *et al.*, 2004).

A possible reason for the difference may be due to possible nutrient differences between the rocks and liquid. The rock may provide greater or different nutrients than the liquid or the bacteria require attachment to the rock. Certainly surface-active particles in soil and sediment do adsorb and bind organic and inorganic materials (Stotzky, 1986). Another explanation is that not enough clones were sampled for the flasks and therefore the libraries are not showing all phyla that were present. Certainly the rarefaction curves (Figure 4.10) were not saturated. Had more clones been sampled, it may be that *Chloroflexi* and *Nitrospirae* would have been detected in the liquid samples as well. However, even with partial clone libraries, rocks were more diverse as observed in the rarefaction curves. Therefore, it is likely that direct contact with the rocks provided more nutrients for the bacteria, or the bacteria required attachment to the rocks to obtain nutrients.

One issue that may arise from analysing the DNA in the flasks may be whether some of the DNA detected by the clone libraries, especially in the rock, may be due to dead cells. PCR does not discriminate viable cells from dead cells.

Extracellular DNA released from lysed and by growing bacteria has been recovered from soil (Steffan *et al.*, 1988), sediment (Ogram *et al.*, 1987), and fresh and marine waters (DeFlaun *et al.*, 1986). The primary mechanism for extracellular DNA degradation in soil is believed to be bacterial DNases (Blum *et al.*, 1997). Soil bacteria

actively secrete nucleases into the soil to increase the rate at which the nutrients in extracellular DNA become accessible, and production of DNase in soil occurs rapidly following DNA entry (Levy-Booth *et al.*, 2007). Blum *et al.* (1997) found that the number of viable microorganisms increase one order of magnitude 12 hours after DNA entry to loamy soil. In addition, during this time about 68 % of the 50 μg DNA added to the soil was degraded (Blum *et al.*, 1997). Though it appears naked DNA may not be an issue if it is degraded quickly, this is something that needs to be addressed in future work.

Rudi *et al.* (2005) have found a solution to this, whereby the viable/dead stain ethidium monoazide (EMA) was used in combination with real-time PCR. EMA inhibits the amplification of DNA from dead cells, penetrating the dead cells and binding to the DNA (Rudi *et al.*, 2005). A similar process has been reported by Lin *et al.* (2011) where they used propidium monoazide (PMA) in conjunction with PCR. PMA is a DNA-intercalating dye that only penetrates dead cells with compromised cell membrane integrity, but not viable cells with intact cell membranes (Lin *et al.*, 2011). The PMA cross links to DNA strands and forms stable covalent nitrogen-carbon bonds which prevent the DNA PCR amplification (Nocker *et al.*, 2006; Lin *et al.*, 2011).

5.4.3. Comparison of communities between high and low ratios

In terms of ratios and the microorganisms emerging, isolate sequencing did not show a clustering of isolates based on ratios. All phyla were represented in each of the three ratios obtained through isolation. However, when looking at the clone libraries on the low and high ratios, specifically at the MOTHUR-created tree (Figure 5.9), there is clustering of the two ratios, with exceptions for the rocks, that clustered together, and for 5 d, which cluster together also. The MOTHUR tree would suggest that the two

ratios, in terms of the liquid sampling, take different routes after five days; however the rocks are similar at the end of the experiment. Libshuff results also show that the rock communities are not significantly different from each other; however, the libraries of the liquid samples between the two ratios are significantly different. From this, one could suggest that communities are affected by ratios. However, it is important to note that the clone libraries were only carried out on one replicate in both high and low ratio conditions, and no libraries on the medium ratio. Thus, more concrete conclusions could be drawn if libraries were also carried out on the replicates, and whether results in the libraries could be replicated.

DGGE was performed for all samples. As Figure 5.5, however, demonstrates, the DGGE results give conflicting viewpoint as no clustering pattern emerges. As all samples were run, one might prefer the DGGE results over the clone libraries due to a more complete sampling. However, if the clustering analysis is only performed on the samples that were used in the clone library (Figure 5.12) one does see a similar clustering pattern as with the MOTHUR tree. The matching, though, may be just down to chance as similar clustering is not seen when other ratios are analysed. Perhaps if clone libraries had been done in all replicates and the medium ratio (as with the DGGE) a similar clustering pattern would have been observed.

As was the case with the clone libraries, the need for caution and more replicates is amplified when looking at the DGGE bands between replicates. Though replicates were run, differences in replicates were observed on the gel. Bands that were seen in one flask did not always show in its replicate. Cluster analysis based on the presence and absence of bands also showed no clustering of replicates. It is not inconceivable to think that if replicates were done on the clone libraries, differences might also be seen there.

The cluster analysis also showed no discernable pattern between ratios, or between time points. It appears that water-rock ratios do not exert an influence on community succession. One may go even as far as saying that, based on the differences between replicates, each rock has its own unique successional story - a microbial island so to speak. Perhaps, in contrast to a single species such as with *A. ferrooxidans*, a natural community is too complex in structure to be influenced by water-rock ratios, and also gives rise to differences between replicates.

The DGGE cluster analysis is, however, qualitative, in that the program GelCompar creates a dendogram based on the presence and absence of bands. A future analysis could possibly be on the intensity of bands and how these compare and change over time and between ratios.

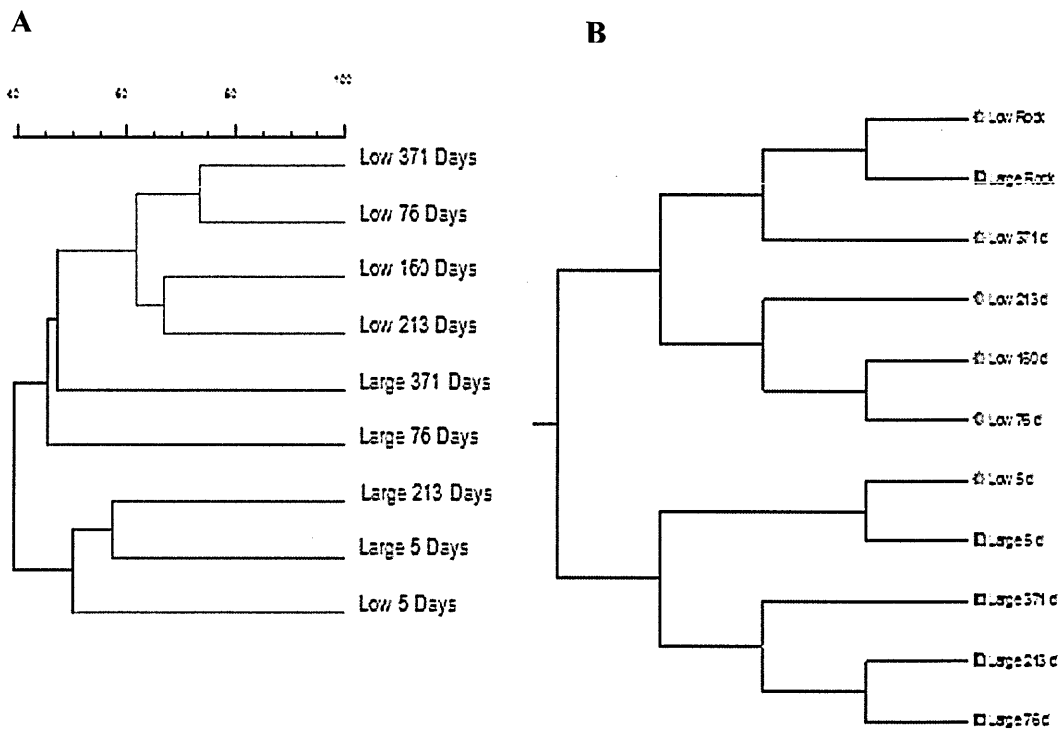

Figure 5.12. DGGE cluster analysis (A) based on the presence and absence of bands on same samples that clone libraries were carried out on. The MOTHUR tree seen first in Figure 5.9 is shown alongside (B) to compare clustering. Red colouring denotes the high ratio, whilst green is the low ratio.

5.5. Conclusions

Plant succession has been documented by ecologists for centuries. However, the successional patterns of microbial communities have received very little attention in comparison. In addition, the role microorganisms may have in weathering make them a group worthy of investigation. This chapter looked at succession in a one year-long experiment with different water-rock ratios, using molecular and culturing techniques. It was found that community structure changed over time, becoming more diverse, with a switch from r- to K-selected microorganisms over the course of the year, as reported

by previous literature. At later time points, phyla that were not culturable using conventional culturing techniques emerged. DGGE results would suggest each flask has a distinctive population - there is no correlation between ratios, and replicates also do not conform to each other. Therefore, though community does change over time as witnessed by the clone libraries, DGGE suggests that ratios do not have an effect and each flask is developing with its own 'microbial island'.

Chapter 6: Microbial Successional Changes in a One Year Laboratory Experiment on the Weathering of Basalt Glass With Different Water-Rock Ratios – Chemical Analyses and Weathering Rates

6.1. Introduction

6.1.1. Aim of Chapter

The aim of this chapter was to focus on the chemical analyses and weathering rates related to the natural community experiment first discussed in Chapter 5. In addition, a number of isolates from Chapter 5 were chosen for further experiments.

Microbes have been associated with alteration of basalt glass, which is abundant in the Earth's crust. Due to the concentration of biologically important elements present, alteration of glass makes it an important process in global biogeochemical cycling. As previously discussed, rock weathering by microbes can be influenced by varying conditions, and though variables such as temperature and pH have been investigated, water-rock ratios have not. In natural environments one can find differing water-rock ratios, from low ratios of water in rock vesicles to high ratios, such as rocks in a flowing river bed.

Though Chapter 5 allowed one to know what was in the rock and how this changed over time and with different water-rock ratios, it did not provide information on what was happening with the chemistry in the flask. With elemental release rates we should be able to correlate the microbiology to weathering conditions; were the communities accelerating weathering of the glass? As described in Chapter 5, this work has implications for the rates of rock weathering in natural environments where water-rock ratios may affect the balance between optimum energy and nutrient supply.

6.1.2. Weathering of volcanic glass

As previously described in Chapter 2, the weathering of volcanic minerals is recognised to make a significant contribution to the global silicate weathering budget (Louvat and Allégre, 1998; Dessert *et al.*, 2001; Kisakurek *et al.*, 2004). This influences carbon dioxide drawdown and climate control, since CO_2 is consumed in mineral weathering reactions. Prokaryotic involvement in volcanic rock weathering has been inferred in deep ocean basalt glass in which a diversity of microbial alteration textures has been reported (e.g. Thorseth *et al.*, 1992; Fisk *et al.*, 1998; Torsvik *et al.*, 1998; Furnes and Staudigel, 1999; Thorseth *et al.*, 2001; Etienne and Dupont, 2002; Thorseth *et al.*, 2003).

The idea that microbes can influence basalt weathering is not new (Staudigel *et al.*, 1995, 1998; Daughney *et al.*, 2004). Indeed, weathering by *A. ferrooxidans* was studied in Chapter 3. However, the majority of studies have focussed on single species and their effect on weathering of rocks. A community is a more complex matter, and a more natural set up for studying weathering rates.

6.1.3. Effect of communities on weathering

Several studies related to the weathering of minerals and rocks have indicated a complex interaction of not only physical and chemical factors, but also of the activity of microorganisms (Thorseth *et al.*, 1995). Weathering studies have typically tended to focus on single microorganisms rather than communities (e.g. Santelli *et al.*, 2001; Lüttge and Conrad, 2004; Song *et al.*, 2007; Wu *et al.*, 2007a; Wu *et al.*, 2008). In nature, the diversity of microorganisms offers a much greater variety of direct and indirect mechanisms that may responsible for basalt weathering than single organisms would (Karl, 1995; Daughney *et al.*, 2004). Microorganisms selectively oxidise, reduce

and chelate a large number of elements. In addition, during microbial activity inorganic/organic acids and alkalies resulting from metabolism will appear (Thorseth *et al.*, 1995). This will cause changes in the pH of the original environment. Chemo-organotrophic microbial communities may lower the pH to 2-4, while phototrophic communities may increase pH to above 10 due to CO_2 utilisation (Golubic, 1973; Krumbein *et al.*, 1991). As observed in Chapter 4, phototrophs began appearing in flasks from 76 d onwards. It would be expected that this would affect pH. The emergence of phototrophs would also provide a new carbon source which would encourage more microorganisms to grow, which could change the weathering rates.

In a study of basaltic glass weathering using a microbial enrichment culture from Loihi seamount, Hawaii, Staudigel *et al.* (1998) showed that the population of microorganisms, which included heterotrophic bacteria, cyanobacteria and diatoms, induced an enrichment of calcium in the sediments produced by weathering, but a loss of magnesium. In contrast, the controls showed the opposite trend. Herrera *et al.* (2008) examined bacterial communities within obsidian in Iceland. They showed a diverse population of bacteria which were shown to be associated with weathering alteration fronts in the rocks. However, Einen *et al.* (2006) observed that the bioalteration of glass with a community of microorganisms present was not different from abiotic controls. This difference may be explained by the timescale that the two studies looked at. The obsidian studied by Herrera *et al.* (2008) was approximately 2000 years old and from the field, whilst Einen *et al.* (2006) studied weathering of glass for one year in the laboratory. It may take centuries for visible alterations to occur which may explain why bioalteration in the lab does not always occur.

As with this experiment, Einen *et al.* (2006) incubated their flasks for one year whilst studying the colonisation of seafloor basalts and alteration of the glass. However, they

did not study the weathering rates of the glass or monitor the pH of the flasks, relying on visual observations of alterations instead. This chapter attempts to further information on weathering rates of glass with a succeeding natural community.

6.2. Results

6.2.1. pH measurements

The pH of the flasks was monitored every month for the entirety of the experiment. The results are depicted in Figure 6.1 and Table 6.1. The starting pH for all three ratios, control and biology, was pH 7.0. Whilst the pH of the abiotic ratios rose over time, the biotic ratios decreased in pH. By the end of the experiment, pH in the biological experiment had dropped to 5.98 for the low ratio, 6.00 for the medium and 5.27 in the high ratio. On the other hand, the controls rose from pH 7.0 to 7.33 (high ratio), 7.08 (medium ratio) and 7.03 (low ratio).

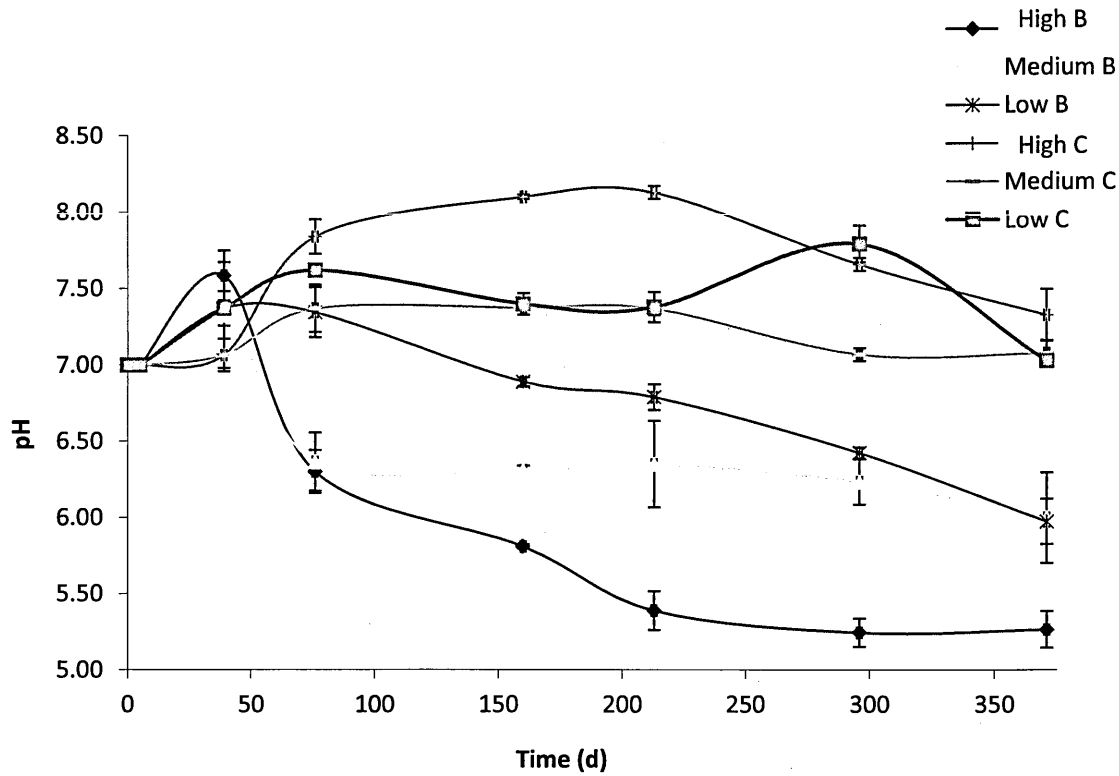

Figure 6.1. The change in average pH for the three ratios under abiotic and biotic conditions over one year. The end values are also show in Table 6.1. 'B' denotes biological flasks and 'C' denotes controls. The average pH is calculated from two replicates.

Table 6.1. Average pH values at the start and end of the one year experiment (standard deviation in brackets).

Time (d)	0	371
High B	7.00	5.27 (± 0.12)
High C	7.00	7.33 (± 0.17)
Medium B	7.00	6.00 (± 0.30)
Medium C	7.00	7.08 (± 0.08)
Low B	7.00	5.98 (± 0.15)
Low C	7.00	7.03 (± 0.01)

6.2.2. Elemental analysis

ICP-MS and –AES were carried out on the flasks to analyse REEs and trace elements. As with Chapter 4, the REEs all followed a similar pattern. A representative for REEs is shown in Figure 6.2. This shows the average release of the REE Cerium per gram of rock at the start and at day 216 of the experiment. The high ratios had the highest release whilst the low ratios had the lowest. Between the abiotic and biotic conditions, the biological experiment released more Ce than the controls in the medium and low ratios (Figure 6.2b). In the case of the high ratio, the concentration of Ce at 216 d for the high ratio was 9.25×10^{-8} g (biological experiment) and 9.37×10^{-8} g (control). However, the error bars for the two overlap, and a T-test of the means showed no significant difference (P-value >0.05). The rates of release are shown in Table 6.2.

The average release of Si and Mg are shown in Figure 6.3 and 6.4, respectively. For both elements, similar trends were observed. The average release was highest in the high ratios and lowest in the low ratios. The biological experiments had an increased release over controls for all ratios and both elements, with the exception of the low ratio for Si. In this instance, the control had a higher rate in the first 5 days (Figure 6.3b). After this, control and biological experiments were very similar in their release of Si. The linear elemental rates (Table 6.2) replicate this. In terms of Mg, the rates were fastest in the biological experiment. With Si, biological experiments had the fastest release rate in the high and medium ratios, whilst the low ratio had the fastest rate in the control. The fastest rates were found in the high ratio and the slowest in the low ratio.

The other elements analysed using ICP-AES (Ca, Fe, Na and K) were found not to produce reliable data, possibly due to concentrations being below detection limits by the machine.

Table 6.2. Linear elemental release rates (μmol per m^2 per day) from ICP-MS and -AES analysis over 213 days. The fastest release rates, when comparing biological (B) and control experiments (C), are underlined.

μmol/m^2/d	Ce	Mg	Si
High B	3.31×10^{-7}	$\underline{9.28 \times 10^{-6}}$	$\underline{1.79 \times 10^{-3}}$
High C	$\underline{3.36 \times 10^{-7}}$	3.58×10^{-6}	6.91×10^{-4}
Med B	$\underline{3.72 \times 10^{-8}}$	$\underline{1.19 \times 10^{-5}}$	$\underline{6.99 \times 10^{-4}}$
Med C	2.13×10^{-8}	6.27×10^{-6}	4.00×10^{-4}
Low B	$\underline{1.36 \times 10^{-9}}$	$\underline{2.13 \times 10^{-8}}$	1.51×10^{-6}
Low C	2.03×10^{-10}	1.42×10^{-8}	$\underline{2.02 \times 10^{-6}}$

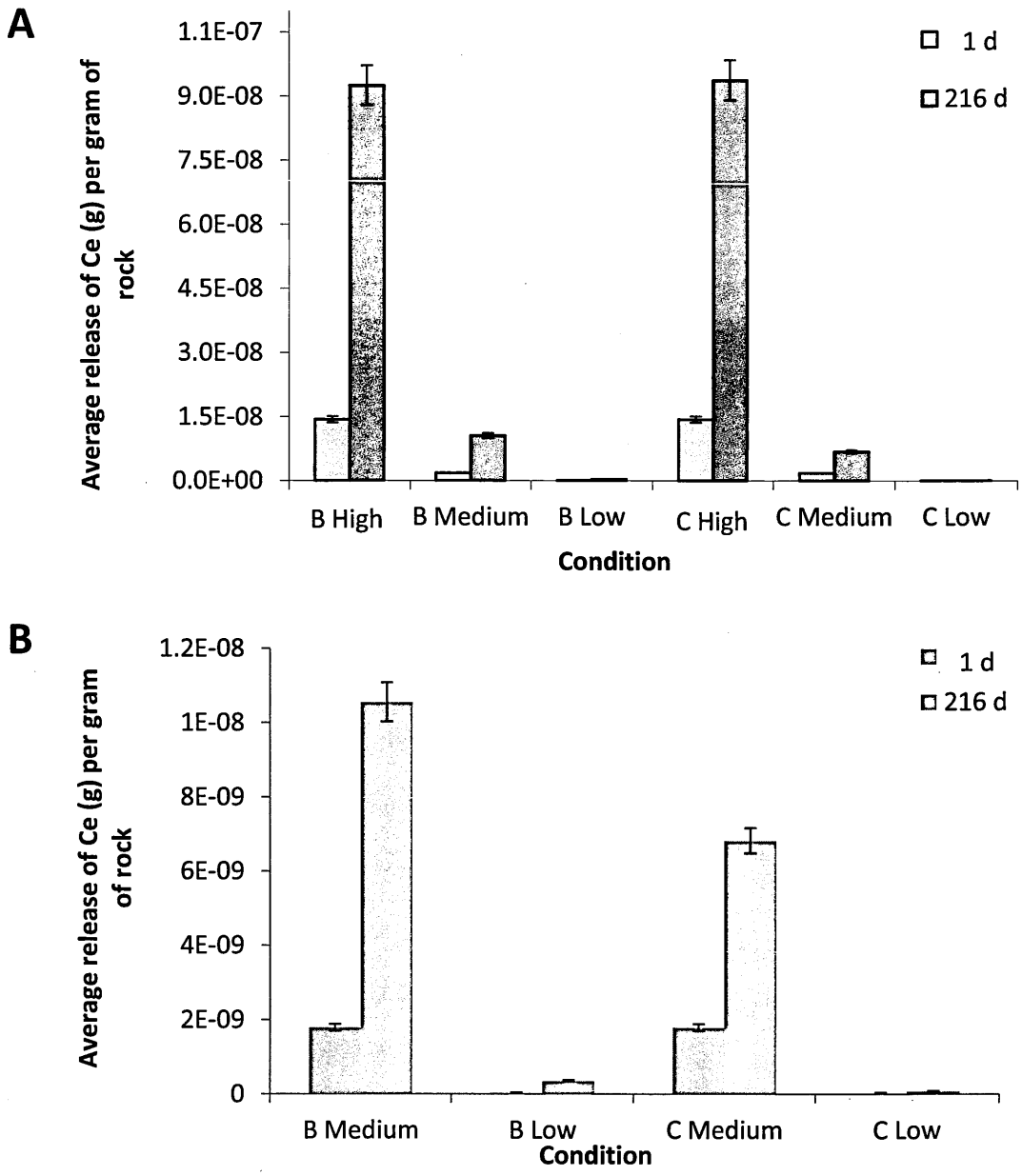

Figure 6.2. Average release of REE Ce per gram of rock at start of the experiment and at 216 d for all three ratios, controls and biology.

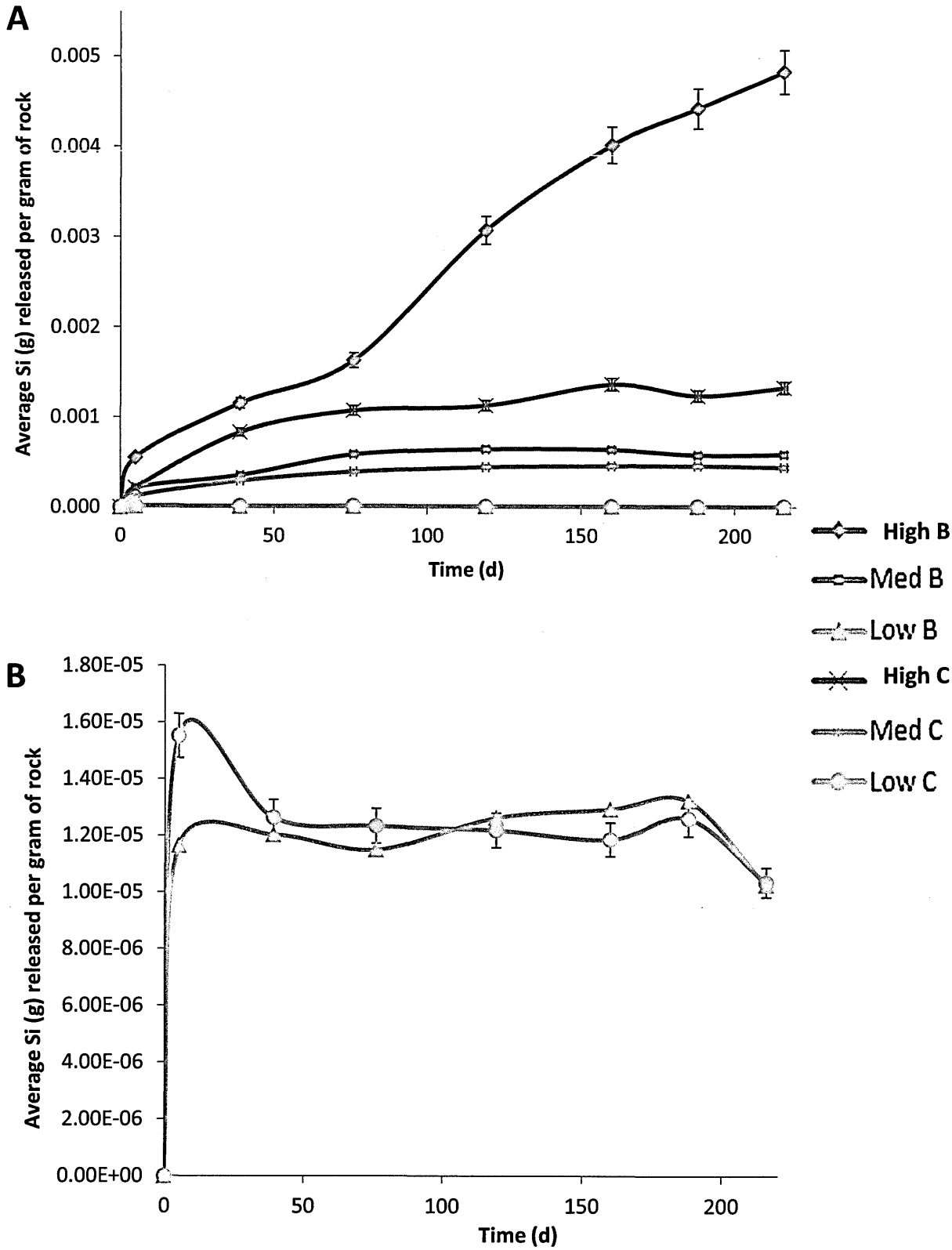

Figure 6.3. Average release over 261 d of Si per gram of rock in biotic and abiotic conditions, for high, medium and low ratios.

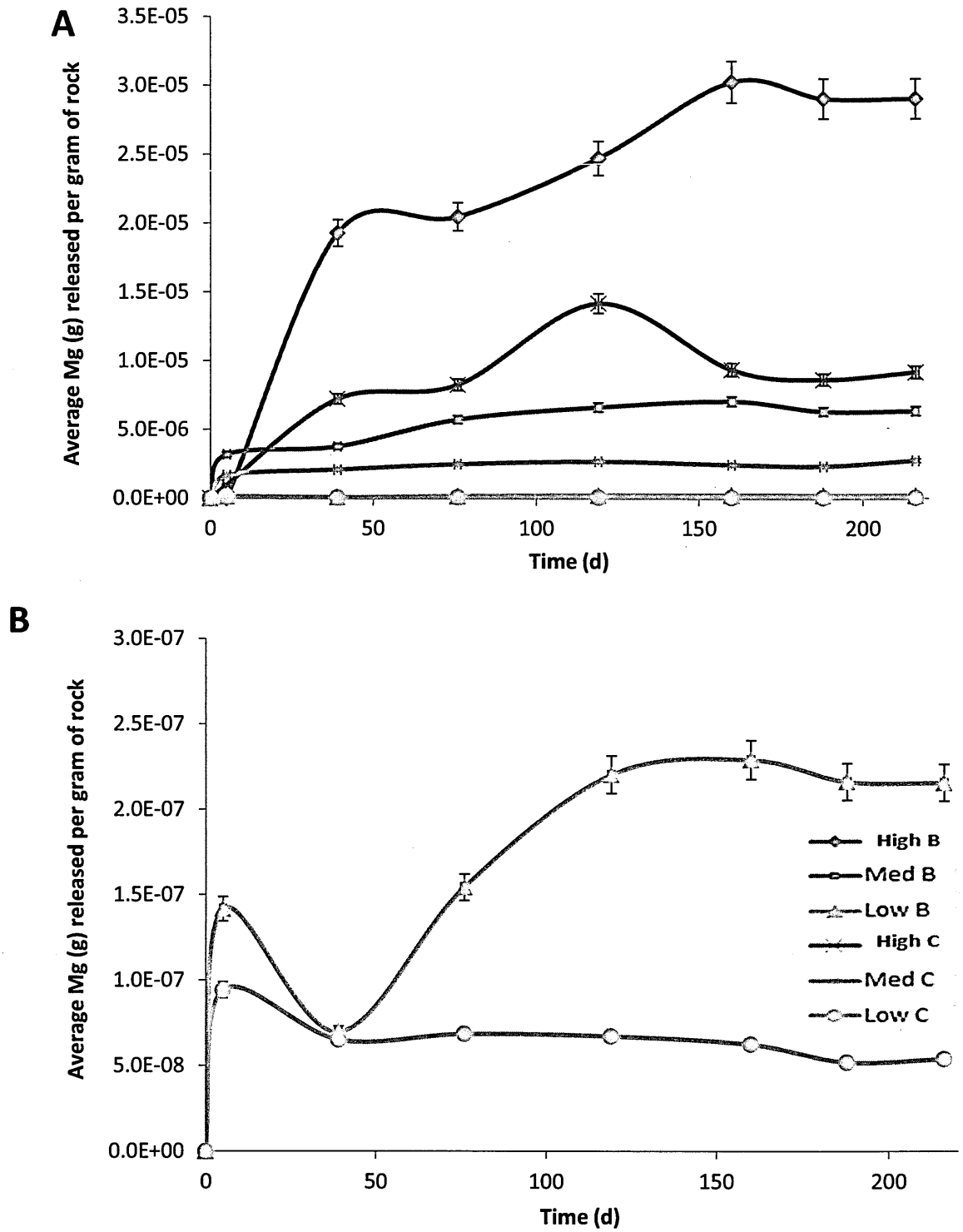

Figure 6.4. Average release over 261 d of Mg per gram of rock in biotic and abiotic conditions, for high, medium and low ratios.

6.2.3. Volcanic glass surface morphology using SEM

At the end of the experiment, SEM analysis was carried out on the rocks from the flasks to observe whether biofilms had formed on the surface of the rocks. Representative images are shown in Figure 6.5. Rod-shaped cells were observed in the medium and low ratios (Figure 6.5b and c), covering approximately 30 and 65% of the surface, respectively. That, however, was the extent of microbial attachment to the rock surfaces. Vesicles in the rock surfaces were observed in all three ratios, approximately 20 μm in diameter (Figure 6.5a, b and c) but appeared to be naturally-occurring rock features rather than biologically influenced.

A

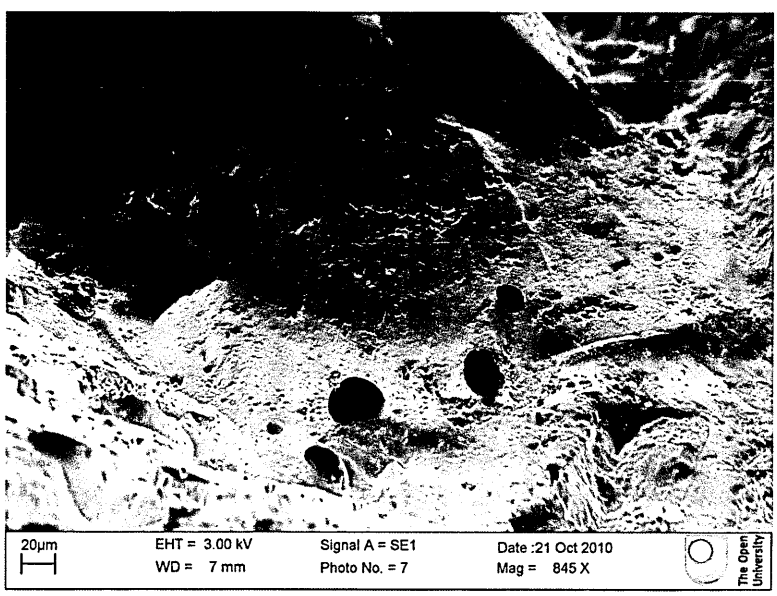

Figure 6.5. Continued overleaf.

B

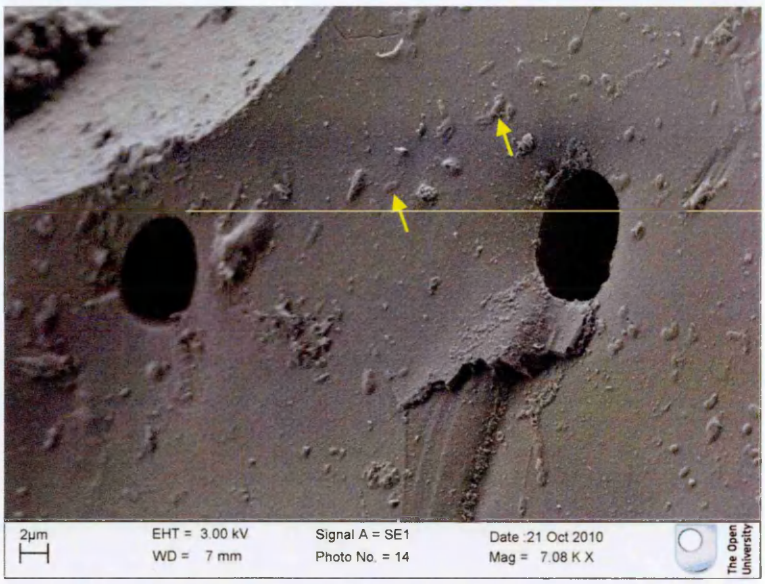
2µm
EHT = 3.00 kV
WD = 7 mm
Signal A = SE1
Photo No. = 14
Date :21 Oct 2010
Mag = 7.08 K X
The Open University

C

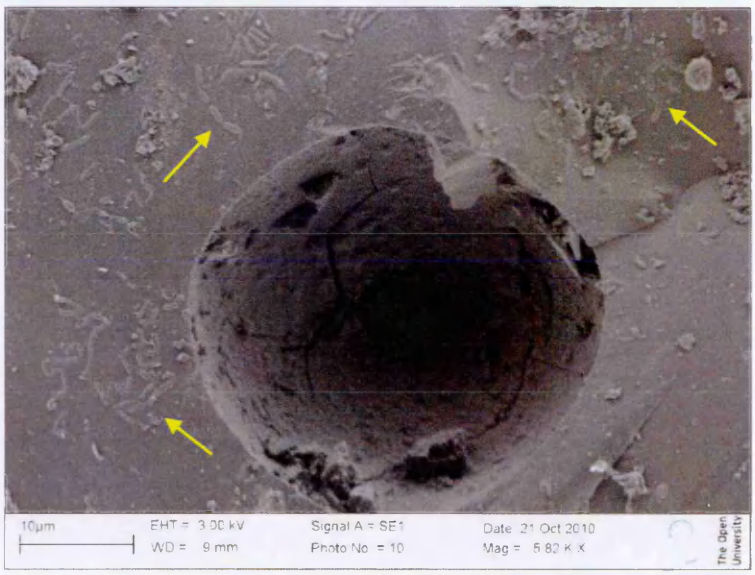
10µm
EHT = 3.00 kV
WD = 9 mm
Signal A = SE1
Photo No. = 10
Date :21 Oct 2010
Mag = 5.82 K X
The Open University

D

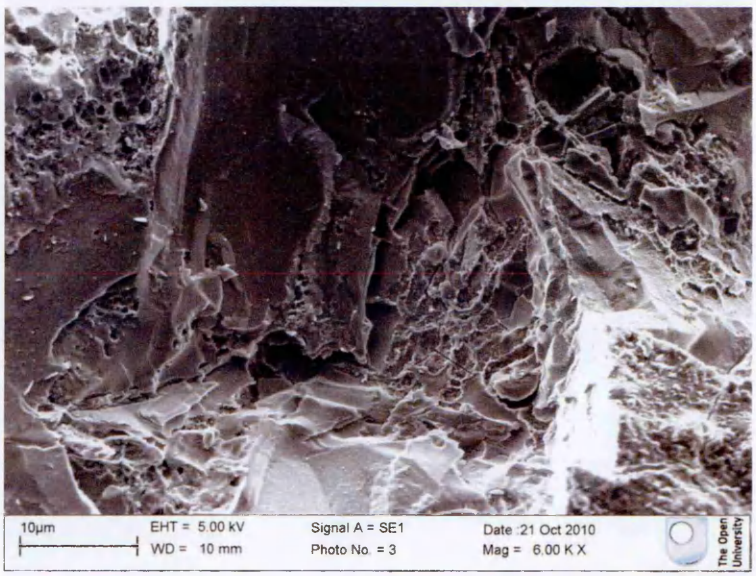
10µm
EHT = 5.00 kV
WD = 10 mm
Signal A = SE1
Photo No. = 3
Date :21 Oct 2010
Mag = 6.00 K X
The Open University

E

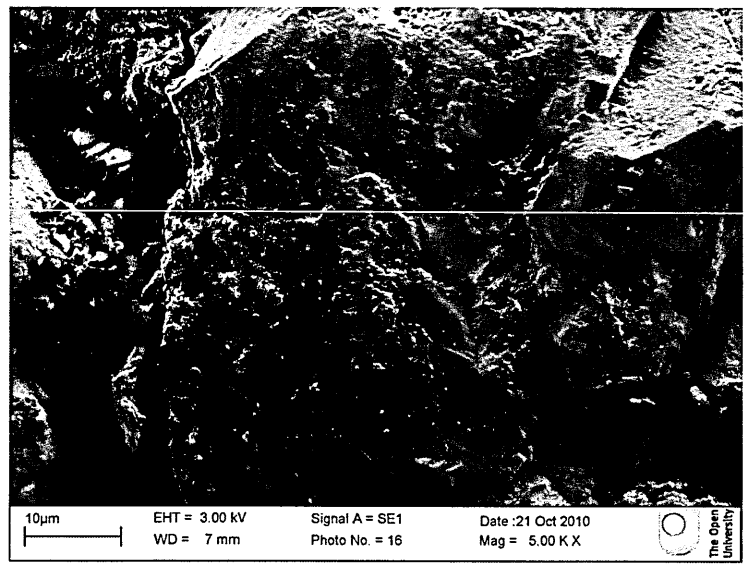

Figure 6.5. SEM images of the rock surfaces, taken at the end of the experiment. Biological experiments are shown in A-C (A: high ratio, B: medium ratio, C: low ratio) and representative controls in D-E (D: high ratio, E: medium ratio). Rod-shaped cells are seen in B and C (as shown by arrows).

6.3. Discussion

The molecular biology of the natural community experiment (Chapter 5) had drawn up a picture of what microorganisms are present in the glass and how this changes over time. Chapter 6 has gone one step further and analysed the chemistry over time and how this may be linked to the microorganisms present. At the same time as the flasks were sampled for molecular analysis, samples were also taken for elemental analysis with ICP-AES. ICP-MS analysis was also carried out at the start and at 216 d. pH was also monitored for all flasks.

6.3.1. pH

There is a large amount of evidence from observations of naturally weathered minerals (Barker and Banfield, 1996, 1998; Thorseth *et al.*, 1992, 1995a), *in situ* field experiments (Bennet *et al.*, 1996; Hiebert and Bennett, 1992; Ullman *et al.*, 1996), and *in vitro* experiments (Berthelin, 1983; Vandevivere *et al.*, 1994, Thorseth *et al.*, 1995b) that microorganisms accelerate the degradation rates of rocks and minerals by both physical and chemical processes.

Results from the study described here show that pH decreased in the biotic conditions, with the greatest drop in the high water-rock ratio flask (from pH 7 to 5.27), whilst rising slightly in the abiotic. The pH decreased despite the growth of phototrophs, which began to appear from 76 d onwards (noted by the flasks turning green). Phototrophs produce bicarbonate ions during photosynthesis, which acts to increase pH. It is possible that the phototrophs were overwhelmed by other organisms, which microorganisms may have produced strong acids that counteracted the bicarbonate ions. It is also possible that the phototrophs are not playing as large a part in the community as other microorganisms, which would also explain why they did not have a noticeable impact on pH. Interestingly, phototrophs were present even at the lowest pH observed (Flask B high water-rock ratio at 371 d – pH 5.27). As the pH is decreasing in the flasks over time, it would be interesting to examine whether they are healthy during this time or under stress by measuring Fv/Fm (the maximum quantum efficiency of photosystem II). It is a measure of how healthy phototrophs are in the sense of efficiency of photosynthesis (Genty *et al.*, 1989).

The microorganisms appeared to be influencing the pH, rather than water-rock ratios: if the latter had been the case, then the control (abiotic) flasks would have seen similar decreases in pH. The decrease in pH is in contrast to the results in Chapter 3 with *A.*

ferrooxidans, where pH increased. However, Chapter 3 dealt with the effect of only one organism instead of a community, and *A. ferrooxidans* does not produce organic acids. With communities there are more possibilities for obtaining minerals from the rocks or influencing the surrounding environment, as described in the literature review at the beginning of this thesis (Chapter 2). The production of organic acids may have influenced the environment in the flasks. It is possible that the pH decrease resulted from production of organic acids.

Barker *et al.* (1998) observed that microbial colonisation of surfaces, production of inorganic and organic acids, and extracellular polymers greatly accelerated mineral weathering reactions and released up to two orders of magnitude more material to solution than abiotic controls. Indeed, Wu *et al.* (2007a) suggested that lowered pH in the presence of microorganisms resulted from production of organic acids. Previous literature has shown that bacteria as well as fungi can acidify the surrounding medium through an ionic exchange involving the uptake of NH_4^+ and extrusion of H^+ with a 1:1 stoichiometry (Roos and Luckner, 1984; Gyaneshwar *et al.*, 1998; Reyes *et al.*, 1999). Many dissolution and precipitation reactions result in a decrease in the pH of the solution phase, although the extent of the pH change depends on which minerals are dissolving, which (if any) secondary minerals are forming, and the kinetics of the reaction(s) (Langmuir, 1997).

6.3.2. Elemental analysis

REEs rose from day 0 to day 216, with the high control and high ratio biological experiment showing similar values. However, the medium and low biological experiments showed higher releases than their control counterparts. In terms of trace elements, only Si and Mg were above detection levels for the ICP-AES (due to the

dilutions carried out on the samples in order to run them). On the whole, release rates were fastest in the biological experiments with the exception of Low B for Si, in which case the control had the fastest rate. SEM images appear to show no continuous biofilm is established on the rock surface. This would refute the theory put forward in Chapter 3 that the bacteria would contribute to the retardation of leaching of elements in this case.

One may raise the question as to whether the increased release rates in the biology are due to the microorganisms weathering the rocks directly or due to the increased acidity increasing dissolution rates, or a combination of the two. Wu *et al.* (2007a) attributed the accelerated elemental release during microbe-basalt interactions at 28°C to pH lowering during biomass production.

Releases of major structural elements such as Si, Al and Fe have been used as indicators of mineral dissolution (Barker *et al.*, 1998). Several previous experimental weathering studies have shown that release of these framework elements is most sensitive to changes in solution chemistry (Acker and Bricker, 1992; Welch and Ullman, 1993). The drop in pH in the biotic flasks may have directly affected the release of elements. For example, the dissolution rates of other, principally basaltic constituent minerals, such as olivines and pyroxenes, increase at acidic pH, which can be associated with organic acids produced by heterotrophic bacteria, fungi and plants (Wogelius and Walther, 1991; Knauss *et al.*, 1993; Drever and Stillings, 1997; Oelkers and Schott, 2001). This is in contrast to some cases where alkaline conditions will increase the dissolution of some of the key rock-forming silicate components, such as feldspars (Chou and Wollast, 1984; Schweda, 1989). Si becomes more soluble as pH becomes more basic.

Future work should involve changing the pH in abiotic flasks and observing whether there is a similar increase in release of these elements. If there is, one could also suggest that the microorganisms present are causing the mineral dissolution through affecting the pH of the solution rather than attacking the rock through other means (as described in Chapter 2). In contrast, Na, Ca, and K are preferentially leached from the mineral (Barker *et al.*, 1998). There is often no systematic variation in cation leaching with changes in solution chemistry (Welch and Ullman, 1993). Barker *et al.* (1998) studied the effects of bacteria on aluminosilicate weathering and observed that non-metabolising bacteria released Si at a factor of two higher compared to abiotic controls. They suggested that the increase in mineral dissolution may reflect complexing of mineral ions by microbial cell surfaces (Barker *et al.*, 1998). It could also be the result of lysis of microbial cells, which release low molecular weight ligands to solution, thereby catalysing mineral dissolution (Barker *et al.*, 1998).

The effect of microbially derived chemicals is amplified by increases in the amount of reactive surface area due to physical disruption by micro- and macro-organisms (Barker and Banfield, 1996, 1998). Experimental weathering studies have demonstrated that microbial extracellular polymers can react chemically with mineral surfaces and mineral ions, increasing dissolution by up to several orders of magnitude (Welch *et al.*, in preparation). With this in mind, it is not surprising that faster rates of elemental release are observed in the biological flasks. Uptake and enrichment of silica by different species of bacteria and cyanobacteria have been reported earlier by several authors (Lauwers and Heinen, 1974; Krumbein and Werner, 1983; Heinen and Lauwers, 1988). Bacteria acting as a sink for elements lost during dissolution of the glass are important when considering the chemical budget for the alteration of basaltic glass. Thus, even when the chemical/physical conditions are unsuitable for precipitation of dissolved

compounds, they may not be lost but housed in bacteria or extracellular polymers (Fyfe, 1987; Thorseth *et al.*, 1995b). As discussed in Chapter 4, intracellular elemental 71analysis should be carried out to ascertain whether elements are being housed in bacteria. There was not enough sampling liquid in this experiment to analyse both cell content and solution content but future work should aim to analyse both.

6.3.2.1. Rates

In their characterisation of elemental release during microbe-basalt interactions at 28 °C, Wu *et al.* (2007a) observed faster rates of release of elements (including Mg and Si) when bacteria were present. This is consistent with what was found in this chapter. The authors reported linear release rates for Mg and Si as 1.01×10^{-7} and 1.65×10^{-7} mol/m^2/d, respectively. Table 6.3 lists weathering rates found in literature for Si and Mg in glass and other rocks, both in the field and laboratory.

Many previous studies have reported that weathering rates in the laboratory are as much as five orders of magnitude faster than those determined from field-based studies (e.g. Swobada-Colberg and Drever, 1993; Yokoyama and Banfield, 2002; White and Brantley, 2003). For example, Yokoyama and Banfield (2002) studied the rates of rhyolite dissolution and compared them with lab measurements. Despite the authors' attempts to keep the laboratory experiment as closely comparable to field conditions as possible (not vigorously agitated), the experimental dissolution rate of the powder was approximately 84 times faster than the field rate (Table 6.3). Dahlgreen *et al.* (1999), when looking at field weathering rates of Mt. St. Helens tephra (fragmentary volcanic materials, such as ash, dust, cinders and volcanic bombs, given off during an eruption), found weathering rates of Si ranging from 8.64×10^{-10} to 8.64×10^{-11} mol/m^2/d. These rates were one to three orders of magnitude less than for glass (Si = 8.64×10^{-8} to 8.64

$\times 10^{-9}$ mol/m^2/d) (White and Claasen, 1980; White, 1983) in laboratory dissolution experiments at pH 5-7 and 25 °C. The one to three orders of magnitude discrepancy is consistent with other estimates of natural weathering rates from soils, watersheds, and groundwater aquifers (e.g. Claasen and White, 1979; Sverdrup, 1990; Swodoba-Coldberg and Drever, 1993; Velbel, 1993; White, 1995; White *et al.*, 1996). Indeed, the maximum rates in this chapter are faster than field observations in Table 6.3.

The studies on weathering rates have focussed on chemical processes (dissolution) and the slow rates in the field have mostly been attributed to uncertainties in estimations of the reactive surface area and reaction time in the field, differences in solution chemistry, and differences in surface reactivity of minerals. Dahlgreen *et al.* (1999) state that the principal factors contributing to the discrepancy between field and laboratory rates are availability of water, temperature, and the extent of solution-solid mixing which serves to reduce the influence of solute diffusion on the rates. Dissolution studies in the laboratory typically involve vigorous mixing and high solution/solid ratios to minimise the influence of diffusion (Dahlgreen *et al.*, 1999). In contrast, field rates may be limited by the lack of mixing and low solution/solid ratios ($\leq$ 1), so that solutions approach equilibrium with secondary phases (Dahlgreen *et al.*, 1999). Previous studies examining the effects of precipitation and temperature on field rates have shown a linear increase in rates with precipitation and an exponential increase with temperature (Jenny, 1941; White and Blum, 1995). Despite the numerous studies on laboratory rates being faster than field rates, the opposite has been shown as well.

Yokoyama and Matsukura (2006) showed that, in some cases, the overall weathering rate in the field can be faster than in the laboratory if physical processes are taken into account. In this instance, the weathering of granodiorite in an aquifer was inferred to proceed by initial dissolution of the mineral grain boundary (chemical process) and

subsequent detachment of the mineral grain (physical process) (Yokoyama and Matsukura, 2006). To evaluate the amount of weathering caused only by the chemical process, a laboratory dissolution experiment was conducted on granodiorite. The obtained rates were approximately 50 times slower than the field rate in the aquifer (Yokoyama and Matsukura, 2006). The authors proposed that this showed that the contribution of the physical process to granodiorite weathering in the aquifer is very large compared to that of the chemical process (Yokoyama and Matsukura, 2006).

Table 6.3. Weathering rates from literature for Si and Mg, compared to the High ratio rates in this chapter's experiment for both the biological and control experiments. 'L' denotes rates determined in the laboratory, whilst 'F' indicates field-based rates.

Type	Si (mol/m^2/d)	Mg (mol/m^2/d)	Literature
Basalt (L)	1.65×10^{-7}	1.01×10^{-7}	Wu *et al.* (2007a)
Basalt glass (L)	2.43×10^{-7}	4.43×10^{-8}	Gislason and Eugster (1987b)
Basalt glass, pH 7, 25 °C (L)	1.19×10^{-8}	-	Gislason and Oelkers (2003)
Chapter 5 rates – Biology (L)	1.79×10^{-8}	9.28×10^{-11}	This thesis
Chapter 5 rates – Control (L)	6.91×10^{-9}	3.58×10^{-11}	This thesis
Granitic gneiss bedrock (L)	$8.64 \times 10^{-7} - 8.64 \times 10^{-8}$	-	Schnoor (1990)
Granitic gneiss bedrock (F)	$8.64 \times 10^{-8} - 8.64 \times 10^{-10}$	-	Schnoor (1990)
Rhyolite powder (L)	$\sim 4.32 \times 10^{-10}$	-	Yokoyama and Banfield (2002)
Ryholite block (L)	$\sim 4.32 \times 10^{-11}$	-	Yokoyama and Banfield (2002)
Rhyolite (F)	$\sim 5.18 \times 10^{-12}$	-	Yokoyama and Banfield (2002)

There are discrepancies between rates in the literature which may results from different to experimental conditions. For example, Gislason and Eugster (1987b) determined their rates at pH 9, whereas Wu *et al.* (2007a) determined their rates at pH 4.5-6 (Oelkers and Gislason, 2001; Brantley, 2003; Gislason and Oelkers, 2003). Another example may be because of the rock surface area. In previous studies, the rocks have typically been crushed into powder and fine particles - Wu *et al.* (2007a), for example, used 45-850 μm size fractions. This would have provided fresh rock surface for the microorganisms. Bacterial access to elements, presence of fresh surfaces, and higher dissolution rates of elements could be increased with use of powder rather than crushed rock. The activity of the surfaces is important: weathered surfaces are frequently covered with oxide layers which provide a protective layer and passivate reaction and leaching. Less crushed rock is more representative of nature because the surfaces are less fresh and will weather at rates more comparable to natural rocks that are weathered.

The topic of rock surface area is further illustrated by Yokoyama and Banfield (2002). As shown in Table 6.3, the dissolution rates of silica in rhyolite was fastest in the powdered rhyolite (53-106 μm) compared to the block of rhyolite (height ~8 cm, radius ~1.5 cm) and field based rhyolite. Yokoyama and Banfield (2002) concluded that the difference between the powdered rate and field rate were probably due to the state of the samples (e.g. changes induced by crushing, in the case of powdered samples) and the conditions under which field and lab weathering reactions occur. This chapter's use of roughly crushed rock, with less fresh surface available may be more indicative of rates in the environment, where basalt is not routinely found finely crushed, with fresh surfaces available. The rates for Mg and Si in this chapter were 9.28×10^{-11} and 1.79×10^{-8} mol/m^2/d, respectively as observed in the high biological experiment and 3.58×10^{-11} and 6.91×10^{-9} mol/m^2/d, respectively as observed in the high ratio control

experiment. The values are lower than reported by Wu *et al.* (2007a). The difference between the controls and biological experiment are approximately 1.5-fold for Si and 2.6-fold for Mg. The Si values are similar to Wu *et al.* (2007a) who observed a 2-fold increase in the biological experiment; however, they also observed a 6- to 9-fold increase for Mg, which is lower than what was observed in this chapter. The discrepancy in Mg may be because of the distribution of Mg in basalt and basalt glass. The element is homogenously distributed across glass but in basalt it is located in minerals, and not evenly distributed. The difference in rates is may also be due to the rock surface. In addition, the difference in rates between the rhyolite powder and rhyolite block observed by Yokoyama and Banfield (2002) is particularly relevant.

To investigate the effects of water absorption ratio on dissolution rates and whether this may be the cause of differences between powder and block dissolution rates, Yokoyama and Banfield (2002) vacuum treated one block to completely saturate the block with water, whilst the other was just soaked in water. The same dissolution rates were obtained for samples with and without vacuum treatment (Yokoyama and Banfield, 2002). This would indicate that water penetrates into all pores - the complete surface area was wet to some extent and all pore water was connected to the external bulk water. Thus, it is unlikely that the main reason for the difference between powder and block experiments is due to restricted access of water to the reactive surfaces (Yokoyama and Banfield, 2002).

The dissolution of glass proceeds by many complicated reactions such as ion exchange, hydration, and hydrolysis of the glass framework (Yokoyama and Banfield, 2002). As a result of this, an alteration layer composed of allophane-like material and/or secondary minerals forms at the surface and a hydration layer (or diffusion layer) moves into the glass (Casey and Bunker, 1990; Bourcier, 1994; Yokoyama and Banfield, 2002). From

observations of weathered rhyolites, the thickness of both the alteration and hydration layers increase as the reaction proceeds (Yokoyama and Banfield, 2002). In the case of Yokoyama and Banfield (2002), they carried out dissolution experiments with powder and block samples of lava that had undergone weathering over 1100 years, and the surface of the glass had approximately a 6 μm wide alteration (hydration) layer (Taniguchi, 1980; Yokoyama and Banfield, 2002). In the case of the block samples, most reactive surfaces of block samples were unaffected by sample preparation. However, fresh surfaces were created for the powder by crushing. The authors suggest that it is possible that the freshly broken surfaces dissolve faster than those with an alteration/hydration layer, explaining the differences between powder, block, and field rates (Yokoyama and Banfield, 2002). This would also explain why the results in this chapter are slower than observed in other papers that used finely crushed rock. It has been suggested by Techer *et al.* (2001) that the formation of an alteration film on basaltic glass decreased the dissolution rate. In hindsight, this chapter could have been improved by running parallel flasks that had powdered rock instead of blocks of rock. If fresh surface area is the key, one would have seen faster dissolution rates in the powdered flasks compared to the flasks with larger pieces of glass.

6.3.3. Chapter 5 and chemistry

It was noted in Chapter 5 that the increase in microbial community diversity may be due to an increase in the diversity and amount of energy and carbon inputs into the system, in forms of available light and organic material deposition (Nemergut *et al.*, 2007). An increase in energy would permit the growth of more diverse sets of microorganisms. As suggested in Chapter 4, further work should involve the analysis of intracellular concentrations of the elements (Wu *et al.*, 2007a). This would allow one to analyse

whether there is a preferential uptake of some elements and would also provide more information on the nutrient requirements of the different communities emerging in the flasks, as would the concentration of carbon in the flasks over time. Knowing if there was a change in carbon over time would allow one to dispel or corroborate the r/K selection theory put forward in Chapter 5 to explain the succession patterns. Biolog plates on some of the isolates were carried out and described in Chapter 7, which offer some insight into the carbon utilisation in the flasks.

The molecular results, specifically DGGE, in Chapter 5 suggested no correlation between ratios, with each flask possibly developing its own distinctive population. However, results in this chapter would indicate that the biological experiments showed differences in pH and elemental release between ratios. This is a similar trend as observed in Chapter 4, where the high ratio had the lowest pH and fastest rates, and the low ratio had the higher pH and the slowest rates. As discussed in Chapter 4, pH affects the dissolution of minerals. For example, Blum and Lasaga (1988) showed that as acidity increases, below pH 5.5, the rates of silicate mineral dissolution increases. Biology was certainly affecting pH, which was affecting elemental release rates; however, the populations between replicates may not be so distinct from each other that they do not affect the solution chemistry in a similar way. Succession may be different between replicates, which may overwhelm the ratios; however, the chemistry they produce is similar, suggesting that the community profile differences between replicates are not enough to overpower the chemistry in the flasks.

6.4. Conclusions

In conclusion, pH decreased in the biotic flasks and rose or stayed near the starting pH in the abiotic flasks. On the whole, elemental release rates were faster in the biological

experiments, with the high ratio having faster rates and the low ratios the slowest, as observed in Chapter 4. The natural communities affected mineral dissolution, possibly through the release of organic acids, which would also account for the drop in pHs which would affect mineral dissolution in itself. The difference in dissolution rates between the results in this chapter and previous literature is possibly due to using crushed rock rather than powder. In previous studies, the rocks have typically been crushed into powder and fine particles which would have a combination of effects. Bacterial access to elements, presence of fresh surfaces, and a better ability of chemicals to be dissolved could be increased with use of powder rather than crushed rock.

Though Chapter 5 suggested no correlation between ratios, and that each flask was developing its own distinctive population, results in this chapter indicate that chemistry-wise, the biology showed differences in pH and elemental release between ratios, a similar trend as observed in Chapter 4.

Chapter 7: Microbial Successional Changes in a One Year Laboratory Experiment on the Weathering of Basalt Glass With Different Water-Rock Ratios – Physiological Profiles

7.1. Introduction

7.1.1. Aim of Chapter

The aim of this chapter was to focus on some of the microorganisms isolated from the natural community experiment first described in Chapter 5. Microbial communities from basalt glass were observed under different water-rock ratios for one year. Chapter 4 dealt with the community composition over time through isolation, 16S rDNA clone libraries and DGGE, whereas Chapter 6 analysed the chemistry in the flasks. This chapter selected a number of isolates from Chapter 5 and carried out further investigations on them. Carbon utilisation profiles and tolerance to pH and heavy metals were carried out. On one isolate (Medium-4-188d), the possibility of magnetotaxis was also analysed.

7.1.2. Individual isolates

The isolates picked for further analysis are shown in Table 7.1, alongside their closest relative matches on BLAST. These were selected because bacteria matching to *Paenibacillus* sp., *Arthrobacter* sp. and *Bacillus* sp. were isolated in all three ratios at various time points. The Firmicutes, Actinobacteria and Proteobacteria were found in all three ratios (Chapter 5). The isolates tested in this chapter were found in a range of pHs, from pH 7.35 to 5.25. The pH of the medias ranged from pH 7.59 (maximum) to pH 5.27 (minimum) (Chapter 6).

Table 7.1. Isolates used for pH and heavy metal tolerance tests, alongside their closest relative matches on BLAST. The isolate naming system is as follows: ratio-isolate number-day of experiment. Algal-1-160d was found in all three ratios from 76 d onwards, however, the isolate used in this chapter was from 160 d (the pH given for this isolate is the range it was found at, from 76 d to 371 d).

Isolate (Accession #)	pH of flask when sampled	Closest relative (BLASTn)
High-5-213d (JN627971)	5.39	*Humicoccus* sp.
High-7-296d (JN627973)	5.27	*Cohnella* sp.
Medium-3-188d (JN628001)	6.31	*Bradyrhizobium* sp.
Medium-4-188d (JN628002)	6.31	*Rhodococcus erythropolis*
Medium-6-188d (JN628004)	6.31	*Arthrobacter* sp.
Medium-7-213d (JN628005)	6.35	*Streptomyces* sp.
Medium-12-371d (JN627994)	6.00	*Microbacterium* sp.
Medium-13-371d (JN627995)	6.00	*Bosea thiooxidans*
Low-4-39d (JN627986)	7.37	*Variovorax paradoxus*
Low-8-188d (JN627990)	6.89	*Bacillus cereus*
Low-11-213d (JN627976)	6.79	*Paenibacillus alginolyticus*
Low-15-371d (JN627980)	5.98	*Skermanella* sp.
Low-16-371d (JN627982)	5.98	*Sphingomonas* sp.
Algal-1-160d (JN628008)	6.30 – 7.35	Uncultured bacterium clone QB78

7.2. Experimental design

The isolates chosen for further investigation are shown in Table 7.2. Pure cultures were obtained as described in Chapter 5. Colonies were picked from each of the pure cultures and transferred to 250 ml Erlenmeyer conical flasks containing 100 ml 0.2 g l^{-1} yeast extract medium. The cultures were incubated at 21 °C in Milton Keynes, UK, in natural sunlight with a natural diurnal illumination cycle. The cultures were monitored

for growth, and after approximately 5 days of growth, the cultures were ready for downstream applications.

Table 7.2. Isolates used for pH and heavy metal tolerance tests, alongside their closest relative matches on BLAST.

Isolate (Accession #)	Closest relative (BLASTn)		
	ID (Accession #)	Max. ident. (%)	Sampling environment
HIGH RATIO			
High-5-213d (JN627971)	*Humicoccus* sp. A24MTO (FN293194.1)	99 %	Alpine tundra
High-7-296d (JN627973)	*Cohnella* sp. GT-L22 (GQ355279.1)	96 %	Tidal flat sediment
MEDIUM RATIO			
Medium-3-188d (JN628001)	*Bradyrhizobium* sp. CCBAU 85080 (EU256466.1)	99 %	Rhizobial resource in Tibet
Medium-4-188d (JN628002)	*Rhodococcus erythropolis* strain cmmb1 (GU120079.1)	100 %	Marine water from the Gulf of Mannar
Medium-6-188d (JN628004)	*Arthrobacter* sp. MNPB6 (FM213396.2)	100 %	Glacier and cold environments of Lahaul and Spiti, India
Medium-7-213d (JN628005)	*Streptomyces* sp. ZS1-2 (DQ408296.1)	100 %	Antarctica
Medium-12-371d (JN627994)	*Microbacterium* sp. DVS4a2 (AY864634.1)	99 %	Dry Valley in Antarctica
Medium-13-371d (JN627995)	*Bosea thiooxidans* strain MGV6-VS (AJ250799.1)	99 %	Rhizoplane of *Medicago sativa* (alfalfa)
LOW RATIO			
Low-4-39d (JN627986)	*Variovorax paradoxus* strain B55 (EU169153.1)	100 %	Rhizosphere soil of *Bashania fangiana* (bamboo)
Low-8-188d (JN627990)	*Bacillus cereus* strain ZY-02 (GU181319.1)	100 %	Wastewater of Sibao (China) sewage treatment plant
Low-11-213d (JN627976)	*Paenibacillus alginolyticus* strain ST7 (FJ982934.1)	99 %	Anaerobic granular sludge
Low-15-371d (JN627980)	*Skermanella* sp. VTT E-073090 (EU438962.1)	98 %	Paper mill pulps containing recycled fibres
Low-16-371d (JN627982)	*Sphingomonas* sp. AKB-2008-VA4 (AM989065.1)	99 %	Treated drinking water
SEEN IN ALL			
Algal-1-160d (JN628008)	Uncultured bacterium clone QB78 (FJ790633.1)	99 %	Quartz Pavement in the High-Altitude Tundra of Central Tibet

7.2.1 Biolog plates

Carbon source utilisation profiles were constructed for the isolates listed in Table 7.3 using Biolog-GN2 and -GP2 Microplates (Biolog Inc., Hayward, California, USA). The Biolog-GN2 was designed for Gram-negative bacteria and the GP2 for Gram-positive. Isolates were removed from growing culture by pelleting cells gently for five minutes at 2000 rpm. Cells were then re-suspended in sterile distilled water. The microplates were then inoculated by adding 100 µl of suspended cells into each well and incubated at 21 °C. The plates were monitored over three days by observing colour change (whether the well changed from colourless to purple).

Table 7.3. Isolates used for Biolog plates and the type of Biolog plate used for each.

Isolate (Accession #)	Biolog plate
Low-4-39d (JN627986)	GN2
Medium-3-188d (JN628001)	GN2
Medium-13-371d (JN627995)	GN2
Low-15-371d (JN627980)	GN2
Low-16-371d (JN627982)	GN2
Low-11-213d (JN627976)	GP2
Low-8-188d (JN627990)	GP2
High-5-213d (JN627971)	GP2
High-7-296d (JN627973)	GP2

7.2.2. Tolerance experiments

The pH and heavy metal tolerances of the isolates were tested. The heavy metal tolerance of the isolates was tested to ascertain whether the heavy metal concentrations observed in the experiment may have had an effect on isolate growth or the absence of isolates later in the timeline. Table 7.4 outlines the different conditions set up.

Table 7.4. Outline of different conditions tested with the isolates.

Flask	Tolerance	Concentration
Condition 1	Untreated	-
Condition 2	Heavy metals	Maximum leach
Condition 3	pH 5	-
Condition 4	pH 6	-
Condition 5	pH 7	-
Condition 6	pH 8	-

As with Chapter 5, for the heavy metal tolerance tests, concentrations were based in ICP-MS data obtained on the leach solution at the end of the experiment. Table 7.5 lists the heavy metals added to 0.2 g l^{-1} yeast extract agar plates and the concentrations tested. Isolates were streaked onto plates and incubated at 21 °C. If growth occurred, the isolate was recorded as tolerant to the condition, and no growth as negative tolerance. In addition to the isolates, samples were directly taken from the flasks and inoculated into liquid yeast media which had had the heavy metals added. Untreated liquid cultures were also run. The reason for sampling the flasks directly was to record phototroph tolerance as some of the phototrophs would only grow in liquid culture and could not be isolated for individual tests.

Similarly to the heavy metal tolerance tests, pH tolerance was tested by streaking the isolates onto yeast extract with pH altered. The pH of the agar was adjusted with HCl or NaOH prior to autoclaving. In addition to the isolates, samples were again taken directly from the flasks and added to liquid yeast media that had had its pH altered. Growth was recorded as tolerance, no growth as negative tolerance.

Table 7.5. Heavy metal composition in heavy metal tolerance flasks. They are the maximum concentrations as found in solution at the end of the experiment (from ICP-MS data).

Metal	Chemical form	Leach concentration (mM)
Copper	$CuSO_4.5H_2O$	2.00×10^{-3}
Cobalt	$CoSO_4.7H_2O$	1.36×10^{-5}
Zinc	$ZnSO_4.7H_2O$	5.01×10^{-3}
Nickel	$NiSO_4.6\ H_2O$	9.69×10^{-5}
Lead	$Pb(NO_3)_2$	1.21×10^{-5}
Tin	$SnCl_2$	2.02×10^{-6}

7.2.3. Magnetotaxis with Medium-4-188d

From sequencing matching, isolate Medium-4-188d matched 100 % to *Rhodococcus erythropolis* strain cmmb1 (GU120079.1), a strain which was reported by its submitting authors as exhibiting magnetotaxis. A small experiment was devised to test whether this was true for the isolate.

Four petri dishes were set up on the lab bench: two would be controls (no magnet), and two would have a magnet attached, either with a South polarity or a North polarity (if the isolate had a polarity preference). The yeast extract media was made up with 0.25 % agar and autoclaved. Thirty ml of media was added to each petri dish along with 3 ml of culture and mixed. The petri dishes were set up as in Figure 7.1. The marked distances were drawn into onto the bottom of the petri dishes and these acted as the sampling points. For five days the points were sampled, with one ml removed and filtered stained with SYBR green (Chapter 3) and viewed under the fluorescence microscope. Fifty fields of view were counted for each point and plate and converted to cells per ml. If the isolate was magnetotactic, one would expect more cells nearer the

magnet and less further away. However, if they were not magnetotactic, one would expect no difference between the distances.

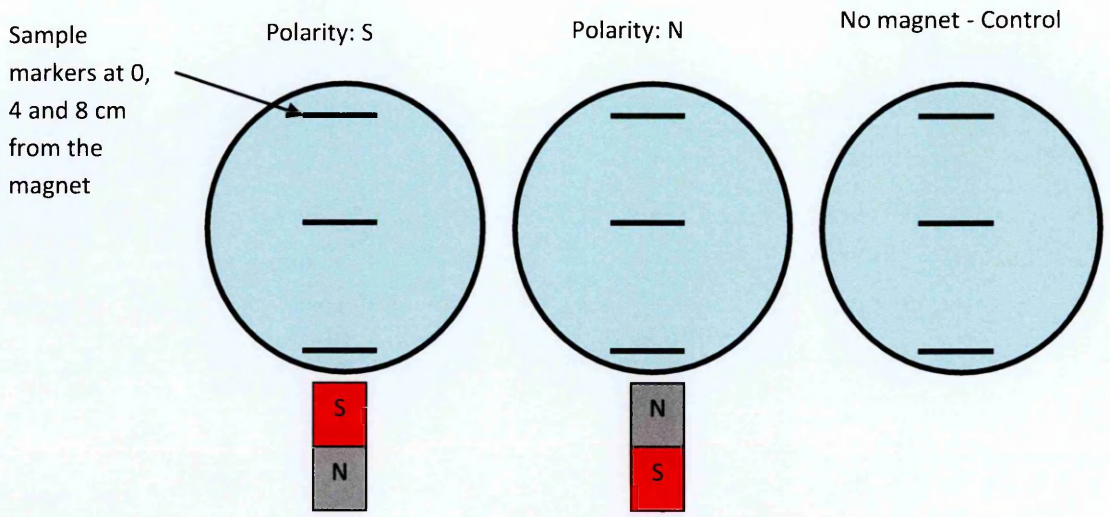

Figure 7.1. Set up of magnetotaxis experiment with petri dishes for isolate Medium-4-188d. The strength of the magnet decreases the further away the magnet is.

7.3. Results

7.3.1. Biolog plates

The carbon utilisation of selected isolates is shown in Table 7.6 (Gram-negative plates) and Table 7.7 (Gram-positive plates). The isolates were all capable of degrading numerous common sugars and amino acids. On the whole, the isolates shared a number of carbon sources between each other, and also utilised a great number. The exception was isolate Medium-3-188d, which utilised 8.42 % of the carbon substrates available. In comparison, the rest of the isolates utilised 22-51.56 % of the carbon substrates available (Table 7.8).

Table 7.6. Carbon utilisation of Gram-negative isolates on Biolog GN2 microplates. A positive marker denotes utilisation of the carbon (by way of a change in colour), and the negative sign denotes no use.

Carbon Source	Low-4-39d	Medium-3-188d	Medium-13-371d	Low-15-371d	Low-16-371d
Tween 40	+	-	+	+	-
Tween 80	+	-	+	+	-
N-Acetyl-D Galactosamine	+	-	-	-	-
N-Acetyl-D Glucosamine	+	-	-	+	+
Adonitol	+	-	-	-	+
L-Arabinose	+	-	+	-	-
D-Arabitol	+	-	+	+	-
i-Erythritol	-	-	-	-	+
D-Fructose	+	-	+	+	+
L-Fucose	+	-	-	-	-
D-Galactose	+	-	+	+	-
Gentiobiose	-	-	-	-	-
α-D-Glucose	+	-	+	+	-
m-Inositol	+	-	+	-	+
α-D-Lactose	-	-	-	-	+
Maltose	-	-	-	-	+
D-Mannitol	+	-	+	+	-
D-Mannose	+	-	-	-	-
D-Raffinose	-	-	+	+	-
L-Rhamnose	-	-	-	-	+
D-Sorbitol	+	-	+	+	-
Sucrose	-	-	+	+	-
D-Trehalose	-	-	+	+	-
Turanose	-	-	-	+	-
Xylitol	+	-	-	-	-
Pyruvic Acid Methyl Ester	-	-	+	-	-
Succinic Acid Mono-Methyl-Ester	+	-	-	-	-
Cis-Aconitic Acid	-	+	+	+	-
Citric Acid	-	+	+	+	-
Formic Acid	+	-	-	-	-
D-Galactonic Acid Lactone	+	-	+	+	-
D-Galacturonic Acid	-	+	+	+	-
D-Gluconic Acid	+	+	+	+	-
D-Glucosaminic Acid	-	-	+	+	-
D-Glucuronic Acid	-	+	+	+	-
α-Hydroxybutyric Acid	+	-	-	-	+
β-Hydroxybutyric Acid	+	-	+	+	-
Itaconic Acid		-	-	-	+
α-Keto Butyric Acid	+	-	-	-	-

α-Keto Glutaric Acid	+	-	+	+	-
D,L-Lactic Acid	+	-	+	+	-
Malonic Acid	-	-	+	-	-
Propionic Acid	+	-	+	-	+
Quinic Acid	+	-	+	+	-
D-Saccharic Acid	-	+	+	-	-
Sebacic Acid	+	-	-	-	+
Succinic Acid	+	-	+	-	-
Bromosuccinic Acid	+	+	+	+	-
Succinamic Acid	+	-	-	-	-
Glucuronamide	-	-	-	-	+
L-Alaninamide	+	-	-	-	-
D-Alanine	+	-	+	+	+
L-Alanine	+	-	+	+	-
L-Alanylglycine	+	-	-	-	-
L-Asparagine	+	-	+	+	-
L-Aspartic Acid	+	-	+	+	+
L-Glutamic Acid	+	+	+	+	
Glycyl-LAspartic Acid	-	-	-	-	+
Glycyl-LGlutamic Acid	+	-	-	-	-
L-Histidine	+	-	+	+	-
Hydroxy-LProline	+	-	-	-	-
L-Leucine	+	-	-	-	-
LPhenylalanine	+	-	-	-	+
L-Proline	+	-	+	+	+
L-Pyroglutamic Acid	+	-	+	+	-
D-Serine	-	-	-	-	+
L-Serine	-	-	+	+	+
D,L-Carnitine	+	-	-	-	-
γ-Amino Butyric Acid	-	-	+	-	-
Urocanic Acid	+	-	+	+	-
Inosine	+	-	+	+	-
Uridine	-	-	-	-	+
Phenyethylamine	+	-	-	-	-
Putrescine	-	-	+	+	-
Glycerol	-	-	+	+	-
D,L-α-Glycerol Phosphate	-	-	+	+	-

Table 7.7. Carbon utilisation of Gram-positive isolates on Biolog GP2 microplates. A positive marker denotes utilisation of the carbon (by way of a change in colour), and the negative sign denotes no use.

Carbon Source	Low-11-213d	High-5-213d	Low-8-188d	High-7-296d
Dextrin	+	-	-	-
Glycogen	-	-	-	+
Inulin	-	-	-	+

Tween 40	+	+	-	-
Tween 80	+	+	+	-
N-Acetyl-D Glucosamine	+	+	-	+
N-Acetyl-β-D Mannosamine	-	-	-	+
L-Arabinose	+	+	+	-
D-Arabitol	+	+	+	+
D-Cellobiose	-	-	-	+
D-Fructose	+	+	+	-
L-Fucose	-	-	+	+
D-Galactose	-	-	+	-
D-Galacturonic Acid	+	+	+	-
Gentiobiose	-	+	-	-
D-Gluconic Acid	+	+	+	-
α-D-Glucose	+	+	+	+
m-Inositol	-	+	+	
Maltotriose	-	-	-	+
D-Mannitol	+	+	+	
D-Mannose	+	+	+	+
D-Melezitose	-	-	-	+
D-Melibiose	-	-	-	+
3-Methyl Glucose	-	-	-	+
α-Methyl-DMannoside	-	-	-	+
Palatinose	-	-	-	+
D-Psicose	+	-	-	-
L-Rhamnose	-	-	-	+
D-Ribose	-	-	-	+
Salicin	-	-	-	+
Sedoheptulosan	-	-	-	+
D-Sorbitol	+	+	+	-
Stachyose	-	-	-	+
D-Trehalose	+	+	+	-
Xylitol	-	+	+	+
Acetic Acid	-	+	+	+
β-Hydroxybutyric Acid	+	+	+	-
γ-Hydroxybutyric Acid	-	-	-	+
p-Hydroxy-Phenylacetic Acid	-	-	-	+
α- Ketoglutaric Acid	+	+	+	-
α-Ketovaleric Acid	-	-	+	-
Lactamide	-	+	+	+
D-Lactic Acid Methyl Ester	-	-	-	-
L-Lactic Acid	+	+	+	-
D-Malic Acid	-	-	-	-
L-Malic Acid	+	+	+	+
Pyruvatic Acid Methyl Ester	-	+	+	+
Succinic Acid Mono-methyl Ester	+	+	-	-
Propionic Acid	-	+	-	+
Pyruvic Acid	+	+	-	-
Succinamic Acid	-	-	+	+
Succinic Acid	+	+	-	-
N-Acetyl-Lglutamic Acid	-	+	+	-
L-Alaninamide	+	-	+	+

D-Alanine	+	+	-	-
L-Alanine	+	+	-	-
L-Alanyl-Glycine	-	+	-	-
L-Asparagine	+	+	-	-
L-Glutamic Acid	+	+	+	+
Glycyl- LGlutamic Acid	-	+	-	+
L-Pyroglutamic Acid	+	+	+	-
L-Serine	-	+	-	+
Glycerol	+	+	-	-
Adenosine	-	-	-	+
2'-Deoxy Adenosine	-	-	-	+
Inosine	-	+	+	-
Uridine	-	-	+	-
Adenosine-5'-Monophosphate	-	+	-	+
D-Fructose-6-Phosphate	-	-	-	+
D-Glucose-6-Phosphate	-	+	+	-
D-L-α-Glycerol Phosphate	+	+	+	-

Table 7.8. Utilisation of carbon in percentage by the isolates tested (calculated by dividing the number of carbon substrates tested positive by 95 and converting to percentage, where 95 is the number of wells in the Biolog microplate containing a carbon source).

Isolate (Accession #)	Carbon utilisation (%)
High-5-213d (JN627971)	43.16
High-7-296d (JN627973)	40.00
Medium-3-188d (JN628001)	8.42
Medium-13-371d (JN627995)	47.37
Low-4-39d (JN627986)	51.56
Low-8-188d (JN627990)	33.68
Low-11-213d (JN627976)	31.58
Low-15-371d (JN627980)	41.05
Low-16-371d (JN627982)	22.11

7.3.2. Tolerance tests

Heavy metal and pH tolerance of the isolates was tested by plating them onto yeast extract plates that either contained different pHs (5-8) or the maximum heavy metal concentrations as found in the leach samples at the end of the natural community

experiment. The results are shown in Table 7.9. All isolates showed growth at pHs 5, 6, 7 and 8. In addition, liquid cultures at these pHs which contained samples from the high and medium ratios at 371 d showed growth of phototrophs. This suggested that the phototrophs viewed under the microscope but unable to be isolated were tolerant at these pHs. The same case was true for the heavy metal leach test. All isolates showed growth, and liquid cultures of the flasks also showed phototrophic growth.

7.3.3. Magnetotaxis

Isolate Medium-4-188d matched 100 % to *Rhodococcus erythropolis* strain cmmb1. According to the submitting authors to BLAST (Accession number: GU120079.1), this strain exhibited magnetotaxis. Tests were set up to see whether this was the case for Medium-4-188d. The results for the test with petri dishes are shown in Table 7.10. There was no difference observed with the presence of a magnet. The number of cells per ml was similar regardless of distance from the magnet, polarity or no magnet present.

Table 7.9. Tolerances of the isolates selected for further analysis.

Isolate (Accession #)	pH tolerance				Metal tolerance
	5	6	7	8	
High-5-213d (JN627971)	+	+	+	+	+
High-7-296d (JN627973)	+	+	+	+	+
Medium-3-188d (JN628001)	+	+	+	+	+
Medium-4-188d (JN628002)	+	+	+	+	+
Medium-6-188d (JN628004)	+	+	+	+	+
Medium-7-213d (JN628005)	+	+	+	+	+
Medium-12-371d (JN627994)	+	+	+	+	+
Medium-13-371d (JN627995)	+	+	+	+	+
Low-4-39d (JN627986)	+	+	+	+	+
Low-8-188d (JN627990)	+	+	+	+	+
Low-11-213d (JN627976)	+	+	+	+	+
Low-15-371d (JN627980)	+	+	+	+	+
Low-16-371d (JN627982)	+	+	+	+	+
Algal-1-160d (JN628008)	+	+	+	+	+
B1A 371 d	+	+	+	+	+
B1B 371 d	+	+	+	+	+
B2A 371 d	+	+	+	+	+
B2B (371 d)	+	+	+	+	+

Table 7.10. Number of cells per ml at different distances from magnet and with no magnet present.

Magnet and polarity	Distance	Number of cells per ml
S	0	2.5×10^4
S	4	2.4×10^4
S	8	2.4×10^4
N	0	2.8×10^4
N	4	2.8×10^4
N	8	2.5×10^4
No magnet	0	2.3×10^4
No magnet	4	2.5×10^4
No magnet	8	2.4×10^4

7.4. Discussion

As companion work to Chapters 5 and 6, several isolates were chosen for physiological studies to better understand what was being observed in the flasks. Chapter 5 reported increased diversity as time progressed, shifting to more non-culturable organisms, whilst Chapter 6 reported decreases in pH and increased elemental release rates where biotic conditions were concerned. The physiological tests on the isolates in this chapter aimed to understand what type of conditions the isolates could tolerate.

Regarding the matching of Medium-4-188d to a strain of *R. erythropolis* that had been linked to magnetotaxis by the submitting authors to BLAST, the isolate itself did not exhibit magnetotaxis. However, the submission to BLAST is unpublished data and so far there is no further literature to support these claims, nor any information that any strain of *R. erythropolis* exhibits magnetotaxis.

The isolates tested in this chapter were found in a range of pHs, from pH 7.35 to 5.27. The pH of the media ranged from pH 7.59 (maximum) to pH 5.27 (minimum) (Chapter 6,). Icelandic rain water is acidic and previously measured as 5.1-5.6 (Gislason and Eugster, 1987a). Cockell *et al.* (2009b) reported, through their study on bacteria in weathered Icelandic basaltic glass, that the growth of many microorganisms is retarded at the pH of Icelandic rain water (pH 5.6), compared with neutral and alkaline pH. The authors suggest that this raises two possibilities:

1. The pH changes due to rock weathering may change the community of active microorganisms.
2. Through their metabolic activity, the microorganisms may change the rate of weathering and therefore the rate of pH change (Cockell *et al.*, 2009b).

Results from the natural community experiment show that the lowest pH in the experiment was 5.27 and the communities were still thriving and becoming more diverse. pH tolerance tests on the isolates have shown them to grow at pH 5 to 8, though growth rates would need to be observed to ascertain whether the pH are retarding growth in any way.

To be active in the rock, microorganisms must also be able to tolerate numerous heavy metals; these include copper, cobalt and nickel (Carmichael, 1964; Walsh and Clarke, 1982). Using the highest concentrations found in solution at the end of the experiment, all isolates were found to be able to tolerate the heavy metal concentrations tested. The concentrations were over ten times lower than what Cockell *et al.* (2009b) examined, and were at least 100 times lower than that recorded for some microorganisms from metal-contaminated industrial soils (e.g. Bopp *et al.*, 1983; Malik and Jaiwal, 2000). However, for this experiment, it appears that heavy metals do not have an influence on the community composition on the basis of the results in this chapter. There, however,

is a caveat to this. The physiological tests were not able to be carried out on the non-culturables emerging at later stages due to inability to grow them outside the flasks. As described in Chapter 5, according to the r/K selection, microorganisms emerging in later succession stages are increasingly non-culturable types, which may be a result of a narrow niche width they inhabit. It is possible that these microorganisms may be influenced to a larger degree by pH and heavy metals compared to the isolates in this chapter.

The r/K selection theory is also relevant to the carbon profiles obtained using Biolog plates. Though the majority of the isolates showed similar percentages for carbon utilisation and shared a number of carbon sources between each other, preferences for certain types of carbon sources were observed. Medium-3-188d, High-5-213d and Low-8-188d were poor at utilising sugars, whilst Medium-3-188d did not utilise many amino acids but Low-4-39d did. This suggests there is a cross-community use of carbon sources in the community, with the microorganisms utilising different carbon sources when other microorganisms die or release carbon.

The similar precentages for carbon utilisation is not surprising considering the isolates belonged to Actinobacteria, Firmicutes and Proteobacteria. Their presence throughout the experiment would suggest that they are able to utilise a variety of carbon sources to thrive. Indeed, it has been shown that *Actinomycetes* can use a variety of organic nutrients, even though special media are often preferable (Rahman *et al.*, 2000; Sultan *et al.*, 2002). Carbon utilisation data can provide a valuable measure of potential microbial activity. For example, reduced carbon utilisation activity has been observed previously in systems disturbed by elevated metals and thus microbial communities are affected (Knight *et al.*, 1997; Kelly and Tate, 1998; Dobler *et al.*, 2000, Moynahan *et al.*, 2002). Had some of the non-culturable organisms that had emerged later in the

succession been able to be cultured and analysed using Biolog plates, one may have observed less broad carbon utilisation profiles. If following the r/K selection theory, being K-strategists, the non-culturables would have lower energy demands (Chapter 5). Indeed, Button *et al.* (1993) suggested that the fastidious nature of non-culturables may be due to a specialised use of a narrow range of carbon sources.

7.5. Conclusions

In conclusion, physiological tests were carried out on a selection of isolates obtained in Chapter 5. The isolates all showed tolerances to pHs 4-8. And to the maximum heavy metal concentrations found in solution. The carbon utilisation profiles for the isolates showed a variety of carbon sources were used, and shared amongst the isolates. The isolates were composed of Actinobacteria, Firmicutes and Proteobacteria, which emerged early in the succession stages and could be classified as r-strategists – inhabiting a broad niche. However, non-culturables emerging later on may have shown less broad carbon utilisation profiles and narrow pH tolerance ranges that would fit with the K-strategist profile. It would appear that at least these three phyla are able to colonise the rock throughout the succession period due to their broad tolerances. This may be why they may dominate early on and persist even when K-strategists begin to thrive.

Chapter 8: *Geobacter metallireducens* and Using Basaltic Glass as an Iron Source

8.1. Introduction

8.1.1. Aim of Chapter

The aim of this chapter was to investigate whether the iron reducer *Geobacter metallireducens* could weather basaltic glass. The thesis began with studying the effect of an iron oxidiser, *A. ferrooxidans*, and ends with the opposite, studying the effect of an iron reducer. The work also acts as preliminary work to further work that is planned to investigate whether *G. metallireducens* would be able to obtain iron from Martian meteorite. As mentioned in Chapter 4, iron is the fourth most abundant element in the Earth's crust (5.63 %) (Taylor, 1964). It exists naturally as a metal and in two oxidation states on Earth's surface: ferrous (Fe^{2+}) and ferric (Fe^{3+}) (Madigan and Martinko, 2005). Chapter 4 focussed on iron oxidation (Fe^{2+} to Fe^{3+}).

8.1.2. Iron reduction

The environmental relevance of Fe(III) has been well documented (Thamdrup, 2000; Lovley, 1991). Geochemical and microbiological evidence suggests that the reduction of Fe(III) may have been an early form of respiration on Earth (Vargas *et al.*, 1998), and is a candidate for the basis of life on other planets (Nealson and Cox, 2002). On modern Earth, Fe (III) can be the dominant electron acceptor for microbial respiration in many subsurface environments (Lovley and Chapelle, 1995). As such, Fe(III)-reducing communities can be responsible for the majority of the organic matter oxidised in such environments (Lovley, 1993). The cycling of iron in the environment is to a large

extent controlled by dissimilatory iron (III) reducing microorganisms (Burdige, 1993; Thamdrup *et al.*, 1994; Krebs *et al.*, 1997). In a process termed dissimilatory iron reduction (Lovley, 1991), the bacteria couple hydrogen and organic carbon oxidation to the reduction of Fe(III). Iron reducing bacteria utilise Fe(III) from a wide variety of oxyhydroxide and clay minerals (Lovley *et al.*, 2004). Such microorganisms have a great geological impact in terms of biomineralisation as they reduce and solubilise iron (III) present in many minerals in nature, e.g. ferrihydrite ($Fe_5HOH_8.4H_2O$), goethite (α-FeOOH), hematite (α-Fe_2O_3) or clay minerals (Roden and Zachara, 1996, Zacchara *et al.*, 1998; Kostka *et al.*, 1999; Zachara *et al.*, 2002; Dong *et al.*, 2003). In marine ecosystems, iron reduction in marine sediments is the contribution to the cycling of iron, carbon, sulphur, phosphorus and trace elements, which is an important influence regarding, for example, the growth of phytoplankton which strongly influences global food chains (Burdige, 1993; Thamdrup *et al.*, 1994; Morel and Price, 2003).

8.1.3. *Geobacter metallireducens*

Dissimilatory iron-reducing microorganisms are found throughout the phylogenetically distinct kingdoms *Archaea* and *Bacteria* (Nealson and Little, 1997; Lovley *et al.*, 2004) and are widespread in many different marine or freshwater environments (Coates *et al.*, 1996; Venkateswaran *et al.*, 1999). Microbial reduction has been known of since the 1920s, but only after the isolation of the first *Geobacter* strain, *Geobacter metallireducens*, was this metabolic group studied in more detail (Lovley *et al.*, 1987; Lovley and Phillips, 1988).

G. metallireducens, an obligate anaerobe, was first isolated from freshwater sediment, and was able to gain energy through dissimilatory reduction of iron, manganese, uranium and other metals (Lovley *et al.*, 1993). The bacteria is also able to oxidise

short chain fatty acids, alcohols and monoaromatic compounds such as toluene and phenol using iron as its electron acceptor (Lovley *et al.*, 1993). This has stimulated a great deal of interest in the possibility of using iron reducing bacteria for bioremediation (Lovley *et al.*, 1993; Nealson *et al.*, 1994).

Although Fe(III) oxides are often abundant, the bacteria are faced with the problem of how to effectively access an electron acceptor that cannot diffuse to the cell. *G. metallireducens* specifically expresses flagella and pili (Figure 8.1) when grown on insoluble Fe(III) oxide, and is chemotactic towards Fe(II) under these conditions (Childers *et al.*, 2002). These results suggest that *the bacteria* sense when soluble electron acceptors are depleted and then synthesise the appropriate appendages to permit it to search and establish contact with insoluble Fe(III). This approach may explain why the *Geobacter* species predominate over other Fe(III) oxide-reducing microorganisms in a wide variety of sedimentary environments (Childers *et al.*, 2002).

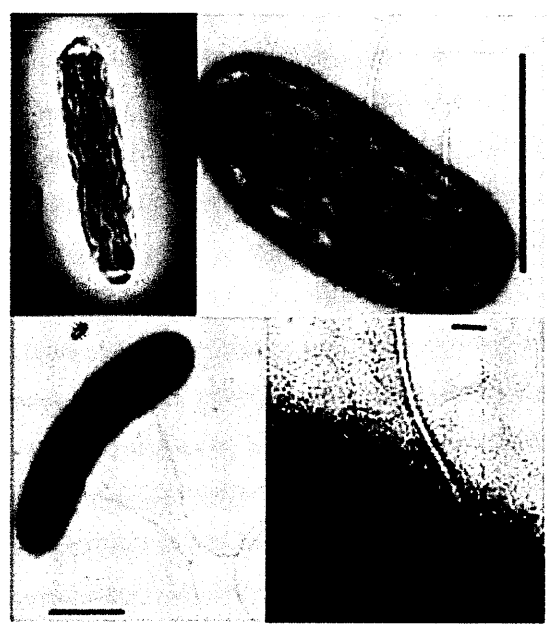

Figure 8.1. SEM images showing the absence of flagella on cells grown with Fe(III)-citrate (top left), in contrast to cells grown with Fe(III) (top right) or Mn(IV) (bottom left) oxides as the terminal electron acceptor. Scale bars, 1 mm (Childers *et al.*, 2002).

8.1.4. Implications

Microbes interact with nearly every metal on Earth, the interaction often leading to oxidation and/or reduction of the metal ions with changes in solubility of the altered product. Given that iron is the fourth most abundant element in the Earth's crust, iron redox reactions have the potential to support substantial microbial populations in soil and sedimentary environments (Weber *et al.*, 2006). As such, biological iron distribution has been described as one of the most ancient forms of microbial metabolism on Earth, and as a possible extraterrestrial metabolism on other iron-mineral-rich planets such as Mars (Weber *et al.*, 2006). Mars is an iron-rich planet, with a mantle more concentrated in iron relative to Earth's (Boynton *et al.*, 2008; Brückner *et al.*, 2008). Though the dominant oxidation state of the iron is Fe^{2+}, spectroscopic data have indicated presence of Fe^{3+} across numerous mineral phases, with hematite, goethite and magnetite having been detected (Christensen *et al.*, 2001; Klingelhöfer *et al.*, 2004; Morris *et al.*, 2006; Christensen et al., 2008; Brückner *et al.*, 2008). Knowing this, it was decided to study if Martian meteroites could be used by bacteria as a food source.

This chapter acts as a precursor to further work to be carried out to observe whether *G. metallireducens* is able to utilise the iron in a Martian meteorite. Microorganisms that metabolise anaerobically on Earth are the most plausible candidates for understanding potentially analogus metabolisms on Mars. The iron-rich nature of Mars raises important questions as to whether the planet could support energy acquisition by iron reducing microorganisms. If the bacteria can use basaltic glass as their iron source, it is possible that they are able to utilise iron from Martian rock which could mean life was or still is present on Mars.

8.2. Experimental design

8.2.1. Overview

The aim of this chapter was to investigate whether the iron reducer *Geobacter metallireducens* could weather basaltic glass. In addition, work in this chapter was also aimed as groundwork for a future experiment that is planned (outside of this thesis' timeline) to examine if the bacteria can use Martian meteorite. This was in the form of studying three different iron sources (basalt glass, vesicular basalt and hematite) and three different ratios (high, medium and low). The three different iron sources were tested to ascertain whether the bacteria could utilise iron from different sources. The ratios were tested as only a small amount of meteorite would be available to use – 40 mg for biology and a control, along with duplicates. Thus, the optimum volume of media was needed so that optimum results could be achieved from the Martian meteorite experiment once underway.

8.2.2. Set up of hungates and cultures

To observe the effect of *G. metallireducens* on volcanic glass, Hungate tubes were set as shown in Figure 8.2. Each Hungate had 2 g of powdered volcanic glass added; the glass was powdered using a disc mill (TEMA, Woodford Halse, UK). DSMZ 579 media was prepared without the addition of iron citrate (579 Fe- media). Powdered rock was used in this experiment (rather than crushed rock as in previous chapters) as time was limited. Powdered rock allowed for a greater surface area for reactions to take place and for organisms to access Fe3+ for iron reduction.

Ten ml of 579 Fe- media was added to each Hungate. One hundred µl of *Geobacter* stock culture (4×10^6 cells per ml) was added to three Hungates. The inoculum had

previously been centrifuged gently and the pellet re-suspended in 579 Fe- media to remove residual iron from the culture. Three other Hungates acted as the control, with no addition of bacteria. The Hungates were incubated at 29 °C for approximately 50 d. All manipulations were carried out in an anaerobic cabinet (H_2:CO_2:N_2 at a ratio of 10:10:80).

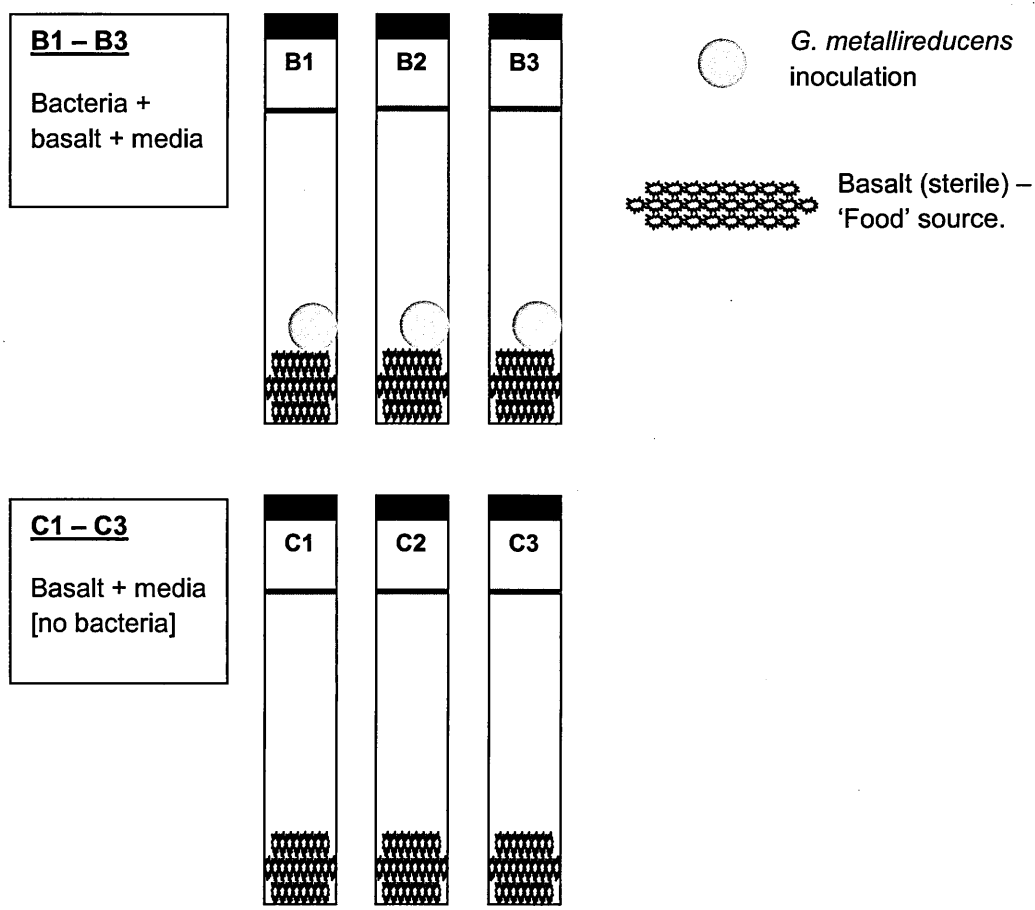

Figure 8.2. The experimental set up of the Hungates to study the effect of *G. metallireducens* on basaltic glass.

8.2.3. Sampling

At intervals, the Hungates were sampled in the anaerobic cabinet and Ferrozine assays (Chapter 3) were carried out. Sampling frequency was limited by the volume of liquid present. Future experiments should be scaled up so more liquid can be removed.

XRD (X-ray diffraction) was carried out on the glass at the start and end of the experiment, the work was carried out by the Natural History Museum, London, UK using an INEL X-ray diffractometer (XRD) (Inel, Strasbourg, France) with a curved position sensitive detector. Two hundred mg of the powdered rock was removed from the abiotic and biotic tubes and placed in eppendorfs and sent for analysis.

8.2.4. Effect of different iron sources and ratios

Preliminary tests were set up in order to observe the effect of different iron sources and water-rock ratios on *G. metallireducens*. Three iron sources were used: vesicular basalt (as used in Chapter 4), basaltic glass (as used in Chapter 5-7) and hematite, due to its high iron content. In 20 ml glass tubes, 40 mg of rock was added. Three ratios were set up for each rock type: 2 ml, 4 ml and 6 ml of 579 Fe- media (Table 8.1). As before, 100 µl of inoculum, which had been centrifuged to remove residual iron, was added to biotic tubes whilst controls were also set up. The tubes were in triplicate and incubated stationary at 29 °C for 20 days. Ferrozine assays were carried out at intervals during the time period.

Table 8.1. Conditions to test different iron sources and ratios on *G. metallireducens*.

Ratio	Volume of media (ml)	Mass of rock (mg)
High (0.15)	6	40
Medium (0.1)	4	40
Low (0.05)	2	40

8.3. Results

8.3.1. Basalt glass and *G. metallireducens*

G. metallireducens reduced Fe^{3+} obtained from the basalt glass as indicated by the production of Fe^{2+} in Figure 8.3. The production of Fe^{2+} was higher in the biology than the control up until 31 days where, when taking into account error bars, the two were almost identical. Fe^{3+} reduction was still occurring in the controls as indicated by the production of Fe^{2+}. The initial rate of Fe^{2+} production was 1.83 µM per day for biology and 0.67 µM per day for the control.

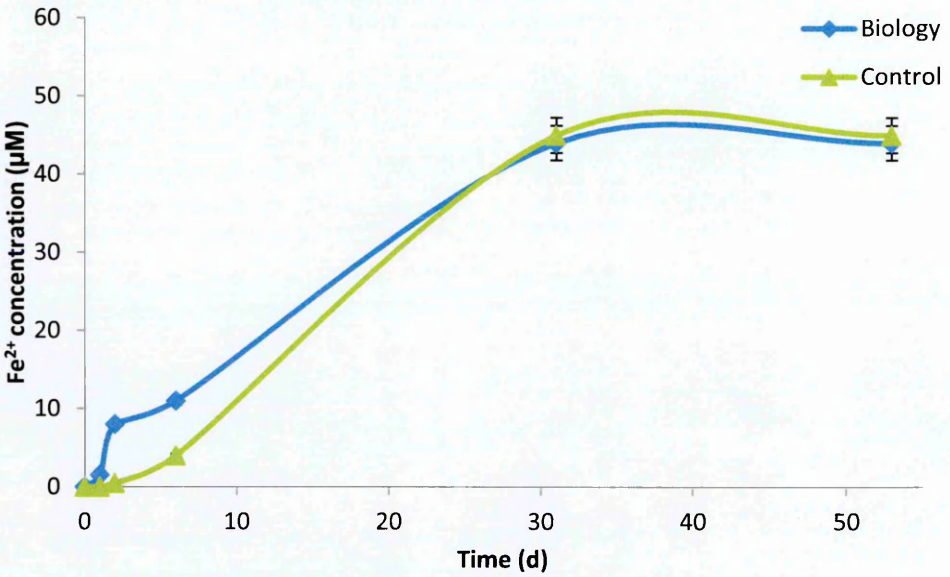

Figure 8.3. Fe^{2+} release from basalt glass over time for control and biology.

XRD on the weathering of basalt glass by *G. metallireducens* showed no difference between the rock at time zero and the end of the experiment (Figure 8.4), and between the control and biology (Figure 8.5). The general 'hump' shape of the curve is typical of a glassy material and the high background intensity indicates high iron content in the samples. The samples appear to contain feldspar, as indicated by the pink lines in Figure 7.3b. The samples at day zero and biology at the end of the experiment appear

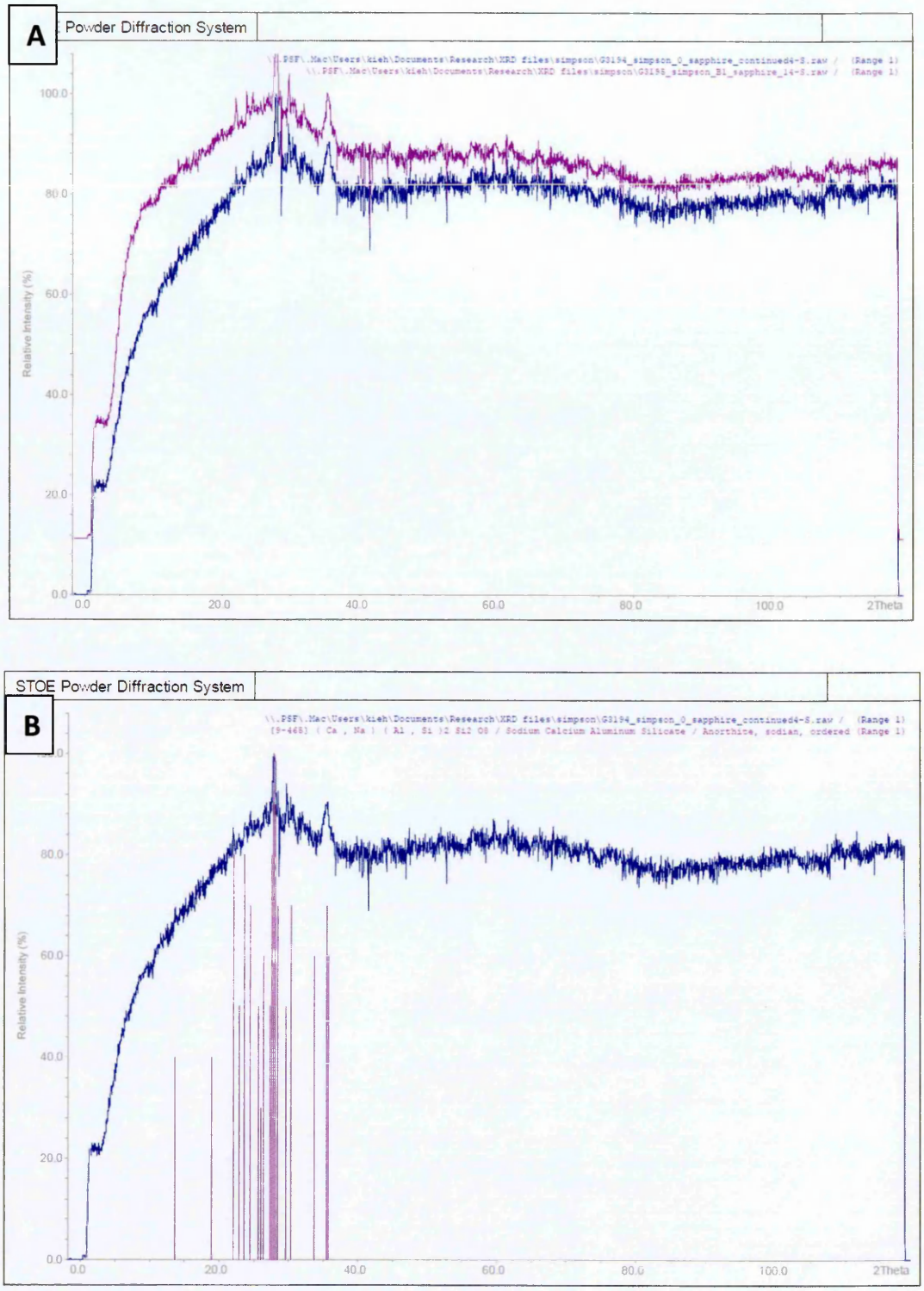

Figure 8.4. XRD analysis on (A) the glass at day zero and the biology at the end of the experiment, indicated by blue and pink lines, respectively. Also shown is day zero on its own (B) with pink lines indicating feldspar signatures.

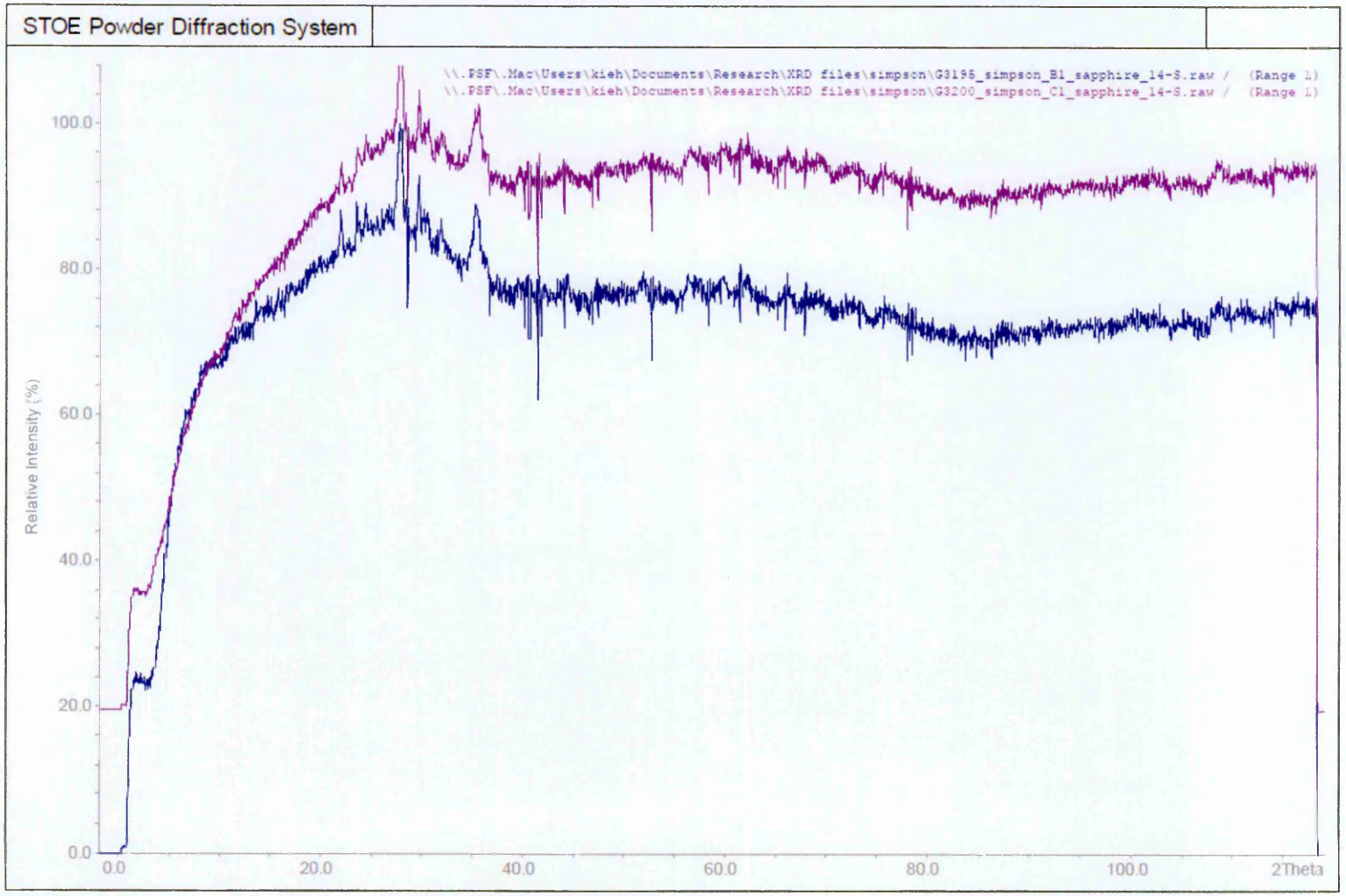

Figure 8.5. XRD analysis of biology and control basalt glass at the end of the experiment.

identical. This is replicated when the control and biology samples from the end of the experiment are compared. The shape of the curve at low angles might reflect perhaps a development of very early phyllosilicates. However, overall no discernable differences have been observed.

8.3.2. Iron sources and water-rock ratios

In terms of water-rock ratios and basalt glass, Fe^{2+} production rates are shown in Table 8.2. The fastest rate was observed in the hematite biological low ratio, whilst the slowest rate was observed in the basalt control high ratio. On the whole, biological rates were faster in the biology compared to the control, and low ratios tending to be faster and high ratios slower.

Table 8.2. Rate of Fe^{2+} production with different iron sources and water-rock ratios. 'B' denotes biology and 'C' indicates controls. The rate was calculated from Figure 8.3 and normalised for volume of liquid and mass of rock used (no BET data was available on the rocks used and thus the rate equations used for Chapters 4 and 6 cannot be used in this case).

Ratio	Rock	Fe^{2+} (μM) release rate (mg/ml/d)
Low	Basalt glass B	5.00×10^{-4}
	Basalt glass C	3.75×10^{-4}
	Basalt B	1.00×10^{-3}
	Basalt C	3.75×10^{-4}
	Hematite B	8.00×10^{-3}
	Hematite C	1.25×10^{-4}
Medium	Basalt glass B	6.25×10^{-5}
	Basalt glass C	6.25×10^{-5}
	Basalt B	1.25×10^{-4}
	Basalt C	1.88×10^{-4}
	Hematite B	1.25×10^{-4}
	Hematite C	6.25×10^{-5}
High	Basalt glass B	4.17×10^{-5}
	Basalt glass C	4.17×10^{-5}
	Basalt B	8.33×10^{-5}
	Basalt C	1.39×10^{-5}
	Hematite B	8.33×10^{-5}
	Hematite C	4.17×10^{-5}

8.4. Discussion

The aim of this chapter was to investigate whether *G. metallireducens* was able to utilise Fe(III) in basaltic glass. Though basalt glass contains primarily Fe^{2+}, the Fe^{3+} is present in the palagonite that the glass is weathered to. In addition, work in this chapter was also aimed as groundwork for a future experiment that is planned (outside of this thesis' timeline) to examine if the bacteria can use Martian meteorite. This was in the form of studying three different iron sources (basalt glass, vesicular basalt and hematite)

and three different ratios (high, medium and low). The three different iron sources were tested to ascertain whether the bacteria could utilise iron from different sources. The ratios were tested as only a small amount of meteorite would be available to use – 40 mg for biology and a control, along with duplicates. Thus, the optimum volume of media was needed so that optimum results could be achieved from the Martian meteorite experiment once underway.

With regards to the results from the effect of *G. metallireducens* on basaltic glass, the bacteria showed a faster initial rate of Fe^{2+} production compared to the control but when both reached a steady state they were almost identical in Fe^{2+} production. XRD analysis showed no discernable difference between the biology and control, or a change from day 0. This, however, only means that any mineralogical changes are not resolvable by XRD. Activity may still be affecting nano-scale mineralogy which may not be able distinguished from the glass pattern (both nano-phases and glass produce 'hump' like reflections as seen in the patterns in this chapter). It is possible that the bacteria needed longer than the 50 or so days the experiment ran for to make a noticeable difference to the glass. Future work should let the experiment for several months to a year to see whether this would make a difference. It is also possible that in this short time scale, changes in glass are not different between abiotic and biotic conditions (as evidenced by the Fe^{2+} production) but a longer timescale would allow the bacteria to establish themselves and begin to weather the rocks more than abiotic conditions. Differences between controls and biology were certainly seen when testing different ratios; perhaps the ratio used for the basalt glass experiment (2 g in 10 ml) was too large.

In terms of ratios and different iron sources, *G. metallireducens* appeared to favour the low ratios and hematite. The preference for low ratios may be explained by the way *G. metallireducens* obtains its iron. As described in the introduction to this chapter, Fe(III)

oxides are abundant but bacteria face the problem of how to effectively access an electron acceptor that cannot diffuse into the cell. Childers *et al.* (2002) reported that *G. metallireducens* overcomes this problem by expressing flagella and pili when grown on insoluble Fe(III) oxide (and not when grown on dissolved iron citrate), and is chemotactic towards Fe(II) under these conditions. The bacteria sense when soluble electron acceptors are depleted and to search and establish contact with insoluble Fe(III), they synthesise the appropriate appendages to do this. A low ratio would mean that any iron being released into solution is not being diluted, as in the high ratio, making it more difficult for the bacteria to sense 'food'. It would mean less distance for the bacteria to move to find more iron. The preference for hematite may be due to the higher iron found in this iron source. This, however, is contradicted in the literature.

A significant portion of the Fe(III) in soils and sediments may be in crystalline forms such as hematite which Fe(Ill)-reducing microorganisms may only poorly reduce, if at all (Lovley 1991; Phillips *et al.*, 1993). When Lovley *et al.* (1998) incubated hematite in cell suspensions of *G. metallireducens* there was little Fe(III) reduction. Only the addition of soil humic acids or the humic analogue, anthraquinone-2,6,-disulfonate allowed significant reduction Fe(III) from hematite. No humic acids were added in the experiments in this chapter. This raises the question of whether the results in this experiment may have been a fluke or if the low water rock ratio may have played a part in allowing the bacteria to obtain the iron more easily, perhaps by affecting the pH of the solution that affected the stability of the bound iron.

The pH was not monitored in the experiments due to the small volumes being used, but future work could involve a larger scale repeat that monitored pH in case it deviated from the starting pH of 7. Indeed, pH has had a role to play in the dissolution of jarosite (Bridge and Johnson, 2000) and schwertmannite (Küsel *et al.*, 2002) where iron

reducing bacteria under acidic (pH <2.5) conditions has been demonstrated. Experimental evidence indicates that at low pH, *Acidiphilium* spp. can accelerate the dissolution of ferric iron minerals by way of an indirect mechanism in which bacterial reduction of dissolved Fe^{3+} results in a shift in equilibrium between solid phase Fe(III) and dissolved Fe^{3+}, thereby driving dissolution of the mineral phase (Jones *et al.*, 2006).

The preference for hematite would bode well in implications for Mars. As mentioned in the introduction to this chapter, crystalline iron oxides such as hematite, goetjite and magnetite have been detected on Mars through spectroscopic data from orbital and ground-based missions, with hematite being the dominant mineral (Christensen *et al.*, 2001; Klingelhöfer *et al.*, 2004; Morris *et al.*, 2006; Christensen et al., 2008; Brückner *et al.*, 2008). *G. metallireducen*'s preference and ability to acquire iron from hematite, in addition to its preference to low-water rock ratios could provide could prove hopeful on the search for life is or having been present on Mars. More work, however, would need to be carried out to provide more concrete implications.

8.5. Conclusions

In conclusion, it was found that *G. metallireducens* did not greatly affect the production of Fe^{2+} from basalt glass when compared to controls. However, when the ratio of rock to media was altered, an effect in Fe^{2+} production was seen, especially in the case of hematite. Low ratios were also favoured by the bacteria. This may be due to the iron being released being less diluted and allowing the bacteria to sense the presence of iron and produce pili/flagella enabling them to move towards the iron source. In Chapter 4, it was found that low ratios inhibited weathering by *A. ferrooxidans*, however, this

thesis ends with the opposite – *G. metallireducens* preferred a low water-rock ratio when it came to obtaining iron. The low ratio possibly allowed *G. metallireducens* to obtain the iron more easily by affecting the pH of the solution which in turn affected the stability of the bound iron. In addition, the low ratio would mean that any iron being released into solution was not being diluted, as in the high ratio, which would have made it more difficult for the bacteria to sense 'food'. The low ratio would have meant less distance for the bacteria to move to find more iron.

Chapter 9: Concluding Remarks

The weathering of volcanic minerals is recognised to make a significant contribution to the global weathering budget (Louvat and Allègre, 1998; Dessert *et al.*, 2001, 2003; Kisakurek *et al.*, 2004), influencing CO_2 drawdown and climate control. It is thought that microorganisms play an important part in rock weathering. However, it is only recently that work has begun in the laboratory to understand the role of bacteria (e.g. Wu *et al.*, 2007a, 2007b). The involvement of bacteria has been inferred in deep-ocean basaltic glass in which a diversity of microbial alteration textures has been reported (e.g. Thorseth *et al.*, 1992; Fisk *et al.*, 1998; Torsvik *et al.*, 1998; Furnes and Staudigel, 1999; Thorseth *et al.*, 2001; Etienne and Dupont, 2002; Thorseth *et al.*, 2003).

Chapter 4 aimed to investigate what effect water-rock ratios would have on the iron-oxidiser *A. ferrooxidans*. It was found that the medium water-rock ratio (50:1) provided the optimum conditions for growth whilst the low water-rock ratio (1:1) had a lower release of iron because of pH. The pH affected the release of iron and REEs, with less released the higher the pH. Bacteria retarded the release of REEs through formation of biofilms on the surface of the basalt in the medium water-rock ratio biological experiment. In addition, XANES analysis suggested localised areas of hematite on the treated rocks, as well as oxidised layers that did not correspond to specific mineralogy. The lack of specific mineral signatures on the rock surface, but the apparent oxidation of the surface, would provide some evidence that the surface had been passivated with Fe^{3+} binding to the mineral surface. This was consistent with speculations advanced by

Santelli *et al.* (2001). They observed the passivation of olivines during microbial dissolution.

Linear elemental release rates for the trace elements showed no overall preference for controls or biology-containing flasks. It is possible that a lack of preference for either controls or biology-containing flasks could be due to uptake of some of the elements by the cells as soon as the elements were released.

On the opposite side, Chapter 8 studied the effect of an iron reducer (Chapter 8). Chapter 8 was a preliminary investigation as whether the iron reducer *G. metallireducens* could weather basaltic glass. The work also acted as preliminary work to further that is planned to investigate whether *G. metallireducens* would be able to obtain iron from Martian meteorite. It was found the bacteria did not affect the production of Fe^{2+} from basalt glass when compared to controls. However, when low water-rock ratios and hematite were tested, a difference was observed between abiotic and biotic flasks. The low ratio was favoured by the bacteria, the opposite to what was seen in Chapter 4 with *A. ferrooxidans*. It was suggested the low water-rock ratio possibly allowed *G. metallireducens* to obtain the iron more easily by affecting the pH of the solution which in turn affected the stability of the bound iron. In addition, the low water-rock ratio would mean that any iron being released into solution was not being diluted, which would have made it more difficult for the bacteria to sense 'food'. The low water-rock ratio would have meant less distance for the bacteria to move to find more iron.

The pH was not monitored in the experiments due to the small volumes being used, but it is suggested that future work would involve a larger scale repeat that monitored pH in case it deviated from the starting pH of 7, as pH has been shown to play a role in dissolution of minerals (Bridge and Johnson, 2000; Küsel *et al.*, 2002). It is also

suggested that a longer experiment is run (longer than the 50 or so days this experiment was run for) to ascertain whether the bacteria would make a more noticeable difference to the glass (analysed through XRD), preferably for several months to a year. It is possible that in the short time scale of the experiment, changes in glass were not different between abiotic and biotic conditions but a longer timescale would allow the bacteria to establish themselves and begin to weather the rocks more than abiotic conditions. Once this future work is carried out, it is also suggested that Martian meteorite is used in place of the basalt to ascertain whether the bacteria can weather the meteorite.

Though work in Chapters 4 and 8 provided information on how one organism affected weathering of volcanic rocks, it was not representative of a natural environment where microbial communities exist. In addition, succession occurs in the environment as communities change with changing nutrient profiles. The successional patterns of microbial communities have received very little attention. The aim of the work in Chapters 5-7 was to shed more light on this area, alongside how weathering rates are affected in community-based weathering, and how water-rock ratios may affect the communities.

It was found that community structure changed over time, becoming more diverse, with a switch from r- to K-selected microorganisms over the course of the year, similarly to results obtained in the field. DGGE results showed each flask had a distinctive population – with no correlation between ratios, and replicates different in composition to each other. Though the molecular biology in Chapter 5 suggested no correlation between ratios, and that each flask was developing its own distinctive population, the results of the chemistry of the flask solutions in Chapter 6 indicated that the biological

experiments showed differences in pH and elemental release between ratios, a similar trend as observed in Chapter 4.

Elemental release rates were, on the whole, faster in the biological experiments, with the high water-rock ratio having faster rates and the low water-rock ratios the slowest, as observed in Chapter 4.

Though this experiment provided further information on microbial succession in volcanic rocks, and weathering rates by communities, future work is suggested to obtain a better understanding. It is recommended that the experiment is repeated but with a larger number of replicates. Clone libraries would be carried out on all the replicates (and all water-rock ratios) to be able to better understand the successionsal changes in the different water-rock ratios, and also conclusively identify whether each replicate develops into its own 'microbial island'. In addition, as with Chapter 4, it is suggested that further ICP-AES work should be carried out to measure the intracellular concentrations of elements to provide more information on what elements were being utilised. The organic acid concentrations in the flasks should also be measured over time to ascertain whether they are being produced and link them with the clone library data.

It was proposed that differences in dissolution rates between previous literature and the work in this thesis were caused by the state of the rock surface area (powder with its fresh surface area vs crushed rock). To ascertain whether this assumption is corrected, it would be prudent to run an identical experiment alongside the repeat experiment, but with one difference: the use of powdered rock instead of crushed rock. Thus, one could monitor release rates and succession when crushed rock and powdered rock are added and analyse whether there is a difference.

The general aim of this thesis was to study microbial weathering of volcanic rocks, with an emphasis on water-rock ratios, by looking at the effect of model organisms (*Acidithiobacillus ferrooxidans* and *Geobacter metallireducens*) to natural microbial communities (from basaltic glass). The main objective was to gain a better understanding of the processes by which microbes contribute to weathering and if any knowledge learnt can be put to use in industrial applications (e.g. acid mine drainage) and in the field of astrobiology (e.g. life on Mars). The aim was to address to some degree three broad questions.

1. Do microbes contribute significantly to rock weathering?

This question was investigated specifically in Chapters 4, 6 and 8. In Chapters 4 and 8, no overall preference between biology and controls was seen for elemental release rates. The bacteria, however, were still surviving so they must have been were living off nutrients from the rocks. Despite no real difference between controls and biology in Chapters 4 and 8, work carried out with natural communities in Chapter 6 showed faster rates in the cases where there were microorganisms present. It is possible that the natural communities affected mineral dissolution, possibly through the release of organic acids, which would also account for the drop in pHs observed in the biological experiments. This by itself would affect mineral dissolution. The community working together seems to have a greater influence on weathering than just one species.

It was noted that there were differences in dissolution rates between the results reported in this chapter and previous literature. It is suggested that these are caused by the state of the rock surface area as in previous studies the rocks have typically been crushed into powder and fine particles. This crushed powder would have provided fresh rock surface for the microorganisms and also greater surface area for reactions to take place,

accounting for generally higher weathering rates in previous literature per unit weight of material.

2. How do microbial communities develop under different water-rock ratios?

This question was answered specifically in Chapter 5. It was found that the communities showed no correlation between ratios and rise of different community profiles. It was found, however, that that community structure changed over time, becoming more diverse, with a switch from r- to K-selected microorganisms over the course of the year. It is suggested that, though community diversity does change over time (as shown by the clone libraries), the ratios do not have an effect and each flask is developing with its own 'microbial island'.

3. Can they acquire nutrients and energy supplies from volcanic environments?

This question was broached in Chapters 4, 6 and 8. To answer this question, it is suggested that future work would examine the intracellular element concentrations of the cells to ascertain whether elements were being taken up by the cells as soon as they were released from the rock. If elements that had faster rates of release in the controls were found in high concentrations inside the cells in the biological experiments, it might be argued that the elements were being taken up by the cells as soon as they were released from the rock. In addition, doping the flasks with labelled elements could also be used to track concentration inside and out of the cell.

A larger experiment should also be set up which would include more replicates and cell counts throughout the experiment rather than just at the beginning and end (as carried out in this thesis because of volume constraints). The additional cell counts at regular

intervals would be paired to iron and other element release rates, allowing one to monitor how cell numbers change and attempt to relate this to elemental release rates more thoroughly and to know whether they were acquiring elements.

It is hoped that the findings in this thesis will contribute on some level to the knowledge of microbial weathering of volcanic rocks, and will provide groundwork for further investigations to be carried out.

Appendix A: Growth Media Recipes

Chapter 4: *A. ferrooxidans* (modified K9 medium)

Solution A – per 500 ml dH_2O

NH_4SO_4	3 g
KCl	0.1 g
K_2HPO_4	0.5 g
$MgSO_4.7H_2O$	0.5 g
$Ca(NO_3)$	0.01 g
10 N H_2SO_4	1 ml

Solution A was autoclaved for 15 min at 15 psi pressure, 121°C.

Solution B – per 500 ml dH_2O

$FeSO_4.7H_2O$	44 g

Solution B was prepared fresh before use and filter sterilised.

Solutions A and B are mixed together in a 50:50 ratio.

Chapters 5-7: Natural Community Experiments

0.2 g l^{-1} yeast extract – per 1 l dH_2O:

Yeast extract (Oxoid LP2001)	0.2 g l^{-1}

The media was autoclaved for 15 min at 15 psi pressure, 121°C.

0.2 g l^{-1} yeast extract agar – per 1 l dH_2O:

Yeast extract (Oxoid LP2001) ..... 0.2 g l^{-1}

Agar Bacteriological (Oxoid LP0011) ..... 10 g l^{-1}

The media was autoclaved for 15 min at 15 psi pressure, 121°C.

BG-11 (Stanier et al., 1971):

Stocks per litre

(1) $NaNO_3$ ..... 15.0 g

Per 500 ml

(2) K_2HPO_4 ..... 2.0 g

(3) $MgSO_4.7H_2O$ ..... 3.75 g

(4) $CaCl_2.2H_2O$ ..... 1.80 g

(5) Citric acid ..... 0.30 g

(6) Ammonium ferric citrate green ..... 0.30 g

(7) $EDTANa_2$ ..... 0.05 g

(8) Na_2CO_3 ..... 1.00 g

(9) Trace metal solution: per litre

H_3BO_3 ..... 2.86 g

$MnCl_2.4H_2O$ ..... 1.81 g

$ZnSO_4.7H_2O$ ..... 0.22 g

$Na_2MoO_4.2H_2O$ ..... 0.39 g

$CuSO_4.5H_2O$ ..... 0.08 g

$Co(NO_3)_2.6H_2O$ ..... 0.05 g

Medium per litre

Stock solution **1** ..... 100.0 ml

Stock solutions **2-8** ..... 10.0 ml each

Stock solution **9** ..... 1.0 ml

Agar ..... 15 g

This medium was made up to 1 litre with dH_2O and adjusted to pH 7.1 with 1M NaOH or HCl.

The medium was autoclaved for 15 min at 15 psi pressure, 121°C, before being poured into plates.

Luria Broth (LB) agar plates – per 1 l dH_2O:

Tryptone ..... 10 g

Yeast Extract ..... 5 g

NaCl ..... 10 g

Agar ..... 15 g

The components were dissolved in 950 ml dH_2O and the pH adjusted to 7.0 with NaOH. The volume was brought up to 1 l. The medium was autoclaved for 15 min at 15 psi pressure, 121°C. The medium was then cooled to ~55°C, the antibiotic ampicillin added (50 mg ml^{-1}) and the plates poured. The plates were stored at 4 °C until needed.

Chapter 8: *Geobacter metallireducens*

DSMZ 579. Geobacter medium

Fe(III) citrate ..... 13.70 g

$NaHCO_3$ ..... 2.50 g

NH_4Cl ..... 1.50 g

NaH_2PO_4 ..... 0.60 g

KCl ..... 0.10 g

Na-acetate ..... 2.50 g

Vitamin solution (see below) ..... 10.00 ml

Trace element solution (see below)	10.00 ml
$Na_2WO_4.2H_2O$	0.25 mg
dH_2O	980.00 ml

DSMZ 579 medium was prepared and dispensed medium under an oxygen-free 80% N_2 + 20% CO_2 gas mixture. The ferric citrate was dissolved in 900 ml dH_2O by heating and adjusting to pH 6.0. The other components were added, except the vitamin solution, to dH_2O and the volume brought to 990 ml. The media was sparged with 80% N_2 + 20% CO_2 and autoclaved for 15 min at 15 psi pressure, 121°C. The media was cooled to 25°C and 10 ml vitamin solution was added aseptically and anaerobically.

Trace element solution:

Nitrilotriacetic acid	1.50 g
$MgSO_4.7H_2O$	3.00 g
$MnSO_4.H_2O$	0.50 g
NaCl	1.00 g
$FeSO_4.7H_2O$	0.10 g
$CoSO_4.7H_2O$	0.18 g
$CaCl_2.2H_2O$	0.10 g
$ZnSO_4.7H_2O$	0.18 g
$CuSO_4.5H_2O$	0.01 g
$KAl(SO_4)_2.12H_2O$	0.02 g
H_3BO_3	0.01 g
$Na_2MoO_4.2H_2O$	0.01 g
$NiCl_2.6H_2O$	0.03 g
$Na_2SeO_3.5H_2O$	0.30 mg

dH_2O ..... 1000 ml

Nitrilotriacetic acid was first dissolved and adjusted to pH 6.5 with KOH. The remaining components were then added. Final pH was 7.0 (with KOH).

Vitamin solution:

Biotin ..... 2.00 mg

Folic acid ..... 2.00 mg

Pyridoxine-HCl ..... 10.00 mg

Thiamine-HCl.$2H_2O$ ..... 5.00 mg

Riboflavin ..... 5.00 mg

Nicotinic acid ..... 5.00 mg

D-Ca-pantothenate ..... 5.00 mg

Vitamin B12 ..... 0.10 mg

p-Aminobenzoic acid ..... 5.00 mg

Lipoic acid ..... 5.00 mg

dH_2O ..... 1000 ml

Appendix B: Libshuff Statistics for Chapter 5

Figure B.1. Libshuff comparisons for clone libraries.

Comparison	Significance	Comparison	Significance	Comparison	Significance
A-B	0.0002	E-C	<0.0001	J-E	<0.0001
B-A	<0.0001	F-I	<0.0001	E-K	0.0038
A-C	<0.0001	I-F	<0.0001	K-E	0.0367
C-A	<0.0001	F-J	<0.0001	F-G	<0.0001
A-D	<0.0001	J-F	<0.0001	G-F	<0.0001
D-A	<0.0001	F-K	<0.0001	F-H	<0.0001
A-E	0.0784	C-F	<0.0001	H-F	<0.0001
E-A	<0.0001	F-C	<0.0001	K-F	<0.0001
A-F	<0.0001	C-G	<0.0001	G-H	0.0693
F-A	<0.0001	G-C	<0.0001	H-G	0.0456
A-G	<0.0001	C-H	<0.0001	G-I	0.0319
G-A	<0.0001	H-C	<0.0001	I-G	<0.0001
A-H	<0.0001	C-I	<0.0001	G-J	<0.0001
H-A	<0.0001	I-C	<0.0001	J-G	<0.0001
A-I	0.0004	C-J	<0.0001	G-K	<0.0001
I-A	<0.0001	J-C	<0.0001	K-G	<0.0001
A-J	<0.0001	C-K	<0.0001	H-I	0.3915
J-A	<0.0001	K-C	<0.0001	I-H	0.0008
A-K	<0.0001	D-E	<0.0001	H-J	<0.0001
K-A	<0.0001	E-D	<0.0001	J-H	<0.0001
B-C	0.2376	D-F	<0.0001	H-K	<0.0001
C-B	0.2803	F-D	<0.0001	K-H	<0.0001
B-D	0.0017	D-G	<0.0001	I-J	<0.0001
D-B	<0.0001	G-D	<0.0001	J-I	<0.0001
B-E	<0.0001	D-H	<0.0001	I-K	<0.0001
E-B	<0.0001	H-D	<0.0001	K-I	<0.0001
B-F	<0.0001	D-I	<0.0001	J-K	<0.0001
F-B	<0.0001	I-D	<0.0001	K-J	<0.0001
B-G	<0.0001	D-J	<0.0001		
G-B	<0.0001	J-D	<0.0001		
B-H	<0.0001	D-K	<0.0001		
H-B	<0.0001	K-D	<0.0001		
B-I	<0.0001	E-F	<0.0001		
I-B	<0.0001	F-E	<0.0001		
B-J	<0.0001	E-G	<0.0001		
J-B	<0.0001	G-E	<0.0001		
B-K	<0.0001	E-H	<0.0001		
K-B	<0.0001	H-E	<0.0001		
C-D	0.0076	E-I	<0.0001		
D-C	<0.0001	I-E	<0.0001		
C-E	<0.0001	E-J	<0.0001		

Appendix C: Chapter 5 Sequences

Table C.1. OTU sequences with nearest RDP classification.

OTU (no. of clones)	Accession number	Phylum (>95% confidence)	Family (>95% confidence)	Genus (>95% confidence)
OTU1 (33)	JN222427	OD1	OD1 genera incertae sedis	
OTU2 (7)	JN222428	Actinobacteria	Intrasporangiaceae	Phycicoccus
OTU3 (42)	JN222429	Firmicutes	Bacillaceae	Bacillus
OTU4 (1)	JN222430	Betaproteobacteria	Nitrosomonadaceae	Nitrosospira
OTU5 (12)	JN222431	Betaproteobacteria	Oxalobacteraceae	
OTU6 (12)	JN222432	Betaproteobacteria	Oxalobacteraceae	
OTU7 (24)	JN222433	Firmicutes	Paenibacillaceae	Paenibacillus
OTU8 (26)	JN222434	Betaproteobacteria	Oxalobacteraceae	Massilia
OTU9 (2)	JN222435	Betaproteobacteria	Oxalobacteraceae	
OTU10 (4)	JN222436	Actinobacteria		
OTU11 (1)	JN222437	Firmicutes	Paenibacillaceae	Paenibacillus
OTU12 (3)	JN222438	Firmicutes	Clostridia	
OTU13 (12)	JN222439	Acidobacteria		GP10
OTU14 (3)	JN222440	Betaproteobacteria	Oxalobacteraceae	Massilia
OTU15 (32)	JN222441	Actinobacteria	Micrococcaceae	Arthrobacter
OTU16 (4)	JN222442	Unclassified		
OTU17 (8)	JN222443	Betaproteobacteria	Oxalobacteraceae	Janthinobacterium
OTU18 (1)	Not accepted	Gemmatimonadetes	Gemmatimonadaceae	Gemmatimonas
OTU19 (12)	JN222444	Alphaproteobacteria	Bradyrhizobiaceae	Bradyrhizobium
OTU20 (2)	JN222445	Alphaproteobacteria	Sphingomonadaceae	Sphingomonas
OTU21 (10)	JN222446	Actinobacteria		

OTU22 (17)	JN222447	Betaproteobacteria	Oxalobacteraceae	
OTU23 (6)	JN222448	Betaproteobacteria	Oxalobacteraceae	Massilia
OTU24 (8)	JN222449	Unclassified		
OTU25 (2)	JN222450	Betaproteobacteria	Burkholderiales incertae sedis	Ideonella
OTU26 (12)	JN222451	OD1	OD1 genera incertae sedis	
OTU27 (3)	JN222452	Gemmatimonadetes	Gemmatimonadaceae	Gemmatimonas
OTU28 (53)	JN222453	Betaproteobacteria	Oxalobacteraceae	
OTU29 (4)	Not accepted	Unclassified		
OTU30 (3)	JN222454	Firmicutes	Paenibacillaceae	Paenibacillus
OTU31 (22)	JN222455	Betaproteobacteria	Oxalobacteraceae	Herbaspirillum
OTU32 (2)	JN222456	Unclassified		
OTU33 (7)	JN222457	Gemmatimonadetes	Gemmatimonadaceae	Gemmatimonas
OTU34 (1)	JN222458	Betaproteobacteria	Oxalobacteraceae	
OTU35 (1)	JN222459	Firmicutes		
OTU36 (1)	JN222460	Unclassified		
OTU37 (3)	JN222461	Firmicutes	Paenibacillaceae	Cohnella
OTU38 (6)	JN222462	Betaproteobacteria	Oxalobacteraceae	
OTU39 (5)	JN222463	Betaproteobacteria	Oxalobacteraceae	Massilia
OTU40 (8)	JN222464	Alphaproteobacteria	Bradyrhizobiaceae	Bradyrhizobium
OTU41 (10)	Not accepted	Unclassified		
OTU42 (2)	JN222465	Nitrospira	Nitrospiraceae	Nitrospira
OTU43 (1)	JN222466	Gemmatimonadetes	Gemmatimonadaceae	Gemmatimonas
OTU44 (3)	JN222467	Firmicutes	Paenibacillaceae	Paenibacillus
OTU45 (1)	JN222468	Firmicutes	Paenibacillaceae	Paenibacillus
OTU46 (4)	JN222469	Betaproteobacteria	Oxalobacteraceae	
OTU47 (6)	JN222470	Unclassified		
OTU48 (4)	JN222471	Firmicutes	Paenibacillaceae	Paenibacillus

OTU49 (13)	JN222472	Betaproteobacteria	Oxalobacteraceae	Massilia
OTU50 (2)	JN222473	Unclassified		
OTU51 (3)	JN222474	Actinobacteria	Propionibacteriaceae	Propionibacterium
OTU52 (2)	JN222475	Gammaproteobacteria	Unclassified Gammaproteobacteria	
OTU53 (3)	JN222476	Unclassified		
OTU54 (1)	JN222477	Cyanobacteria	Chloroplast	
OTU55 (4)	JN222478	Betaproteobacteria	Oxalobacteraceae	Massilia
OTU56 (2)	JN222479	Betaproteobacteria	Oxalobacteraceae	
OTU57 (6)	JN222480	Bacteroidetes	Chitinophagaceae	Flavisolibacter
OTU58 (3)	JN222481	Cyanobacteria	Chloroplast	
OTU59 (2)	JN222482	Alphaproteobacteria	Hyphomicrobiaceae	Devosia
OTU60 (1)	JN222483	Planctomycetes	Planctomycetaceae	Singulisphaera
OTU61 (3)	JN222484	Unclassified		
OTU62 (1)	JN222485	Unclassified		
OTU63 (2)	JN222486	Unclassified		
OTU64 (8)	JN222487	Betaproteobacteria	Oxalobacteraceae	Massilia
OTU65 (2)	JN222488	OD1	OD1 genera incertae sedis	
OTU66 (4)	JN222489	Betaproteobacteria	Oxalobacteraceae	
OTU67 (2)	JN222490	Acidobacteria		GP6
OTU68 (1)	JN222491	Actinobacteria	Micrococcaceae	Arthrobacter
OTU69 (1)	JN222492	Betaproteobacteria	Nitrosomonadaceae	Nitrosospira
OTU70 (1)	JN222493	Betaproteobacteria	Oxalobacteraceae	
OTU71 (1)	JN222494	Unclassified		
OTU72 (1)	JN222495	Firmicutes	Paenibacillaceae	Paenibacillus
OTU73 (3)	JN222496	Betaproteobacteria	Nitrosomonadaceae	Nitrosospira
OTU74 (1)	JN222497	Verrucomicrobia	Verrucomicrobiaceae	Verrucomicrobium
OTU75 (1)	Not accepted	Firmicutes	Unclassified Firmicutes	

OTU76 (1)	JN222498	Betaproteobacteria	Oxalobacteraceae	
OTU77 (2)	Not accepted	Firmicutes	Paenibacillaceae	
OTU78 (1)	JN222499	Actinobacteria	Micrococcaceae	Arthrobacter
OTU79 (1)	JN222500	Betaproteobacteria	Oxalobacteraceae	Herbaspirillum
OTU80 (1)	JN222501	Alphaproteobacteria	Bradyrhizobiaceae	Bosea
OTU81 (2)	JN222502	Betaproteobacteria	Oxalobacteraceae	
OTU82 (1)	JN222503	Firmicutes		
OTU83 (2)	JN222504	Betaproteobacteria	Oxalobacteraceae	
OTU84 (1)	Not accepted	Betaproteobacteria	Oxalobacteraceae	
OTU85 (2)	JN222505	Planctomycetes	Planctomycetaceae	Singulisphaera
OTU86 (1)	JN222506	Proteobacteria	Unclassified Proteobacteria	
OTU87 (1)	JN222507	Betaproteobacteria	Oxalobacteraceae	
OTU88 (1)	JN222508	Alphaproteobacteria	Unclassified Alphaproteobacteria	
OTU89 (1)	JN222509	Unclassified		
OTU90 (1)	JN222510	Betaproteobacteria	Oxalobacteraceae	
OTU91 (2)	Not accepted	Deltaproteobacteria	Myxococcacea	Myxococcus
OTU92 (1)	Not accepted	Alphaproteobacteria	Unclassified Alphaproteobacteria	
OTU93 (1)	JN222511	Bacteroidetes	Chitinophagaceae	
OTU94 (1)	JN222512	Gammaproteobacteria	Xanthomonadaceae	Dokdonella
OTU95 (1)	JN222513	OD1	OD1 genera incertae sedis	
OTU96 (1)	JN222514	Firmicutes	Paenibacillaceae	Paenibacillus
OTU97 (1)	JN222515	Betaproteobacteria	Comamonadaceae	Polaromonas
OTU98 (2)	JN222516	Gammaproteobacteria	Unclassified Gammaproteobacteria	
OTU99 (1)	JN222517	Firmicutes	Paenibacillaceae	Paenibacillus
OTU100 (1)	JN222518	Unclassified		
OTU101 (1)	Not accepted	Firmicutes		
OTU102 (2)	JN222519	Betaproteobacteria	Oxalobacteraceae	

OTU103 (1)	JN222520	Gemmatimonadetes	Gemmatimonadaceae	Gemmatimonas
OTU104 (1)	Not accepted	Firmicutes	Bacillaceae	Bacillus
OTU105 (1)	JN222521	Betaproteobacteria	Oxalobacteraceae	
OTU106 (1)	Not accepted	Betaproteobacteria	Rhodocyclaceae	Shinella
OTU107 (2)	JN222522	Planctomycetes	Planctomycetaceae	Pirellula
OTU108 (1)	JN222523	Betaproteobacteria	Oxalobacteraceae	
OTU109 (1)	JN222524	Betaproteobacteria	Nitrosomonadaceae	Nitrosospira
OTU110 (1)	JN222525	OD1	OD1 genera incertae sedis	
OTU111 (1)	JN222526	Betaproteobacteria	Burkholderiales incertae sedis	Ideonella
OTU112 (1)	JN222527	Deltaproteobacteria	Unclassified Deltaproteobacteria	
OTU113 (1)	JN222528	Gammaproteobacteria	Unclassified Gammaproteobacteria	
OTU114 (1)	JN222529	Betaproteobacteria	Oxalobacteraceae	Massilia
OTU115 (1)	JN222530	Deltaproteobacteria	Nannocystineae	
OTU117 (1)	JN222532	Betaproteobacteria	Oxalobacteraceae	
OTU118 (1)	JN222533	Planctomycetes	Planctomycetaceae	Pirellula
OTU119 (1)	JN222534	OD1	OD1 genera incertae sedis	
OTU120 (1)	JN222535	Actinobacteria	Lamiaceae	Lamia
OTU121 (1)	Not accepted	Unclassified		
OTU122 (2)	JN222536	Actinobacteria		
OTU123 (1)	JN222537	Bacteroidetes	Chitinophagaceae	Terrimonas
OTU124 (1)	JN222538	Firmicutes	Bacillaceae	
OTU125 (1)	JN222539	Firmicutes	Bacillaceae	Geobacillus
OTU126 (1)	JN222540	Deltaproteobacteria	Polyangiaceae	
OTU127 (1)	JN222541	Uncultured Proteobacteria		
OTU128 (1)	JN222542	Betaproteobacteria	Oxalobacteraceae	
OTU129 (1)	JN222543	Firmicutes		
OTU130 (1)	JN222544	Unclassified		

Table C.2. OTU sequences for water-rock ratios and time points, alongside accession numbers and nearest RDP classification.

Time (d)	High water-rock ratio			Low water-rock ratio		
	OTU	Accession #	RDP Classification	OTU	Accession #	RDP Classification
5	OTU6 (12)	JN222432	Betaproteobacteria/Oxalobacteraceae	OTU5 (12)	JN222431	Betaproteobacteria/Oxalobacteraceae
	OTU7 (24)	JN222433	Firmicutes/Paenibacillus	OTU6 (12)	JN222432	Betaproteobacteria/Oxalobacteraceae
	OTU9 (2)	JN222435	Betaproteobacteria/Oxalobacteraceae	OTU7 (24)	JN222433	Firmicutes/Paenibacillus
	OTU38 (6)	JN222462	Betaproteobacteria/Oxalobacteraceae	OTU8 (26)	JN222434	Betaproteobacteria/Massilia
	OTU48 (4)	JN222471	Firmicutes/Paenibacillus	OTU9 (2)	JN222435	Betaproteobacteria/Oxalobacteraceae
	OTU55 (4)	JN222478	Betaproteobacteria/Massilia	OTU17 (8)	JN222443	Betaproteobacteria/Janthinobacterium
	OTU64 (8)	JN222487	Betaproteobacteria/Massilia	OTU22 (17)	JN222447	Betaproteobacteria/Oxalobacteraceae
	OTU75 (1)	Not accepted	Firmicutes	OTU23 (6)	JN222448	Betaproteobacteria/Massilia
	OTU77 (2)	Not accepted	Firmicutes/Paenibacillaceae	OTU31 (22)	JN222455	Betaproteobacteria/Herbaspirillum
	OTU102 (2)	JN222519	Betaproteobacteria/Oxalobacteraceae	OTU34 (1)	JN222458	Betaproteobacteria/Oxalobacteraceae
				OTU48 (4)	JN222471	Firmicutes/Paenibacillus
				OTU49 (13)	JN222472	Betaproteobacteria/Massilia
				OTU55 (4)	JN222478	Betaproteobacteria/Massilia

				OTU66 (4)	JN222489	Betaproteobacteria/Oxalobacteraceae
				OTU70 (1)	JN222493	Betaproteobacteria/Oxalobacteraceae
				OTU72 (1)	JN222495	Firmicutes/Paenibacillus
				OTU76 (1)	JN222498	Betaproteobacteria/Oxalobacteraceae
				OTU81 (2)	JN222502	Betaproteobacteria/Oxalobacteraceae
				OTU83 (2)	JN222504	Betaproteobacteria/Oxalobacteraceae
				OTU90 (1)	JN222510	Betaproteobacteria/Oxalobacteraceae
				OTU108 (1)	JN222523	Betaproteobacteria/Oxalobacteraceae
				OTU128 (1)	JN222542	Betaproteobacteria/Oxalobacteraceae
76	OTU6 (12)	JN222432	Betaproteobacteria/Oxalobacteraceae	OTU1 (33)	JN222427	OD1/OD1 genera incertae sedis
	OTU22 (17)	JN222447	Betaproteobacteria/Oxalobacteraceae	OTU6 (12)	JN222432	Betaproteobacteria/Oxalobacteraceae
	OTU28 (53)	JN222453	Betaproteobacteria/Oxalobacteraceae	OTU8 (26)	JN222434	Betaproteobacteria/Massilia
	OTU46 (4)	JN222469	Betaproteobacteria/Oxalobacteraceae	OTU13 (12)	JN222439	Acidobacteria
	OTU56 (2)	JN222479	Betaproteobacteria/Oxalobacteraceae	OTU19 (12)	JN222444	Alphaproteobacteria/Bradyrhizobium
	OTU57 (6)	JN222480	Bacteroidetes/Chitinophagaceae	OTU20 (2)	JN222445	Alphaproteobacteria/Sphingomonas
	OTU84 (1)	Not accepted	Betaproteobacteria/Oxalobacteraceae	OTU26 (12)	JN222451	OD1/OD1 genera incertae sedis

	OTU87 (1)	JN222507	Betaproteobacteria/Oxalobacteraceae	OTU31 (22)	JN222455	Betaproteobacteria/Herbaspirillum
	OTU97 (1)	JN222515	Betaproteobacteria/Comamonadaceae	OTU32 (2)	JN222456	Unclassified bacterium
	OTU105 (1)	JN222521	Betaproteobacteria/Oxalobacteraceae	OTU41 (10)	Not accepted	Unclassified bacterium
	OTU127 (1)	JN222541	Uncultured Proteobacteria	OTU57 (6)	JN222480	Bacteroidetes/Flavisolibacter
				OTU65 (2)	JN222488	OD1/OD1 genera incertae sedis
				OTU86 (1)	JN222506	Unclassified Proteobacteria
				OTU89 (1)	JN222509	Unclassified bacterium
				OTU110 (1)	JN222525	OD1/OD1 genera incertae sedis
				OTU119 (1)	JN222534	OD1/OD1 genera incertae sedis
160	Clone library unsuccessful			OTU1 (33)	JN222427	OD1/OD1 genera incertae sedis
				OTU6 (12)	JN222432	Betaproteobacteria/Oxalobacteraceae
				OTU13 (12)	JN222439	Acidobacteria
				OTU16 (4)	JN222442	Unclassified bacterium
				OTU26 (12)	JN222451	OD1/OD1 genera incertae sedis
				OTU36 (1)	JN222460	Unclassified bacterium

				OTU41 (10)	Not accepted	Unclassified bacterium
				OTU47 (6)	JN222470	Unclassified bacterium
				OTU65 (2)	JN222488	OD1/OD1 genera incertae sedis
				OTU95 (1)	JN222513	OD1/OD1 genera incertae sedis
				OTU113 (1)	JN222528	Unclassified Gammaproteobacteria
				OTU126 (1)	JN222540	Deltaproteobacteria/Polyangiaceae
				OTU130 (1)	JN222544	Unclassified bacterium
213	OTU2 (7)	JN222428	Actinobacteria/Phycicoccus	OTU1 (33)	JN222427	OD1/OD1 genera incertae sedis
	OTU5 (12)	JN222431	Betaproteobacteria/Oxalobacteraceae	OTU8 (26)	JN222434	Betaproteobacteria/Massilia
	OTU22 (17)	JN222447	Betaproteobacteria/Oxalobacteraceae	OTU13 (12)	JN222439	Acidobacteria
	OTU28 (53)	JN222453	Betaproteobacteria/Oxalobacteraceae	OTU14 (3)	JN222440	Betaproteobacteria/Massilia
	OTU31 (22)	JN222455	Betaproteobacteria/Herbaspirillum	OTU16 (4)	JN222442	Unclassified bacterium
	OTU57 (6)	JN222480	Bacteroidetes/Flavisolibacter	OTU19 (12)	JN222444	Alphaproteobacteria/Bradyrhizobium
	OTU69 (1)	JN222492	Betaproteobacteria/Nitrosospira	OTU24 (8)	JN222449	Unclassified bacterium
	OTU73 (3)	JN222496	Betaproteobacteria/Nitrosospira	OTU31 (22)	JN222455	Betaproteobacteria/Herbaspirillum

	OTU74 (1)	JN222497	Verrucomicrobia/Verrucomicrobium	OTU33 (7)	JN222457	Gemmatimonadetes/Gemmatimonas
	OTU79 (1)	JN222500	Betaproteobacteria/Herbaspirillum	OTU39 (5)	JN222463	Betaproteobacteria/Massilia
	OTU93 (1)	JN222511	Bacteroidetes/Chitinophagaceae	OTU47 (6)	JN222470	Unclassified bacterium
	OTU109 (1)	JN222524	Betaproteobacteria/Oxalobacteraceae	OTU49 (13)	JN222472	Betaproteobacteria/Massilia
	OTU114 (1)	JN222529	Betaproteobacteria/Massilia	OTU62 (1)	JN222485	Unclassified bacterium
	OTU117 (1)	JN222532	Betaproteobacteria/Oxalobacteraceae	OTU71 (1)	JN222494	Unclassified bacterium
				OTU98 (2)	JN222516	Unclassified Gammaproteobacteria
				OTU107 (2)	JN222522	Planctomycetes/Pirellula
				OTU111 (1)	JN222526	Betaproteobacteria/Ideonella
				OTU112 (1)	JN222527	Unclassified Deltaproteobacteria
				OTU118 (1)	JN222533	Planctomycetes/Pirellula
	OTU4 (1)	JN222430	Betaproteobacteria/Nitrosospira	OTU3 (42)	JN222429	Firmicutes/Bacillus
	OTU15 (32)	JN222441	Actinobacteria/Arthrobacter	OTU10 (4)	JN222436	Actinobacteria
371	OTU30 (3)	JN222454	Firmicutes/Paenibacillus	OTU13 (12)	JN222439	Actinobacteria
	OTU37 (3)	JN222461	Firmicutes/Cohnella	OTU19 (12)	JN222444	Alphaproteobacteria/Bradyrhizobium
	OTU40 (8)	JN222464	Alphaproteobacteria/Bradyrhizobium	OTU21 (10)	JN222446	Actinobacteria

	OTU51 (3)	JN222474	Actinobacteria/Propionibacterium	OTU24 (8)	JN222449	Unclassified bacterium
	OTU58 (3)	JN222481	Cyanobacteria	OTU25 (2)	JN222450	Betaproteobacteria/Ideonella
	OTU78 (1)	JN222499	Actinobacteria/Arthrobacter	OTU27 (3)	JN222452	Gemmatimonadetes/Gemmatimonas
	OTU80 (1)	JN222501	Alphaproteobacteria/Bosea	OTU29 (4)	Not accepted	Unclassified bacterium
	OTU82 (1)	JN222503	Firmicutes	OTU33 (7)	JN222457	Gemmatimonadetes/Gemmatimonas
	OTU88 (1)	JN222508	Unclassified Alphaproteobacteria	OTU35 (1)	JN222459	Firmicutes
	OTU125 (1)	JN222539	Firmicutes/Geobacillus	OTU50 (2)	JN222473	Unclassified bacterium
				OTU53 (3)	JN222476	Unclassified bacterium
				OTU54 (1)	JN222477	Cyanobacteria
				OTU63 (2)	JN222486	Unclassified bacterium
				OTU92 (1)	Not accepted	Unclassified Alphaproteobacteria
				OTU122 (2)	JN222536	Actinobacteria
Rock	OTU6 (12)	JN222432	Betaproteobacteria/Oxalobacteraceae	OTU3 (42)	JN222429	Firmicutes/Bacillus
	OTU7 (24)	JN222433	Firmicutes/Paenibacillus	OTU7 (24)	JN222433	Firmicutes/Paenibacillus
	OTU12 (3)	JN222438	Firmicutes/Clostridia	OTU8 (26)	JN222434	Betaproteobacteria/Massilia

	OTU13 (12)	JN222439	Acidobacteria	OTU11 (1)	JN222437	Firmicutes/Paenibacillus
	OTU15 (32)	JN222441	Actinobacteria/Arthrobacter	OTU12 (3)	JN222438	Firmicutes/Clostridia
	OTU33 (7)	JN222457	Gemmatimonadetes/Gemmatimonas	OTU14 (3)	JN222440	Betaproteobacteria/Massilia
	OTU37 (3)	JN222461	Firmicutes/Cohnella	OTU18 (1)	Not accepted	Gemmatimonadete/Gemmatimonas
	OTU42 (2)	JN222465	Nitrospira/Nitrospira	OTU19 (12)	JN222444	Alphaproteobacteria/Bradyrhizobium
	OTU43 (1)	JN222466	Gemmatimonadetes/Gemmatimonas	OTU30 (3)	JN222454	Firmicutes/Paenibacillus
	OTU45 (1)	JN222468	Firmicutes/Paenibacillus	OTU33 (7)	JN222457	Gemmatimonadete/Gemmatimonas
	OTU48 (4)	JN222471	Firmicutes/Paenibacillus	OTU44 (3)	JN222467	Firmicutes/Paenibacillus
	OTU52 (2)	JN222475	Unclassified Gammaproteobacteria	OTU48 (4)	JN222471	Firmicutes/Paenibacillus
	OTU58 (3)	JN222481	Cyanobacteria	OTU49 (13)	JN222472	Betaproteobacteria/Massilia
	OTU60 (1)	JN222483	Planctomycetes/Singulisphaera	OTU59 (2)	JN222482	Alphaproteobacteria/Devosia
	OTU61 (3)	JN222484	Unclassified bacterium	OTU67 (2)	JN222490	Acidobacteria
	OTU68 (1)	JN222491	Actinobacteria/Arthrobacter	OTU77 (2)	Not accepted	Firmicutes/Paenibacillaceae
	OTU85 (2)	JN222505	Planctomycetes/Singulisphaera	OTU91 (2)	Not accepted	Deltaproteobacteria/Myxococcacea

	OTU94 (1)	JN222512	Gammaproteobacteria/Dokdonella	OTU100 (1)	JN222518	Unclassified bacterium
	OTU96 (1)	JN222514	Firmicutes/Paenibacillus	OTU101 (1)	Not accepted	Firmicutes
	OTU99 (1)	JN222517	Firmicutes/Paenibacillus	OTU104 (1)	Not accepted	Firmicutes/Bacillus
	OTU103 (1)	JN222520	Gemmatimonadetes/Gemmatimonas	OTU106 (1)	Not accepted	Betaproteobacteria/Shinella
	OTU123 (1)	JN222537	Bacteroidetes/Terrimonas	OTU115 (1)	JN222530	Deltaproteobacteria/Nannocystineae
	OTU124 (1)	JN222538	Firmicutes/Bacillaceae	OTU120 (1)	JN222535	Actinobacteria/Lamia
				OTU121 (1)	Not accepted	Unclassified bacterium
				OTU129 (1)	JN222543	Firmicutes

Appendix D: ICP-AES Rates

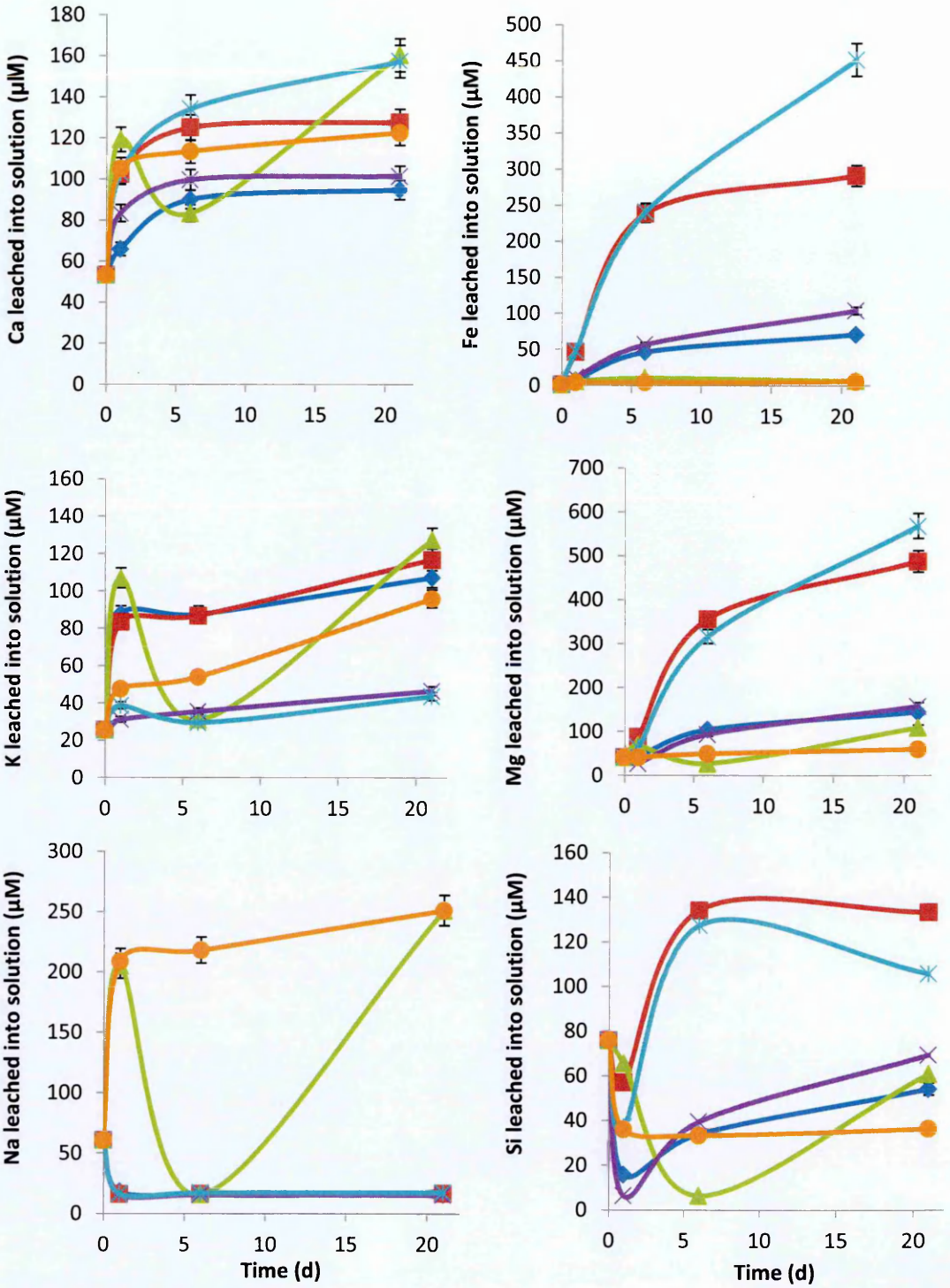

Figure D.1. Chapter 4, Experiment 2. The average release of trace elements over time for all ratios. The slopes were used to calculate the linear elemental release rates in Table 4.6.

Appendix E: ICP-MS data for Chapter 4 and 6

Table E.1. Chapter 4 Experiment 1. REE raw data in ppb and not normalised for water-rock ratios. 'B' denotes biological flasks and 'C' control. 1 = high ratio, 2 = medium ratio, 3 = low ratio.

Sample:	Sc / 45	Y / 89	La / 139	Ce / 140	Sm / 147	Eu / 151	Gd / 156	Dy / 161	Ho / 165	Er / 166	Yb / 172	Lu / 175
B1 0	0.087	0.463	5.669	3.121	0.078	0.020	0.119	0.072	0.015	0.040	0.033	0.005
B2 0	0.550	2.936	2.820	4.139	0.490	0.134	0.516	0.479	0.096	0.255	0.212	0.031
B3 0	18.126	96.963	64.490	130.718	17.750	5.104	18.090	16.768	3.351	8.835	7.271	1.010
C1 0	0.076	0.335	0.429	0.592	0.057	0.015	0.061	0.057	0.011	0.027	0.021	0.003
C2 0	0.871	3.756	2.417	4.745	0.616	0.167	0.634	0.586	0.120	0.322	0.274	0.038
C3 0	21.244	122.113	79.545	161.713	21.899	6.367	22.350	21.180	4.202	11.112	9.122	1.274
B1 30 m	0.208	1.128	0.999	1.646	0.184	0.051	0.196	0.179	0.037	0.096	0.081	0.012
B2 30 m	1.227	6.363	3.939	8.390	1.045	0.290	1.111	1.027	0.210	0.569	0.475	0.068
B3 30 m	26.371	143.600	95.705	199.143	26.838	7.852	27.272	25.784	5.148	13.615	11.277	1.581
C1 30 m	0.191	0.957	0.755	1.415	0.158	0.040	0.168	0.148	0.032	0.081	0.067	0.009
C2 30 m	1.766	7.501	4.305	9.136	1.196	0.333	1.251	1.186	0.245	0.659	0.569	0.082
C3 30 m	28.570	158.399	100.259	207.886	28.554	8.424	29.006	27.755	5.547	14.658	12.070	1.702
B1 1H	0.274	1.619	1.126	2.283	0.271	0.076	0.285	0.268	0.054	0.142	0.124	0.018
B2 1 H	1.730	9.108	5.241	11.557	1.488	0.401	1.538	1.480	0.301	0.813	0.679	0.098
B3 1H	29.325	166.913	106.508	220.987	30.373	8.901	30.735	29.766	5.874	15.613	13.045	1.822
C1 1H	0.248	1.324	0.855	1.817	0.221	0.059	0.238	0.212	0.044	0.113	0.089	0.013
C2 1 H	2.433	10.061	6.016	13.208	1.644	0.454	1.751	1.637	0.338	0.908	0.772	0.114
C3 1H	33.275	186.112	118.199	246.750	33.375	9.965	34.028	32.784	6.496	17.183	14.257	1.997
B1 24H	1.874	8.161	5.153	10.790	1.397	0.379	1.479	1.364	0.285	0.755	0.651	0.095
B2 24H	9.856	36.601	21.043	47.020	6.305	1.750	6.604	6.210	1.287	3.440	2.969	0.435

B3 24H	23.803	239.813	143.037	293.090	39.756	11.951	41.319	40.222	8.015	21.341	17.960	2.529
C1 24H	1.854	6.932	4.065	9.093	1.185	0.306	1.243	1.160	0.234	0.629	0.521	0.076
C2 24H	14.072	46.589	24.923	56.888	7.829	2.156	8.157	7.736	1.570	4.234	3.670	0.539
C3 24H	21.592	236.112	141.995	286.800	38.746	11.734	40.331	39.079	7.768	20.733	17.272	2.422
B1 3D	4.133	14.375	8.139	17.834	2.413	0.656	2.538	2.406	0.492	1.308	1.144	0.170
B2 3D	20.544	62.574	36.184	83.980	11.477	3.191	11.779	11.167	2.280	6.121	5.275	0.780
B3 3D	21.305	282.562	162.731	326.464	44.403	13.389	46.629	45.695	9.138	24.435	20.349	2.882
C1 3D	3.981	12.302	6.661	15.383	2.058	0.551	2.190	2.052	0.419	1.124	0.962	0.144
C2 3D	24.835	74.729	42.394	98.518	13.734	3.853	14.195	13.412	2.712	7.266	6.379	0.944
C3 3D	19.666	284.128	162.441	323.129	43.574	13.184	46.095	45.199	8.974	24.067	19.893	2.813
B1 7D	7.443	21.820	12.048	27.024	3.686	1.016	3.855	3.644	0.743	1.980	1.734	0.258
B2 7D	32.335	86.829	50.362	118.570	16.184	4.566	16.671	15.679	3.192	8.415	7.421	1.083
C1 7D	6.346	17.501	10.159	23.384	3.106	0.826	3.272	3.058	0.624	1.652	1.435	0.214
C2 7D	38.552	109.664	61.943	145.427	20.582	5.803	20.855	20.044	4.064	10.770	9.418	1.389
B1 14D	11.498	30.477	17.585	39.933	5.379	1.481	5.607	5.361	1.088	2.899	2.540	0.382
B2 14D	38.769	102.543	61.570	144.669	20.162	5.751	20.532	19.313	3.930	10.484	9.221	1.346
C1 14D	8.235	21.544	11.874	27.443	3.627	0.975	3.863	3.624	0.740	1.963	1.688	0.250
C2 14D	44.063	129.288	71.263	171.776	23.950	6.839	24.330	23.054	4.687	12.609	11.053	1.614
B1 24D	13.135	35.392	20.277	46.347	6.333	1.742	6.532	6.178	1.272	3.402	2.994	0.445
B2 24D	51.578	124.507	75.016	166.829	23.720	6.836	23.823	22.678	4.585	12.160	10.836	1.548
C1 24D	11.141	26.566	15.697	33.824	4.703	1.277	4.777	4.569	0.930	2.459	2.161	0.316
C2 24D	47.660	129.494	77.952	174.361	25.471	7.348	25.573	24.383	4.941	13.117	11.714	1.687
B1 37D	16.969	40.874	24.352	52.236	7.429	2.104	7.592	7.261	1.479	3.928	3.470	0.504
B2 37D	50.366	129.104	78.952	176.180	25.410	7.370	25.393	24.458	4.922	13.125	11.451	1.645
B3 37D	27.755	628.168	340.274	695.641	95.457	29.104	101.268	96.562	19.078	51.325	43.175	5.982
C1 37D	11.427	29.925	17.876	38.103	5.462	1.461	5.497	5.190	1.048	2.827	2.397	0.353
C2 37B	50.022	146.652	90.444	206.710	29.613	8.576	29.593	28.235	5.660	15.162	13.259	1.906
C3 37D	25.553	454.952	240.540	486.251	66.585	20.332	74.079	70.691	14.126	38.113	31.692	4.508

Table E.2. Chapter 4 Experiment 2. REE raw data in ppb and not normalised for water-rock ratios. 'B' denotes biological flasks and 'C' control. 1 = high ratio, 2 = medium ratio, 3 = low ratio.

Sample:	Sc / 45	Y / 89	La / 139	Ce / 140	Sm / 147	Eu / 151	Gd / 156	Dy / 161	Ho / 165	Er / 166	Yb / 172	Lu / 175
T0	0.024	0.022	0.033	0.074	0.004	0.004	0.006	0.006	0.003	0.004	0.002	0.002
B1A T1d	0.087	2.085	34.784	16.342	0.412	0.095	0.541	0.369	0.075	0.199	0.160	0.023
B1B T1d	0.062	1.289	1.801	3.252	0.248	0.065	0.255	0.232	0.046	0.122	0.101	0.014
B2A T1d	0.412	9.234	6.794	15.137	1.711	0.411	1.782	1.582	0.319	0.867	0.691	0.095
B2B T1d	0.452	12.552	9.438	20.448	2.339	0.550	2.452	2.167	0.435	1.175	0.956	0.129
B3A T1d	0.414	4.084	2.291	3.493	0.372	0.112	0.482	0.420	0.098	0.271	0.217	0.035
B3B T1d	0.382	4.711	2.859	4.721	0.499	0.150	0.640	0.565	0.121	0.333	0.239	0.037
C1A T1d	0.136	1.676	1.193	2.595	0.309	0.080	0.325	0.286	0.061	0.163	0.124	0.021
C1B T1d	0.072	1.569	1.441	2.996	0.326	0.082	0.347	0.290	0.060	0.156	0.117	0.020
C2A T1d	0.475	10.272	7.791	17.343	2.028	0.501	2.044	1.817	0.364	0.975	0.793	0.115
C2B T1d	0.624	6.151	4.195	9.245	1.108	0.294	1.182	1.075	0.217	0.591	0.494	0.072
C3A T1d	0.286	0.871	0.528	0.938	0.105	0.032	0.130	0.120	0.025	0.075	0.057	0.009
C3B T1d	0.229	0.885	0.602	1.021	0.098	0.028	0.132	0.114	0.022	0.067	0.055	0.008
B1A T6d	0.326	4.250	30.649	17.181	0.816	0.183	0.969	0.755	0.149	0.413	0.327	0.045
B2B T6d	0.292	2.862	9.154	7.285	0.547	0.135	0.592	0.495	0.096	0.278	0.223	0.028
B2A T6d	1.668	15.409	12.340	25.243	2.829	0.647	2.955	2.611	0.524	1.453	1.223	0.169
B2B T6d	1.589	21.138	15.633	34.044	3.852	0.910	3.997	3.527	0.717	1.970	1.603	0.220
B3A T6d	0.458	2.569	1.608	2.578	0.291	0.085	0.351	0.308	0.064	0.191	0.155	0.025
B3B T6d	0.362	2.663	1.787	2.398	0.231	0.070	0.316	0.268	0.057	0.165	0.125	0.017
C1A T6d	0.467	3.003	2.761	4.821	0.543	0.141	0.576	0.534	0.102	0.286	0.230	0.033
C1B T6d	0.279	3.008	2.632	5.472	0.593	0.142	0.608	0.523	0.101	0.293	0.218	0.029
C2A T6d	1.444	16.979	12.668	28.738	3.257	0.800	3.323	3.025	0.597	1.654	1.357	0.192
C2B T6d	2.270	13.101	8.591	19.103	2.325	0.619	2.470	2.289	0.455	1.269	1.080	0.156
C3A T6d	0.349	0.959	0.604	1.058	0.125	0.039	0.151	0.120	0.027	0.074	0.068	0.008
C3B T6d	0.181	0.498	0.355	0.633	0.066	0.020	0.074	0.071	0.011	0.045	0.036	0.004

B1A T21d	0.574	4.869	39.769	32.173	0.916	0.206	1.134	0.821	0.169	0.452	0.364	0.050
B2B T21d	0.503	2.847	9.249	8.626	0.526	0.129	0.582	0.483	0.096	0.266	0.216	0.029
B2A T21d	2.490	17.198	14.170	28.136	3.114	0.722	3.250	2.954	0.601	1.609	1.371	0.189
B2B T21d	2.370	21.761	16.431	34.492	3.916	0.902	3.969	3.601	0.733	2.031	1.665	0.228
B3A T21d	0.350	1.790	1.071	1.678	0.187	0.054	0.223	0.207	0.040	0.125	0.096	0.016
B3B T21d	0.434	1.849	1.295	1.781	0.191	0.054	0.236	0.203	0.040	0.122	0.097	0.014
C1A T21d	1.004	5.174	10.631	12.688	0.951	0.253	1.054	0.926	0.187	0.493	0.406	0.055
C1B T21d	0.516	5.355	19.538	16.964	1.057	0.251	1.168	0.964	0.185	0.505	0.401	0.052
C2A T21d	2.300	23.886	21.332	41.668	4.465	1.116	4.624	4.137	0.822	2.323	1.868	0.270
C2B T21d	3.069	16.688	11.848	24.058	2.881	0.763	3.042	2.830	0.573	1.580	1.375	0.202
C3A T21d	0.208	0.399	0.312	0.443	0.045	0.012	0.058	0.052	0.009	0.027	0.024	0.002
C3B T21d	0.144	0.420	0.287	0.529	0.060	0.016	0.068	0.063	0.011	0.037	0.032	0.004
B1A T43d	0.800	6.112	5.002	15.690	1.113	0.256	1.187	1.030	0.208	0.574	0.470	0.065
B2B T43d	0.536	3.518	2.622	5.933	0.657	0.162	0.654	0.607	0.120	0.336	0.277	0.039
B2A T43d	2.851	18.566	12.676	28.754	3.251	0.781	3.386	3.149	0.639	1.736	1.469	0.208
B2B T43d	2.894	23.951	16.752	37.224	4.296	1.008	4.380	3.978	0.809	2.248	1.838	0.258
B3A T43d	0.394	2.691	1.618	2.336	0.253	0.082	0.323	0.277	0.062	0.176	0.146	0.023
B3B T43d	0.492	2.957	2.475	3.189	0.270	0.079	0.366	0.297	0.062	0.167	0.134	0.018
C1A T43d	1.128	6.021	4.190	9.334	1.125	0.290	1.161	1.068	0.207	0.578	0.467	0.065
C1B T43d	0.634	6.379	5.475	11.800	1.295	0.299	1.285	1.138	0.224	0.594	0.462	0.065
C2A T43d	2.418	30.831	21.824	49.671	5.525	1.377	5.677	5.077	1.019	2.862	2.361	0.346
C2B T43d	2.640	18.696	11.627	26.452	3.170	0.825	3.342	3.126	0.632	1.765	1.564	0.228
C3A T43d	0.281	0.746	0.562	0.914	0.094	0.022	0.107	0.097	0.017	0.054	0.044	0.007
C3B T43d	0.345	1.161	0.686	1.232	0.133	0.040	0.163	0.145	0.030	0.083	0.074	0.010

Table E.3. Chapter 5. REE raw data in ppb and not normalised for water-rock ratios at day 0 and day 216. 'B' denotes biological flasks and 'C' control. 1 = high ratio, 2 = medium ratio, 3 = low ratio.

Sample:	Sc / 45	Y / 89	La / 139	Ce / 140	Eu / 151	Gd / 156	Dy / 161	Er / 166
T = 0 Stock (13/02/09)	0.008	0.009	0.012	0.036	-0.002	-0.002	0.000	0.000
B1A T = 216 d	0.112	0.053	0.280	0.291	0.002	0.009	0.007	0.003
B1B T = 216 d	0.051	0.016	0.265	0.172	-0.001	0.002	0.004	0.000
B2A T = 216 d	0.109	0.074	0.111	0.183	0.002	0.018	0.012	0.007
B2B T = 216 d	0.102	0.052	0.328	0.239	0.001	0.008	0.009	0.003
B3A T = 216 d	0.185	0.206	0.155	0.321	0.011	0.039	0.035	0.019
B3B T = 216 d	0.181	0.167	0.335	0.393	0.008	0.033	0.029	0.014
C1B T = 216 d F.C.	0.039	0.006	0.514	0.279	-0.002	0.001	-0.002	0.000
C2A T = 216 d	0.107	0.007	0.162	0.190	-0.002	0.003	0.000	-0.002
C2B T = 216 d	0.095	0.016	0.068	0.083	-0.002	0.000	0.001	-0.001
C3A T = 216 d	0.107	0.023	0.040	0.076	-0.001	0.002	0.003	0.000
C3B T = 216 d	0.131	0.052	0.048	0.091	0.000	0.005	0.008	0.003

Appendix F: Published Abstracts

Oral Presentation: Astrobiology Society of Britain Conference (2008)

Weathering with *Thiobacillus* – The effect of changing liquid to rock ratios on microbial weathering of basalt

Simpson, A.E.[1], Grady, M.M.[1], Cockell, C.S.[1]

[1] The Open University, Geomicrobiology Research Group, CEPSAR, Walton Hall, Milton Keynes, Buckinghamshire, MK7 6AA, United Kingdom. a.e.simpson@open.ac.uk

Rock weathering has a large effect on biogeochemical cycling. It controls nutrient flux in the biosphere and long term climate. However, weathering does not only occur by chemical and physical factors. Microorganisms play a central role in the weathering of rocks. This, however, is little understood and one major mystery is why weathering rates are so different in the laboratory compared to the field. The aim of this work is to understand the influence of the water-rock ratio on the rate of microbial rock weathering.

To investigate how pH and rates of elemental release were affected by changing the liquid to rock ratio, batch cultures of the acidophilic, iron-oxidising bacterium *Thiobacillus ferrooxidans* were set up in polycarbonate flasks, with the iron required provided by basalt from the volcano Eldfell in Heimaey, Iceland. Three different liquid to rock ratio conditions were used: high, medium and low ratios. Controls to compare abiotic effects were set up, with flasks containing only media and basalt.

An optimum liquid to rock ratio was found to be the medium volume condition. The large volume diluted the released iron, potentially limiting its supply. In the low volume

flasks, which had a low liquid to rock ratio, the acid in the media was quickly quenched, with pH increasing nearly two-fold after the first 24 hours, which in natural closed environments might increase the pH to above the optimum for growth. The medium volume flask achieved a near optimum balance between iron concentration and proton quenching by rock weathering.

Work is ongoing using inductively coupled plasma mass spectrometry (ICP-MS) to determine the concentration of other elements being released from the basalt. In addition, the basalt from the different conditions is being examined by SEM to record the abiotic and biotic effect of weathering on the rock's surface.

This work has implications for the rates of rock weathering in natural environments where a balance between optimum energy and nutrient supply and pH conditions for growth occurs including, for example, in acid mine drainage sites. From an astrobiological perspective, this work has implications for micro-scale conditions for habitability in basaltic environments on Mars, where low water to rock ratios have been postulated to be present in combination with acidic conditions. Such conditions may also have existed in geothermal regions on the Archaean Earth.

Oral Presentation: Goldschmidt Conference (2009)

The effect of water-rock ratios on microbial weathering of basalt

Simpson, A.E.[1], Grady, M.M.[1], Mosselmans J.F.W.[2], Cockell, C.S.[1]

[1]CEPSAR, Open University, Milton Keynes, MK7 6AA, UK (a.e.simpson@open.ac.uk)

[2]Diamond Light Source, Didcot, OX11 0DE, UK

Rock weathering has an important influence on biogeochemical cycling. It controls nutrient flux in the biosphere and long term climate through CO_2 drawdown. However, weathering does not only occur by chemical and physical factors. Microorganisms play a role in the weathering of rocks. This, however, is little understood and one major question is why weathering rates are so different in the laboratory compared to the field.

This work aimed to understand the influence of water-rock ratios on the rate of microbial weathering of basalt.

To investigate how pH and rates of elemental release were affected by changing the water-rock ratio, batch cultures of the acidophilic iron-oxidising bacterium *Acidithiobacillus ferrooxidans* were set up in polycarbonate flasks and monitored for 37 days. The iron required was provided by basalt from the volcano Eldfell in Heimaey, Iceland. Three different water-rock ratios were used: high (800ml media, 2g basalt), medium (100ml, 2g) and low (25ml, 25g).

An optimum water-rock ratio was found to be the medium ratio, which achieved the highest cell numbers, . Additional experiments showed that in the low ratio case neither an increase in pH due to rock weathering reactions or high heavy metal concentrations present in rocks was the cause of cell death. XANES at the Fe-K edge analysis showed localised areas of heamatite but the surface of the rock also showed Fe oxidation without a change in gross mineralogy. It is proposed that Fe^{3+} ions bind to the rock surface and preventing the release of reduced iron to provide energy for the bacteria, which might cause rapid reduction in Fe availability in the low water rock ratio environment.

This work has implications for the rates of rock weathering in natural environments where water-rock ratios may effect the balance between optimum energy and nutrient supply, as for example in the case of organisms in vesiculated basalt (low water-rock

ratio) and acid mine drainage sites (high water rock-ratio). Water-rock ratio effects may contribute to differences in laboratory and field-measured weathering rates.

Oral Presentation: Astrobiology Society of Britain Conference (2010)

Effect of Water-Rock Ratios on Microbial Weathering: A Strategy for Site Selection on Mars?

Simpson, A.E.[1], Cockell, C.S.[1], Olsson-Francis, K.[1], Grady, M.M.[2],

[1] The Open University, Geomicrobiology Research Group, CEPSAR, Walton Hall, Milton Keynes, Buckinghamshire, MK7 6AA, United Kingdom. a.e.simpson@open.ac.uk

[2] The Open University, Planetary and Space Sciences Research Institute, CEPSAR, Walton Hall, Milton Keynes, Buckinghamshire, MK7 6AA, United Kingdom.

Several paleoclimate models have shown early Mars to have been a wet and warm planet, similar to early Earth, before losing its atmosphere and becoming a cold, dry planet. Elemental and mineralogical data from the Mars Rover Missions have revealed both low and high water-rock ratio alterations on Mars. The aim of this work is to, through understanding the influence of water-rock ratios on microbial rock weathering, find suitable sites that would or could have sustained life.

The experiment investigated how pH and rates of elemental release were affected by changing the water-rock ratio. Batch cultures of the acidophilic iron-oxidising bacterium *Acidithiobacillus ferrooxidans* were set up in flasks and monitored for 37 days using Icelandic basalt as the iron source. Three different water-rock ratios were used: high (2g in 800ml), medium (2g in 100ml) and low (25g in 25ml).

The optimum water-rock ratio was found to be the medium ratio, which achieved the highest cell numbers. Experiments showed that in the low ratio case neither an increase

in pH due to proton quenching in rock weathering reactions or high heavy metal concentrations present in rocks was the cause of cell death. XANES at the Fe-K edge analysis showed localised areas of heamatite but the surface of the rock also showed Fe oxidation without a change in gross mineralogy. It is proposed that Fe^{3+} ions bind to the rock surface and preventing the release of reduced iron to provide energy for the bacteria. High water-rock ratios create too dilute an iron source for energy acquisition. This suggests that sites on Mars of medium water-rock ratios would be more likely to support or have supported microbial life.

Oral Presentation: International Society for Microbial Ecology Conference (2010)

Microbial successional changes in a one year laboratory experiment on the weathering of basalt glass with different water-rock ratios

Simpson, A.E.[1], Cockell, C.S.[1], Olsson-Francis, K.[1], Grady, M.M.[2],

[1] The Open University, Geomicrobiology Research Group, CEPSAR, Walton Hall, Milton Keynes, Buckinghamshire, MK7 6AA, United Kingdom. a.e.simpson@open.ac.uk

[2] The Open University, Planetary and Space Sciences Research Institute, CEPSAR, Walton Hall, Milton Keynes, Buckinghamshire, MK7 6AA, United Kingdom.

Microbes have been associated with alteration of basalt glass, which is abundant in the Earth's crust. Due to the concentration of biologically important elements present (including iron), alteration of glass makes it an important process in global biogeochemical cycling. Rock weathering by microbes can be influenced by varying conditions, and though variables such as temperature and pH have been investigated, water-rock ratios have not. In natural environments one can find differing water-rock ratios, from low ratios in rock vesicles to high ratios, such as rocks in a river bed.

To gain a better understanding of the process of microbial alteration of basalt glass, three water-rock ratios were established (high - 2.5×10^{-3} g/ml, medium - 0.02 g/ml and low - 1 g/ml) and inoculated with basalt glass that contained a natural microbial community. For 12 months, the flasks were sampled for pH, elemental release, and to build a community profile over time using denaturing gradient gel electrophoresis (DGGE) in combination with 16S rDNA clone libraries and sequencing of isolates. Preliminary DGGE analysis has shown different community profiles emerging with the varying ratios, as each condition brings about different solution chemistries.

Cyanobacteria and algae appeared at 76 days and at 12 months were present under all conditions, even at pH 5 (pH of high ratio flask after one year). Representatives of the Actinobacteria and Firmicutes are some of the dominant organisms. pH dropped in all biological flasks, with the greatest drop in the high ratio flask (from pH 7 to 5.2). With elemental release rates we are able to correlate the microbiology to weathering conditions.

This work has implications for the rates of rock weathering in natural environments where water-rock ratios may affect the balance between optimum energy and nutrient supply.

References

Åström M (2001) Abundance and fractionation patterns of rare earth elements in streams affected by acid sulphate soils. *Chem. Geol.* **175**, 249–258.

Åström M, Corin N (2003) Distribution of rare earth elements in anionic, cationic and particulate fractions in boreal humus-rich streams affected by acid sulphate soils. *Water Res.* **37**, 273–280.

Abed RMM, Zein B, Al-Thukair A, de Beer D (2007) Phylogenetic diversity and activity of aerobic heterotrophic bacteria from a hypersaline oil-polluted microbial mat. *Syst Appl Microbiol* **30**, 319–330.

Ascaso A, Wierzchos J, De Los Rios A (1995) Cytological investigations of lithobiontic microorganisms in granitic rocks. *Bot. Acta* **108**, 474–481.

Acker JG, Bricker OP (1992) The influence of pH on biotite dissolution and alteration kinetics at low temperature. *Geochimica et Cosmochimica Acta* **56**, 3073–3092.

Adamo P, Violante P (1991) Weathering of volcanic rocks from Mt. Vesuvius associated with the lichen Stereocaulon vesuvianum. *Pedobiologia* **35**, 209–217.

Adamo P, Violante P (2000) Weathering of rocks and neogenesis of minerals associated with lichen activity. *Appl Clay Sci* **16**, 229–256.

Adams JB, Palmer F, Staley JT (1992) Rock weathering in deserts: mobilization and concentration of ferric iron by microorganisms. *Geomicrobiol. J.* **10**, 99-114.

Altschul SF, Madden TL, Schäffer AA, Zhang Z, Zhang Z, Miller W, Lipman DJ (1997) Gapped BLAST and PSI-BLAST: a new generation of protein database search programs. *Nucl Acids Res* **25**, 3389-3402.

Andrews JH, Harris RF (1986) r- and K selection and microbial ecology. *Adv. Microb. Ecol.* 9, 99-147.

Antweiler RC, Drever JI (1983) The weathering of a late Tertiary volcanic ash: importance of organic solutes. *Geochim et Cosmochim Acta* **47**, 623-629.

Arinõ X, Ortega-Calvo JJ, Gomez-Bolea A, Saiz-Jimenez C (1995) Lichen colonization of the Roman pavement at Baelo Claudia (Cadiz, Spain): Biodeterioration vs. bioprotection. *Sci. Total Environ.* **167**, 353–363.

Baas Becking LGM, Parks GS (1927) Energy relations in the metabolism of autotrophic bacteria. *Physiol. Rev.* **7**, 85-106.

Bach W Edwards KJ (2003) Iron and sulfide oxidation within the basaltic ocean crust: Implications for chemolithoautotrophic microbial biomass production. *Geochimica et Cosmochimica Acta*. **67**, 3871-3887.

Bailey RM, Stokes S, Bray H (2003) Inductively-coupled plasma mass spectrometry (ICP-MS) for dose rate determination: some guidelines for samples prepararttion and analysis. *Ancient TL.* **21**, 11-14.

Baillet F, Magnin JP, Cheruy A (1997) Cadmium tolerance and uptake by a *Thiobacillus ferrooxidans* biomass. *Environ Technol* **18**, 631–638.

Baillet F, Magnin JP, Cheruy A, Ozil P (1998) Chromium precipitation by acidophilic bacterium *Thiobacillus ferrooxidans*. *Biotechnol Lett* **20**, 95–99.

Baker VR (2001) Water and the Martian landscape. *Nature.* **412**, 228-236.

Baker VR (2002) High-energy megafloods: Planetary settings and sedimentary dynamics. *International Association of Sedimentologists Special Publications*. 3-15.

Baker BJ, Banfield JF (2003) Microbial communities in acid mine drainage. *FEMS Microbiology Ecology* **44**, 139-152.

Balamurugan R, Janardhan HP, George S, Chittaranjan SP, Ramakrishna BS (2008) Bacterial succession in the colon during childhood and adolescence: molecular studies in a southern Indian village. *Am. J. Clin. Nutr.* **88**, 1643-1647.

Banerjee NR, Muehlenbachs K (2003) Tuff life: bioalteration in volcaniclastic rocks from the Ontong Java Plateau. *Geochemistry, Geophysics, and Geosystems* **4**, 1037-1059.

Banfield JF, Barker WW, Welch SA, Taunton A (1999) Biological impact on mineral dissolutions: Application of the lichen model to understanding mineral weathering in the rhizosphere. *Proc. Natl. Acad. Sci.* **96**, 3404-3411.

Barker WW, Banfield JF (1996) Biologically versus inorganically mediated weathering reactions: Relationships between minerals and extracellular microbial polymers in lithobiontic communities. *Chemical Geology* **132**, 5–69.

Barker WW, Banfield JF (1998) Zones of chemical and physical interaction at interfaces between microbial communities and minerals. A model. *Geomicrobiology Journal* **15**, 223–244.

Barker WW, Welch SA, Chu S, Banfield JF (1998) Experimental observations of the effects of bacteria on aluminosilicate weathering. *Am. Mineral.* **83**, 1551-1563.

Battin T (2007). Biophysical controls on community sucession in stream biofilms. *Appl. Environ. Microbiol.* **73**, 4966-4974.

Bawden TM, Einaudi MT, Bostick BC, Meibom A, Wooden J, Norby JW, Orobona MJT, Chamberlain CP (2003) Extreme 34S depletions in ZnS at the Mike gold deposit, Carlin Trend, Nevada: Evidence for bacteriogenic supergene sphalerite. *Geology* **31**, 913-916.

BBC (2010) A guide to Iceland's volcanoes. http://news.bbc.co.uk/1/hi/world/europe/8623239.stm. Last accessed: 24/8/11

Benedict JB (1993) Influence of snow on rates of granodiorite weathering, Colorado Front Range, USA. *Boreas* **22**, 87-92.

Bennett PC, Hiebert FK, Choi WJ (1996) Microbial colonization and weathering of silicates in a petroleum-contaminated groundwater. *Chemical Geology*. **132**, 45–53.

Benzerara K, Barakat M, Menguy N, Guyot F, Luca GD, Audrain C, Heulin T (2004) Experimental colonization and alteration of orthopyroxene by the pleomorphic bacteria *Ramlibacter tataouinensis*. *Geomicrobiol. J.* **21**, 341–349.

Benzerara K, Menguy N, Guyot F, Vanni C, Gillet P (2005) TEM study of a silicate-carbonate-microbe interface prepared by focused ion beam milling. *Geochim. Cosmochim. Acta* **69**, 1413–1422.

Berg KA, Lyra C, Sivonen K, Paulin L, Suomalainen S, Tuomi P, Rapala J (2009) High diversity of cultivable heterotrophic bacteria in association with cyanobacterial water blooms. *The ISME Journal* **3**, 314–325.

Berner RA, Lasaga AC, Garrels RM (1983) The carbonate-silicate geochemical cycle and its effect on atmospheric carbon dioxide over the past 100 millions years. *Am. J. Sci.* **284**, 641–683.

Berner RA, Lasaga AC (1989) Modeling the geochemical carbon cycle. *Scientific American.* 74-81.

Berthelin J (1983) Microbial weathering processes. **In**. W.E. Krumbein, Ed., *Microbial Geochemistry*, 223–262. Blackwell Scientific Publications, Oxford, UK.

Besemer K, Singer GA, Limberger R, Chlup AK, Hochedlinger G, Hoedl I, Baranyi C,

Bik EM, Long CD, Armitage GC, Loomer P, Emerson J, Mongodin EF et al. (2010) Bacterial diversity in the oral cavity of 10 healthy individuals. *ISME J.* 4:8, 962-74.

Bland W, Rolls D (2005) Weathering: An introduction to the scientific principles. Arnold, London.

Blum AE, Lasaga AC (1988) Role of surface speciation in the low-temperature dissolution of minerals. *Nature* **331**, 431–433.

Blum SAE, Lorenz MG Wackernagel W (1997) Mechanism of retarded DNA degradation and prokaryotic origin of DNases in nonsterile soils. *Systematic and Applied Microbiology.* **20**, 513–521.

Bonferroni CE (1935) Il calcolo delle assicurazioni su gruppi di teste. *Studi in Onore del Professore Salvatore Ortu Carboni.* 13-60.

Bonetta S, Bonetta S, Carraro E, Rantsiou K, Cocolin L (2008) Microbiological characterisation of Robiola di Roccaverano cheese using PCR–DGGE. *Food Microbiology* 25:6, 786–792.

Bopp HL, Chakrabarty AM, Ehrlich HL (1983) Chromate resistance plasmid in *Pseudomonas fluorescens. J Bacteriol* **155**, 1105–1109.

Borrel G. Lehours AC, Bardot C, Bailly X, Fonty G (2010) Members of candidate divisions OP11, OD1 and SR1 are widespread along the water column of the meromictic Lake Pavin (France). *Archives of Microbiology* **192(7)**, 559-567.

Bourcier WL (1994) Waste glass corrosion modeling: Comparison with experimental results. *Mat. Res. Soc. Symp. Proc.* **333**, 69–82.

Boyer A, Magnin JP, Ozil P (1998) Copper ion removal by *Thiobacillus ferrooxidans* biomass. *Biotechnol Lett* **20**, 187–190.

Boynton WV, Taylor GJ, Karunatillake S, Reedy RC, Keller JM (2008) Elemental abundances determined via the Mars Odyssey GRS. J.F. Bell (Ed.) *The Martian Surface: Composition, Mineralogy and Physical Properties*, Cambridge University Press, p. 105–124

Brahmaprakash GP, Devasia P, Jagadish KS, Natarajan KA, Rao GR (1988) Development of *Thiobacillus ferrooxidans* ATCC 19859 strains tolerant to copper and zinc. *Bull Mater Sci* **10**, 461–465.

Brantley SL (2003) Reaction kinetics of primary rock-forming minerals under ambient conditions. In *Treatise on Geochemistry, Surface and Ground Water, Weathering, and Soils* (ed. J. I. Drever, vol. 5.). Elsevier Pergamon, 73–119.

Brehm U, Gorbushina A, Mottershead D (2005) The role of microorganisms and biofilms in the breakdown and dissolution of quartz and glass. *Palaeogeography, Palaeoclimatology, Palaeoecology.* **219**, 117-129.

Bridge TAM, Johnson DB (2000) Reductive dissolution of ferric iron minerals by *Acidiphilium* SJH, *Geomicrobiol. J.* **17**, 193– 206.

Brown MV, Bowman JP (2001) A molecular phylogenetic survey of sea-ice microbial communities (SIMCO). *FEMS Microbiol Ecol* **35**, 267–275.

Bruce KD, Hiorns WD, Hobman JL, Osborn AM, Strike P, Ritchie DA (1992) Amplification of DNA from native populations of soil bacteria by using polymerase chain reaction. *Appl Environ Microbiol.* **58**, 3413-3416.

Brunauer S, Emmett PH, Teller E (1938) Adsorption of gases in multimolecular layers. *J Am Chem Soc.* **60**, 309-319.

Brückner J, Dreibus G, Gellert R, Squyres SW, Wänke H, Yen A, Zipfel J (2008) Mars exploration rovers: chemical composition by the APX. J. Bell (Ed.), *The Martian*

Surface: Composition, Mineralogy and Physical Properties, Cambridge University Press (2008), 58–102.

Budyko M., Ronov A (1979) Chemical evolution of the atmosphere in the Phanerozoic. *Geochemical International.* **16**, 1–9.

Burdige DJ (1993) The biogeochemistry of manganese and iron reduction in marine sediments. *Earth-Sci. Rev.* **35**, 249-284.

Burger D (1968) Relative weatherability of calcium containing minerals. *Canadian Journal of Soil Science.* **49**, 21-28.

Button DK, Schut F, Quang P, Martin R, Robertson BR (1993) Viability and Isolation of Marine Bacteria by Dilution Culture: Theory, Procedures, and Initial Results. *Appl Environ Microbiol.* **59(3)**, 881–891.

Bünzli JCG, Choppin GR (eds.) (1989) *Lanthanide Probes in Life, Chemical and Earth Sciences*. Elsevier Science Publishers B.V., Amsterdam, 432 pp.

Böckelmann U, Manz W, Neu TR, Szewzyk U (2000) Characterization of the microbial community of lotic organic aggregates ('river snow') in the Elbe River of Germany by cultivation and molecular methods. *FEMS Microbiol Ecol* **33**, 157–170.

Cabrera G, Gómez JM. Cantero D (2005) Influence of heavy metals on growth and ferrous sulphate oxidation by *Acidithiobacillus ferrooxidans* in pure and mixed cultures. *Process Biochemistry* **40**, 2683-2687

Caldeira K (1995) Long-term control of atmospheric carbon dioxide; low temperature seafloor alteration or terrestrial silicate-rock weathering? *Am. J. Sci.* **295**, 1077-1114.

Carmichael ISE (1964) The petrology of Thingmuli, a Tertiary volcano in eastern Iceland. *J Petrol* **5**, 425-460.

Casey WH, Bunker B (1990) Leaching of mineral and glass surfaces during dissolution. **In:** Hochella Jr MF, White AF, Editors (1990) *Mineral-water Interface Geochemistry: Reviews in Mineralogy* 23, Mineralogical Society of America 397–426.

Cavicchioli R (2002) Extremophiles and the Search for Extraterrestrial Life. *Astrobiology*. **2**, 281-292.

Chang TT, Li CY (1998) Weathering of limestone, marble, and calcium phosphate by ectomycorrhizal fungi and associated microorganisms. *Taiwan J. Forest Sci.* **13**, 85–90.

Chao A (1984) Non-parametric estimation of the number of classes in a population. *Scand. J. Stat.* **11**, 265-270.

Chen J, Blume HP, Beyer L (2000) Weathering of rocks induced by lichen colonization. *Catena*. **39**, 121–146.

Childers SE, Ciufo S, Lovley DR (2002) *Geobacter metallireducens* accesses insoluble Fe(III) oxide by chemotaxis. *Nature* **416**, 767-9.

Christensen PR, Bandfield JL, Hamilton VE, Ruff SW, Kieffer HH, Titus TN, Malin MC, Morris RV, Lane MD, Clark RL, Jakosky BM, Mellon MT, Pearl JC, Conrath BJ, Smith MD, Clancy RT, Kuzmin RO, Roush T, Mehall GL, Gorelick N, Bender K, Murray K, Dason S, Greene E, Silverman SGM (2001) Mars Global Surveyor Thermal Emission Spectrometer experiment: investigation description and surface science results. *Journal of Geophysical Research*, **106**, 823-871.

Christensen PR, Bandfield JL, Rogers AD, Glotch TD, Hamilton VE, Ruff SW, Wyatt MB (2008) Global mineralogy mapped from the Mars Global Surveyor Thermal Emission Spectrometer. J. Bell (Ed.), *The Martian Surface: Composition, Mineralogy and Physical Properties*, Cambridge University Press, 195–220.

Claassen HC, White AF (1979) Application of geochemical kinetic data to groundwater systems, Part 1. A tuffaceous-rock system in southern Nevada. **In:** *Chemical Modeling in Aqueous Systems* (ed. E. Jenne); *Am. Chem. Soc.* **93,** 447–473.

Coates JD, Phillips EJP, Lonergan DJ, Jenter HL, Lovley DR (1996) Isolation of *Geobacter* species from diverse sedimentary environments. *Appl. Environ. Microbiol.* **62**, 1531-1536.

Cockell CS, Olsson-Francis K, Herrera A, Meunier A (2009a) Alteration textures in terrestrial volcanic glass and the associated bacterial community. *Geobiology* **7**, 50-65.

Cockell CS, Olsson K, Knowles F, Kelly L, Herrera A, Thorsteinsson T, Marteinsson V (2009b) Bacteria in weathered basaltic glass, Iceland. *Geomicrobiology Journal* **26**, 491-507.

Cockell CS (2009) Investigations on Microbial Rock Weathering using XAS and the Implications for Earth System Processes. Diamond Experimental Report. Proposal reference no. SP752.

Cockell CS, Pybus D, Olsson-Francis K, Kelly L, Petley D, Rosser N, Howard K, Mosselmans F (2011). Molecular Characterization and Geological Microenvironment of a Microbial Community Inhabiting Weathered Receding Shale Cliffs. *Microbial Ecology*. **61(1)**, 166-181.

Cole JR, Chai B, Marsh TL, Farris RJ, Wang Q, Kulam SA, Chandra S, McGarrell DM, Schmidt TM, Garrity GM, Tiedje JM (2003) The Ribosomal Database Project (RDP-II): previewing a new autoaligner that allows regular updates and the new prokaryotic taxonomy. *Nucleic Acids Research* **31**, 442–443.

Costello E, Lauber C, Hamady M, Fierer N, Gordon J, Knight R (2009) Bacterial community variation in human body habitats across space and time. *Science* **326**, 1694-1697.

Cottrell MT, Kirchman DL (2000) Natural assemblages of marine proteobacteria and members of the Cytophaga-Flavobacter cluster consuming low- and high-molecular-weight dissolved organic matter. *Appl Environ Microbiol* **66**, 1692–1697.

Cousins CR (2011) Volcano - Ice Interaction: A Haven for Life on Mars? *Astronomy and Geophysics.* **52**, 36 - 38.

Crovisier J-L, Advocat T., Dussossoy J-L (2003) Nature and role of natural alteration gels formed on the surface of ancient volcanic glasses (natural analogs of waste containment glasses). *Journal of Nuclear Materials* **321**, 91–109.

Dahlgren RA, Ugolini FC, Casey WH (1999) Field weathering rates of Mt. St. Helens tephra. *Geochimica et Cosmochimica Acta* **63**, 587-598.

Danin A (1993) Pitting of calcareous rocks by organisms under terrestrial conditions. *Isr. J. Earth-Sci.* **41**, 201-207

Danin A, Caneva G (1990) Deterioration of limestone walls in Jerusalem and marble monuments in Rome caused by cyanobacteria and cyanophilous lichens. *Int. Biodeterior.* **26**, 397-417.

Danon M, Franke-Whittle IH, Insam H, Chen Y, Hadar Y (2008) Molecular analysis of bacterial community succession during prolonged compost curing. *FEMS Microbiol. Ecol.* **65**, 133-144.

Das A, Modak JM Natarajan KA (1997) Technical note studies on multi-metal ion tolerance of *Thiobacillus ferrooxidans*. *Min Eng* **10**, 743–749.

Daughney CJ, Rioux J-P, Fortin D, Pichler T (2004) Laboratory investigation of the role of bacteria in the weathering of basalt near deep sea hydrothermal vents. *Geomicrobiol J.* **21**, 21–31.

DeFlaun MF, Paul JH, Davis D (1986) Simplified method for dissolved-DNA determination in aquatic environments. *Applied and Environmental Microbiology* **52**, 654-659.

de la Torre JR, Goebel BM, Friedmann EI, Pace NR (2003) Microbial diversity of cryptoendolithic communities from the McMurdo Dry Valleys, Antarctica. *Appl Environ Microbiol* **69**, 3858–3867.

Dessert C, Dupré B, François LM, Schott J, Gaillardet J, Chakrapani G, Bajpai S (2001) Erosion of Deccan Traps determined by river geochemistry: impact on the global climate and the 87Sr/86Sr ratio of seawater. *Earth Planet Sc Lett.* **188**, 459-474.

Dessert C, Dupré B, Gaillardet J, Francois LM, Allegre CJ (2003) Basalt weathering laws and the impact of basalt weathering on the global carbon cycle. *Chem Geol.* **202**, 257-273.

Dobler R, Saner M, Bachofen R (2000) Population changes of soil microbial communities induced by hydrocarbon and heavy metal contamination. *Bioremediation Journal* **4**, 41–56.

Dong H, Kukkadapu RK, Fredrickson JK, Zachara JM, Kennedy DW, Kostandarithes HM (2003) Microbial reduction of structural Fe(III) in illithe and goethite. *Environ. Sci. Technol.* **37**, 1268-1276.

Dopson M, Baker-Austin C, Koppineedi PR, Bond PL (2003) Growth in sulfidic mineral environments: metal resistance mechanisms in acidophilic microorganisms. *Microbiology* **149**, 1959–1970.

Drees KP, Neilson JW, Betancourt JL, Quade J, Henderson DA, Pryor BM, Maier RM (2006) Bacterial community structure in the hyperarid core of the Atacama Desert, Chile. *Appl Environ Microbiol* **72**, 7902–7908.

Drever JI (1994) The effect of land plants on weathering rates of silicate minerals: *Geochimica et Cosmochimica Acta*. **58**, 2325–2332.

Drever JI, Vance GF (1994) A Role of Soil Organic Acids in Mineral Weathering Processes. **In:** E.D. Pittman and M.D. Lewan (eds.) *Organic Acids in Geological Processes*. SpringerVerlag, Berlin, Germany. 138-161

Drever JI, Stillings LL (1997) The role of organic acids in mineral weathering. *Colloids and Surfaces A: Physicochemical and Engineering Aspects* **120**, 167-181.

Edwards KJ, Bond PL, Banfield JF (2000) Characteristics of attachment and growth of *Thiobacillus caldus* on sulphide minerals: a chemotactic response to sulphur minerals? *Environmental Microbiology* **2**, 324-332.

Edwards KJ, McCollom TM, Konishi H, Buseck PR (2003) Seafloor bioalteration of sulfide minerals: results from in situ incubation studies. *Geochimica et Cosmochimica Acta*. **67**, 2843-2856.

Ehrich S, Behrens D, Lebedeva E, Ludwig W, Bock E (1995) A new obligately chemolithoautotrophic, nitrite-oxidizing bacterium, *Nitrospira moscoviensis* sp. nov. and its phylogenetic relationship. *Arch Microbiol.* **164(1)**, 16-23.

Eick MJ, Grossl PR, Golden DC, Sparks DL, Ming DW (1996) Dissolution kinetics of a lunar glass simulant at 298 K. The effect of pH and organic acids. *Geochim. Cosmochim. Acta* **58**, 4259–4279.

Eiler A, Bertilsson S (2004) Composition of freshwater bacterial communities associated with cyanobacterial blooms in four Swedish lakes. *Environ Microbiol.* **6**, 1228-1243.

Einen J, Kruber C, Øvreås L, Thorseth IH, Torsvik T (2006) Microbial colonization and alteration of basaltic glass. *Biogeosciences Discuss.* **3**, 273-307.

Elderfield H, Upstill-Goddard R, Sholkovitz ER (1990) The rare earth elements in rivers, estuaries, and coastal seas and their significance to the composition of ocean waters. *Geochim. Cosmochim. Acta* **54**, 971–991.

Embley TM, Stackebrandt E (1994) The molecular phylogeny and systematics of the Actinomycetes. *Annu Rev Microbiol.* **48**, 257–289.

Ercolini D, Mauriello G, Blaiotta G, Moschetti G, Coppola S (2004) PCR-DGGE fingerprints of microbial succession during a manufacture of traditional water buffalo mozzarella cheese. *J. Appl. Microbiol.* **96**, 263-270.

Etienne S, Dupont J (2002) Fungal weathering of basaltic rocks in a cold oceanic environment (Iceland): comparison between experimental and field observations. *Earth Surface Processes and Landforms* **27**, 737–748.

Felsenstein J (1989) PHYLIP – phylogeny inference package (version 3.2). *Cladistics* **5**, 164-166.

Ferris FG, Lowson EA (1997) Ultrastructure and geochemistry of endolithic microorganisms in limestone of the Niagara Escarpment. *Can J Microbiol.* **43**, 211–219.

Fierer N, Hamady M, Lauber C, Knight R (2008) The influence of sex, handedness, and washing on the diversity of hand surface bacteria. *Proc. Natl. Acad. Sci. USA* **105**, 17994-17999.

Fierer, N, Nemergut DR, Knight R, Craine JM (2010) Changes through time: integrating microorganisms into the study of succession. *Research in Microbiology*. **161**, 635-642.

Fisk MR, Giovannoni SJ, Thorseth IH (1998) Alteration of oceanic volcanic glass: textural evidence of microbial activity. *Science* **281**, 978–980.

Friedmann EI, Kibler AP (1980) Nitrogen economy of endolithic microbial communities in hot and cold deserts. *Microbial Ecology*. **6**, 95-108.

Friedmann EI (1982) Endolithic microorganisms in the Antarctic cold desert. *Science* **215**, 1045–1053.

Friedmann EI, Weed R (1987) Microbial trace-fossil formation, biogenous and abiotic weathering in the Antarctic cold desert. *Science* **236**, 703–705.

Fry EJ (1927) The mechanical action of crustaceous lichens on substrata of shale, schist, gneiss, limestone, and obsidian. *Annals of Botany* **41**, 437-460.

Furnes H. (1978) Element mobility during palagonitization of a subglacial hyaloclastite in Iceland. *Chemical Geology* **22**, 249–264.

Furnes H, Staudigel H (1999) Biological mediation in ocean crust alteration: How deep is the deep biosphere? *Earth and Planetary Science Letters* **166**, 97–103.

Furnes H, Banerjee NR, Muehlenbachs K, Kontinen A (2005) Preservation of biosignatures in metaglassy volcanic rocks from the Jormua ophiolite complex, Finland. *Precambrian Research* **136**, 125–137.

Furnes H, Banerjee NR, Staudigel H, Muehlenbachs K, McLoughlin N, de Wit M, van Kranendonk M (2007) Comparing petrographic signatures of bioalteration in recent to Mesoarchean pillow lavas: Tracing subsurface life in oceanic igneous rocks. *Precambrian Research* **158**, 156–176.

Fyfe WS (1987) From molecules to planetary environments: understanding global change. **In:** W. Stumm, Editor, *Aquatic Surface Chemistry: Chemical Processes at the Particle-Water Interface*, Wiley, New York, 495–508.

Gaillardet J, Dupré B, Louvat P, Allègre CJ (1999) Global silicate weathering and CO_2 consumption rates deduced from the chemistry of the large rivers. *Chem. Geol.* **159**, 3–30.

García Jr. O, Silva LL (1991) Differences in growth and iron oxidation among *Thiobacillus ferrooxidans* cultures in the presence of some toxic metals. *Biotechnol Lett* **13**, 567–570.

Garland JL, Cook KL, Adams JL, Kerkhof L (2001) Culturability as an Indicator of Succession in Microbial Communities. *Microbial Ecology.* **42(2)**, 150-158.

Garrels RM, Mackenzie F (1971) *Evolution of Sedimentary Rocks*. Norton, New York.

Genty B, Briantais JM, Baker, NR (1989) The relationship between the quantum yield of photosynthetic electron transport and quenching of chlorophyll fluorescence. Biochimica et Biophysica Acta. **990**, 87-92.

Gislason SR, Eugster HP (1987a) Meteoric water-basalt interactions. II: A field study in N.E. Iceland. *Geochim Cosmochim Acta* **51**, 2841-2855.

Gislason SR, Eugster HP (1987b) Meteoric water–basalt interactions. I: A laboratory study. *Geochim. Cosmochim. Acta* **51**, 2827–2840.

Gislason SR, Arnorsson S, Armannsson H (1996) Chemical weathering of basalt in Southwest Iceland; effects of runoff, age of rocks and vegetative/glacial cover. *American Journal of Science* **296**, 837-907.

Gislason SR, Oelkers EH (2003) Mechanism, rates, and consequences of basaltic glass dissolution: II. An experimental study of the dissolution rates of basaltic glass as a function of pH and temperature. *Geochim. Cosmochim. Acta* **67**, 3817–3832.

Goldschmidt VM (1958) *Geochemistry*. Oxford University Press.

Golubic S (1973) The Relationship between Blue–Green Algae and Carbonate Deposits. In: *The Biology of Blue-Green Algae*. Carr, N.G. and Whitton, B.A., Eds., Berkeley: Univ. of California Press. **9**, 434–472.

Gomez-Alvarez V, King GM, Nusslein K (2007) Comparative bacterial diversity in recent Hawaiian volcanic deposits of different ages. *FEMS Microbiol. Ecol.* **60**, 60–73.

Gorbushina AA, Krumbein WE, Volkmann M (2002) Rock surfaces as life indicators: new ways to demonstrate life and traces of former life. *Astrobiology* **2**, 203-213.

Goudie AS, Parker AG (1999) Experimental simulation of rapid rock block disintegration by sodium chloride in a foggy coastal desert. *Journal of Arid Environment* **40**, 347–355.

Gundlapally SR, Garcia-Pichel F (2006) The community and phylogenetic diversity of biological soil crusts in the Colorado Plateau studied by molecular fingerprinting and intensive cultivation. *Microb Ecol* **52**, 345–357.

Gupta RS (2000) The phylogeny of proteobacteria: relationships to other eubacterial phyla and eukaryotes. *FEMS Microbiol Rev.* **24(4)**, 367-402.

Gyaneshwar P, Kumar GN, Parekh LJ (1998) Effect of buffering on the phosphate-solubilizing ability of microorganisms. *World J. Microb. Biot.* **14**, 669–673.

Hackl E, Zechmeister-Boltenstern S, Bodrossy L, Sessitsch A (2004) Comparison of diversities and compositions of bacterial populations inhabiting natural forest soils. *Appl Environ Microbiol.* **70**, 5057-5065.

Haley BA, Klinkhammer GP, McManus J (2004) Rare earth elements in pore waters of marine sediments. *Geochim. Cosmochim. Acta* **68**, 1265–1279.

Hannigan RE, Sholkovitz ER (2001) The development of middle rare earth element enrichments in freshwaters: weathering of phosphate minerals. *Chem. Geol.* **175**, 495–508.

Haruta S, Ueno S, Egawa I, Hashiguchi K, Fujii A, Nagano M *et al.* (2006) Succession of bacterial and fungal communities during a traditional pot fermentation of rice vinegar assessed by PCR-mediated denaturing gradient gel electrophoresis. *Int. J. Food Microbiol.* **109**, 79-87.

Haukka K, Heikkinen E, Kairesalo T, Karjalainen H, Sivonen K (2005) Effect of humic material on the bacterioplankton community composition in boreal lakes and mesocosms. *Environ Microbiol.* **7**, 620-630.

Haukka K, Kolmonen E, Hyder R, Hietala J, Vakkilainen K, Kairesalo T, Haario H, Sivonen K (2006) Effect of nutrient loading on bacterioplankton community composition in lake mesocosms. *Microb Ecol.* **51**, 137-146.

Harris JK, Kelley ST, Pace NR (2004) New perspective on uncultured bacterial phylogenetic division OP11. Appl *Environ Microbiol* **70**, 845–849.

He J, Xu Z, Hughes J (2006) Molecular bacterial diversity of a forest soil under residue management regimes in subtropical Australia. *FEMS Microbiol Ecol.* **55**, 38-47.

Head IM, Hiorns WD, Embley TM, McCarthy AJ, Saunders JR (1993) The phylogeny of autotrophic ammonia-oxidizing bacteria as determined by analysis of 16S ribosomal RNA gene sequences. J Gen Microbiol. **139(6)**, 1147-53.

Heinen W, Lauwers AM (1988) Leaching of silica and uranium and other quantitative aspects of the lithobiontic colonization in a radioactive thermal spring. *Microb. Ecol.* **15**, 135–149.

Henderson P (ed.) (1984) *Rare Earth Element Geochemistry*. Elsevier Science Publishers B.V., Amsterdam, 510 pp.

Henriksen JR (2004) Documentation for webLIBSHUFF version 0.96. http://libshuff.mib.uga.edu/doc.html. Accessed: 10/03/2011.

Herrera A, Cockell CS, Self S, Blaxter M, Reitner J, Thorsteinsson T, Arp G, Dröse W, Tindle AG (2009) A Cryptoendolithic Community in Volcanic Glass. *Astrobiology*. **9**, 369-381.

Hersman L, Lloyd T, Sposito G (1995) Siderophore-promoted dissolution of hematite. *Geochimica et Cosmochimica Acta*. **59**, 3327–3330.

Hersman L, Maurice P, Sposito G (1996) Iron acquisition from hydrous Fe (III)-oxides by an aerobic *Pseudomonas* sp. *Chem. Geol* **132**, 25–31.

Hersman L, Huang A, Maurice PA, Forsythe JH (2000) Siderophore production and iron reduction by *Pseudomonas mendocina* in response to iron deprivation. *Geomicrobiol. J.* **17**, 1–13.

Hiebert FK, Bennett PC (1992) Microbial control of silicate weathering in organic-rich ground water. *Science*. **258**, 278–281.

Hinsinger P, Gilkes RJ (1993) Root-induced irreversible transformation of trioctahedral mica on the rhizosphere of rape. *J. Soil Sci.* **44**, 535–545.

Hinsinger P, Gilkes RJ (1995) Root-induced dissolution of phosphate rock in the rhizosphere of lupines grown in alkaline soil. *Aust. J. Soil Res.* **33**, 477–489.

Hirsch P, Eckhardt FEW, Palmer Jr RJ (1995a) Methods for the study of rock-inhabiting microorganisms - A mini review. *J. Microbiol. Methods* **23**, 143-167.

Hirsch P, Eckhardt FEW, Palmer Jr RJ (1995b) Fungi active in weathering of rock and stone monuments. *Can. J. Bot.* **73**, 1384-1390.

Holland HD (1978) *The Chemistry of Oceans and Atmosphere*. Wiley, New York.

Holmén BA, Casey WH (1996) Hydroxamate ligands, surface chemistry, and the mechanism of ligand-promoted dissolution of goethite [-FeOOH(s)]. *Geochim. Cosmochim. Acta* **60**, 4403–4416.

Hoppert M, Flies C, Pohl W, Gunzl B, Schneider J (2004) Colonization strategies of lithobiontic microorganisms on carbonate rocks. *Environ. Geol.* **46**, 421–428.

Hossner LR, Doolittle JJ (2003) Iron sulphide oxidation as influenced by calcium carbonate application. *Journal of Environmental Quality* **32**, 773–780.

Huber H, Stetter KO (1990) *Thiobacillus cuprinus* sp. *nov.*, a novel facultative organotrophic metal-mobilizing bacterium. *Appl Environ Microbiol* **56**, 315–322.

Hugenholtz P, Pitulle C, Hershberger KL, Pace NR (1998) Novel division level bacterial diversity in a Yellowstone hot spring. *J Bacteriol* **180**, 366–376.

Humphry DR, George A, Black GW, Cummings SP (2001) Flavobacterium frigidarium sp. nov., an aerobic, psychrophilic, xylanolytic and laminarinolytic bacterium from Antarctica. *Int J Syst Evol Microbiol* **51**, 1235–1243.

Hurowitz JA, McLennan SM (2007) A y3.5 Ga record of waterlimited, acidic weathering conditions on Mars. *EPSL* **260**, 432–443.

Hurowitz JA (2008) A ~3.5By record of water-limited, acidic weathering on Mars. *Geochimica et Cosmochimica Acta*. **72(12)**, 404.

Illmer P, Schinner F (1995) Solubilization of inorganic calcium phosphatesolubilization mechanisms. *Soil Biol. Biochem.* **27**, 257–263.

Illmer P, Barbato A, Schinner F (1995) Solubilization of hardy-soluble AlPO4 with P-solubilizing microorganisms. *Soil Biol. Biochem.* **27**, 265–270.

Imai K, Sugio T, Tsuchida T, Tano T (1975) Effect of heavy metal ions on the growth and iron-oxidizing activity of *Thiobacillus ferrooxidans*. *Agric Biol Chem* **39**, 1349–1354.

Iskandar IK, Syers JK (1972) Metal-complex formation by lichen compounds. *J. Soil Sci.* **23**, 255–265.

Jaccard P (1908) Nouvelles recherches sur la distribution florale. *Bulletin Societe Vaudoise des Sciences Naturelles.* **44**, 223-270.

Jackson TA, Keller WD (1970) A comparative study of the role of lichens and "inorganic" processes in the chemical weathering of recent Hawaiian lava flows. *American Journal of Science* **269**, 446–466.

Jenny H (1941) *Factors of Soil Formation*. McGraw-Hill, New York.

Johannesson, KH, Lyons WB, Yelken MA, Gaudette HE, Stetzenbach KJ (1996) Geochemistry of the rare-earth elements in hypersaline and dilute acidic natural terrestrial waters: complexation behavior and middle rare-earth element enrichments. *Chem. Geol.* **133**, 125–144.

Johannesson, KH, Hawkins Jr DL, Alejandra Cortés A (2006) Do Archean chemical sediments record ancient seawater rare earth element patterns? *Geochim. Cosmochim. Acta* **70**, 871–890.

Johnson RE, Tuchman NC, Peterson CG (1997) Changes in the vertical microdistribution of diatoms within a developing periphyton mat. *J. North Am. Benth. Soc.* **16**, 503-519.

Jones DL (1998) Organic acids in the rhizosphere – a critical review. *Plant and Soil* **205**, 25–44.

Jones EJP, Nadeau TL, Voytek MA, Landa ER (2006) Role of microbial iron reduction in the dissolution of iron hydroxysulfate minerals. *J Geophys Res* **111**.

Jones RT, Robeson MS, Lauber CL, Hamady M, Knight R, Fierer N (2009) A comprehensive survey of soil acidobacterial diversity using pyrosequencing and clone library analyses. *ISME J.* **3(4)**, 442-53.

Jukes TH, Cantor CR, Munro HN (1969) Evolution of protein molecules. In: (eds) Mammalian protein metabolism. Academic Press, pp 21-132.

Kanokratana P, Chanapan S, Pootanakit K, Eurwilaichitr L (2004) Diversity and abundance of Bacteria and Archaea in the Bor Khlueng hot spring in Thailand. *J Basic Microbiol.* **44**, 430-444.

Karl DM (1995) The ecology of hydrothermal vent microbial communities. **In:** Karl DM, editor. *The microbiology of deep-sea hydrothermal vents.* Boca Raton, FL: CRC Press, 25-124.

Kelly JJ, Tate RL (1998) Effects of heavy metal contamination and remediation on soil microbial communities in the vicinity of a zinc smelter. *Journal of Environmental Quality* **27**, 609–617.

Kelly DP, Wood AP (2000) Reclassification of some species of Thiobacillus to the newly designated genera *Acidithiobacillus* gen. nov., *Halothiobacillus* gen. nov. and *Thermithiobacillus* gen. nov. *Int J Syst Evol Microbiol.* **50**, 511-516.

Kelly L, Cockell CS, Piceno YM, Anderson G, Thorsteinsson T, Marteinsson V (2010) Bacterial Diversity of Weathered Terrestrial Icelandic Volcanic Glasses. *Microb Ecol.* **60**, 740-752.

Keszthelyi L, McEwen AS, Thordarson TH (2000) Terrestrial analogs and thermal models for Martian flood lavas. *J. Geophys. Res.* **105**, 15027-15050.

Kisakurek B, Widdowson M, James RH (2004) Behaviour of Li isotopes during continental weathering: the Bidar laterite profile. India.*Chemical Geology* **212**, 27–44.

Klingelhöfer G, Morris RV, Bernhardt B, Schröder C, Rodionov DS, de Souza Jr PA, Yen A, Gellert R, Evlanov EN, Zubkov B, Foh J, Bonnes U, Kankeleit E, Gütlich P, Ming DW, Renz F, Wdowiak T, Squyres SW, Arvidson RE (2004) Jarosite and hematite at Meridiani Planum from Opportunity's Mössbauer spectrometer. *Science*, **306**, 1740–1745.

Knight BP, McGrath SP, Chaudri AM (1997) Biomass carbon measurements and substrate utilization patterns of microbial populations from soils amended with cadmium, copper, or zinc. *Applied and Environmental Microbiology* **63**, 39–43.

Kolenbrander PE, Palmer RJ, Rickard AH, Jakubovics NS, Chalmers NI, Diaz PI (2006) Bacterial interactions and successions during plaque development. *Periodontology* **42**, 47-79.

Kondratyeva TF, Muntyan LN, Karavaiko GI (1995) Strain diversity of *Thiobacillus ferrooxidans* and its significance in biohydrometallurgy. *Microbiology* **141**, 1157–1162.

Konhauser KO, Fyfe WS, Schultze-Lam S, Ferris FG Beveridge TJ (1994) Iron phosphate precipitation by epilithic microbial biofilms in Arctic Canada. *Can. J. Earth Sci.* **31**, 1320–1324.

Konhauser K (2007) Introduction to Geomicrobiology, Blackwell Science, UK.

Korenaga J (2004) Mantle mixing and continental breakup magmatism. *Earth and Planetary Science Letters*. **218**, 463-473.

Kostka JE, Wu J, Nelson KH, Struck JW (1999) The impact of structural Fe(III) reduction by bacteria on the surface chemistry of smectite clay minerals. *Geochim. Cosmochim. Acta* **63**, 3705-3713.

Kraemer SM (2004) Iron oxide dissolution and solubility in the presence of siderophores. *Aquat. Sci.* **66**, 3–18.

Krebs W, Brombacher C, Bosshard PP, Bachofen R, Brandl H (1997) Microbial recovery of metals from solids. *FEMS Microbiol. Rev.* **20**, 605-617.

Krumbein WE, Werner D (1983) The microbial silica cycle. **In:** W.E. Krumbein, Editor, *Microbial Geochemistry*, Blackwell, Oxford, 125–157.

Krumbein WE, Urzi CE, Gehrmann C (1991) Biocorrosion and biodeterioration of antique and medieval glass. *Geomicrobiology Journal* **9**, 139–160.

Kupka D, Kupsáková I (1999) Iron(II) oxidation kinetics in *Thiobacillus ferrooxidans* in the presence of heavy metals. In: Amils R, Ballester A (Eds.), Biohydrometallurgy and the environment toward the mining of the 21st century, Part A, Elsevier Press, Amsterdam, 387-396.

Küsel K, Roth U, Drake HL (2002) Microbial reduction of Fe(III) in the presence of oxygen under low pH conditions. *Environ. Microbiol.* **4**, 414–421.

Landesman J, Duncan DW, Walden CC (1966) Oxidation of inorganic sulfur compounds by washed cell suspensions of *Thiobacillus ferrooxidans*. *Can J Microbiol.* **12**, 957-964.

Langmuir D (1997) Aqueous Environ Geochem. Englewood Cliffs, NJ. Prentice-Hall. 600 p.

Lauwers AM, Heinen W (1974) Bio-degradation and utilization of silica and quartz. *Arch. Microbiol.* **95**, 67–78.

Lawrence JR, Kwong YTJ, Swerhone GDW (1997) Colonization and weathering of natural sulfide mineral assemblages by *Thiobacillus ferrooxidans*. *Canadian Journal of Microbiology*. **43**, 178-188.

Lawver LA, Muller RD (1994) Iceland hotspot track. *Geology* **22**, 311-314.

Le Bas MJ, Le Maitre RW, Streckeisen A, Zanettin B (1986). A Chemical Classification of Volcanic Rocks Based on the Total Alkali-Silica Diagram. *J. Petrology* 27:3, 745-750.

Leduc LG, Trevors JT, Ferroni GD (1993) Thermal characterization of different isolates of *Thiobacillus ferrooxidans*. *FEMS Microbiology Letters*, **108,** 189-193.

Leduc LG, Ferroni GD (1994) The chemolithotrophic bacterium *Thiobacillus ferrooxidans*. *FEMS Microbiology Reviews*. **14**, 103-119.

Leduc LG, Ferroni GD, Trevors JT (1997) Resistance to heavy metals in different strains of *Thiobacillus ferrooxidans*. *World J Microb Biot* **13**, 453–455.

Lees II, Kwok SC, Suzuki I (1969) The thermo dynamics of iron oxidation by the ferrobacilli. *Canadian Journal of Microbiology*. **15**, 43-46.

Leyval C, Berthelin J (1991) Weathering of a mica by roots and rhizospheric microorganisms of pine. *Soil Sci. Soc. Am. J.* **55**, 1009-1016.

Levy-Booth DJ, Campbell RG, Gulden RH, Hart MM, Powell JR, Klironomos JN, Pauls KP, Swanton CJ, Trevors JT, Dunfield KE (2007) Cycling of extracellular DNA in the soil environment. *Soil Biology and Biochemistry*. **39(12)**. 2977-2991.

Liang L, McNabb JA, Paulk JM, Gu B McCarthy JF (1993) Kinetics of Fe(II) Oxygenation at Low Partial Pressure of Oxygen in the Presence of Natural Organic Matter. *Environ. Science and Technol.* **27(9)**, 1864-1870.

Lin WT, Luo JF, Guo Y (2011) Comparison and Characterization of Microbial Communities in Sulfide-rich Wastewater with and without Propidium Monoazide Treatment. *Curr Microbiol.* **62**, 374–381.

Lindstrom ES, Kamst-Van Agterveld MP, Zwart G (2005) Distribution of typical freshwater bacterial groups is associated with pH, temperature, and lake water retention time. *Appl Environ Microbiol.* **71**, 8201-8206.

Lopez BR, Bashan Y, Bacilio M (2011) Endophytic bacteria of *Mammillaria fraileana*, an endemic rock-colonizing cactus of the southern Sonoran Desert. *Archives of Microbiology* **193**, 527-541.

Louvat P, Allègre CJ (1998) Riverine erosion rates on Sao Miguel volcanic island, Azores Archipelago. *Chem. Geol.* **148**, 177–200.

Lovley DR, Stolz JF, Nord J, Phillips, EJP (1987) Anaerobic production of magnetite by a dissimilatory iron-reducing microorganism. *Nature* **330**, 252-254.

Lovley DR, Phillips EJP (1988) Novel mode of microbial energy metabolism: organic carbon oxidation coupled to dissimilatory reduction of iron or manganese. *Appl. Environ. Microbiol.* **54**, 1472-1480.

Lovley DR (1991) Dissimilatory Fe(III) and Mn(IV) reduction. *Microbiol. Rev.* **55**, 259-287.

Lovley DR (1993) Dissimilatory metal reduction. *Annual Review of Microbiology* **47**, 263–290.

Lovley DR, Chapelle FH (1995) Deep subsurface microbial processes. *Rev Geophys* **33**, 365–381.

Lovley DR, Fraga JL, Blunt-Harris EL, Hayes LA, Phillips EJP, Coates JD (1998) Humic substances as a mediator for microbially catalyzed metal reduction. *Acta Hydrochim Hydrobiol* **26**, 152-157.

Lovley DR, Holmes DE, Nevin KP (2004) Dissimilatory Fe(III) and Mn(IV) reduction. **In:** *Adv. Microb. Physiol.* Press, P. (ed), 219-286.

Lüttge A, Conrad PG (2004) Direct Observation of Microbial Inhibition of Calcite Dissolution. *Appl. Environ. Microbiol.* **70(3)**, 1627-1632.

Lyalikova NN (1958) A study of chemosynthesis in *Thiobacillus ferrooxidans*. *Mikrobiologiya.* **27**, 556-559.

Lysnes K, Thorseth IH, Steinsbu BO, Øvreås L, Torsvik T, Pedersen RB (2004) Microbial community diversity in seafloor basalt from the Arctic spreading ridges. *FEMS Microbiology Ecology*. **50(3)**, 213-230

MacArthur RH, Wilson EO (1967) The theory of island biogeography. Princeton University Press, Princeton, NJ, USA.

MacDonald DG, Clark RH (1970) The oxidation of aqueous ferrous sulphate by *Thiobacillus ferrooxidans*. *The Canadian Journal of Chemical Engineering*. **48**, 669-676.

Mackenzie FT, Pigott JD (1981) Tectonic controls of Phanerozoic sedimentary rock cycling. *Journal of the Geological Society of London.* **138**, 183–196.

Madigan MT, Martinko JM (2005) Brock Biology of Microorganisms 11e. Pearson Prentice Hall, USA.

Malik A, Jaiswal R (2000) Metal resistance in *Pseudomonas* strains isolated from soil treated with industrial wastewater. *World J Microbiol Biotech* **16**, 177–182.

Manzano M, Iacumin L, Giusto C, Cecchini F, Patthey C (2013) Utilization of Denaturing Gradient Gel Electrophoresis (DGGE) to evaluate the Intestinal Microbiota of Brown Trout Salmo trutta fario. *J Vet Sci Med Diagn* 1:2.

Martiny AC, Jorgensen TM, Albrechtsen HJ, Arvin E, Molin S (2003). Long-term succession of structure and diversity of a biofilm formed in a model drinking water distribution system. *Appl. Environ. Microbiol.* **69**, 6899-6907.

Matthews JA (1992) The Ecology of Recently-Deglaciated Terrain: A Geoecological Approach to Glacier Forelands and Primary Succession. Cambridge University Press, Cambridge.

McCammon SA, Innes BH, Bowmann JP, Franzmann PD, Dobson SJ, Holloway PE, Skerratt JH, Nichols PD, Rankin LM (1998) Flavobacterium hibernum sp. nov., a lactoseutilizing bacterium from a freshwater Antarctic lake. *Int J Syst Bacteriol* **48**, 1405–1412.

McEwen A, Burr D, Hardardottir J, Hoskuldsson A, Keszthelyi L, Lanagan P, Snorrason A, Thordarson T (2001) Icelandic Analogs for Volcanic and Fluvial Processes on Mars. *American Geophysical Union*, abstract P32D-0573.

McLennan SM (1989) Rare-earth elements in sedimentary-rocks—Influence of provenance and sedimentary processes. In: Lipin BR, McKay GA (1989) Editors, *Geochemistry and Mineralogy of Rare Earth Elements Reviews in Mineralogy 21*, Mineralogical Society of America, Washington, p. 169–200.

McSween HY, Taylor GJ, Wyatt MB (2009) Elemental Composition of the Martian Crust. *Science*. **324**, 736-739.

Meruane G, Vargas T (2003) Bacterial oxidation of ferrous iron by *Acidithiobacillus ferrooxidans* in the pH range 2.5–7.0. *Hydrometallurgy*. **71**, 149-158.

Mielke RE, Pace DL, Porter T, Southam G (2003) A critical stage in the formation of acid mine drainage: Colonization of pyrite by *Acidithiobacillus ferrooxidans* under pH-neutral conditions. *Geobiology*. **1**, 81-90.

Morel FMM, Price NM (2003) The biogeochemical cycles of trace metals in the ocean. *Science* **300**, 944-947.

Morris RV, Klingelhöfer G, Schröder C, Rodionov DS, Yen A, Ming DW, De Souza Jr PA, Fleischer I, Wdowiak T, Gellert R, Bernhardt B, Evlanov EN, Zunkov B, Foh J, Bonnes U, Kankeleit E, Gütlich P, Renz F, Squyres SW, Arvidson RE (2006) Mössbauer mineralogy of rock, soil, and dust at Gusev Crater, Mars: Spirit's journey though weakly altered olivine basalt on the plains and pervasively altered basalt in the Columbia Hills. *Journal of Geophysical Research*, **111**, E02S13.

Mosselmans JFW, Quinn PD, Rosell JR, Atkinson KD, Dent AJ, Cavill SI, Hodson ME, Kirk CA, Schofield PF (2008) The first environmental science experiments on the new microfocus spectroscopy beamline at Diamond. *Mineral Mag.* **72**, 197–200.

Moynahan OS, Zabinski CA, Gannon JE (2002) Microbial Community Structure and Carbon-Utilization Diversity in a Mine Tailings. Revegetation Study. *Restoration Ecology* **10**, 77-87

Mustoe GE (2010) Biogenic origin of coastal honeycomb weathering. *Earth Surface Processes and Landforms* **35**, 424-434.

Muyzer G, de Waal EC, Uitterlinden AG (1993) Profiling of complex microbial populations by denaturing gradient gel electrophoresis analysis of polymerase chain reaction-amplified genes coding for 16S rRNA. *Appl Environ Microbiol.* **59**, 695-700.

Männistö MK, Tiirola M, Häggblom MM (2009) Effect of freeze-thaw cycles on bacterial communities of arctic tundra soil. *Microb Ecol.* **58(3)**, 621-31.

Nagy ML, Perez A, Garcia-Pichel F (2005) The prokaryotic diversity of biological crusts in the Sonoran desert (Organ Pipe Cactus National Monument, AZ). *FEMS Microb Ecol* **54**, 233–245.

Nakamura K, Noike T, Matsumoto J (1986) Effect of operation conditions on biological Fe^{2+} oxidation with rotating biological contactors. *Water Resources.* **20(1)**, 73-77.

Nakasaki K, Nag K, Karita S (2005) Microbial succession associated with organic matter decomposition during thermophilic composting of organic waste. *Waste Manag. Res.* **23**, 48-56.

Nance WB, Taylor SR (1976) Rare earth patterns and crustal evolution, I. Australian post-Archean sedimentary rocks. *Geochim. Cosmochim. Acta* **40**, 1539–1551.

Nealson KH, Saffarini D (1994) Iron and manganese in anaerobic respiration: environmental significance, physiology, and regulation. *Annu. Rev. Microbiol.* **48**, 311-343.

Nealson KH, Little B (1997) Breathing manganese and iron: Solid-state respiration. *Adv. Appl. Microbiol.*, 213-239.

Nealson KH, Cox BL (2002) Microbial metal-ion reduction and Mars: extraterrestrial expectations? *Current Opinion in Microbiology* **5**, 296–300.

Neilands JB (1981). Microbial iron compounds. *Annual Review of Biochemistry* **50**, 15-73.

Neilands JB (1982). Microbial envelope proteins related to iron. *Annual Review of Microbiology* **36**, 285-309.

Nemergut DR, Costello EK, Meyer AF, Pescador MY, Weintraub MN, Schmidt SK (2005) Structure and function of alpine and arctic soil microbial communities. *Research in Microbiology* **156(7)**, 775-784.

Nemergut DR, Anderson SP, Cleveland CC, Martin AP, Miller AE, Seimon A, Schmidt SK (2006) Microbial community succession in an unvegetated, recently deglaciated soil. *Microbial Ecology* **53**, 110-122.

Nicol GW, Tscherko D, Embley TM, Prosser JI (2005) Primary succession of soil Crenarchaeota across a receding glacier foreland. *Environ Microbiol.* **7**, 337–347.

Nocker A, Cheung CY, Camper AK (2006) Comparison of propidium monoazide with ethidium monoazide for differentiation of live vs dead bacteria by selective removal of DNA from dead cells. *J Microb Methods* **67**, 310–320.

Noll M, Matthies D, Frenzel P, Derakshani M, Liesack W (2005) Succession of bacterial community structure and diversity in a paddy soil oxygen gradient. *Environ Microbiol.* **7**, 382-395.

Novinscak A, DeCoste NJ, Surette C, Filion M (2009) Characterization of bacterial and fungal communities in composted biosolids over a 2 year period using denaturing gradient gel electrophoresis. *Can. J. Microbiol.* **55**, 375-387.

O'Sullivan LA, Rinna J, Humphreys G, Weightman AJ, Fry JC (2006) Culturable phylogenetic diversity of the phylum '*Bacteroidetes*' from river epilithon and coastal water and description of novel members of the family *Flavobacteriaceae*: *Epilithonimonas tenax* gen. nov., sp. nov. and *Persicivirga xylanidelens* gen. nov., sp. nov. *Int J Syst Evol Microbiol* **56**, 169-180.

Odum EP (1985) Trends expected in stressed ecosystems. *Bioscience* **35**, 419–422.

Oelkers EH, Gislason SR (2001) The mechanism, rates and consequences of basaltic glass dissolution: I. An experimental study of the dissolution rates of basaltic glass as a function of aqueous Al, Si and oxalic acid concentration at 25 °C and pH = 3 and 11. *Geochim. Cosmochim. Acta* **65**, 3671–3681.

Ogram A, Sayler GS, Barkay T (1987) The extraction and purification of microbial DNA from sediments. *Journal of Microbiological Methods* **7**, 57-66.

Okabe S, Odagiri M, Ito T, Satoh H (2007) Succession of sulfur-oxidizing bacteria in the microbial community on corroding concrete in sewer systems. *Appl. Environ. Microbiol.* **73**, 971-980.

Oros-Sichler M, Gomes NCM, Neuber G, Smalla K (2006) A new semi-nested PCR protocol to amplify large 18S rRNA gene fragments for PCR-DGGE analysis of soil fungal communities. *Journal of Microbiological Methods* 65, 63–75.

Osono T (2005) Colonization and succession of fungi during decomposition of Swida controversa leaf litter. *Mycologia* **97**, 589-597.

Palmer C, Bik EM, DiGiulio DB, Relman DA, Brown PO (2007) Development of the human infant intestinal microbiota. *Plos Biol.* **5**, 1556-1573.

Parasuraman CS (1995) Mechanism of potential ennoblement on passive metals due to biofilms in seawater. **In:** Doctoral dissertation, Univ. Delaware.

Pesic B, Oliver DJ, Wichlacz P (1989) An electrochemical method to measuring the rate of ferrous to ferric iron with oxygen in the presence of *Thiobacillus ferrooxidans*. *Biotechnology and Bioengineering*. **33**, 428-439.

Phillips EJP, Lovley DR, Roden EE (1993) Composition of non-microbially reducible Fe(III) in aquatic sediments. *Appl. Environ. Microbiol.* **59**, 2727–2729.

Polymenakou PN, Bertilsson S, Tselepides A, Stephanou EG (2005) Bacterial community composition in different sediments from the Eastern Mediterranean Sea: a comparison of four 16S ribosomal DNA clone libraries. *Microb Ecol.* **50**, 447-462.

Prieto B, Rivas T, Silva B (1994) Colonization by lichens of granite dolmens in Galicia (NW Spain). *Int. Biodeterior. Biodegrad.* **34**, 47–60.

Pronk JT, De Bruyn JC, Bos P, Kuenen JG (1992) Anaerobic Growth of *Thiobacillus ferrooxidans*. *Appl. Environ. Microbiol.* **58**, 2227-2230.

Puente ME, Bashan Y, Li CY, Lebsky VK (2004) Microbial populations and activities in the rhizoplane of rock-weathering desert plants, I. Root colonization and weathering of igneous rocks. *Plant Biology* **6**, 629-642.

Puente ME, Li CY, Bashan Y (2009) Rock-degrading endophytic bacteria in cacti. *Environmental and Experimental Botany* **66**, 389-401.

Purvis OW (1984) The occurrence of copper oxalate in lichens growing on copper sulphide-bearing rocks in Scandinavia. *Lichenologist* **16**, 197–204.

Quinn RC, Zent AP, Grunthaner P, Taylor CL, Garry JRC (2005) Detection and characterization of oxidizing acids in the Atacama Desert using the Mars Oxidation Instrument. *Planet. Space Sci.* **53(13)**, 1376–1388.

Rahman MZA, Azam ATMZ, Gafur MA (2000) *In vitro* antibacterial principles of two flavonoids and extracts from *Clerodendrum indicum* linn. *Pak. J. Biol. Sci.* **3**, 1769-1771.

Ravel B, Newville M (2005) ATHENA, ARTEMIS, HEPHAESTUS: data analysis for X-ray absorption spectroscopy using IFEFFIT. *J Synchrotron Radiat.* **12**, 537–540.

Redford AJ, Fierer N (2009) Bacterial succession on the leaf surface: a novel system for studying successional dynamics. *Microb. Ecol.* **58**, 189-198.

Reichenbach H (1989) Nonphotosynthetic, nonfruiting gliding bacteria. Genus 1. In. *Bergey's Manual of Systematic Bacteriology*, 2nd edn, vol. 3, pp. 2015–2050. Edited by Staley J, Bryant MP, Pfennig N, Holt JG.

Reyes I, Bernier L, Simard RR, Antoun H (1999) Effect of nitrogen source on the solubilization of different inorganic phosphates by an isolate of *Penicillium rugulosum* and two UV-induced mutants. *FEMS Microbiol. Ecol.* **28**, 281–290.

Roback SS, Richardson JW (1969) The Effects of Acid Mine Drainage on Aquatic Insects. *Proceedings of the Academy of Natural Sciences of Philadelphia.* **121**, 81-107.

Roden EE Zachara JM (1996) Microbial reduction of crystalline iron(III) oxides: Influence of oxide surface area and potential for cell growth. *Environ. Sci. Technol.* **30**, 1618-1628.

Roos W, Luckner M (1984) Relationships between proton extrusion and fluxes of ammonium ions and organic acids in *Penicillium cyclopium*. *J. Gen. Microbiol.* **130**, 1007–1014.

Rudi K, Moen B, Drømtorp SM, Holck AL (2005) Use of Ethidium Monoazide and PCR in Combination for Quantification of Viable and Dead Cells in Complex Samples. *Applied and Environmental Microbiology.* **71(2)**, 1018–1024.

Rui JP, Peng JJ, Lu YH (2009). Succession of bacterial populations during plant residue decomposition in rice field soil. *Appl. Environ. Microbiol.* **75**, 4879-4886.

Santegoeds CM, Ferdelman TG, Muyzer G, de Beer D (1998) Structural and functional dynamics of sulfate-reducing populations in bacterial biofilms. *Appl. Environ. Microbiol.* **64**, 3731-3739.

Santelli CM, Welch SA, Westrich HR, Banfield JF (2001) The effect of Fe-oxidizing bacteria on Fe-silicate mineral dissolution. *Chemical Geology.* **180**, 99-115.

Schloss PD, Westcott SL, Ryabin T, Hall JR, Hartmann M, Hollister EB, Lesniewski RA, Oakley BB, Parks DH, Robinson CJ, et al. (2009) Introducing mothur: Open-Source, Platform-Independent, Community-Supported Software for Describing and Comparing Microbial Communities. *Appl Environ Microbiol.* **75**, 7537-7541.

Schnoor JL (1990) Kinetics of Chemical Weathering: A Comparison of Laboratory and Field Weathering Rates. **In:** Aquatic Chemical Kinetics: Reaction Rates of Processes in Natural Waters. Environmental Science and Technology Series. John Wiley & Sons, New York. 475-504.

Schutte UME, Abdo Z, Bent SJ, Williams CJ, Schneider GM, Solheim B, Forney LJ (2009). Bacterial succession in a glacier foreland of the High Arctic. *ISME J.* **3**, 1258–1268.

Schwertmann U, Cornell RM (2008) Iron oxides in the laboratory. Wiley-VCH, Weinheim, Germany.

Schwieger F, Tebbe CC (1998) A new approach to utilize PCR-single-strand-conformation polymorphism for 16S rRNA gene-based microbial community analysis. *Appl Environ Microbiol.* **64**, 4870-4876.

Servin JA, Herbold CW, Skophammer RG, Lake JA (2008) Evidence excluding the root of the Tree of Life from the Actinobacteria. *Mol Biol Evol.* **25(1)**, 1-4.

Shivaji S, Reddy GSN, Aduri RP, Kutty R, Ravenschlag K (2004) Bacterial diversity of a soil sample from Schirmacher Oasis, Antarctica. *Cell Mol Biol* **50**, 525–536.

Sholkovitz ER (1995) The aquatic chemistry of rare earth elements in rivers and estuaries. *Aquatic Geochemistry* **1**, 1-34.

Sigler WV, Crivii S, Zeyer J (2002a) Bacterial succession in glacial forefield soils characterized by community structure, activity and opportunistic growth dynamics. *Microb Ecol.* **44**, 306–316.

Sigler WV, Zeyer J (2002b) Microbial diversity and activity along the forefields of two receding glaciers. *Microb Ecol.* **43**, 397–407.

Sigler WV, Zeyer J (2004) Colony forming analysis of bacterial community succession in deglaciated soils indicates pioneer stress tolerant opportunists. *Microb. Ecol.* **48**, 316-323.

Sigmarsson O, Steinthórsson S (2007) Origin of Icelandic basalts: A review of their petrology and geochemistry. *Journal of Geodynamics*. **43**, 87–100.

Silva B, Prieto B, Rivas T, Sanchez-Biezma MJ, Paz G, Carballal G (1997) Rapid biological colonization of a granitic building by lichens. *Int. Biodeterior. Biodegrad.* **40**, 263–267.

Silverman MP, Lundgren DG (1959) Studies on the chemoautotrophic iron bacterium *Ferrobacillus ferrooxidans*: An improved medium and a harvesting procedure for securing high cell yields. *J. Bacteriol.* **77**, 642-647.

Singer PC, Stumm W (1970) Acidic Mine Drainage: The Rate-Determining Step. *Science.* **167**, 1121-1123.

Singleton DR, Furlong MA, Rathbun SL, Whitman WB (2001) Quantitative Comparisons of 16S rRNA Gene Sequence Libraries from Environmental Samples. *Appl Environ Microbiol.* **67**, 4374-4376.

Singleton P, Sainsbury D (2006) Dictionary of Microbiology and Molecular Biology 3 ed., Wiley.

Sisti F, Allegretti P, Donati E (1998) Bacterial reduction of hexavalent chromium by species of *Thiobacilli* grown on sulphur. *Appl Biol Sci* **4**, 47–58.

Smellie JL (2009) Terrestrial subice volcanism: Landform morphology, sequence characteristics, environmental influences, and implications for candidate Mars examples. *Special Paper of the Geological Society of America.*

Sogin ML, Morrison HG, Huber JA, Welch DM, Huse SM, Neal PR, Arrieta JM, Herndl GJ (2006) Microbial diversity in the deep sea and the underexplored "rare biosphere". *PNAS.* **103(32)**, 12115-12120.

Song W, Ogawa N, Oguchi CT, Hatta T, Matsukura Y (2007) Effect of *Bacillus subtilis* on granite weathering: A laboratory experiment. *Catena.* **70(3)**, 275-281.

Soucek DJ, Cherry DS Trent GC (2000) Relative Acute Toxicity of Acid Mine Drainage Water Column and Sediments to Daphnia magna in the Puckett's Creek Watershed, Virginia, USA. *Archives of Environmental Contamination and Toxicology.* **38**, 305-310.

Stackebrandt E., Murray RGE, Trüper HG (1988) Proteobacteria classis nov., a name for the phylogenetic taxon that includes the 'purple bacteria and their relatives'. *Int. J. Syst. Bacteriol.* **38**, 321-325.

Stackebrandt E, Sproer C, Rainey FA, Burghardt J, Pauker O, Hippe H (1997). Phylogenetic analysis of the genus *Desulfotomaculum*: evidence for the misclassification of *Desulfotomaculum guttoideum* and description of *Desulfotomaculum orientis* as *Desulfosporosinus orientis* gen. nov., comb. nov. *Int. J. Syst. Bacteriol.* **47**, 1134–1139.

Stanier RY, Kunisawa R, Mandel M, Cohen-Bazire G (1971) Purification and properties of unicellular blue-green algae (Order Chroococcales). *Bacteriol. Rev.* **35**, 171-205.

Staudigel H, Hart SR (1983) Alteration of basaltic glass: Mechanisms and significance for the oceanic crust-sea water budget. *Geochimica et Cosmochimica Acta* **47**, 337-350.

Staudigel H, Davies GR, Hart SR, Marchant KM, Smith BM (1995) Large scale isotopic Sr, Nd and O isotopic anatomy of altered oceanic crust: DSDP/ODP sites 417/418. *Earth and Planetary Science Letters*. **130**, 169-185.

Staudigel H, Yayanos A, Chastain R, Davies G, Verdurmen EA, Schiffman P, Boucier R, de Baar H (1998) Biologically mediated dissolution of volcanic glass in seawater. *Earth and Planetary Science Letters* **164**, 233–244.

Staudigel H, Furnes H, Banerjee NR, Dilek Y, Muehlenbachs K (2006) Microbes and volcanoes: a tale from the oceans, ophiolites, and greenstone belts. *GSA Today* **16**, 4–102.

Staudigel H, Furnes H, McLoughlin N, Banerjee NR, Connell LB, Templeton A (2008) 3.5 billion years of glass bioalteration: Volcanic rocks as a basis for microbial life? *Earth Science Reviews* **89**, 156–176.

Stefánsson A, Gíslason SR (2001) Chemical weathering of basalts, SW Iceland. Effect of rock crystallinity, weathering minerals and vegetative cover on chemical fluxes to the ocean. *American Journal of Science* **301**, 513-556.

Steffan RJ, Goksoyr J, Bej AK, Atlas RM (1988) Recovery of DNA from soils and sediments. *Applied and Environmental Microbiology*. **54**, 2908-2915.

Steven B, Briggs G, McKay CP, Pollard WH, Greer CW, Whyte LG (2007) Characterization of the microbial diversity in a permafrost sample from the Canadian

High Arctic using culture-dependent and culture-independent methods. *FEMS Microbiol Ecol* **59**, 513–523.

Stevens H, Stübner M, Simon M, Brinkhoff T (2005) Phylogeny of *Proteobacteria* and *Bacteroidetes* from oxic habitats of a tidal flat ecosystem. *FEMS Microbiology Ecology*. **54(3)**, 351–365.

Stoker C (2003) Rio Tinto area of Spain where the Mars Analog Research and Technology Experiment (MARTE) is to take place. NASA Ames Research Center. Photograph.

Stone AT (1997) Reactions of extracellular organic ligands with dissolved metal ions and mineral surfaces. **In**: Geomicrobiology: Interactions between microbes and minerals (eds. Banfield J. F. and Nealson K. H.), *Mineral. Soc. Am.* **35**, 309-344.

Stookey LL (1970) Ferrozine: a new spectrophotometric reagent for iron. *Anal. Chem.* **42**, 779–781.

Storrie-Lombardi MC, Fisk MR (2004) Elemental abundance distributions in suboceanic basalt glass: evidence of biogenic alteration. *Geochemistry, Geophysics, and Geosystems* **5**, 1–15.

Stotzky G. (1986) Influence of soil mineral colloids on metabolic processes, growth, adhesion, and ecology of microbes and viruses. In. *Interactions of Soil Minerals with Natural Organics and Microbes.* Soil Science Society of America, Madison, USA. 305-428.

Stumm W, Sulzberger B (1992) The cycling of iron in natural environments: Considerations based on laboratory studies of heterogeneous redox processes. *Geochim. Cosmochim. Acta* **56**, 3233-32.

Sultan MZ, Khatune NA, Sathi ZS, Bhuiyan SA, Sadik MG, Choudury MA, Gafur MA, Rahman AA (2002) *In vitro* antibacterial activity of an active metabolite isolated from *Streptomyces* species. *Biotechnol.* **1**, 100-106.

Sverdrup H (1990) The Kinetics of Base Cation Release Due to Chemical Weathering. Lund University Press.

Swoboda-Colberg NG, Drever JI (1993) Mineral dissolution rates in plot-scale field and laboratory experiments. *Chemical Geology* **105**, 51–69.

Tamura KD J, Nei M, Kumar S (2007) MEGA4: Molecular evolutionary genetics analysis (MEGA) software version 4.0. *Mol Biol Evol.* **24**, 1596-1599.

Taniguchi H (1980) Some volcano-geological significances of the hydration layer observed in the glassy groundmass of Kozu-shima rhyolite. *Bull. Volcanol. Soc. Jpn.* **25**, 217–229.

Taylor SR (1964) Abundance of chemical elements in the continental crust: a new table. *Geochim. Cosmochim. Acta.* **28**, 1273–1285.

Taylor SR, McLennan SM (1985) The Continental Crust: Its Composition and Evolution. *Oxford, Blackwell*, p. 312.

Techer T, Advocat J, Lancelot, Liotard JM (2001) Dissolution kinetics of basaltic glasses: Control by solution chemistry and protective effect of the alteration film. *Chem. Geol.* **176**, 235–263.

Temple KI, Colmer AR (1951) The autotrophic oxidation of iron by a new bacterium: *Thiobacillus ferrooxidans*. *J. Bacteriol.* **62**, 605-611.

Teske A, Alm E, Regan JM, Toze S, Rittmann BE, Stahl DA (1994) Evolutionary relationships among ammonia- and nitrite-oxidizing bacteria. *J Bacteriol.* **176(21)**, 6623-30.

Thamdrup B, Fossing H, Jørgensen BB (1994) Manganese, iron and sulfur cycling in a coastal marine sediment, Aarhus bay, Denmark. *Geochim. Cosmochim. Acta* **58**, 5115-5129.

Thamdrup B (2000) Bacterial manganese and iron reduction in aquatic sediments. **In:** Schink B (ed) Advances in microbial ecology. Kluwer/Plenum, New York, 16, 41-84.

Thorseth IH, Furnes H, Heldal M (1992) The importance of microbiological activity in the alteration of natural basaltic glass. *Geochimica et Cosmochimica Acta* **56**, 845–850.

Thorseth IH, Torsvik T, Furnes H, Muehlenbachs K (1995a) Microbes play an important role in the alteration of oceanic crust. *Chemical Geology* **126**, 137–146.

Thorseth IH, Furnes, H, Tumyr O (1995b) Textural and chemical effects of microbial activity on basaltic glass: an experimental approach. *Chemical Geology*. **119**, 139-60.

Thorseth IH, Torsvik T, Torsvik V, Daae FL, Pedersen RB, Keldysh-98 Scientific Party (2001). Diversity of life in ocean floor basalt. *Earth Planet. Sci. Lett.* **194**, 31–37.

Thorseth IH, Pedersen RB, Christie DM (2003) Microbial alteration of 0–30-Ma seafloor and sub-seafloor basaltic glasses from the Australian Antarctic Discordance. *Earth and Planetary Science Letters* **215**, 237–247.

Torsvik T, Furnes H, Muehlenbachs K, Thorseth IH, Tumyr O (1998) Evidence for microbial activity at the glass-alteration interface in oceanic basalts. *Earth and Planetary Science Letters* **162**, 165–176.

Tuovinen O, Niemelä S, Gyllenberg H (1971) Tolerance of *Thiobacillus ferrooxidans* to some metals. Antonie van Leeuwenhoek **37**, 489-496.

Qin YY, Liu DT, Yang H (2007) Investigation of total bacterial and ammonia oxidizing bacterial community composition in a full-scale aerated submerged biofilm reactor for drinking water pretreatment in China. *FEMS Microbiol Lett* **268**, 126–134.

Quaiser A, Ochsenreiter T, Lanz C, Schuster SC, Treusch AH, Eck J, Schleper C (2003) Acidobacteria form a coherent but highly diverse group within the bacterial domain: evidence from environmental genomics. *Molecular Microbiology* **50**, 563–575.

Ullman WJ, Kirchman DL, Welch SA, Vandevivere P (1996) Laboratory evidence for microbially mediated silicate mineral dissolution in nature. *Chem. Geol.* **132**, 11–17.

Urey HC (1952). *The Planets, their Origin and Development*. Yale University Press, New Haven.

van der Gast CJ, Ager D, Lilley AK (2008) Temporal scaling of bacterial taxa is influenced by both stochastic and deterministic ecological factors. *Environ. Microbiol.* **10**, 1411-1418.

Vandevivere P, Welch SA, Ullman WJ, Kirchman DL (1994) Enhanced dissolution of silicate minerals by bacteria at near-neutral pH. *Microbial Ecology*. **27**, 241–251.

Varadachari C, Barman AK, Ghosh K (1994) Weathering of silicate minerals by organic acids: II. Nature of residual products. *Geoderma* **61**, 251–268.

Vargas M, Kashefi K, Blunt-Harris EL, Lovley DR (1998) Microbiological evidence for Fe(III) reduction on early Earth. *Nature* **395**, 65–67.

Vazquez P, Holguin G, Puente ME, Lopez-Cortes A, Bashan Y (2000) Phosphate-solubilizing microorganisms associated with the rhizosphere of mangroves growing in a semiarid coastal lagoon. *Biol. Fertil. Soils* **30**, 460–468.

Velbel MA (1993) Constancy of silicate-mineral weathering-ratios between natural and experimental weathering: Implications for hydrologic control of differences in absolute rate. *Chem. Geol.* **105** 89–99.

Venkateswaran K, Moser DP, Dollhopf ME, Lies DP, Saffarini DA, MacGregor BJ *et al.* (1999) Polyphasic taxonomy of the genus *Shewanella* and description of *Shewanella oneidensis* sp. nov.. *Int. J. Sys. Micobiol.* **49**, 705-724.

Ventura M, Canchaya C, Tauch A, Chandra G, Fitzgerald GF, Chater KF, van Sinderen D (2007) Genomics of *Actinobacteria*: tracing the evolutionary history of an ancient phylum. *Microbiol Mol Biol Rev.* **71**, 495-548.

Verplanck PL, Nordstrom DK, Taylor HE, Kimball BA (2004) Rare earth element partitioning between hydrous ferric oxides and acid mine water during iron oxidation. *Appl. Geochem.* **19**, 1339–1354.

Viles H (1995) Ecological perspectives on rock surface weathering: Towards a conceptual model. *Geomorphology* **13**, 21-35

Viollier E, Inglett PW, Hunter K, Roychoudhury AN Van Cappellen P (2000) The ferrozine method revisited: Fe(II)/Fe(III) determination in natural waters. *Applied Geochemistry*. **15**, 785-790.

Walker JJ, Pace NR (2007) Phylogenetic composition of rocky mountain endolithic microbial ecosystems. *Appl Environ Microbiol* **73**, 3497-3504.

Walker AW, Ince J, Duncan SH, Webster LM, Holtrop G et al. (2011) Dominant and diet-responsive groups of bacteria within the human colonic microbiota. *ISME J.* 5:2, 220–230.

Walsh JN, Clarke E (1982) The role of fractional crystallisation in the formation of granitic and intermediate rocks of the Beinn Chaisgidle Centre, Mull, Scotland. *Mineral Mag* **45**, 247-255.

Walton AW (2008) Microtubules in basalt glass from Hawaii Scientific Driling Project #2 phase 1 core and Hilina slope, Hawaii: evidence of the occurrence and behavior of endolithic microorganisms. *Geobiology* **6**, 351–364.

Warner NH, Farmer JD (2010) Subglacial hydrothermal alteration minerals in Jökulhlaup deposits of Southern Iceland, with implications for detecting past or present habitable environments on mars. *Astrobiology*. **10**, 523-547.

Watteau F, Berthelin J (1994) Microbial dissolution of iron and aluminium from soil minerals: Efficiency and specificity of hydroxamate siderophores compared to aliphatic acids. *Eur. J. Soil Biol.* **30**, 1–9.

Weber KA, Achenbach LA, Coates JD (2006) Microorganisms pumping iron: anaerobic microbial iron oxidation and reduction. *Nat Rev Micro* **4**,752-764.

Welch SA, Ullman WJ (1993) The effect of organic acids on plagioclase dissolution rates and stoichiometry. *Geochimica et Cosmochimica Acta* **57**, 2725–2736.

Welch SA, Barker WW, Banfield JF (1999) Microbial extracellular polysaccharides and plagioclase dissolution. *Geochim. Cosmochim. Acta* **63**, 1405–1419.

Welch, SA, Christy AG, Isaacson L, Kirste D (2009) Mineralogical control of rare earth elements in acid sulfate soils. *Geochimica et Cosmochimica Acta*. 73, 44-64.

White AF, Classen HC (1980) Kinetic model for the short-term dissolution of a rhyolitic glass. *Chem. Geol.* **28**, 91–109.

White AF (1983) Surface chemistry and dissolution kinetics of glassy rocks at 25°C. *Geochim. Cosmochim. Acta* **47**, 805–815.

White AF (1995) Chemical weathering rates of silicate minerals in soils. In *Chemical Weathering Rates of Silicate Minerals* (eds. A. F. White and S. L. Brantley, vol. **31**.). Mineralogical Society of America, 407–458.

White AF, Blum AE (1995) Effects of climate on chemical weathering in watersheds. *Geochim. Cosmochim. Acta* **59**, 1729–1747.

White AF, Blum AE, Schulz MS, Bullen TD, Harden JW, Peterson ML (1996) Chemical weathering of a soil chronosequence on granitic alluvium: I. Quantification of mineralogical and surface area changes and calculation of primary silicate reaction rate. *Geochim. Cosmochim. Acta* **60**, 2533–2550.

White AF, Brantley SL (1995) (eds.) Chemical Weathering Rates of Silicate. *Minerals, Mineralogical Society of America Shortcourse*, **31**.

White AF, Brantley SL (2003) The effect of time on the weathering of silicate minerals: Why do weathering rates differ in the laboratory and field? *Chemical Geology* **202**, 479–506.

Wierzchos J, Ascaso C (1994) Application of back-scattered electron imaging to the study of the lichen–rock interface. *J. Microsc.* **175**, 54–59.

Wierzchos J, Ascaso C (1996) Morphological and chemical features of bioweathered granitic biotite induced by lichen activity. *Clays Clay Miner.* **44**, 652–657.

Williamson MA (1998) *Iron.* Encyclopedia of Earth Science. 348-353.

Wogelius RA, Walther JV (1991) Olivine dissolution at 25°C: Effects of pH, CO_2, and organic acids. *Geochim. Cosmochim. Acta* **55**, 943–954.

Wolff-Boenisch D, Gislason SR, Oelkers EH (2006) The effect of crystallinity on dissolution rates and CO_2 consumption capacity of silicates. *Geochim. Cosmochim. Acta* **70**, 858–870.

Wong C, Silver M, Kunshner DJ (1982) Effect of chromium and manganese on *Thiobacillus ferrooxidans*. *Can J Microbiol* **28**, 536–544.

Wood SA (1990) The aqueous geochemistry of the rare-earth elements and yttrium 1. Review of available low-temperature data for inorganic complexes and the inorganic REE speciation of natural waters. *Chem. Geol.* **82**, 159–186.

Wu L, Jacobson AD, Chen HC, Hausner M (2007a) Characterization of elemental release during microbe-basalt interactions at T = 28°C. *Geochimica et Cosmochimica Acta.* **71(9)**, 2224-2239.

Wu L, Jacobson AD, Hausner M (2008) Characterization of elemental release during microbe-granite interactions at T = 28°C. *Geochimica et Cosmochimica Acta.* **72(4)**, 1076-1095.

Wu X, Xi WY, Ye WJ, Yang H (2007b) Bacterial community composition of a shallow hypertrophic freshwater lake in China. *FEMS Microb Ecol* **61**, 85–96.

Yamanaka T, Li CY, Bormann B, Okabe H (2003) Tripartite associations in an alder: effects of Frankia and Alpova diplophloeus on the growth, nitrogen fixation and mineral acquisition of Alnus tenuifolia. *Plant Soil* **254**, 179–186.

Yokoyama T, Banfield JF (2002) Direct determinations of the rates of rhyolite dissolution and clay formation over 52,000 years and comparison with laboratory measurements. *Geochimica et Cosmochimica Acta* **66**, 2665–2681.

Yokoyama T, Matsukura Y (2006) Field and laboratory experiments on weathering rates of granodiorite: Separation of chemical and physical processes. *Geology* **34**, 809–812.

Zachara JM, Fredrickson JK, Li SM, Kennedy DW, Smith SC, Gassman PL (1998) Bacterial reduction of crystalline Fe^{3+} oxides in single phase suspensions and subsurface materials. *Am. Miner.* **83**, 1426-1443.

Zachara JM, Kukkadapu RK, Fredrickson JK, Gorby YA, Smith SC (2002) Biomineralization of poorly crystalline Fe(III) oxides by dissimilatory metal-reducing bacteria (DMRB). *Geomicrobiol. J.* **19**, 179-2002.

Zhang H, Sekiguchi Y, Hanada S, Hugenholtz P, Kim H, Kamagata Y, Nakamura K (2003) Gemmatimonas aurantiaca gen. nov., sp. nov., a gram-negative, aerobic, polyphosphate-accumulating micro-organism, the first cultured representative of the new bacterial phylum Gemmatimonadetes phyl. nov. *Int J Syst Evol Microbiol* **53(4)**, 1155–63.

Zhou JP, Gu YQ, Zou CS, Mo MH (2007) Phylogenetic diversity of bacteria in an earth-cave in Guizhou Province, Southwest of China. *J Microbiol* **45**, 105–112.